UNIVERSITÀ DEGLI STUDI DI PALERMO
Dottorato di Ricerca in Scienze Agrarie, Alimentari, Forestali e Ambientali
Dipartimento di Scienze Agrarie, Alimentari e Forestali
Settore Scientifico Disciplinare "AGR/08 Idraulica Agraria e Sistemazioni Idraulico-Forestali"

INVESTIGATIONS ON INFILTRATION METHODS FOR AN IMPROVED SOIL HYDRAULIC CHARACTERIZATION

IL DOTTORE
PAOLA CONCIALDI

IL COORDINATORE
PROF. VINCENZO BAGARELLO

IL TUTOR
PROF. VINCENZO BAGARELLO

IL CO TUTOR
PROF. MASSIMO IOVINO

CICLO XXXII
ANNO CONSEGUIMENTO TITOLO 2020

TABLE OF CONTENTS

CHAPTER 1: General introduction……..……..……..…….1

References…….……..…...6

CHAPTER 2: Laboratory investigation on the Simplified Falling Head technique….....9

2.1 Introduction…….……..……..…….9

2.2 Theory……..……..……....10

2.3 Applications of the SFH technique…….....12

2.4 A novel investigation on the SFH technique……..…16

2.5 Perspectives of future research…….……..17

Appendix A: Laboratory evaluation of falling-head infiltration for saturated soil hydraulic conductivity determination……..……..…..….21

References……..…….…….…..….30

CHAPTER 3: Using single-ring infiltration methods to determine the soil hydraulic properties in a hydrological perspective……...……...…….35

3.1 Introduction……...……..…...35

3.2 Theory……...……..……..40

3.3 Applications of BEST methods……...……..……..…..45

3.4 Characterization of non-rigid soils by single-ring infiltration experiments……...……49

Appendix B: Laboratory testing of Beerkan infiltration experiments for assessing the role of soil sealing on water infiltration……..……...…..53

Appendix C: A test of water pouring height and run intermittence effects on single-ring infiltration rates…….65

Appendix D: Testing an adapted Beerkan infiltration run for a hydrologically relevant soil hydraulic characterization.……...77

References……..…….....86

CHAPTER 4: Intensive soil characterization with automatic single-ring infiltrometers……...…….……...…..95

4.1 Introduction……..…….....95

4.2 An innovative instrumentation package for soil characterization.……96

Appendix E: An open-source instrumentation package for intensive soil hydraulic characterization…….....97

References……..……...……..110

CHAPTER 5: Additional investigations on soil hydraulic characterization by single-ring infiltration methods…….....112

5.1 Parameterization of an explicit model for single-ring infiltration…….……..112

5.1.1 Introduction…….....112

5.1.2 Infiltration model……..……...113

5.1.3 Materials and methods……..……...114

5.1.4 Results……...……...116

5.1.5 Conclusions……...……...121

5.2 Monitoring saturated hydraulic conductivity of a loam soil by different application methodologies of a Beerkan infiltration run …….121

5.2.1 Introduction……..……...121

5.2.2 Materials and methods……...……..122

5.2.3 Results and discussion……...……...124

5.2.4 Conclusions……...……...136

References……..…….137

CHAPTER 6: Summary and conclusions……....140

CHAPTER 1: General introduction

Water flow in heterogeneous, variably saturated porous media is an important topic in any branch of hydrology, soil science, and agricultural engineering dealing with both surface and subsurface flow and chemical transport processes. The unsaturated soil zone plays an important role on extremely important hydrological processes such as surface runoff formation and aquifer recharge since it controls the partition of rainfall into infiltration and infiltration excess. Most groundwater pollution problems are a consequence of the release of contaminants from near surface sources such as landfills, septic tanks or tailing ponds. The groundwater contaminants reach the aquifer moving through the unsaturated soil zone that therefore represents the hydrological connection between the surface water component of the hydrologic cycle and the groundwater component. The characteristics of this zone also influence design and monitoring of irrigation and drainage systems (Hillel, 1998). The unsaturated zone may lose water through evaporation, transpiration, and drainage. Environmental problems caused by intense degradation and desertification of the land, that have an obvious importance for the society, require accurate investigations on soil physical and hydraulic properties of the unsaturated soil zone (Romano, 2000).

In particular, understanding and characterizing the hydrological cycle and transfer of contaminants transported by water relies on determining the soil hydraulic characteristic curves, that is, the water retention and the hydraulic conductivity curves. The water retention curve describes the relation between the volumetric soil water content, θ (L^3L^{-3}), and the soil water pressure head, h (L). The hydraulic conductivity function describes the relation between the soil hydraulic conductivity, K (L T^{-1}), and either θ or h. Soil hydraulic conductivity was originally introduced by Darcy (1856) for saturated soils and it was then extended to unsaturated soils by Buckingham (1907) and Richards (1931). The soil hydraulic conductivity depends on the soil pores characteristics, the moving fluid and the fluid content in the soil. The soil hydraulic conductivity at saturation is referred to as the saturated soil hydraulic conductivity, K_s (L T^{-1}). When expressed as a function of the volumetric soil water content, the hydraulic conductivity function is strongly nonlinear. Generally speaking, as soil dries, K rapidly decreases by several orders of magnitude.

Soil hydrodynamic parameters and, among these, saturated soil hydraulic conductivity are very complicated to be determined accurately since soil pores, and particularly the largest ones, are extremely unstable and fragile (Jarvis et al., 2013). Consequently, any attempt to determine these parameters implies a high risk to modify the soil pore arrangement. This circumstance has to be considered as unfavorable since it implies for example that the conductivity of the absolutely intact porous medium cannot be determined without any uncertainty. On the other hand, it has also to be taken into account that determining K_s has in general a given hydrological purpose and the hydrological processes stress the soil when they occur. Consequently, the soil does not behave in practice as a rigid and immutable porous medium.

Many experimental investigations have been devoted over the last decades to the development of measurement or estimation methodologies of soil hydraulic characteristics. Roughly speaking, two categories of methods can be distinguished for the determination of the unknown soil hydraulic properties: i) direct or indirect measurement techniques, and ii) predictive methods (Di Prima, 2016). The first category of techniques has been developed mainly for measurement of the soil hydraulic properties at a local scale and is difficult to apply over large areas. The second category allows to estimate soil hydraulic properties through the use of pedotransfer functions (PTFs). These are generally empirical relationships that allow the hydraulic properties of a given soil to be predicted from easily accessible data, such as textural characteristics (e.g., percentages of sand, silt, and clay), bulk density and soil organic matter content. The PTFs can either be applied at the local scale using point properties or at the watershed scale where textural information has been aggregated (soil maps). Due to their empirical nature, PTFs are typically characterized by large uncertainties and they should only be applied after checking their usability for the particular scope in the particular environment (Tomasella et al., 2000).

Soil hydrodynamic parameters are very difficult to be determined since they depend on the complex and also rapidly changing pore-size distribution. In particular, many methods have been developed over time for determination of K_s that is a fundamental soil hydraulic property (Reynolds and Elrick, 1990). However, different methods often yield dissimilar K_s values since this parameter is extremely sensitive to sample size, flow geometry, sample collection procedures, and various soil physical-hydrological characteristics (Bouma, 1983). In addition, perhaps all K_s methods are neither appropriate nor accurate for all applications, soil types, or soil conditions (Bouma, 1983). Methods for measuring K_s should therefore be evaluated carefully before use to ensure that they provide practicable results (Reynolds et al., 2000). The problem is of enormous complexity taking for example into account that Reynolds et al. (2000) also concluded that comparing techniques for measuring the saturated hydraulic conductivity of intact soil is an imprecise and perhaps even dubious enterprise because there is no independent K_s datum or benchmark upon which evaluations and judgments can be made. It is nonetheless important to make such comparisons because they provide one of the few sources of information that practitioners can draw upon to select K_s methods that are appropriate for their circumstances.

In general, the measurement techniques rely on precise and time-consuming experimental procedures that can be categorized as being either laboratory- or field-based.

While laboratory methods allow accurate measurement of flow processes, they are performed on samples taken from the field and, as a result, their representativeness of field conditions can be questioned. The presence of aggregates, stones, fissures, fractures, tension cracks, and root holes, commonly encountered in unsaturated soil profiles, is difficult to represent in small-scale laboratory samples. Field techniques can be more difficult to control in terms of initial and imposed boundary conditions, but they have the advantage of estimating in situ soil hydraulic properties that are more representative of the real world, which is of considerable value in the subsequent use of the hydraulic information. Moreover, working directly in the field is the preferred option to obtain reliable data since the functional connection of the sampled soil volume with the surrounding porous medium is maintained in this case (Bouma, 1982). Therefore, it is desirable to aim at field methods that can ease, to some extent, the time-consuming constraints. Lassabatere et al. (2006) concluded that field based methods should be considered more advantageous over laboratory based methods insofar as (i) they are less expensive and time-consuming, (ii) the gain in precision in the laboratory is limited because soil cores usually provide a poor picture of the real soil, and (iii) laboratory devices are badly adapted for revealing the hydraulic behavior of watersheds at field scale (Minasny and McBratney, 2002).

Infiltration-based methods are recognized as valuable tools to determine hydrodynamic soil properties directly in the field (Angulo-Jaramillo et al., 2000, 2016). In particular, single-ring infiltration methods have a great interest for estimating the hydrodynamic properties of the field saturated soil. A great contribution to the success of these methods has to be attributed to the Canadian soil physics scientists D.E. Elrick and W.D. Reynolds since these authors developed the three-dimensional (3D) theory of infiltration from within a single-ring inserted to a short depth into the soil taking into account the three main components of steady flow, i.e. hydrostatic pressure of the ponded water in the cylinder, capillarity of the unsaturated soil under and adjacent to the cylinder, and gravity (Reynolds and Elrick, 1990). The so-called single-ring pressure infiltrometer method makes use of a metal ring that is inserted into the soil to a given, small, depth. A constant hydraulic head, H, is established within the infiltration ring, and the flow rate into the soil is monitored. Flow goes through an initial decreasing phase, and then it approaches steady state conditions. Three dimensional, steady, ponded flow out of the ring is then used to estimate K_s (Reynolds and Elrick, 1990). The method is attractive for field use because it is simple and reasonably rapid. It is now a routinely used K_s measurement method (Vauclin et al., 1994; Ciollaro and Lamaddalena, 1998; Bagarello and Iovino, 1999; Bagarello et al., 2000; Reynolds et al., 2000; Bagarello and Sgroi, 2004; Angulo-Jaramillo et al., 2000, Mertens et al., 2002; Gómez et al., 2005).

The work done by Reynolds and Elrick in the nineties stimulated many other scientists to test and possibly improve existing infiltration methods for determining soil hydrodynamic properties and also to develop new methods. Two of these methods are the Simplified Falling Head (SFH) technique by

Bagarello et al. (2004) and the Beerkan Estimation of Soil Transfer parameters (BEST) procedure of soil hydraulic characterization by Lassabatere et al. (2006). Both methods are based on robust physical theories but they differ in many other respects.

The SFH technique is usable to determine the field saturated hydraulic conductivity of an initially unsaturated soil by a one-dimensional falling head infiltration process. The technique is based on the Philip (1992) relationship which describes one-dimensional cumulative infiltration for falling head conditions using the Green and Ampt (1911) approach. The technique consists of applying quickly a small volume of water on the soil surface confined by a ring inserted at a fixed distance into the soil and in measuring the time from the application of water to the instant at which
the infiltration surface is no longer covered by water. Estimation of K_s also requires data on the initial and saturated volumetric soil water content and also an estimate of the relative importance of gravity and capillary forces on infiltration.

The BEST procedure of soil hydraulic characterization allows simultaneous estimation of the soil water retention and hydraulic conductivity curves by a limited experimental information that includes particle-size distribution of the soil, dry soil bulk density, cumulative 3D infiltration, and initial and final soil water contents. BEST focuses specifically on the van Genuchten (1980) relationship for the water retention curve and the Brooks and Corey (1964) relationship for hydraulic conductivity. In the field, water infiltration experiments are carried out by the beerkan method, pioneered by Braud et al. (2005). A ring with a diameter of several centimeters is inserted a short distance into the soil to pour water volumes at soil surface while avoiding lateral loss of ponded water. A fixed, small volume of water is poured into the cylinder at time zero to establish a small ponded head of water and the time elapsed during infiltration of the known volume of water is measured. When the first volume has completely infiltrated, a second equal volume of water is added to the cylinder, and the time needed for it to infiltrate is measured. The procedure is repeated for about 8 to 15 known volumes to allow flow into the soil to nearly stabilize (Lassabatere et al., 2006), and cumulative infiltration, I (L), is recorded. The infiltration data are analyzed using the approximations of the quasi-exact implicit infiltration model by Haverkamp et al. (1994).

A great interest by the scientific community for both the SFH technique and the BEST procedure of soil hydraulic characterization can be recognized. For example, the Scopus database indicated that the paper by Bagarello et al. (2004) was cited 92 times while 174 citations were reported for the paper by Lassabatere et al. (2006). The larger interest for BEST than the SFH technique probably relies on the fact that the former method provides a complete soil hydraulic characterization while the latter one is limited to the determination of K_s.

The research on single-ring infiltration into an initially unsaturated soil appears to still attract the interest by the scientific community and even in the most recent years attempts to further improve determination of soil hydraulic properties, with particular reference to K_s, by single-ring infiltration data were made. In particular, Stewart and Abou Najm (2018a) developed a new comprehensive model for single ring infiltration data by combining the infiltration models by Reynolds and Elrick (1990) and Wu et al. (1999). These authors then proposed four different approaches for estimating K_s from both transient and steady-state single-ring infiltration data (Stewart and Abou Najm, 2018b). The proposed model has still received little attention but it seems to have some practical interest in that it treats both transient and steady-state infiltration data and can analyze experiments carried out with different ring sizes and ring insertion depths.

The soil physics research group of the Agricultural, Food and Forest Sciences Department of the University of Palermo has actively contributed in the past years to the doctoral training of several PhD students, including Antonio De Santis (2004), Mirko Castellini (2005), Chiara Caponnetto (2006), Angelo Sgroi (2006), Chiara Antinoro (2008), Sebastiano Sferlazza (2011), Simone Di Prima (2016) and Vincenzo Alagna (2017), some of which are today researchers working at Universities or other Research Centers in the field of soil physics. Most if not all of these older colleagues developed specific topics related with determinations of soil physical and hydraulic properties with both laboratory and field methodologies.

Starting from these premises, the research activity for this PhD thesis was consistent with the activity carried out in the past and it had the general objective to contribute to improving applicability of single-ring infiltration methods for soil hydraulic characterization. The reasoning at the basis of all the activity that was carried out was that measurement of soil hydraulic properties has to be useful for solving a specific problem. Therefore, the method to be applied, its application procedure and the applied approach to analyze the data should be appropriate in the perspective to solve the problem under consideration. This is a relevant problem since, for example, some literature appears to suggest that infiltrometer methods could not yield data usable for explaining rainfall partition into infiltration and rainfall excess in any circumstance (Ben-Hur et al., 1987; Cerdà, 1996; Cerdà et al. 1997; van De Giesen et al., 2000; Bagarello et al., 2013).

The investigations of this thesis were mainly focused on the SFH technique and the BEST procedure of soil hydraulic characterization, given the recognized interest for these two methodologies. The recently proposed infiltration model by Stewart and Abou Najm (2018a) was also investigated since it appears to have the potential to simplify application of single-ring infiltration methods. More in detail, this dissertation is composed by the following six chapters.

Chapter 1 is this introduction.

Chapter 2 is titled "Laboratory investigation on the Simplified Falling Head technique" and it summarizes the research activity on the SFH technique. The general objective of this investigation was to check falling head one-dimensional infiltration procedures for K_s determination in controlled situations, that is in the laboratory and using homogenized soil samples. Chapter 2 contains an introduction, the theory of the SFH technique, an overview of the use that has been made of the SFH technique up to now, a brief description of the research activity on the SFH technique developed during the PhD course and a short discussion on some aspects that could be investigated in some detail in the future. The paper <Concialdi P., Bagarello V., Alagna V., Iovino M. 2020. Laboratory evaluation of falling-head infiltration for saturated soil hydraulic conductivity determination. Journal of Agricultural Engineering, LI:1003, 27-35, doi: 10.4081/jae.2019.1003> that contains all the details on the investigations that were made specifically, is enclosed as the appendix A to the chapter.

Chapter 3 is titled "Using single-ring infiltration methods to determine the soil hydraulic properties in a hydrological perspective" and it focuses mainly on the BEST methodology. This chapter is organized into four sections and three appendices. In particular, after an introduction, the theory of the BEST methods is presented. An overview of the use that has been made of the BEST methodology up to now is then provided. The research activity on the BEST methodology developed during the PhD course is subsequently described. Finally, the appendices B, C and D are the following published papers during the PhD course: <Di Prima S., Concialdi P., Lassabatere L., Angulo-Jaramillo R., Pirastru M., Cerdà A., Keesstra S. 2018a. Laboratory testing of Beerkan infiltration experiments for assessing the role of soil sealing on water infiltration. Catena, 167: 373-384>; <Alagna V., Bagarello V., Cecere N., Concialdi P., Iovino M. 2018b. A test of water pouring height and run intermittence effects on single-ring infiltration rates. Hydrological Processes, 32: 3793-3804>, and <Auteri N., Bagarello V., Concialdi P., Iovino M. 2020. Testing an adapted beerkan infiltration run for a hydrologically relevant soil hydraulic characterization. Journal of Hydrology, 584, 12469714, 9 pp.>.

Chapter 4 is titled "Intensive soil characterization with automatic single-ring infiltrometers" and it mainly focuses on development of an automatic infiltrometer in view to reduce analysis time and improve data consistency. This chapter contains an introduction, an overview of the currently available automated devices and a description of the activity that was carried out during the PhD course. Finally, the paper <Concialdi, P., Di Prima, S., Bhanderi, H.M., Stewart, R.D., Abou Najm, M.R., Lal Gaur, M., Angulo-Jaramillo, R., Lassabatere, L., 2020. An open-source instrumentation package for intensive soil hydraulic characterization. J. Hydrol. 582, 124492. https://doi.org/10.1016/j.jhydrol.2019.124492> is reported at the end of the chapter. This part of the thesis represents the result of a six-month period spent at the Laboratoire d'Ecologie des Hydrosystèmes Naturels et Anthropisés, Lyon, France, under the supervision of Dr. Laurent Lassabatere.

Chapter 5 is titled “Additional investigations on soil hydraulic characterization by single-ring infiltration methods”. This chapter contains the “parameterization of an explicit model for single-ring infiltration” by Stewart and Abou Najm (2018a) with some theoretical reasoning to show that parameterization of the model can be simplified in practice. “Monitoring saturated hydraulic conductivity of a loam soil by different application methodologies of a beerkan infiltration run” was also included in this chapter.
Finally, **Chapter 6** reports the main conclusions of all the research activity that was carried out during the PhD course.

References

Alagna, V., Bagarello, V., Cecere, N., Concialdi, P., Iovino, M., 2018. A Test of water pouring height and run intermittence effects on single-ring infiltration rates. Hydrol. Process. https://doi.org/10.1002/hyp.13290

Angulo-Jaramillo, R., Bagarello, V., Iovino, M., Lassabatere, L., 2016. Unsaturated soil hydraulic properties, in: infiltration measurements for soil hydraulic characterization. Springer International Publishing

Angulo-Jaramillo, R., Vandervaere, J.-P., Roulier, S., Thony, J.-L., Gaudet, J.-P., Vauclin, M., 2000. Field measurement of soil surface hydraulic properties by disc and ring infiltrometers: A review and recent developments. Soil Tillage Res. 55, 1–29. https://doi.org/10.1016/S0167-1987(00)00098-2

Auteri, N., Bagarello, V., Concialdi, P., Iovino, M., 2020. Testing an adapted beerkan infiltration run for a hydrologically relevant soil hydraulic characterization. J. Hydrol. 584, 124697. https://doi.org/10.1016/j.jhydrol.2020.124697

Bagarello, V., Di Stefano, C., Iovino, M., Sgroi, A., 2013. Using a transient infiltrometric technique for intensively sampling field-saturated hydraulic conductivity of a clay soil in two runoff plots. Hydrol. Process. 27, 3415–3423. https://doi.org/10.1002/hyp.9448

Bagarello, V., Sgroi, A., 2004. Using the single-ring infiltrometer method to detect temporal changes in surface soil field-saturated hydraulic conductivity. Soil Tillage Res. 76, 13–24. https://doi.org/10.1016/j.still.2003.08.008

Bagarello, V., Iovino, M., Tusa, G., 2000. Factors affecting measurement of the near-saturated soil hydraulic conductivity. Soil Sci. Soc. Am. J. 64, 1203. https://doi.org/10.2136/sssaj2000.6441203x

Bagarello, V., Iovino, M., 1999. Spatial and temporal variability of saturated hydraulic conductivity in a central Sicily soil. Int. Workshop EurAgEngs Field Interest Soil Water Leuven Belg. 24-26 Nov 1999 Wagening. Pers.

Ben-Hur, M., Shainberg, I., Morin, J., 1987. Variability of infiltration in a field with surface-sealed Soil. Soil Sci. Soc. Am. J. 51, 1299–1302. https://doi.org/10.2136/sssaj1987.03615995005100050037x

Braud, I., De Condappa, D., Soria, J.M., Haverkamp, R., Angulo-Jaramillo, R., Galle, S., Vauclin, M., 2005. Use of scaled forms of the infiltration equation for the estimation of unsaturated soil hydraulic properties (the beerkan method). Eur. J. Soil Sci. 56, 361–374. https://doi.org/10.1111/j.1365-2389.2004.00660.x

Brooks, R.H., Corey, T., 1964. hydraulic properties of porous media. Hydrol Pap. 3 Colo. State Univ. Fort Collins.

Bouma, J., 1983. Use of soil survey data to select measurement techniques for hydraulic conductivity. Agric. Water Manag. 6, 177–190. https://doi.org/10.1016/0378-3774(83)90007-0

Bouma, J., 1982. Measuring the hydraulic conductivity of soil horizons with continuous macropores. Soil Sci. Soc. Am. J. 46, 438. https://doi.org/10.2136/sssaj1982.03615995004600020047x

Buckingham, E., 1907. Studies on the movement of soil moisture. US Dept Agr Bur Soils Bull 38

Cerdà, A., Ibáñez, S., Calvo, A., 1997. Design and operation of a small and portable rainfall simulator for rugged terrain. Soil Technol. 11, 163–170. https://doi.org/10.1016/S0933-3630(96)00135-3

Cerdà, A., 1996. Seasonal variability of infiltration rates under contrasting slope conditions in southeast Spain. Geoderma 69, 217–232. https://doi.org/10.1016/0016-7061(95)00062-3

Ciollaro, G., Lamaddalena, N., 1998. Effect of tillage on the hydraulic properties of a vertic soil. J. Agric. Eng. Res. 71, 147–155. https://doi.org/10.1006/jaer.1998.0312

Concialdi, P., Di Prima, S., Bhanderi, H.M., Stewart, R.D., Abou Najm, M.R., Lal Gaur, M., Angulo-Jaramillo, R., Lassabatere, L., 2020. An open-source instrumentation package for intensive soil hydraulic characterization. J. Hydrol. 582, 124492. https://doi.org/10.1016/j.jhydrol.2019.124492

Concialdi, P., Bagarello, V., Alagna, V., Iovino, M., 2019. Laboratory evaluation of falling-head infiltration for saturated soil hydraulic conductivity determination. J. Agric. Eng. https://doi.org/10.4081/jae.2019.1003

Darcy, H., 1856. Les fontaines publiques de la ville de Dijon: exposition et application... Victor Dalmont.

Di Prima, S., Concialdi, P., Lassabatere, L., Angulo-Jaramillo, R., Pirastru, M., Cerda, A., Keesstra, S., 2018. Laboratory testing of beerkan infiltration experiments for assessing the role of soil sealing on water infiltration. Catena 167, 373–384. https://doi.org/10.1016/j.catena.2018.05.013

Di Prima, S., 2016. Improvement of BEST (Beerkan Estimation of Soil Transfer parameters) method for soil hydraulic characterization (doctoral thesis)

Gómez, J.A., Vanderlinden, K., Nearing, M.A., 2005. Spatial variability of surface roughness and hydraulic conductivity after disk tillage: implications for runoff variability. J. Hydrol. 311, 143–156. https://doi.org/10.1016/j.jhydrol.2005.01.014

Green, W.H., Ampt, G.A., 1911. Studies on soil phyics. J. Agric. Sci. 4, 1–24. https://doi.org/10.1017/S0021859600001441

Haverkamp, R., Ross, P.J., Smettem, K.R.J., Parlange, J.Y., 1994. Three-dimensional analysis of infiltration from the disc infiltrometer: 2. Physically based infiltration equation. Water Resour. Res. 30, 2931–2935. https://doi.org/10.1029/94WR01788

Hillel, D., 1998. Environmental soil physics: Fundamentals, applications, and environmental considerations. Academic press.

Jarvis, N., Koestel, J., Messing, I., Moeys, J., Lindahl, A., 2013. Influence of soil, land use and climatic factors on the hydraulic conductivity of soil. Hydrol Earth Syst Sci 17, 5185–5195. https://doi.org/10.5194/hess-17-5185-2013

Lassabatere, L., Angulo-Jaramillo, R., Soria Ugalde, J.M., Cuenca, R., Braud, I., Haverkamp, R., 2006. Beerkan estimation of soil transfer parameters through infiltration experiments—BEST. Soil Sci. Soc. Am. J. 70, 521. https://doi.org/10.2136/sssaj2005.0026

Mertens, J., Jacques, D., Vanderborght, J., Feyen, J., 2002. Characterisation of the field-saturated hydraulic conductivity on a hillslope: in situ single ring pressure infiltrometer measurements. J. Hydrol. 263, 217–229. https://doi.org/10.1016/S0022-1694(02)00052-5

Minasny, B., McBratney, A.B., 2002. The efficiency of various approaches to obtaining estimates of soil hydraulic properties. Geoderma 107, 55–70.

Philip, J.R., 1992. Falling head ponded infiltration. Water Resour. Res. 28, 2147–2148. https://doi.org/10.1029/92WR00704

Stewart, R.D., Abou Najm, M.R., 2018a. A comprehensive model for single ring infiltration I: initial water content and soil hydraulic properties. Soil Sci. Soc. Am. J. 0, 0. https://doi.org/10.2136/sssaj2017.09.0313

Stewart, R.D., Abou Najm, M.R., 2018b. A comprehensive model for single ring infiltration II: estimating field-saturated hydraulic conductivity. Soil Sci. Soc. Am. J. 0, 0. https://doi.org/10.2136/sssaj2017.09.0314

Reynolds, W.D., Bowman, B.T., Brunke, R.R., Drury, C.F., Tan, C.S., 2000. Comparison of tension infiltrometer, pressure infiltrometer, and soil core estimates of saturated hydraulic conductivity. Soil Sci. Soc. Am. J. 64, 478–484. https://doi.org/10.2136/sssaj2000.642478x

Reynolds, W.D., Elrick, D.E., 1990. Ponded infiltration from a single ring: I. Analysis of steady flow. Soil Sci. Soc. Am. J. 54, 1233. https://doi.org/10.2136/sssaj1990.03615995005400050006x

Richards, L.A. 1931. Capillary conduction of liquids through porous mediums. Journal of Applied Physics, 1, 318-333. http://dx.doi.org/10.1063/1.1745010

Romano N., 2000. Applicazioni di tecniche geostatistiche per la caratterizzazione idraulica dei suoli. Rivista di Ingegneria Agraria. Vol 4. 216-225.

Tomasella, J., Hodnett, M.G., Rossato, L., 2000. Pedotransfer functions for the estimation of soil water retention in Brazilian soils. Soil Sci. Soc. Am. J. 64, 327. https://doi.org/10.2136/sssaj2000.641327x

van De Giesen, N.C., Stomph, T.J., de Ridder, N., 2000. Scale effects of Hortonian overland flow and rainfall–runoff dynamics in a West African catena landscape. Hydrol. Process. 14, 165–175. https://doi.org/10.1002/(SICI)1099-1085(200001)14:1<165::AID-HYP920>3.0.CO;2-1

van Genuchten, M.T., 1980. A closed-form equation for predicting the hydraulic conductivity of unsaturated soils. Soil Sci. Soc. Am. J. 44, 892–898.

Vauclin, M., Elrick, D.E., Thony, J.L., Vachaud, G., Revol, P., Ruelle, P., 1994. Hydraulic conductivity measurements of the spatial variability of a loamy soil. Soil Technol. 7, 181–195. https://doi.org/10.1016/0933-3630(94)90020-5

Wu, L., Pan, L., Mitchell, J., Sanden, B., 1999. Measuring saturated hydraulic conductivity using a generalized solution for single-ring infiltrometers. Soil Sci. Soc. Am. J. 63, 788. https://doi.org/10.2136/sssaj1999.634788x

CHAPTER 2: Laboratory investigation on the Simplified Falling Head Technique

2.1. Introduction

The saturated soil hydraulic conductivity, K_s (L T^{-1}), is one of the most important soil properties controlling water infiltration and surface runoff, leaching of pesticides from agricultural lands and migration of pollutants from contaminated sites to the groundwater. Saturated conductivity depends on soil texture and structure and therefore can vary widely in space. Since K_s is determined essentially at points in the fields, a large number of determinations is required to assess the magnitude and structure of the variation within the area of interest (Logsdon and Jaynes, 1996). Saturated conductivity also shows a temporal variability that depends on different interrelated factors, including soil physical and chemical characteristics affecting aggregate stability, climate, land use, dynamics of plant canopy and roots, tillage operations, activity of soil organisms (Fuentes et al., 2004). Therefore, spatially distributed determinations of K_s have to be repeated at different times for understanding and modelling hydrological phenomena at the field scale.

On the premise that K_s should be determined directly in the field with simple, rapid, cheap and water-parsimonious methods, Bagarello et al. (2004, 2006) developed and tested a technique for field determination of K_s by a transient, one-dimensional infiltration experiment under falling head condition. This technique was named Simplified Falling Head (SFH).

The early stages of the proposal of the SFH technique to the scientific community were summarized in **Table 2.1** and they were also described in brief in the following.

The SFH technique consists of measuring the total infiltration time, t_a (T), of a given volume of water instantaneously poured on the soil surface confined by a ring inserted into the initially unsaturated soil to a given depth. Saturated conductivity is determined from the measured t_a value using the Green and Ampt (1911) representation of a falling head, one-dimensional infiltration process, using the expression including gravity proposed by Philip (1992). Theory of the SFH technique is described in more detail in the 2.2 section of this chapter.

Due to the one-dimensional nature of the experiment, the water volume to be applied must be chosen in such a way that the wetting front does not go beyond the bottom of the inserted ring into the soil at the time $t = t_a$. Determination of initial and saturated soil water content and estimation of the relative importance of gravity and capillarity forces during infiltration, through the so-called α^* (L^{-1}) parameter (Elrick and Reynolds, 1992), are also necessary to estimate K_s.

The experimental activity initially carried out for testing the SFH technique included the following stages (Bagarello et al., 2004; **Table 2.1**): i) comparison in the laboratory with the so-called Early-Time Constant-Head (ECH) technique (Fallow et al., 1994; Odell et al., 1998) that is another technique considering the early stage of the infiltration process; and ii) comparison in the field with the Pressure Infiltrometer (PI) technique (Reynolds and Elrick, 1990). Reasons for choosing this last technique for the comparison included the fact that the PI is a well-tested K_s measurement method (Reynolds, 2008; Reynolds et al., 2000) and also that the same surface area can be sampled with the SFH and PI techniques, which was expected to simplify interpretation of the K_s results.

Additional testing and attempts to develop the SFH technique were made later (Bagarello et al., 2006; **Table 2.1**). In particular, a comparison was established in the laboratory with the constant head permeameter method, largely used and close to a standard K_s measurement method (Klute and Dirksen, 1986). A two-level (TL) data analysis procedure was developed in an attempt to avoid the need to estimate the α^* parameter with a subjective procedure, that is based on visual assessment of the soil textural and structural characteristics (Elrick and Reynolds, 1992).

After 15 years from the proposal of the technique, it was the time to check the interest it has received by the scientific community and signs of appreciation for the developed methodology were clearly perceived by performing a literature review.

This circumstance reinforced the belief that additional investigations on the factors that influence the SFH technique were advisable, also in the perspective of an increasingly aware use of the technique in its practical applications.
A laboratory investigation was therefore carried out with different specific objectives including i) testing water volume effects on K_s determination; ii) comparing K_s determinations for different porous materials; iii) establishing the impact of an increasing final infiltration rate on K_s calculations; iv) checking predictability of the depth of the wetting front at the end of the run; and v) developing alternative methods for estimating α^*.
This chapter is divided into four sections and an appendix. In particular, the theory of the SFH technique is presented in the 2.2 section. An overview of the use that has been made of the SFH technique up to now is provided in the 2.3 section. The research activity on the SFH technique developed during the PhD course is shortly introduced in the 2.4 section. This activity was summarized in the article: Concialdi P., Bagarello V., Alagna V., Iovino M. 2020. Laboratory evaluation of falling-head infiltration for saturated soil hydraulic conductivity determination. Journal of Agricultural Engineering, LI:1003, 27-35, doi: 10.4081/jae.2019.1003. This article is enclosed as the **Appendix A** to this chapter. Finally, some aspects that should be investigated in some detail in the future are briefly suggested in the 2.5 section.

Table 2.1 Summary of the research activity carried out during development of the Simplified Falling Head (SFH) technique (Bagarello et al., 2004, 2006)

	Field and laboratory investigation by Bagarello et al., 2004.	**Laboratory investigation by Bagarello et al., 2006.**
Soil	Laboratory: silty-clay-loam (undisturbed soil cores); sand and commercial kaolin powder (repacked soil columns) Field: loam	repacked sandy loam and loam columns
Experiment	Laboratory: comparison between the ECH and SFH techniques Field: comparison between the SFH and PI techniques	Comparison between the SFH and CHP technique Development of the Two-Level (TL) analysis procedure for the estimation of α^*
Results	Laboratory: similar estimates of K_s with the applied techniques Field: similar estimates of K_s with the applied techniques	Similar estimates of K_s with the applied techniques Plausible estimates of α^* with the TL procedure but high failure rates of the two-level calculations

CHP, Constant Head permeameter; ECH, Early-Time Constant-Head (ECH) technique; K_s, saturated soil hydraulic conductivity; PI, pressure infiltrometer

2.2. Theory

The SFH technique consists of applying quickly a small volume of water, V (L^3), on the soil surface confined by a ring inserted at a fixed distance, d (L), into the soil and in measuring the time, t_a (T),from the application of water to the instant at which the infiltration surface, having a cross-sectional area equal to A (L^2), is no longer covered by water (**Figure 2.1**).

Figure 2.1 Steps of the SFH run in the field: a) exposition of the infiltration surface; b) insertion of the cylinder into the soil; c) check of the contact between the sampled soil volume and the inner walls of the cylinder; d) pouring of the prescribed water volume; e) intermediate stage of the falling head infiltration process; f) infiltration surface at the end of the run (image by Angulo-Jaramillo et al., 2016)

The technique is based on the Green and Ampt (1911) approach to describe a falling head, one-dimensional infiltration process (Philip, 1992):

$$t = \frac{\Delta\theta}{K_{fs}(1-\Delta\theta)}\left[\frac{I(t)}{\Delta\theta} - \frac{H_0 - h_f}{1-\Delta\theta} ln\left(1 + \frac{(1-\Delta\theta)I(t)}{\Delta\theta(H_0 - h_f)}\right)\right] \quad (1)$$

where t (T) is the time, $\Delta\theta$ (L^3L^{-3}) is the difference between the field-saturated (θ_{fs}) and the initial (θ_i) volumetric soil water content, H_0 (L) is the height of the ponded head at t = 0, and h_f (L) is the soil water pressure head at the wetting front, with h_f negative. It may be born in mind that $I = H_0 - H$, where H (L) corresponds to the head of water into the ring. The h_f term can be replaced by the so-called α^* (L^{-1}) parameter by using the following relationship (Elrick et al., 2002):

$$h_f = -\frac{1}{\alpha^*} \quad (2)$$

Then, eq.(1) can be written in the following form:

$$t = \frac{\Delta\theta}{K_s(1-\Delta\theta)}\left[\frac{I(t)}{\Delta\theta} - \frac{H_0 + \frac{1}{\alpha^*}}{1-\Delta\theta}\ln\left(1 + \frac{(1-\Delta\theta)I(t)}{\Delta\theta\left(H_0 + \frac{1}{\alpha^*}\right)}\right)\right] \quad (3)$$

At $t = t_a$, $I(t_a) = H_0 = V/A = D$, D (L) being the depth of water corresponding to V. Therefore, K_s can be calculated as:

$$K_{fs} = \frac{\Delta\theta}{(1-\Delta\theta)t_a}\left[\frac{D}{\Delta\theta} - \frac{\left(D+\frac{1}{\alpha^*}\right)}{1-\Delta\theta}\ln\left(1+\frac{(1-\Delta\theta)D}{\Delta\theta\left(D+\frac{1}{\alpha^*}\right)}\right)\right] \quad (4)$$

Solving eq.(4) needs determining $\Delta\theta$ and estimating α^*. In particular, this last parameter can be estimated on the basis of the textural/structural soil characteristics, according to Elrick and Reynolds (1992) and Reynolds and Lewis (2012) (**Table 2.2**).
Taking into account that this method requires one-dimensional flow, the wetting front should not emerge from the bottom of the ring. Therefore, a volume of water, V (L^3), less than or equal to the volume of voids, V_p (L^3), within the bulk soil volume confined by the ring, V_c (L^3), has to be used:

$$V \leq V_p = V_c\ \Delta\theta = d\ A\ \Delta\theta \quad (5)$$

where d (L) is the depth of the wetting front at the end of the run.

Table 2.2 Texture-structure categories for selecting capillarity category and representative α^* parameter (Reynolds and Lewis, 2012; adapted from Elrick and Reynolds, 1992)

Texture-structure category	**Soil capillarity category**	**Representative α^* (m^{-1})**
Compacted, structureless, clayey or silty materials such as landfill caps and liners, lacustrine or marine sediments	Very strong	≤ 1
Porous materials that are both fine textured and massive; includes unstructured clayey and silty soils, as well as very fine to fine structureless sandy materials	Strong	4
Most structured and medium textured materials; includes structured clayey and loamy soils, as well as medium single-grain sands. This category is generally the most appropriate for agricultural soils	Moderate	12
Coarse and gravelly single-grain sands; may also include some highly structured soils with large and/or numerous cracks and biopores	Weak	36
Gravels, very coarse sands, etc. containing negligible amounts of coarse/medium/fine/very fine sand, silt and clay	Negligible	≥ 100

The soil capillarity categories assume that antecedent pore water pressure head is sufficiently negative to produce near-maximum soil capillarity for that category

2.3. Applications of the SFH technique

The SFH technique has been used in different countries, soils and environmental contexts. In addition, it has been applied under different land uses such as cropping systems, orchards, forests and pastures. The Elsevier's Scopus abstract and citation database of peer-reviewed literature (www.scopus.com) lists a total of 89 citations for the Bagarello et al. (2004) paper and 28 citations for the Bagarello et al. (2006) paper (access April 26, 2020).
A summary of the contexts in which the SFH technique was applied and some detail on the investigations that were carried out is reported in **Table 2.3**. For each mentioned paper, the first column of this table reports the reference. The second column explains the main objective of the investigation. Finally, the third column lists the main conclusions of that study. In a few cases, it was not possible to have access to the bibliographic source. These cases were listed in **Table 2.4**.

Table 2.3 Investigations making use of the SFH technique

Reference	Aim of SFH technique application	Conclusions
Bagarello and Sgroi, 2007	Studying temporal variability (2 years) of K_s determined with the SFH technique and comparison with the PI technique	K_s varied appreciably during the studied period. The lowest values were found in December and January. The SFH technique yielded similar results to the more laborious and time-consuming PI technique
Azam et al., 2008	Impact of cropping systems on soil structural properties	Residue management and tillage direction significantly affected root density and soil shrinkage behavior. In the subsoil, OM, ρ_b, and shrinkage behavior were not significantly influenced by any of the cropping systems studied
Azam et al., 2009	Assessing and developing soil hydraulic quality (SHQ) factor for optimum soil water regime	Factors affecting SHQ were pore-size distribution, shape and grade of water-stable aggregates, shrinking-swelling, infiltration rate, sand fraction of the Ap horizon. A comprehensive SHQ index was developed for both topsoil and subsoil layers under different cropping systems
Bagarello et al., 2010	Characterizing hydraulic properties of a clay soil at the plot scale	The SFH technique was able to measure a large range of K_s values. It appeared suitable to determine the saturated conductivity of soils with only matrix pores or also containing macropores
Agnese et al., 2011	Determination of physical quality indicators of several forest and pasture soils	Forest soils had a higher K_s than pasture soils. Conversion of pasture into forest was expected to reduce the risk of soil erosion. The forest soils had a better soil physical quality as compared with the pasture soils. The SFH technique was considered to be usable to detect land use effects
Bagarello et al., 2012	Sample size effect on K_s determined by the SFH technique. Comparison between SFH and PI techniques. Usability of the literature values of the α^* parameter	Larger ring yielded more reliable predictions of K_s. SFH and PI techniques were complementary methods with the SFH technique more appropriate to describe soil in the early phases of an infiltration process and the PI technique more appropriate at a later stage. Experimental values of α^* were close to the literature values
Keller et al., 2012	Establishing if K_s could be an indicator of yield variability among different crops	A model was developed to predict crop yield as a function of K_s
Bagarello et al., 2013	Intensively sampling a clay soil at the plot scale by the SFH technique	The K_s data were considered to be representative of a soil condition at the beginning of a rainfall event that produces runoff. The transformation of rainfall into runoff needs soil modification
Biddoccu et al., 2013	Effects of management practices on soil surface behavior in rainfall-runoff processes	In the brief period (season), tillage reduced runoff production. In the longer period, the soil surface developed a crusted layer with lower hydraulic conductivity
Rex et al., 2013	Development of a hydrologic hazard assessment procedure in forest environment	A set of hazard indicators was developed to decrease the likelihood of soil disturbance from harvesting. The most effective indicators were pine content and understory, soil texture, drainage density and a topographic index
Aiello et al., 2014	Applicability of BEST procedure in a citrus orchard and comparison with the SFH technique	K_s values obtained with the SFH technique were higher than those determined by BEST
Bagarello et al., 2014a	Applicability of the BEST procedure at the near point scale and comparison with the SFH technique	K_{sSFH} was higher than K_{sBEST}

Bagarello et al., 2014b	Effect of height of water application on soil hydraulic properties obtained by SFH and BEST techniques	The height of pouring did not influence the SFH results. With BEST, soil hydraulic properties were influenced significantly by the height of water application
Bagarello et al., 2014c	Test the applicability of BEST in an area of a few square meters	BEST experiments perturbed the soil more than the SFH experiments
Castellini et al., 2015	Impact of biochar addition on a clay soil	Results showed a non-significant impact of biochar incorporation (from 5 to 30 g kg^{-1} of soil) on K_s values
Leblanc et al., 2015	Hydraulic characterization of bauxite deposits	The combined datasets (remote sensing, hydrochemistry, and hydrodynamics) allowed studying the hydrology of Australians bauxite deposits. The investigation provided a first conceptual hydrogeological model of the spring system functioning on the hydrology of the bauxite oases
Alagna et al., 2016	Hydraulic characterization of a loam soil by different infiltration techniques	Among the applied techniques, the SFH technique, the mini disk infiltrometer and the tension infiltrometer were considered more appropriate to determine the soil hydraulic properties before wetting caused by rainfall events
Biddoccu et al., 2016	Management effects on runoff and soil erosion in sloping vineyards	Highest runoff and soil losses were measured in autumn. Grass cover was effective in reducing soil losses in summer. but not in autumn. Adoption of tillage for more than 8 years caused increasing runoff and soil erosion
Cherubin et al., 2016	Soil physical quality (SPQ) response to sugarcane expansion in Brazil	SPQ decreased from native vegetation to pasture (P) to sugarcane (S). Soil compaction limited soil aeration and water availability under P and S. Soil tillage in S had short-term positive effects on soil compaction. S soils were more susceptible to degradation by erosion process
Servadio et al., 2016	Adaptation of soil tillage to climate change	A significant linear relationship between grain yield and soil penetration resistance was detected
Bagarello et al., 2017	Influence of the shape of the infiltration source on K_s in a sandy loam soil	The SFH technique can be applied with different shapes of the infiltration surface (square, circular) since this shape did not influence determination of K_s
Baiamonte et al., 2017	Determining variability of K_s measured by the SFH technique in a small Sicilian basin	The SFH technique appeared suitable to characterize the soil before wetting. A detailed information on the spatial distribution of the soil textural characteristics throughout the basin should help to develop an appropriate sampling plan for K_s
Capello et al., 2017	Testing soil management effects considering soil moisture and precipitation characteristics	Tillage increased K_s as compared with permanent grass cover. During most of the events, runoff in the tilled plot was higher than in the grassed one
Chyba et al., 2014 and 2017	Influence of soil compaction on water infiltration rate	K_s measurements were higher in the non-compacted than the compacted soil. No differences were detected in soil compaction due to cattle hooves or tractor. The positive effects of controlled traffic farming were demonstrated
Khodaverdiloo et al., 2017	Effects of the ring diameter on the K_s values obtained with the SFH technique in four texturally similar soils with different levels of salinity and sodium	The ring diameter did not have in general a statistically detectable impact on the K_s values. A diameter effect on K_s was only detected for a non-saline, sodic soil, but this effect was moderate
Kovář et al., 2017	Comparison of tillage system effects on water infiltration in a loamy sand soil	The lowest K_s values were obtained under oats by reduced tillage. Conventional tillage was most threatened by excessive runoff. The investigation confirmed the risk of erosion without the use of proper soil conservation techniques

Šařec and Novák, 2017	Effects of manure and OM activators on soil physical properties	High K_s values were detected in all variants of organic management. The study was unable to demonstrate in the short term clear beneficial effects of manure and activators on soil properties
Erban et al., 2018	Impact of herbicide glyphosate on compost-amended soils	The persistence of both glyphosate and its metabolite (AMPA) decreased with soil depth. Compost dose alone did not cause significant differences among samples. Behavioral differences between glyphosate and AMPA were related to K_s and soil moisture
Preti et al., 2018	Modeling of water flow pathways in agricultural terraced landscapes	A multidisciplinary approach allowed establishing that infiltrated water accumulated behind dry-stone walls, increasing pore water pressure and inducing wall bulging and instability. Findings provided field evidences of water circulation and led to the definition of hydrological functioning of farming terraced systems
Scarabeli et al., 2018	Measuring K_s through two distinct techniques	A good agreement was found between the applied techniques, with measured values close to each other. SFH was the better since it had a variation coefficient 1.4 times lower than the standard technique
Bagarello et al., 2019	Comparison between SFH and BEST methods in the Maganoce basin to study the factors that produce variability on infiltration in clay soils	The two techniques yielded similar K_s values. Organic matter content and topography could be used as factors to be considered for choosing points to be sampled
Capello et al., 2019	Effects of soil management and tractor traffic on the spatial and temporal variability of soil compaction and both hydrological and erosional processes	After just one tractor passage on wet soil after tillage, K_s decreased from more than 1000 to near 1 mm h^{-1}. The soil management with permanent grass cover provided higher K_s and soil water recharge, reducing runoff and soil losses
Chai et al., 2019	Effects of trampling by Yak and Tibetan sheep. Response mechanisms of soil to these effects	The soil bulk density increased with heavy trampling and K_s decreased. Heavy grazing is dangerous for soil. Possible solution could be reducing the yak and increasing the sheep grazing or give a spring break to meadow
Cislaghi et al., 2019	Comparing different grazing intensities to identify sustainable pasture management	Maintaining moderate grazing favors a high level of biodiversity, an excellent availability of nutrients, and constant action to guard against surface soil erosion and the instability of shallow soil layers
Novak et al., 2019	Effect of activators of organic matter on soil properties	Beneficial effects of the activators were recognized. Consequently, ρ_b decreased, porosity increased, and K_s also increased
Ramazanpour Esfahani et al., 2020	Effects of short and long-term irrigation with wastewater on the physical, chemical and hydraulic properties in sand and limestone-packed columns	Reduction of K_s in sand columns. K_s of limestone columns decreased in the first two weeks of the experiment and then it slightly increased until the end of the experiment due to calcite dissolution by microbial activities
Etana et al., 2020	Studying the impact of controlled traffic farming with respect to soil physical properties and crop yield for Swedish conditions	In general, the ρ_b values measured in the crop zone were low. K_s was greater in the crop zone than in the trafficked zone

BEST, Beerkan Estimation of Soil Transfer parameters procedure; D, ring diameter; K_s, saturated soil hydraulic conductivity; K_{sBEST}, saturated soil hydraulic conductivity determined with the BEST procedure; K_{sSFH}, saturated soil hydraulic conductivity determined with the SFH technique; OM, organic matter; PI, pressure infiltrometer; R^2, coefficient of determination; SFH, simplified falling-head; ρ_b, dry soil bulk density

Table 2.4 Non-accessible sources making reference to the SFH technique

Category	Authors	Title
Book or Book Chapter	Erickson et al., 2013	Optimizing stormwater treatment practices: A handbook of assessment and maintenance
	Verhoef and Egea, 2013	Soil water and its management
Conference Paper	Chyba, et al., 2013	Impact of land crossing on soil physical properties
	Hanamura et al., 2007	Handy permeability test method with a single-unit apparatus developed at the solid waste landfill construction site
	Chen et al., 2010	Measurement of soil hydraulic conductivity in relation with vegetation
Article	Iwanek, 2008	A method for measuring saturated hydraulic conductivity in anisotropic soils
	Liu et al., 2010	Applicability of explicit functions on cumulative infiltration of Green-Ampt model under different conditions
	Chen and Hsu, 2012a	Study of using multi-step falling-head infiltration to estimate hydraulic conductivity at various depths

2.4. A novel investigation on the SFH technique

An objective of the research activity during the PhD course was to improve our knowledge of the factors that can influence application of the Simplified Falling Head (SFH) technique for saturated soil hydraulic conductivity, K_s, determination and, more in general, of falling head one dimensional infiltration methodologies. Therefore, a laboratory experiment was carried out with three different kinds of porous materials, using in several cases experimental approaches and methodologies that were already tested by Bagarello et al., 2006.

The general objective of the investigation that was carried out was to check falling head one-dimensional infiltration procedures for saturated soil hydraulic conductivity, K_s, determination. The specific objectives were to: i) test water volume effects on K_s determination for three homogeneous soils; ii) compare the K_s values for these three media; iii) establish the impact of an increasing final infiltration rate on K_s calculations; iv) test an experimentally simplified procedure to estimate the α^* parameter; and v) establish the reliability of a theoretical prediction of the depth of the wetting front at the end of the SFH run. In short, it was found that the method used to determine D should not affect very much K_s determination but larger D values can yield smaller K_s values in fine-textured soils. Air escapes from the sampled soil volume when almost all water had infiltrated but this circumstance does not have a great impact on calculation of K_s. A falling-head one-dimensional ponded infiltration process is not recommended to estimate α^*. The theoretical depth of the wetting front can approximately be predicted before the run. Finally, the SFH technique appears a rather robust method to simply and rapidly determine K_s.

The research activity was summarized in the paper Concialdi P., Bagarello V., Alagna V., Iovino M. 2020. Laboratory evaluation of falling-head infiltration for saturated soil hydraulic conductivity determination. Journal of Agricultural Engineering, LI:1003, 27-35, doi: 10.4081/jae.2019.1003. This paper is reported in the **Appendix A** to the Chapter 2.

2.5. Perspectives of future research

In light of the experience gained during this doctoral course, some research questions needing investigation in the future can be suggested. They include i) estimation of the capillarity parameter by a ponded, falling head infiltration experiment; ii) effect of the packing procedure on saturated hydraulic conductivity of repacked soil samples measured with the SFH technique; iii) effect of the reuse of the same soil material on saturated hydraulic conductivity of repacked soil samples measured with the SFH technique; and iv) testing of the multistep falling head infiltration method. A short description of these research questions is reported below.

1)Estimation of the capillarity parameter by a ponded, falling head infiltration experiment - It seems that the one-dimensional falling head ponded infiltration process does not work very well for estimating α^*. The investigation made in this thesis (Concialdi et al., 2020) supported this conclusion that, however, does not seem general since, according to Zeleke and Si (2005), a falling head infiltration experiment could instead be appropriate to also estimate α^*, at least under certain circumstances. This last suggestion justifies further considering and testing other alternative methods to obtain the capillarity parameter as compared with those tested until now.

The infiltration rate, i_r (L/T), can be expressed, using the Green and Ampt (1911) model, by the following relationship (Philip, 1992):

$$ir = \left(\theta_1 - \theta_0\right)\frac{dz}{dt} = K_s\left[1 - \left(\theta_1 - \theta_0\right) + \frac{C + D}{z}\right] \tag{6}$$

in which, using the original symbolism, θ_0 (L^3/L^3) is the initial uniform volumetric moisture content, θ_1 (L^3/L^3) is the mean moisture content of the wetted region, z (L) is the wetting front depth below the pond floor (soil surface), t (T) is the time, K_s (L/T) is the mean conductivity of the wetted region, C (L) is the constant wetting front moisture potential, and D (L) is the water depth in the pond at t = 0. Eq.(6) can be written as (Chen and Hsu, 2012b):

$$ir = K_s\left[1 - \left(\theta_1 - \theta_0\right)\right] + \frac{K_s\left(C + D\right)}{z} = A_1 + \frac{B_1}{z} \tag{7}$$

in which:

$$A_1 = K_s\left[1 - \left(\theta_1 - \theta_0\right)\right] \tag{8a}$$

$$B_1 = K_s\left(C + D\right) \tag{8b}$$

According to Chen and Hsu (2012b), A_1 and B_1 can be estimated by linear regression of i_r vs. $1/z$. Consequently, K_s, C and, hence α^* (Zeleke and Si, 2005), can be deduced as:

$$K_s = \frac{A_1}{1 - \left(\theta_1 - \theta_0\right)} \tag{9a}$$

$$C = \frac{B_1}{K_s} - D \tag{9b}$$

$$\alpha^* = \frac{1}{C} \quad . \tag{9c}$$

Therefore, i_r and z have to be determined repeatedly during the falling head infiltration run to simultaneously determine K_s and α^*. Using infiltration rates and depth of the wetting front for characterizing the soil could be a topic to be developed, at least initially in nearly ideal conditions, that is on homogeneous soil samples in the laboratory.

2)Effect of the packing procedure on saturated hydraulic conductivity of repacked soil samples measured with the SFH technique - Working in the laboratory on repacked, homogeneous soil samples needs choosing an individual sample size (height, diameter) and then applying a soil packing procedure. The few references reported in **Table 2.5** demonstrate that packing procedures are not always reported and also that they are not consistent between investigations.

Table 2.5. Steps of the soil sample preparation for some laboratory investigations

Reference	Main features of the soil sample	Packing procedure
Moutier et al., 1998	120 g of soil packed in a cylinder, 5.4 cm diameter	Not described
Bagarello et al., 2004	5.0 cm diameter × 4.0 or 5.0 high	Step-by-step procedure. At each step, pouring of 1 cm of soil followed by manual compaction
Bagarello et al., 2006 and Concialdi et al., 2020	9.4 cm diameter × 32 cm or more high	Column filled with 40 cm of soil. Manual compaction by dropping the column repeatedly from a height of 5 cm until compaction ceased
Moody et al., 2009	5.1 cm diameter × 20 cm high and 10 cm diameter × 12 cm high	Soil introduced in 5-10 increments
Assouline and Narkis, 2011	5.5 cm diameter × 9 cm high	Not described
Armenise et al., 2018	Soil packed to a bulk density of 1.2 g/cm^3 in PVC columns, 4.6 cm diameter × 5.0 cm high	Not described
Di Prima et al., 2018	Boxes of 13.7 × 9.7 cm^2 (base) × 15.0 cm (height)	Not described
Ghosh and Pekkat, 2019	Cylindrical, 20 cm diameter × 30 cm high	Packed in three layers by imparting an equal number of blows on each layer, depending on the desired state of compaction

There is a limited literature investigating specifically the effect of the sample preparation procedure on the determined soil physical properties. However, these investigations agree in suggesting that the measured soil properties depend appreciably on the applied soil sample preparation procedure (Oliveira et al., 1996; Lewis and Sjöstrom, 2010). With specific reference to K_s, Teng et al. (2019) recently concluded that the difference caused by different sample preparation procedures can be as large as one order of magnitude. Therefore, attempting to standardize procedures for testing K_s methods in the laboratory needs further investigating the effect of the sample preparation procedure on determination of K_s.

A methodology to develop this issue has been planned and will be applied in the near future by the research team of the University of Palermo (Italy). In particular, four different packing procedures will be applied to prepare a soil sample for the SFH experiment using Plexiglas cylinders of 9.4 cm in diameter and 15 cm in height. Initially, the amount of air-dried soil needed to completely fill the cylinder without any compaction will be determined. The following packing procedures will then be applied by using this amount of air-dried soil for each soil sample: i) the cylinder is filled up to the upper rim by simply pouring soil. The soil is then compacted manually by dropping the cylinder repeatedly from a height of approximately 5 cm; ii) the soil mass is subdivided into three equal parts.

One third of the soil mass is poured in the cylinder and the soil is compacted manually by dropping the cylinder repeatedly from a height of approximately 5 cm. The second part is then poured and the same compaction procedure is applied again. Finally, the last part of soil is poured into the cylinder and compacted; iii) the soil mass is subdivided into three equal parts. One third of the soil mass is poured in the cylinder and the soil is compacted manually by a wood pestle. The second part is then poured and the same compaction procedure is applied again. Finally, the last part of soil is poured and compacted; iv) this procedure is similar to the third procedure. The difference is that soil packing is carried out in six subsequent steps.

For a given set of four samples, that is one for each applied packing procedure, the gravimetric water content, w_i (g/g), of the air-dried soil used for the experiment will be determined on small soil samples and this water content will be considered representative of the four samples. Consequently, the dry soil bulk density, ρ_b (g/cm^3), of each prepared soil sample will be determined as:

$$\rho_b = \frac{m_s}{V_t} = \frac{1}{V_t}\left(m_{ad} - \frac{w_i \times m_{ad}}{1+w_i}\right) = \frac{m_{ad}}{V_t(1+w_i)} \tag{10}$$

where m_s (g) is the mass of the dry soil, V_t (cm^3) is the bulk volume of the soil sample and m_{ad} (g) is the mass of the air-dried soil.

The four soil samples are required to have the same, or a very similar, dry bulk density. To reach this objective, a trials and errors approach will be followed. In particular, a sample is prepared with each procedure, by using the same amount of soil for each sample, and the procedure yielding the lowest ρ_b value is identified. Then, the other three procedures are applied again by adapting compaction levels to reproduce the same ρ_b value. Each soil sample will be prepared with a soil mass that was never used before. The SFH technique will finally be applied to determine the saturated conductivity of each soil sample.

3)Effect of the reuse of the same soil material on saturated hydraulic conductivity of repacked soil samples measured with the SFH technique - Performing laboratory experiments on homogeneous soil samples does not make replication of the experiment useless since reproducibility of any experiment has to be demonstrated. The need to replicate the experiment and that to test the effect of different factors on determination of K_s implies that large amounts of sieved soil should be available in general for the laboratory investigations. A way to save time is to reuse previously used soil in subsequent experiments (Concialdi et al., 2020; Moody et al., 2009). However, other authors made a different choice, that is using for each experiment a soil mass that was never used before (Ghosh and Pekkat, 2019). If K_s is measured with the SFH technique, the history of the soil used in the laboratory should be no more than a minor factor influencing the experiments since each infiltration run makes use of small water volumes, which implies that wetting-induced soil alteration should be small and probably negligible. Moreover, the lower part of the soil sample is never wetted since the experiment is designed in such a way to impede the wetting front to reach the bottom of the soil column, due to the need to establish a one-dimensional infiltration process. However, an experimental evidence of the soundness of this expectation is lacking. Therefore, a point to be developed in the laboratory in the future could be to establish comparisons between never used before and re-used soil masses for performing the measurement of K_s with the SFH technique.

4)Testing of the multistep falling head infiltration method - According to Chen and Hsu (2012b), a multistep falling head infiltration method (MSFIT) can be applied to determine K_s at various depths. The method is based on an extension of the Philip's falling head theory to multiple steps. In other words, the starting point of the methodology by Chen and Hsu (2012b) is the same as that of the SFH technique by Bagarello et al. (2004). Chen and Hsu (2012b) suggested that the MSFIT method can be applied both in the laboratory and in the field but this method has not yet received much attention from the scientific community nor any testing. In principle, using a simple method for determining the vertical profile of K_s at a sampling location is practically attractive. Therefore, it could be advisable to examine in detail the theory of the MSFIT method and then to test this method, initially

in highly controlled conditions. The MSFIT method could be considered a step forward compared with the SFH technique, usable when the homogeneity hypothesis, which is at the basis of the SFH technique, is invalid. In any case, the former method requires more experimental information than the latter one, since water has to be repeatedly applied on the soil surface and the drop in water level has to be monitored for each water volume.

Appendix A:

pagepress

Journal of Agricultural Engineering 2020; volume LI:1003

Laboratory evaluation of falling-head infiltration for saturated soil hydraulic conductivity determination

Paola Concialdi,[1] Vincenzo Bagarello,[1] Vincenzo Alagna,[2] Massimo Iovino[1]

[1]Dipartimento di Scienze Agrarie, Alimentari e Forestali, Università di Palermo; [2]Dipartimento di Scienze e Tecnologie Agro-Alimentari, Alma Mater Studiorum Università di Bologna, Italy

Abstract

Falling-head one-dimensional infiltration procedures, such as the simplified falling-head (SFH) technique, yield estimates of saturated soil hydraulic conductivity, K_s, with parsimonious and rapid experiments. Factors that can influence determination of K_s by the SFH technique were tested in the laboratory on three repacked soils differing by particle diameter ranges (0-2000, 0-105 and 105-2000 μm, respectively). Using the theoretically calculated depth of ponding on the infiltration surface, D, instead of the measured one had a small impact on the K_s calculations (means differing by a factor of 1.1-1.2, depending on the soil). For the finest soil, K_s decreased by 3.1 times as D increased from 40 to 135 mm but D did not affect K_s for the coarsest soil, yielding in general the highest K_s values. The abrupt increase of the infiltration rate close to the end of the run did not influence appreciably K_s calculations since it determined an increase in K_s by a mean factor never exceeding 1.1. The most frequent result of the developed procedure for estimating the α* parameter was failure of the experiment although the valid α* calculations were plausible, being higher for the coarse textured soil (17 m^{-1}) than the finer soils (9.2-9.3 m^{-1}). The depth of the wetting front at the end of the run was 1.1-1.2 times deeper than that calculated theoretically before the run, depending on the soil. In conclusion, the method used to determine D should not affect very much K_s determination but larger D values can yield smaller K_s values in fine-textured soils. Air escapes from the sampled soil volume when almost all water had infiltrated but this circumstance does not have a great impact on calculation of K_s. A falling-head one-dimensional ponded infiltration process is not recommended to estimate α*. The theoretical depth of the wetting front can approximately be predicted before the run. The SFH technique appears a rather robust method to simply and rapidly determine K_s.

Correspondence: Vincenzo Bagarello, Dipartimento di Scienze Agrarie, Alimentari e Forestali, Università di Palermo, Viale delle Scienze, Edificio 4, 90128 Palermo, Italia.
E-mail: vincenzo.bagarello@unipa.it

Key words: Laboratory investigation; saturated soil hydraulic conductivity; falling-head one-dimensional infiltration; simplified falling-head technique.

Received for publication: 26 July 2019.
Accepted for publication: 25 September 2019.

©Copyright: the Author(s), 2019
Licensee PAGEPress, Italy
Journal of Agricultural Engineering 2020; LI:1003
doi:10.4081/jae.2019.1003

This article is distributed under the terms of the Creative Commons Attribution Noncommercial License (by-nc 4.0) which permits any noncommercial use, distribution, and reproduction in any medium, provided the original author(s) and source are credited.

Introduction

The saturated soil hydraulic conductivity, K_s, can be determined by a falling-head one-dimensional infiltration process (Philip, 1992). The simplified falling-head (SFH) technique (Bagarello *et al.*, 2004; Angulo-Jaramillo *et al.*, 2016) consists of applying a small volume of water on the surface of a confined soil volume and then measuring the time, t_a, from the application of water to the moment at which the surface area is no longer covered by water. The experiment can be carried out both in the field and on laboratory soil columns. Calculation of K_s requires an independent estimation of the so-called α* parameter on the basis of the soil textural and structural characteristics (Elrick and Reynolds, 1992). If the drop of the water level is monitored in some detail during the transient infiltration run, an estimate of α* can also be obtained by the two-level (TL) analysis (Bagarello *et al.*, 2006). An interest of the scientific community for the SFH determination of K_s is documented (Keller *et al.*, 2012; Biddoccu *et al.*, 2016, 2017; Kovář *et al.*, 2017; Preti *et al.*, 2018).

Methods for measuring K_s should be evaluated carefully to ensure that they provide practicable results. Working in the laboratory on repacked soil samples is a necessary, non-exclusive, step of a method's evaluation because the available analytical solutions were developed for an idealized soil and using homogeneous porous media is expected to make interpretation of the data easier. Several topics deserving testing and developments can be identified with reference to the SFH technique and, more in general, falling-head one-dimensional infiltration methodologies.

In the field, the used water volume, V, must assure one-dimensional infiltration and therefore it depends, for a given soil surface area, A, on the ring insertion depth and the available pore space in the confined soil volume. In theory, the initial depth of ponding, $D = V/A$, is established instantaneously on the soil surface and infiltration starts under a ponded depth of water of D. In practice, pouring water needs a few seconds during which infiltration occurs with smaller ponded depths of water. Bagarello *et al.* (2004) suggested that using $D = V/A$ was a generally reasonable assumption to calculate K_s but alternative ways to obtain D should be tested.

Water volume effects on the K_s values obtained with the SFH technique have to be determined because, for given experimental conditions, more water implies deeper sampling depths, more

Non-commercial use only

opportunities for disturbance of the exposed soil surface during water application and higher hydrostatic pressures at the beginning of the run that could have some soil compaction effect.

In their laboratory test of the one-dimensional falling-head infiltration procedure, Bagarello *et al.* (2006) detected a rather frequent increase of the infiltration rates during the last part of the process, *i.e.* for ponded heads close to zero, and they suggested that this phenomenon, also signaled by Wang *et al.* (1998), was a consequence of the removal of entrapped air bubbles close to the end of the process. The SFH technique is used on initially unsaturated soils. Therefore, establishing if this phenomenon is frequent and determining its impact on K_s determination is important, taking into account that, with the SFH technique, only t_a is measured. In other words, the technique is not suited to signal any change in infiltration rates during the run.

The TL analysis is computationally and experimentally complicate because cumulative infiltration has to be determined at many times during the falling-head run (Bagarello *et al.*, 2006). This circumstance implies that a TL-type experiment has a limited applicability in the field. An alternative way having some practical interest for field estimation of α* could be to develop a methodology requiring a very limited information on the falling-head infiltration process. An approach of this kind, making use of only two measurements of the infiltration time during the run, was developed by Philip (1993) for the Philip-Dunne permeameter.

Finally, the depth of the wetting front at the end of the SFH experiment has to be predicted before the run to be confident that infiltration will be one-dimensional during the run. An analysis of true depths of wetting front appears advisable since a difference between predicted and actual depths of the wetting front could imply a violation of theory during the method's application. In particular, infiltration becomes three-dimensional if the wetting front crosses the bottom of the confined soil volume.

The general objective of this investigation was to check in the laboratory falling-head one-dimensional infiltration procedures for saturated soil hydraulic conductivity, K_s, determination. The specific objectives were to: i) test water volume effects on K_s determination for three homogeneous soils; ii) compare the K_s values for these three media; iii) establish the impact of an increasing final infiltration rate on K_s calculations; iv) test an experimentally simplified procedure to estimate the α* parameter; and v) establish the reliability of a theoretical prediction of the depth of the wetting front at the end of the SFH run.

Theory

According to Philip (1958), the Green and Ampt (1911) or delta function (Philip, 1969) model is useful for one-dimensional ponded infiltration. Under falling-head conditions, cumulative infiltration, I (L), can be described by the following equation that includes gravity:

$$t = \frac{\Delta\theta}{K_s(1-\Delta\theta)}\left[\frac{I(t)}{\Delta\theta} - \frac{D-\psi_f}{1-\Delta\theta}\ln\left(1+\frac{(1-\Delta\theta)I(t)}{\Delta\theta(D-\psi_f)}\right)\right] \quad (1)$$

where t (T) is the time, $\Delta\theta$ (L^3L^{-3}) is the difference between the saturated (θ_s) and the initial (θ_i) volumetric soil water content, K_s ($L\,T^{-1}$) is the saturated soil hydraulic conductivity (mean conductivity of the wetted region, taken as constant), D (L) is the height of the ponded head at $t = 0$, and ψ_f (L) is the soil water pressure head at the wetting front, with ψ_f negative. The ψ_f term can be replaced by the so-called α* (L^{-1}) parameter using the following relationship, derived by assuming an exponential hydraulic conductivity - pressure head relationship (Gardner, 1958) and representing ψ_f according to Philip (1969) (Reynolds and Elrick, 1990; Elrick *et al.*, 2002):

$$\alpha^* \cong -\frac{1}{\psi_f} \quad (2)$$

Eq.(1) can then be written in the following form:

$$t = \frac{\Delta\theta}{K_s(1-\Delta\theta)}\left[\frac{I(t)}{\Delta\theta} - \frac{D+\frac{1}{\alpha^*}}{1-\Delta\theta}\ln\left(1+\frac{(1-\Delta\theta)I(t)}{\Delta\theta\left(D+\frac{1}{\alpha^*}\right)}\right)\right] \quad (3)$$

The depth of the wetting front, d (L), at a given moment during the falling-head experiment can be estimated as (Bagarello *et al.*, 2004):

$$d = \frac{V(t)}{A\Delta\theta} = \frac{I(t)}{\Delta\theta} \quad (4)$$

where $V(t)$ (L^3) is the infiltrated water volume from $t = 0$ up to the considered moment and A (L^2) is the area of the infiltration surface. Bagarello *et al.* (2004) used Eq.(3) to propose a SFH technique for determining K_s. By this technique, a small water volume, V (L^3), is quickly poured on the surface of a confined soil volume and total duration of infiltration, t_a (T), is measured. At $t = t_a$, $I(t_a) = D = V/A$ (L). Then, Eq.(3) solved for K_s becomes:

$$K_s = \frac{\Delta\theta}{t_a(1-\Delta\theta)}\left[\frac{D}{\Delta\theta} - \frac{\left(D+\frac{1}{\alpha^*}\right)}{1-\Delta\theta}\ln\left(1+\frac{(1-\Delta\theta)D}{\Delta\theta\left(D+\frac{1}{\alpha^*}\right)}\right)\right] \quad (5)$$

The need to assure one-dimensional flow during the run implies that, in the field, the d value obtained by Eq.(4) for $t = t_a$ has to be smaller than or equal to the ring insertion depth.

Eq.(3) can be used to predict the infiltration time of any water volume during the falling-head process. In particular, it can be applied to determine $t = t_{0.5}$ that is the infiltration time of the first half of the applied water volume, *i.e.* $I(t_{0.5}) = D/2$. The ratio between t_a and $t_{0.5}$ is then equal to:

$$\frac{t_a}{t_{0.5}} = \frac{\frac{D}{\Delta\theta} - \frac{D+\frac{1}{\alpha^*}}{1-\Delta\theta}\ln\left[1+\frac{(1-\Delta\theta)D}{\Delta\theta\left(D+\frac{1}{\alpha^*}\right)}\right]}{\frac{D}{2\Delta\theta} - \frac{D+\frac{1}{\alpha^*}}{1-\Delta\theta}\ln\left[1+\frac{(1-\Delta\theta)D}{2\Delta\theta\left(D+\frac{1}{\alpha^*}\right)}\right]} \quad (6)$$

Determining $t_{0.5}$ in addition to t_a should be rather easy during a falling-head infiltration experiment, even in the field, and it potentially yields an estimate of α* which is the only unknown parameter of Eq.(6).

Non-commercial use only

OPEN ACCESS

Materials and methods

Laboratory experiment

A loam soil (USDA classification, Gee and Bauder, 1986) with a maximum particle diameter of 2000 μm was used for this investigation. This soil was passed through a 105 μm sieve to obtain three different soils to be tested (Table 1): i) 0-2000 soil (diameter of the soil particles, d_p, varying from 0 to 2000 μm); ii) 0-105 soil ($0 < d_p \leq 105$ μm); and iii) 105-2000 soil ($105 < d_p \leq 2000$ μm).

A total of 48 packed soil columns were prepared in graduated Plexiglas tubes (internal diameter = 0.094 m; height = 0.5 m; Figure 1) for each soil type given that the analysis assumes a homogeneous soil (Bagarello *et al.*, 2006). A nylon guard cloth and a wire net were connected to the base of the tube to support the weight of the soil. According to many other laboratory investigations (*e.g.* Assouline and Narkis, 2011; Moutier *et al.*, 1988; Di Prima *et al.*, 2018), air-dried soil was used to fill the tube to a height of approximately 0.4 m. The soil was then compacted manually by dropping the tube repeatedly from a height of approximately 0.05 m until compaction ceased. The number of drops varied between 18 and 170, depending on the soil sample, and the final height of the soil columns was in the ranges 0.33-0.35, 0.28-0.35 and 0.33-0.36 m (sample volumes of 0.0023-0.0024, 0.0019-0.0024 and 0.0023-0.0025 m^3) for the 0-2000, 0-105 and 105-2000 soils, respectively. For each tube, the weight of the air-dried soil used to fill the tube and the final volume of the soil sample were noted. The gravimetric water content of the air-dried soil was determined on a small soil sample and this water content was assumed to be representative of the whole sample. The dry soil bulk density, ρ_b, and the volumetric soil water content, θ_i, were then calculated and the volumetric saturated soil water content, θ_s, was set equal to total porosity obtained from ρ_b (Table 1).

A wire mesh was placed on the soil surface and a falling-head infiltration experiment was carried out on each soil column by pouring almost instantly a pre-established water volume, V, on the infiltration surface. In particular, the 48 columns filled with a given soil were randomly subdivided into four groups, each constituted by 12 soil columns, and a fixed water volume (V = 280, 624, 833 and 940 cm^3) was used for each group of soil columns. This choice was made to test effects of the initially established ponded depth of water on K_s determination for a presumably homogeneous porous medium. The largest water volume avoided emergence of the wetting front from the bottom of the tube since, according to Eq.(4), d

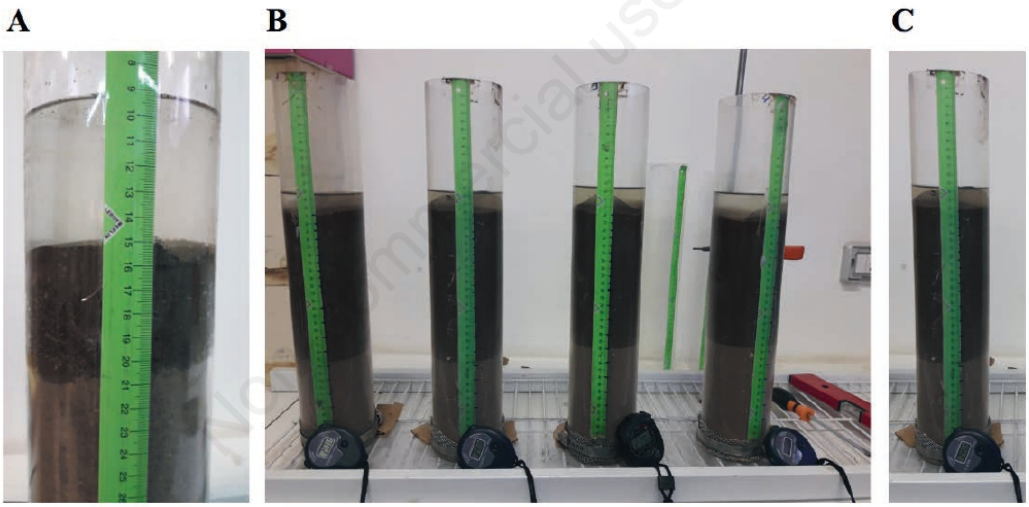

Figure 1. Soil columns during the experiment: A) early-stage; B) close to the end of the experiment; and C) appearance of an air bubble in the final stage of the experiment.

Table 1. Basic statistics of the clay (*cl*), silt (*si*) and sand (*sa*) percentages (sample size, N = 4 for each soil), and dry soil bulk density (ρ_b), volumetric soil water content at the beginning of the transient infiltration experiment (θ_i) and saturated soil volumetric water content (θ_s) for the soil columns used in the investigation (N = 48 for each soil).

Statistic	0-2000 soil						0-105 soil						105-2000 soil					
	cl (%)	si (%)	sa (%)	ρ_b (g cm^{-3})	θ_i (m^3m^{-3})	θ_s (m^3m^{-3})	cl (%)	si (%)	sa (%)	ρ_b (g cm^{-3})	θ_i (m^3m^{-3})	θ_s (m^3m^{-3})	cl (%)	si (%)	sa (%)	ρ_b (g cm^{-3})	θ_i (m^3m^{-3})	θ_s (m^3m^{-3})
Min	16.2	35.2	47.0	1.197	0.033	0.498	17.9	57.2	20.8	1.132	0.042	0.474	14.4	32.1	51.3	1.175	0.026	0.479
Max	17.2	36.4	48.6	1.330	0.068	0.548	21.5	58.3	24.9	1.394	0.144	0.573	16.1	34.2	52.5	1.381	0.075	0.557
Mean	16.7	35.7	47.6	1.254	0.049	0.527	19.7	57.6	22.7	1.199	0.061	0.547	15.4	32.7	51.9	1.281	0.045	0.517
CV (%)	2.5	1.4	1.5	2.7	22.1	2.4	8.0	1.0	7.5	5.3	46.8	4.4	5.2	3.1	1.0	4.2	32.1	3.9

Min, minimum value; Max, maximum value; Mean, arithmetic mean; CV, coefficient of variation.

Non-commercial use only

was not expected to exceed 0.29 (0-2000 soil), 0.28 (0-105 soil) and 0.32 (105-2000 soil) m. The drop of the water level during the transient infiltration experiment was monitored visually through the walls of the Plexiglas tube by noting the time corresponding to every subsequent 5 mm drop. The time, t_a (original SFH experiment), and the actual depth of the wetting front at the end of the run, d_m, were also visually measured (Figure 1). Vertical soil expansion, v_e, at the end of infiltration was recorded when it occurred. Initially dry soil was used for the experiments in accordance with Bagarello *et al.* (2004, 2006).

Dataset development

A dataset was developed for each soil. For each soil column, the dataset comprised ρ_b, θ_i, θ_s, v_e, the measured, D_m, and the theoretical, $D_t = V/A$, ponded depth of water established on the infiltration surface at the beginning of the run, the measured, d_m, and the theoretical, $d_t = I/\Delta\theta$, wetting front depth at the end of the run, t_a and $t_{0.5}$. In particular, D_m was obtained by the difference between the first reading of the water level above a datum (bottom of the soil column) and the height of the soil surface above the same datum when all water had infiltrated. An alternative way to calculate D_m could be considering the height of the soil surface immediately before the run. The D_m values do not change if vertical expansion does not occur during the run. Otherwise, considering this position introduces an inconsistency in the D calculations. In particular, at $t = t_a$, there is no more water on the soil surface but the calculations would indicate that a layer of water, having a height of v_e, is still present on this surface.

Eq.(5) with $\alpha^* = 12$ m^{-1}, that is the first approximation value for this parameter (Elrick and Reynolds, 1992; Reynolds and Lewis, 2012), was used to estimate K_s by the SFH technique (Bagarello *et al.*, 2004). Both D_m and D_t were used in the calculations, and the corresponding K_s values where denoted by $K_{s,m}$ and $K_{s,t}$, respectively.

In many cases, plotting the data on a cumulative infiltration, I, *vs* time, t, graph suggested an increase of the infiltration rate, i, during the last part of the infiltration process, *i.e.*, for ponded heads close to zero. Therefore, two i estimates at, i_e, and near, i_{ne}, the end of the run were obtained for each soil column by linear regression of selected (I, t) data pairs (Figure 2). In particular, i_e was obtained by considering the last two or three data points (only occasionally a few more), depending on the visually detected signs about the final increase of i. The estimate of i_{ne} was obtained by considering the two or three (I, t) data points immediately preceding those signaling the infiltration rate increase. Eq.(3) with $\alpha^* = 12$ m^{-1} was solved for K_s and it was applied to obtain an estimate of K_s, denoted by the symbol $K_{s,ne}$, for an infiltration process starting at $t = 0$ and going on till collecting the last of the (I, t) data points that did not signal any i increase.

Eq.(6) was used in an attempt to obtain an estimate of α^* for each soil column. At this aim, the theoretical $t_a/t_{0.5}$ ratio was calculated for different α^* values, ranging from 1 to 100 m^{-1} with steps of 1 m^{-1}. The α^* value yielding the best agreement between the theoretical and the experimentally determined $t_a/t_{0.5}$ ratio was assumed to be the specific α^* parameter for the soil column. Estimation of α^* was considered to be unsuccessful when the best agreement for $t_a/t_{0.5}$ was detected with reference to one of the two extremes of α^*. A smaller range of α^* values was considered in this investigation as compared with Bagarello *et al.* (2006) ($0.1 \leq \alpha^* \leq 1000$ m^{-1} in that case) since α^* for the considered soils should not be smaller than 1 m^{-1} and larger than 100 m^{-1} (Elrick and Reynolds, 1992; Reynolds and Lewis, 2012) and the investigation by Bagarello *et al.* (2006) was consistent with this expectancy.

Data analysis

A comparison was initially carried out between the measured, D_m, and the theoretical, D_t, ponded depths of water at the beginning of the SFH run. Then, the impact of D on K_s calculation by Eq.(5) was determined by comparing $K_{s,m}$ and $K_{s,t}$. The difference between the two estimates of K_s for a given run was considered to be negligible when their ratio fell in the 0.75 to 1.25 range (Reynolds, 2013) but it was also taken into account that differences by a factor of two or three could be considered small for some practical purposes (Elrick and Reynolds, 1992).

The effect of the used water volume for the run on K_s determination was then checked for each soil. In particular, a regression analysis between K_s ($K_{s,m}$, $K_{s,t}$) and D (D_m and D_t, respectively) was carried out. Linear, logarithmic, power and exponential relationships were considered and the relationship with the highest coefficient of determination, R^2, was retained for the analysis. The Tukey honestly significant difference (THSD) test at P=0.05 was also applied to compare K_s values obtained with the four water volumes. A soil comparison was then carried out with reference to both $K_{s,m}$ and $K_{s,t}$. This analysis was carried out by considering the complete datasets for each soil (*i.e.*, regardless of the used water volume) but also by extracting from the complete dataset the runs corresponding to a given V value. In both cases, a pairwise two-tailed t test at P=0.05 was used to compare the three soils.

The next step was to analyze the final phase of the run, when ponded heads approach zero. The increase of i at the end of the run was quantified by the ratio i_e/i_{ne} and its impact on K_s calculation was checked by comparing $K_{s,m}$ with $K_{s,ne}$.

The estimated α^* values were summarized for each soil and the conditions discriminating between valid and invalid runs in terms of α^* estimation were identified by an analysis of $t_a/t_{0.5}$.

Finally, a comparison between the actual, d_m, and the theoretical, d_t, depths of the wetting front at the end of the run was carried out.

Results and discussion

Theoretical *vs* measured ponded depth of water

The length of the soil column increased upon wetting in 37 (0-2000 soil), 14 (0-105 soil) and 40 (105-2000 soil) cases and, on average, v_e was equal to 4.6 (CV = 70.6%), 2.4 (CV = 177.4%), and 5.1 (CV = 58.9%) mm, respectively. A length increase after wetting

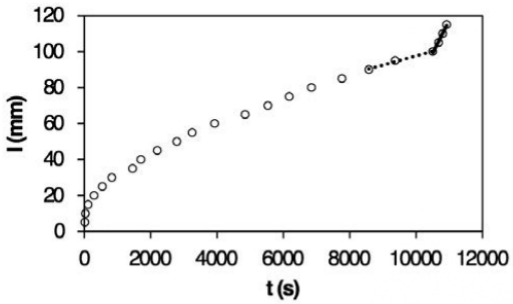

Figure 2. Example of infiltration rates calculation at (i_e, continuous line) and near (i_{ne}, dotted line) the end of the run on a cumulative infiltration, I, *versus* time, t, plot.

OPEN ACCESS

was also noticed as a consequence of soil swelling by other authors (Moutier *et al.*, 1998).

The theoretical ponded depth of water at the beginning of the run, D_t, varied between 40.5 and 135.5 mm, depending on the applied water volume, and D_m was in the range 35 to 135 mm for the 0-105 soil and 30-130 mm for the other two soils. A D_m/D_t ratio ≤ 1 was the most frequent result since $D_m/D_t > 1$ was obtained for only the 6.3% of the 144 runs. The mean of D_m/D_t was closest to one for the 0-105 soil (0.96) and it was significantly lower (0.88-0.89) for the 0-2000 and 105-2000 soils (Table 2).

A D_m value slightly smaller than D_t can be explained by considering that the first water level reading was unavoidably made a few seconds after water started to infiltrate the soil. Moreover, D_m is smaller than D_t if vertical soil expansion occurs during infiltration. Starting from the beginning of water application, many small air bubbles were often detectable in the applied water volume and, in several cases, they remained encapsulated in the water until infiltration finished. The presence of these air bubbles in the water was likely responsible of the rare detection of $D_m/D_t > 1$.

A higher D value for $t = t_a$ means that more water infiltrates the soil. Consequently, $K_{s,t}/K_{s,m} \geq 1$ was the most frequent result. This ratio was closest to one for the 0-105 soil and it was significantly higher for the other two soils (Table 2). On average, however, all differences between two estimates of K_s were negligible since the mean $K_{s,t}/K_{s,m}$ ratios varied from 1.06 to 1.21, depending on the soil. For each soil, the K_s differences were generally negligible even at the single run level since $0.75 \leq K_{s,t}/K_{s,m} \leq 1.25$ was obtained in the 65% or more of the cases (Table 2). The R^2 values of the linear regression line between $K_{s,t}$ and $K_{s,m}$ varied with the soil from 0.91 (0-105 soil) to 0.97 (0-2000 soil) and they were statistically significant in all cases according to a two-tailed t test at $P = 0.05$ (Glantz, 2012). However, none of the linear regression lines did coincide with the identity line according to the calculated 95% confidence intervals for the intercept and the slope. Using D_t for the K_s calculations is common in field application of the SFH technique but water is not poured instantly on the soil surface and possible changes in the height of the soil column during the run cannot be taken into account. These changes were considered with D_m but the initial stage of the infiltration process (*i.e.*, the first few seconds) was neglected in this case. The estimates of K_s obtained with D_t and D_m did not coincide but, on the whole, the differences between $K_{s,m}$ and $K_{s,t}$ were small or even very small, indicating a practical similarity of the two ways to estimate D for the SFH equation.

Table 2. Basic statistics of the D_m/D_t ratio (D_m and D_t = measured and theoretical ponded depth of water at the beginning of the run, respectively), the $K_{s,m}/K_{s,t}$ ratio ($K_{s,m}$ and $K_{s,t}$ = saturated soil hydraulic conductivity estimated by the SFH equation using D_m and D_t, respectively), and the $K_{s,t}$ and $K_{s,m}$ values obtained on the three tested soils (sample size, N = 48 for each soil).

Variable	Statistic	0-2000 soil	0-105 soil	105-2000 soil
D_m/D_t	Min	0.74	0.81	0.74
	Max	1.00	1.24	1.11
	Mean	0.89[a]	0.96[b]	0.88[a]
	CV (%)	5.7	8.6	9.2
$K_{s,t}/K_{s,m}$	Min	1.00	0.72	0.85
	Max	1.60	1.31	1.61
	Mean	1.18[a]	1.06[b]	1.21[a]
	CV (%)	8.8	11.5	13.1
	$P_{0.75\text{-}1.25}$ (%)	85.4	87.5	64.6
$K_{s,t}$ (mm h^{-1})	Min	6.8	5.0	19.2
	Max	132.5	39.3	381.4
	Mean	32.2[a]	17.1[b]	80.9[c]
	CV (%)	64.5	53.9	72.3
$K_{s,m}$ (mm h^{-1})	Min	5.8	4.3	17.3
	Max	106.0	42.6	237.6
	Mean	27.0[a]	16.6[b]	65.5[c]
	CV (%)	59.8	60.8	62.0

Min, minimum value; Max, maximum value; Mean, arithmetic mean; CV, coefficient of variation; $P_{0.75\text{-}1.25}$ = number of cases, in percentage of the total number of cases, for which $K_{s,t}/K_{s,m}$ was in the range 0.75 to 1.25. For a given variable, mean values followed by a different letter are significantly different according to a pairwise two-tailed t test at P = 0.05. Means followed by the same letter are not significantly different.

Effect of ponded depth of water on saturated soil hydraulic conductivity

Regardless of the use of the measured (D_m) or the theoretical (D_t) ponded depth of water for the K_s calculations, a statistically significant effect of D on K_s ($K_{s,m}$, $K_{s,t}$) was detected for the 0-2000 and 0-105 soils, with K_s values decreasing as D increased in both cases (Figure 3). This effect was particularly clear for the latter soil

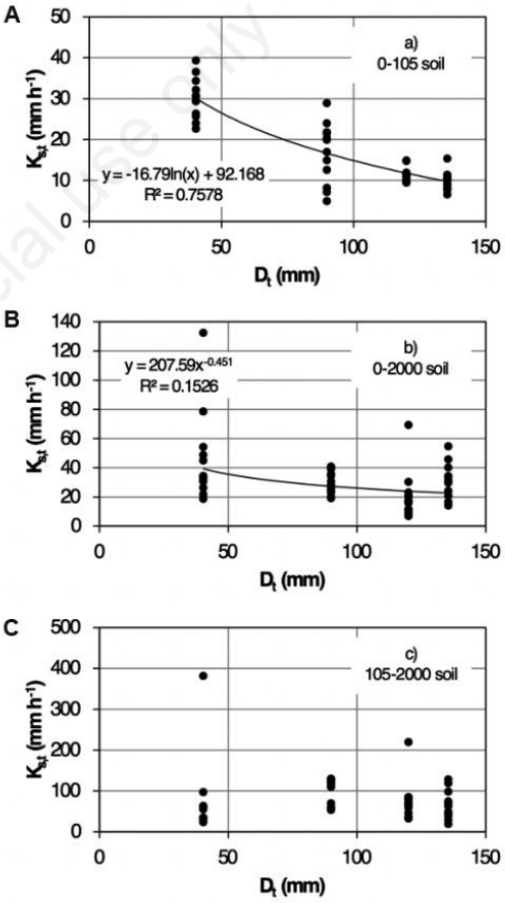

Figure 3. Saturated soil hydraulic conductivity calculated with the simplified falling-head equation, $K_{s,t}$, against the theoretically established ponded depth of water at the beginning of the infiltration run, D_t: A) 0-105 soil; B) 0-2000 soil; and C) 105-2000 soil.

Non-commercial use only

(R^2 = 0.67-0.76, depending on the used D value) and it appeared rather weak for the former one, since the (K_s, D) data points were highly scattered in this case (R^2 = 0.15). According to the fitted $K_{s,t}$ *vs* D_t relationships, an increase of D from 40 to 135 mm determined a decrease of K_s by 3.1 times for the 0-105 soil and by 1.7 times for the 0-2000 soil. An effect of D on K_s was not detected for the 105-2000 soil (R^2 = 0.006-0.01).

The results of the THSD test (Table 3) were similar to those obtained by the regression analysis. In particular, a single difference out of six established comparisons was detected for the 0-2000 soil. For the 0-105 soil, larger water volumes clearly yielded smaller $K_{s,m}$ and $K_{s,t}$ values, with non-significant K_s differences only with reference to the two largest V values. The used water volume did not influence the two estimates of K_s for the 105-2000 soil.

Therefore, the ponded depth of water effect was soil specific since using more water for the SFH run implied measurement of smaller K_s values for the finest soil, had a small and almost negligible effect on K_s determination for the intermediate soil, and was uninfluential for the coarsest soil. An inverse relationship between K_s and D, such as the one detected for the 0-105 soil, could be due to the fact that a higher hydrostatic pressure at the beginning of the run determined more compaction of the surface soil layer and hence lower conductivity values. Therefore, it could be suggested that the 105-2000 soil was the most stable soil among those tested whereas the 0-105 soil was the most unstable one. However, more water for the run implies larger sampling depths. Therefore, an inverse K_s *vs* D relationship could also be a consequence of vertical gradients in soil bulk density, increasing from the surface layer to the bottom, perhaps even due to the downward particle migration during infiltration. Slight differences in soil bulk density resulting from differences in packing were reported in other investigations (Assouline and Narkis, 2011). If this was the cause, gradients in packing density occurred in the finest soil but they were less relevant or even absent in coarser soil conditions. Finally, the accuracy of the Green and Ampt (1911) model is expected to increase with the ponded depth of water on the soil surface (Philip, 1992). Therefore, it could also be suggested that more accurate K_s values were obtained in the finest soil with the largest D values. Instead, nothing can be said about K_s accuracy for the coarsest soil since an effect of D was not detected in this case.

Comparing soils

According to a pairwise two-tailed t test at P = 0.05, the SFH technique was able to statistically discriminate among the three soils, regardless of the considered ponded depth of water for the calculations (D_m, D_t), since the highest mean K_s value (65.5-80.9 mm h^{-1}, depending on D) was obtained for the 105-2000 soil, only containing relatively coarse particles, the lowest mean (16.6-17.1 mm h^{-1}) was detected for the 0-105 soil, with only relatively fine particles, and an intermediate result (27.0-32.2 mm h^{-1}) was obtained for the 0-2000 soil, constituted by both coarse and fine particles (Table 2).

This comparison was based on the premise that the three $K_{s,m}$ (or $K_{s,t}$) datasets were comparable since they were developed by using exactly the same experimental methodology and procedures for each soil. An alternative way to establish a comparison among the three soils was to only consider each time the runs corresponding to a given applied water volume. Therefore, the soil comparison was repeated four times for a given variable ($K_{s,m}$, $K_{s,t}$), *i.e.* for V = 280, 624, 833 and 940 cm^3. With this choice, cases with both negligible and appreciable V effects on K_s were not pooled together and soil layers that did not vary very much from soil to soil were considered (Table 3). However, each comparison was based on a smaller dataset (N = 12 for each soil) as compared with that performed with the complete datasets (N = 48 for each soil).

Regardless of both the considered variable ($K_{s,m}$ or $K_{s,t}$) and the used water volume for the run, the numerically highest and lowest mean K_s values were obtained in the coarsest (105-2000) and the finest (0-105) soils, respectively (Table 3). The soil differences

Table 3. Mean and coefficient of variation, *CV*, of the saturated hydraulic conductivity values, K_s, obtained by using different water volumes, V, for the SFH run and of the measured depth of the wetting front at the end of the run, d_m (sample size, N = 12 for given variable, soil and water volume).

Variable	Soil	Statistic	V = 280 cm^3	V = 624 cm^3	V = 833 cm^3	V = 940 cm^3
$K_{s,m}$ (mm h^{-1})	0-2000	mean	37.6$^{a\,A}$	25.2$^{ab\,A}$	18.1$^{b\,A}$	27.4$^{ab\,A}$
		CV (%)	62.5	26.3	82.1	34.9
	0-105	mean	31.1$^{a\,A}$	15.5$^{b\,B}$	10.8$^{bc\,A}$	9.1$^{c\,B}$
		CV (%)	22.2	46.4	18.2	17.0
	105-2000	mean	59.4$^{a\,A}$	77.5$^{a\,C}$	64.9$^{a\,B}$	60.1$^{a\,C}$
		CV (%)	97.9	34.5	66.8	48.0
$K_{s,t}$ (mm h^{-1})	0-2000	mean	46.4$^{a\,A}$	30.1$^{ab\,A}$	21.0$^{b\,A}$	31.3$^{ab\,A}$
		CV (%)	68.3	26.2	78.8	37.7
	0-105	mean	30.1$^{a\,A}$	16.8$^{b\,B}$	11.5$^{cd\,A}$	9.9$^{d\,B}$
		CV (%)	16.7	43.9	15.6	22.4
	105-2000	mean	78.0$^{a\,A}$	100.7$^{a\,C}$	77.5$^{a\,B}$	67.3$^{a\,C}$
		CV (%)	125.3	30.5	62.3	50.5
d_m (cm)	0-2000	mean	11.0	24.3	28.2	28.5
		CV (%)	9.5	9.8	8.8	5.3
	0-105	mean	9.8	20.4	23.8	27.2
		CV (%)	4.0	13.8	2.4	5.8
	105-2000	mean	11.4	26.4	27.7	30.3
		CV (%)	9.5	8.9	11.6	2.9

$K_{s,m}$ = saturated soil hydraulic conductivity obtained by using Eq.(5) and the measured ponded depth of water at the beginning of the run, D_m. $K_{s,t}$ = saturated soil hydraulic conductivity obtained by using Eq.(5) and the theoretically determined value of the ponded depth of water at the beginning of the run, D_t. For given variable and soil, mean values in a row followed by a different lower-case letter are significantly different according to the Tukey honestly significant difference test at P = 0.05. For given water volume and variable, mean values in a column followed by a different upper-case letter are significantly different according to a pairwise two-tailed t test at P = 0.05.

Non-commercial use only

were not statistically significant for V = 280 cm^3 and with reference to another comparison (V = 833 cm^3, 0-2000 soil *vs* 0-105 soil) and they were statistically significant in all the other cases. Therefore, the expected discrimination among the three soils was generally detectable by using a fixed water volume for the runs and a smaller number of replicated runs. Applying large or relatively large water volumes for the infiltration run appeared appropriate to perceive these soil differences. A possible reason of this result is that more water for the run implies a larger, and presumably more representative, sampled soil volume. Another factor to be considered is that the measurement errors can be expected to have a larger impact on K_s calculation for smaller water volumes.

The detected K_s differences among soils were consistent with those expected on the basis of their textural characteristics, that likely had a noticeable influence on water permeability of the three soils since they were intentionally structureless or with little structure.

Infiltration rate for ponded heads close to zero

Increasing infiltration rates during the last part of the infiltration process, *i.e.* for ponded heads close to zero, were obtained very frequently in this investigation (Figure 2). In particular, i_e was greater than i_{ne} for 40 to 44 runs, depending on the soil. The mean of i_e/i_{ne} varied between 1.9 and 2.6 with some significant, although relatively small, differences among the three tested soils (Table 4). A possible explanation of the increase of infiltration rates close to the end of the run could be that air bubbles entrapped in the upper zone of the soil volume escaped from the soil surface as the hydrostatic pressure due to the ponded head tended to vanish (Bagarello *et al.*, 2006; Figure 1).

The measured ponded depths of water were considered for calculating both $K_{s,m}$ and $K_{s,ne}$ and the former values were 0.78-1.63 times the corresponding latter values (Table 4). The 0-2000 and 105-2000 soils were characterized by a statistically similar $K_{s,m}/K_{s,ne}$ ratio (1.09-1.13), slightly higher than that detected for the 0-105 soil, equal to 1.05. Moreover, $K_{s,m}/K_{s,ne}$ fall in the range 0.75-1.25 in the 92.4% of the cases.

According to the similarity criterion by Reynolds (2013), the abrupt change of the infiltration rate close to the end of the run had a minor, and therefore negligible, impact on calculation of K_s, which means that the SFH determination of K_s was not appreciably affected by the final increase of the infiltration rate. This is a practically relevant result since it is practically impossible to detect an increase of the infiltration rate at the end of the SFH field run.

Estimating the α* parameter

Using Eq.(6) for estimating α* was successful in a limited number of cases, increasing from only five for the 0-105 soil (10.4% of the runs) to 18 for the 105-2000 soil (37.5%, Table 4). The experimental ratio between t_a and $t_{0.5}$ influenced the possibility to obtain valid α* estimates. In particular, considering all infiltration runs, *i.e.* regardless of the soil (N = 144), the procedure was always successful for $3.31 \le t_a/t_{0.5} \le 3.78$ and always unsuccessful for $t_a/t_{0.5} \le 3.16$ and $t_a/t_{0.5} \ge 3.94$. For intermediate $t_a/t_{0.5}$ values ($3.19 \le t_a/t_{0.5} \le 3.29$ and $3.80 \le t_a/t_{0.5} \le 3.93$), both success and failure in the α* estimation were detected.

Notwithstanding this, the means of the few valid estimates of α* fell within the range of reasonable α* values (Elrick and Reynolds, 1992) and the soil differences were also reasonable given that higher α* results were obtained in the coarser-textured soil than the finer-textured ones (17 against approximately 9 m^{-1}, Table 4).

These results provided additional support to the suggestion that a ponding infiltration run does not represent the best way to estimate α* (Bagarello *et al.*, 2006; Reynolds and Elrick, 1990). In other terms, α* should be determined independently.

Actual depth of the wetting front

In general, wetting fronts were easily detectable during the experiments and they exhibited a nearly horizontal shape, probably because a homogeneous porous medium was used in this investigation (Figure 1). The actual depth of the wetting front at the end of the run, d_m, was generally (*i.e.*, in the 75% or more of the cases, depending on the soil) greater than the theoretical value, d_t, that was calculated by Eq.(4) for $t = t_a$ (Table 4) but outflow from the bottom of the column was never detected. On average, the d_m/d_t ratio was in a rather narrow range, relatively close to one (1.06-1.21), for all soils but this ratio was significantly lower for the 0-105 soil than the other two soils. Moreover, d_m/d_t was found to decrease as D_m increased, approximately assuming, in all cases, values close to unity for the largest D_m values (Figure 4) ($R^2 \ge$ 0.3725 depending on the soil, $R > 0$ in all cases).

Perhaps, a d_m/d_t ratio greater than one was a consequence of air entrapment in the sampled soil volume. This phenomenon likely occurred in this investigation, as revealed by the final increase in infiltration rates. Consequently, it could be suggested that d_m/d_t was generally greater than one because some of the pore space was occupied by air instead of water. More water for the run, *i.e.* larger D_m values, implied more opportunities for air displacement during the infiltration process and hence d_m/d_t values closer to one. Even diffusion of the wetting front could be thought to be a factor determining the observed differences between d_m and d_t.

Table 4. Basic statistics of i_e/i_{ne} (i_e and i_{ne} = infiltration rates at and near the end of the run, respectively), $K_{s,m}/K_{s,ne}$ (saturated soil hydraulic conductivity estimated by considering the complete infiltration process and a process stopped immediately before the raise in infiltration rate, respectively), the experimentally determined α* parameter, and d_m/d_t (d_m and d_t = measured and theoretical depth of the wetting front at the end of the run, respectively) for the three sampled soils (sample size, N = 48 for each variable and soil, with an exception for α*, as shown in the table).

Variable	Statistic	0-2000 soil	0-105 soil	105-2000 soil
i_e/i_{ne}	Min	0.59	0.46	0.55
	Max	7.0	10.6	6.0
	Mean	2.57^{a}	1.86^{bc}	2.19^{ac}
	CV (%)	66.3	81.0	49.2
$K_{s,m}/K_{s,ne}$	Min	0.98	0.81	0.78
	Max	1.63	1.35	1.62
	Mean	1.13^{a}	1.05^{b}	1.09^{a}
	CV (%)	14.8	8.5	10.2
α* (m^{-1})	N	14	5	18
	Min	2	2	2
	Max	20	22	67
	Mean	9.3	9.2	17.0
	CV (%)	64.7	84.0	121.6
d_m/d_t	Min	0.91	0.66	0.88
	Max	1.45	1.30	1.55
	Mean	1.18a	1.06b	1.21a
	CV (%)	13.8	14.5	15.7
	N($d_m/d_t > 1$)	38 (79.2%)	36 (75.0%)	42 (87.5%)

Min, minimum value; Max, maximum value; Mean, arithmetic mean; CV, coefficient of variation. For a given variable, means followed by a different letter are significantly different according to a two-tailed t test (P = 0.05). Means followed by the same letter are not significantly different.

Conclusions

This laboratory investigation increased our knowledge of the factors that can influence application of the SFH technique for saturated soil hydraulic conductivity, K_s, determination and, more in general, of falling-head one-dimensional infiltration methodologies. A depth of ponding on the infiltration surface at the beginning of the run, D, simply calculated by the ratio between the used water volume and the soil surface area does not coincide in general with the depth of ponding that can be determined by visually reading water and soil surface heights above a datum. However, this difference should not be expected to have a great impact on K_s calculations which implies that the simplest way to calculate D can be used in practice.

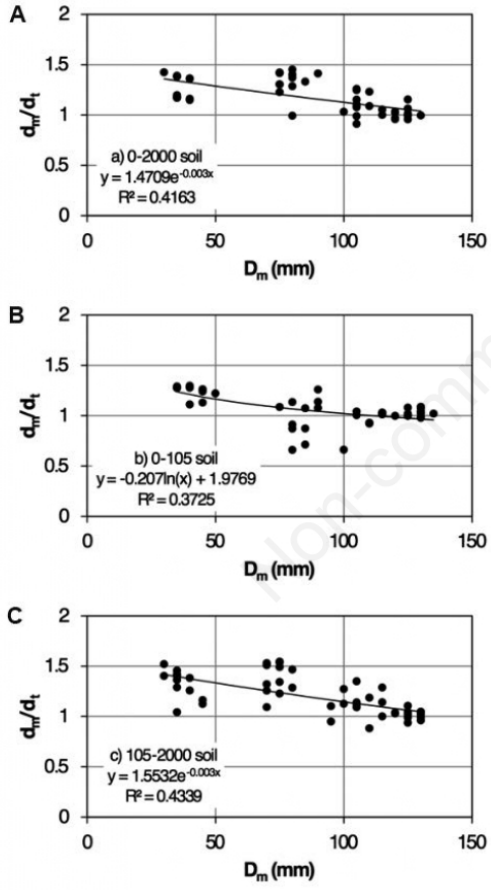

Figure 4. Ratio between the measured, d_m, and the theoretical, d_t, depth of the wetting front at the end of the simplified falling-head run plotted against the measured ponding depth of water at the beginning of the run, D_m, for the: A) 0-2000 soil; B) 0-105 soil; and C) 105-2000 soil.

Ponded depth of water effects on K_s calculation can be detected in nearly homogeneous soil conditions, probably because more compaction of the surface soil layer occurs as a consequence of a greater hydrostatic pressure at the beginning of the run or as a consequence of vertical migration of fine soil particles during the run. Ponded depth of water effects should be expected to occur when the soil contains many mobile small particles but they appear less noticeable or even absent for coarser and more rigid soils.

An abrupt increase of the infiltration rate for ponded heads approaching zero was a very frequent occurrence in this investigation, probably because air bubbles entrapped in the upper zone of the soil volume escaped from the infiltration surface as the hydrostatic pressure due to the ponded head of water tended to vanish. However, the SFH calculations of K_s should not be appreciably affected by the final increase of the infiltration rate. Therefore, this phenomenon, that cannot be detected with the SFH experiment, should not be expected to have a strong impact on the K_s results.

A falling-head one-dimensional ponded infiltration process does not represent a good means to estimate α^* since the run appears to be successful with respect to this objective only in a limited number of cases.

The depth of the wetting front at the end of the run should generally be close to the one calculated theoretically before the run. Even this result supports the SFH procedure since it indicated that a very simple method can be employed to plan a one-dimensional infiltration process. As a precaution, it is recommended to calculate the water volume to be used for the field run by assuming that the ring insertion depth is smaller by a very few centimeters than the actual one.

The information provided by this investigation reinforced our knowledge on the functioning of the SFH technique and it represents a good basis for additional developments. In particular, establishing K_s comparisons with other methods and improving our ability to obtain site-specific estimates of α^* by simple infiltration experiments appears advisable. Going from nearly idealized porous media to field soil conditions is also necessary because, in this last case, other factors that likely were not relevant in this investigation, such as layering or local heterogeneities, could have a relevant impact on the method's performances. These developments have practical importance since falling-head infiltration procedures can give estimates of K_s with experiments that are both parsimonious and rapid.

Non-commercial use only

References

Angulo-Jaramillo R., Bagarello V., Iovino M., Lassabatere L. 2016. Infiltration measurements for soil hydraulic characterization. Springer International Publishing, Switzerland.

Assouline S., Narkis K. 2011. Effects of long-term irrigation with treated wastewater on the hydraulic properties of a clayey soil. Water Resour. Res. 47:W08530.

Bagarello V., Iovino M., Elrick D.E. 2004. A simplified falling-head technique for rapid determination of field-saturated hydraulic conductivity. Soil Sci. Soc. Am. J. 68:66-73.

Bagarello V., Elrick D.E., Iovino M., Sgroi A. 2006. A laboratory analysis of falling head infiltration procedures for estimating the hydraulic conductivity of soils. Geoderma 135:322-34.

Biddoccu M., Ferraris S., Opsi F., Cavallo E. 2016. Long-term monitoring of soil management effects on runoff and soil erosion in sloping vineyards in Alto Monferrato (North-West Italy). Soil Till. Res. 155:176-89.

OPEN ACCESS

Biddoccu M., Ferraris S., Pitacco A., Cavallo E. 2017. Temporal variability of soil management effects on soil hydrological properties, runoff and erosion at the field scale in a hillslope vineyard, North-West Italy. Soil Till. Res. 165:46-58.

Di Prima S., Concialdi P., Lassabatere L., Angulo-Jaramillo R., Pirastru M., Cerdà A., Keesstra S. 2018. Laboratory testing of Beerkan infiltration experiments for assessing the role of soil sealing on water infiltration. Catena 167:373-84.

Elrick D.E., Reynolds W.D. 1992. Methods of analyzing constant-head well permeameter data. Soil Sci. Soc. Am. J. 56:320-3.

Elrick D.E., Angulo-Jaramillo R., Fallow D.J., Reynolds W.D., Parkin G.W. 2002. Analysis of infiltration under constant head and falling head conditions. In: Raats P.A.C. *et al.* (Eds.), Environmental mechanics: Water, mass and energy transfer in the biosphere, Geophysical Monograph Series. AGU, Washington, D.C., 129:47-53.

Gardner W.R. 1958. Some steady-state solutions of the unsaturated moisture flow equation with application to evaporation from a water table. Soil Sci. 85:228-32.

Gee G.W., Bauder J.W. 1986. Particle-size analysis. pp 383-411 in Klute A. (Ed.), Methods of soil analysis. Part 1. Physical and mineralogical methods. 2nd ed. Agronomy no. 9. American Society of Agronomy, Madison, WI, USA.

Glantz S.A. 2012. Primer of Biostatistics. 7th ed. The McGraw-Hill Companies, Inc., New York, NY, USA.

Green W.H., Ampt G.A. 1911. Studies in soil physics. I. The flow of air and water through soils. J. Agr. Sci. 4:1-24.

Keller T., Sutter J.A., Nissen K., Rydberg T. 2012. Using field measurement of saturated soil hydraulic conductivity to detect low-yielding zones in three Swedish fields. Soil Till. Res. 124:68-77.

Kovář S., Mašek J., Novák P. 2017. Comparison of tillage systems in terms of water infiltration into the soil during the autumn season. Agron. Res. 15:1629-35.

Moutier M., Shainberg I., Levy G.J. 1998. Hydraulic gradient, aging, and water quality effects on hydraulic conductivity of a Vertisol. Soil Sci. Soc. Am. J. 62:1488-96.

Philip J.R. 1958. The theory of infiltration, 7. Soil Sci. 85:278-86.

Philip J.R. 1969. Theory of infiltration. Adv. Hydrosci. 5:215-96.

Philip J.R. 1992. Falling head ponded infiltration. Water Resour. Res. 28:2147-8.

Philip J.R. 1993. Approximate analysis of falling-head lined borehole permeameter. Water Resour. Res. 29:3763-8.

Preti F., Guastini E., Penna D., Dani A., Cassiani G., Boaga J., Deiana R., Romano N., Nasta P., Palladino M., Errico A., Giambastiani Y., Trucchi P., Tarolli P. 2018. Conceptualization of water flow pathways in agricultural terraced landscapes. Land Degrad. Dev. 29:651-62.

Reynolds W.D. 2013. An assessment of borehole infiltration analyses for measuring field-saturated hydraulic conductivity in the vadose zone. Eng. Geol. 159:119-30.

Reynolds W.D., Elrick D.E. 1990. Ponded infiltration from a single ring: I. Analysis of steady flow. Soil Sci. Soc. Am. J. 54:1233-41.

Reynolds W.D., Lewis J.K. 2012. A drive point application of the Guelph Permeameter method for coarse-textured soils. Geoderma 187-188:59-66.

Wang Z., Feyen, J., van Genuchten M.Th., Nielsen D.R. 1998. Air entrapment effects on infiltration rate and flow instability. Water Resour. Res. 34:213-22.

Non-commercial use only

References

Agnese, C., Bagarello, V., Baiamonte, G., Iovino, M., 2011. Comparing physical quality of forest and pasture soils in a Sicilian watershed. Soil Sci. Soc. Am. J. 75, 1958. https://doi.org/10.2136/sssaj2011.0044

Aiello, R., Bagarello, V., Barbagallo, S., Consoli, S., Di Prima, S., Giordano, G., Iovino, M., 2014. An assessment of the beerkan method for determining the hydraulic properties of a sandy loam soil. Geoderma 235–236, 300–307. https://doi.org/10.1016/j.geoderma.2014.07.024

Alagna, V., Bagarello, V., Di Prima, S., Iovino, M., 2016. Determining hydraulic properties of a loam soil by alternative infiltrometer techniques. Hydrol. Process. 30, 263–275. https://doi.org/10.1002/hyp.10607

Angulo-Jaramillo, R., Bagarello, V., Iovino, M., Lassabatère, L., 2016. Infiltration measurements for soil hydraulic characterization. Springer International Publishing

Armenise, E., Simmons, R.W., Ahn, S., Garbout, A., Doerr, S.H., Mooney, S.J., Sturrock, C.J., Ritz, K., 2018. Soil seal development under simulated rainfall: Structural, physical and hydrological dynamics. J. Hydrol. 556, 211–219. https://doi.org/10.1016/j.jhydrol.2017.10.073

Assouline, S., Narkis, K., 2011. Effects of long-term irrigation with treated wastewater on the hydraulic properties of a clayey soil: Effects of wastewater irrigation on soil properties. Water Resour. Res. 47. https://doi.org/10.1029/2011WR010498

Azam, M.G., Zoebisch, M.A., Wickramarachchi, K.S., Ranamukarachchi, S.L., 2009. Site-specific soil hydraulic quality index to describe the essential conditions for the optimum soil water regime. Can. J. Soil Sci. 89, 645–656

Azam, M.G., Zoebisch, M.A., Wickramarachchi, K.S., 2008. Effects of cropping systems on selected soil structural properties and crop yields in the Lam Phra Phloeng watershed-Northeast Thailand. J. Agron. 7, 56

Bagarello, V., Baiamonte, G., Caia, C., 2019. Variability of near-surface saturated hydraulic conductivity for the clay soils of a small Sicilian basin. Geoderma 340, 133–145. https://doi.org/10.1016/j.geoderma.2019.01.008

Bagarello, V., De Santis, A., Giordano, G., Iovino, M., 2017. Source shape and data analysis procedure effects on hydraulic conductivity of a sandy-loam soil determined by ponding infiltration runs. J. Agric. Eng. 48, 71–80. https://doi.org/10.4081/jae.2017.597

Bagarello, V., Baiamonte, G., Castellini, M., Di Prima, S., Iovino, M., 2014a. A comparison between the single ring pressure infiltrometer and simplified falling head techniques. Hydrol. Process. 28, 4843–4853. https://doi.org/10.1002/hyp.9980

Bagarello, V., Castellini, M., Di Prima, S., Iovino, M., 2014b. Soil hydraulic properties determined by infiltration experiments and different heights of water pouring. Geoderma 213, 492–501. https://doi.org/10.1016/j.geoderma.2013.08.032

Bagarello, V., Di Prima, S., Giordano, G., Iovino, M., 2014c. A test of the Beerkan Estimation of Soil Transfer parameters (BEST) procedure. Geoderma 221–222, 20–27. https://doi.org/10.1016/j.geoderma.2014.01.017

Bagarello, V., Di Stefano, C., Iovino, M., Sgroi, A., 2013. Using a transient infiltrometric technique for intensively sampling field-saturated hydraulic conductivity of a clay soil in two runoff plots. Hydrol. Process. 27, 3415–3423. https://doi.org/10.1002/hyp.9448

Bagarello, V., D'Asaro, F., Iovino, M., 2012. A field assessment of the Simplified Falling Head technique to measure the saturated soil hydraulic conductivity. Geoderma 187–188, 49–58. https://doi.org/10.1016/j.geoderma.2012.04.008

Bagarello, V., Stefano, C.D., Ferro, V., Iovino, M., Sgroi, A., 2010. Physical and hydraulic characterization of a clay soil at the plot scale. J. Hydrol. 387, 54–64. https://doi.org/10.1016/j.jhydrol.2010.03.029

Bagarello, V., Sgroi, A., 2007. Using the simplified falling head technique to detect temporal changes in field-saturated hydraulic conductivity at the surface of a sandy loam soil. Soil Tillage Res. 94, 283–294. https://doi.org/10.1016/j.still.2006.08.001

Bagarello, V., Elrick, D.E., Iovino, M., Sgroi, A., 2006. A laboratory analysis of falling head infiltration procedures for estimating the hydraulic conductivity of soils. Geoderma 135, 322–334. https://doi.org/10.1016/j.geoderma.2005.12.008

Bagarello, V., Iovino, M., Elrick, D., 2004. A Simplified Falling-Head technique for rapid determination of field-saturated hydraulic conductivity. Soil Sci. Soc. Am. J. 68, 66. https://doi.org/10.2136/sssaj2004.6600

Baiamonte, G., Bagarello, V., D'Asaro, F., Palmeri, V., 2017. Factors influencing point measurement of near-surface saturated soil hydraulic conductivity in a small Sicilian basin: factors influencing saturated soil hydraulic conductivity. Land Degrad. Dev. 28, 970–982. https://doi.org/10.1002/ldr.2674

Biddoccu, M., Ferraris, S., Cavallo, E., Opsi, F., Previati, M., Canone, D., 2013. Hillslope vineyard rainfall-runoff measurements in relation to soil infiltration and water content. Procedia Environ. Sci. 19, 351–360

Biddoccu, M., Ferraris, S., Opsi, F., Cavallo, E., 2016. Long-term monitoring of soil management effects on runoff and soil erosion in sloping vineyards in Alto Monferrato (North–West Italy). Soil Tillage Res. 155, 176–189

Capello, G., Biddoccu, M., Ferraris, S., Cavallo, E., 2019. Effects of tractor passes on hydrological and soil erosion processes in tilled and grassed vineyards. Water 11, 2118. https://doi.org/10.3390/w11102118

Capello, G., Biddoccu, M., Ferraris, S., Pitacco, A., Cavallo, E., 2017. Year-round variability of field-saturated hydraulic conductivity and runoff in tilled and grassed vineyards. Chem. Eng. Trans. 58, 739–744

Castellini, M., Giglio, L., Niedda, M., Palumbo, A.D., Ventrella, D., 2015. Impact of biochar addition on the physical and hydraulic properties of a clay soil. Soil Tillage Res. 154, 1–13. https://doi.org/10.1016/j.still.2015.06.016

Chai, J., Yu, X., Xu, C., Xiao, H., Zhang, J., Yang, H., Pan, T., 2019. Effects of yak and Tibetan sheep trampling on soil properties in the northeastern Qinghai-Tibetan Plateau. Appl. Soil Ecol. 144, 147–154. https://doi.org/10.1016/j.apsoil.2019.07.017

Chen, C.T., Hsu, K.-C., 2012a. Study of using multi-step falling-head infiltration to estimate hydraulic conductivity at various depths. J. Taiwan Agric. Eng. 58, 1–12

Chen, C.-T., Hsu, K.-C., 2012b. Use of falling-head infiltration to estimate hydraulic conductivity at various depths: Soil Sci. 177, 543–553. https://doi.org/10.1097/SS.0b013e318267ed7f

Chen, X., Cheng, Q., Zhang, Z., 2010. Measurement of soil hydraulic conductivity in relation with vegetation, in: Proceedings of the IASTED International Conference. p. 797

Cherubin, M.R., Karlen, D.L., Franco, A.L.C., Tormena, C.A., Cerri, C.E.P., Davies, C.A., Cerri, C.C., 2016. Soil physical quality response to sugarcane expansion in Brazil. Geoderma 267, 156–168. https://doi.org/10.1016/j.geoderma.2016.01.004

Chyba, J., Kroulik, M., Kristof, K., Misiewicz, P.A., 2017. The influence of agricultural traffic on soil infiltration rates. Agron. Res. 15, 664–673

Chyba, J., Kroulík, M., Krištof, K., Misiewicz, P.A., Chaney, K., 2014. Influence of soil compaction by farm machinery and livestock on water infiltration rate on grassland. Agron. Res. 12, 59–64

Chyba, J., Kroulík, M., Kumhála, F. 2013. Impact of land crossing on soil physical properties. In conference Proceeding - 5th International Conference, TAE 2013: Trends in Agricultural Engineering 2013 pp. 273-276

Cislaghi A., Giupponi L., Tamburini A., Giorgi A., Bischetti G.B, 2019. The effects of mountain grazing abandonment on plant community forage value and soil properties: observations and field measurements in an Alpine area. Unimont. URL https://www.unimontagna.it/pubblicazioni/effects-mountain-grazing-abandonment-plant-community-forage-value-soil-properties-observations-field-measurements-alpine-area/ (accessed 10.23.19)

Concialdi, P., Bagarello, V., Alagna, V., Iovino, M., 2020. Laboratory evaluation of falling-head infiltration for saturated soil hydraulic conductivity determination. J. Agric. Eng. https://doi.org/10.4081/jae.2019.1003

Di Prima, S., Concialdi, P., Lassabatere, L., Angulo-Jaramillo, R., Pirastru, M., Cerda, A., Keesstra, S., 2018. Laboratory testing of Beerkan infiltration experiments for assessing the role of soil sealing on water infiltration. Catena 167, 373–384. https://doi.org/10.1016/j.catena.2018.05.013

Elrick, D.E., Angulo-Jaramillo, R., Fallow, D.J., Reynolds, W.D., Parkin, G.W., 2002. Infiltration under constant head and falling head conditions. Wash. DC Am. Geophys. Union Geophys. Monogr. Ser. 129, 47–53. https://doi.org/10.1029/129GM04

Elrick, D.E., Reynolds, W.D., 1992. Methods for analyzing constant-head well permeameter data. Soil Sci. Soc. Am. J. 56, 320. https://doi.org/10.2136/sssaj1992.03615995005600010052x

Erban, T., Stehlik, M., Sopko, B., Markovic, M., Seifrtova, M., Halesova, T., Kovaricek, P., 2018. The different behaviors of glyphosate and AMPA in compost-amended soil. Chemosphere 207, 78–83. https://doi.org/10.1016/j.chemosphere.2018.05.004

Erickson, A.J., Weiss, P.T., Gulliver, J.S., 2013. Optimizing stormwater treatment practices. Handb. Assess. Maint. 1, 1–337

Etana, A., Holm, L., Rydberg, T., Keller, T., 2020. Soil and crop responses to controlled traffic farming in reduced tillage and no-till: some experiences from field experiments and on-farm studies in Sweden. Acta Agric. Scand. Sect. B Soil Plant Sci. 0, 1–8. https://doi.org/10.1080/09064710.2020.1728372

Fallow, D.J., Elrick, D.E., Reynolds, W.D., Baumgartner, N., Parkin, G.W., 1994. Field measurement of hydraulic conductivity in slowly permeable materials using early-time infiltration measurements in unsaturated media, in: Hydraulic Conductivity and Waste Contaminant Transport in Soil. ASTM International

Fuentes, J.P., Flury, M., Bezdicek, D.F., 2004. Hydraulic properties in a silt loam soil under natural prairie, conventional till, and no-till. Soil Sci. Soc. Am. J. 68, 1679–1688

Ghosh, B., Pekkat, S., 2019. A critical evaluation of measurement induced variability in infiltration characteristics for a river sub-catchment. Measurement 132, 47–59. https://doi.org/10.1016/j.measurement.2018.09.018

Green, W.H., Ampt, G.A., 1911. Studies on Soil Phyics. J. Agric. Sci. 4, 1–24. https://doi.org/10.1017/S0021859600001441

Hanamura, T., Matsuzaki, T., Numata, A., 2007. Handy permeability test method with a single-unit apparatus developed at the solid waste landfill construction site, in: 7th FMGM 2007: Field Measurements in Geomechanics. pp. 1–12

Iwanek, M., 2008. A method for measuring saturated hydraulic conductivity in anisotropic soils. Soil Sci. Soc. Am. J. 72, 1527–1531

Keller, T., Sutter, J.A., Nissen, K., Rydberg, T., 2012. Using field measurement of saturated soil hydraulic conductivity to detect low-yielding zones in three Swedish fields. Soil Tillage Res. 124, 68–77. https://doi.org/10.1016/j.still.2012.05.002

Khodaverdiloo, H., Khani Cheraghabdal, H., Bagarello, V., Iovino, M., Asgarzadeh, H., Ghorbani Dashtaki, S., 2017. Ring diameter effects on determination of field-saturated hydraulic conductivity of different loam soils. Geoderma 303, 60–69. https://doi.org/10.1016/j.geoderma.2017.04.031

Klute, A., Dirksen, C., 1986. Hydraulic conductivity and diffusivity: laboratory methods. Methods soil anal. Part 1—Physical Mineral. Methods sssabookseries, 687–734. https://doi.org/10.2136/sssabookser5.1.2ed.c28

Kovář, S., Mašek, J., Novák, P., 2017. Comparison of tillage systems in terms of water infiltration into the soil during the autumn season

Leblanc, M., Tweed, S., Lyon, B.J., Bailey, J., Franklin, C.E., Harrington, G., Suckow, A., 2015. On the hydrology of the bauxite oases, Cape York Peninsula, Australia. J. Hydrol. 528, 668–682. https://doi.org/10.1016/j.jhydrol.2015.06.001

Lewis, J., Sjöstrom, J., 2010. Optimizing the experimental design of soil columns in saturated and unsaturated transport experiments. J. Contam. Hydrol. 115, 1–13. https://doi.org/10.1016/j.jconhyd.2010.04.001

Liu, J.L., Ma, X.Y., Zhang, Z.H., 2010. Applicability of explicit functions on cumulative infiltration of Green-Ampt model under different conditions. J. Basic Sci. Eng. 18, 11–19

Logsdon, S.D., Jaynes, D.B., 1996. Spatial variability of hydraulic conductivity in a cultivated field at different times. Soil Sci. Soc. Am. J. 60, 703. https://doi.org/10.2136/sssaj1996.03615995006000030003x

Moody, J.A., Kinner, D.A., Úbeda, X., 2009. Linking hydraulic properties of fire-affected soils to infiltration and water repellency. J. Hydrol. 379, 291–303. https://doi.org/10.1016/j.jhydrol.2009.10.015

Moutier, M., Shainberg, I., Levy, G.J., 1998. Hydraulic gradient, aging, and water quality effects on hydraulic conductivity of a Vertisol. Soil Sci. Soc. Am. J. 62, 1488–1496. https://doi.org/10.2136/sssaj1998.03615995006200060003x

Novak, P., Sarec, P., Latal, O., Brtnicky, M., Masek, J., 2019. Influence of manure with activators of organic matter on physical properties of soil.

Odell, B.P., Groenevelt, P.H., Elrick, D.E., 1998. Rapid determination of hydraulic conductivity in clay liners by early-time analysis. Soil Sci. Soc. Am. J. 62, 56–62

Oliveira, C.C., Sartini, R.P., Reis, B.F. dos, Zagatto, E.A.G., 1996. Multicommutation in flow analysis. Part 4. Computer-assisted splitting for spectrophotometric determination of copper and zinc in plants. Anal. Chim. Acta 332, 173–178

Philip, J.R., 1992. Falling head ponded infiltration. Water Resour. Res. 28, 2147–2148. https://doi.org/10.1029/92WR00704

Preti, F., Guastini, E., Penna, D., Dani, A., Cassiani, G., Boaga, J., Deiana, R., Romano, N., Nasta, P., Palladino, M., 2018. Conceptualization of water flow pathways in agricultural terraced landscapes. Land Degrad. Dev. 29, 651–662

Ramazanpour Esfahani, A., Batelaan, O., Hutson, J.L., Fallowfield, H.J., 2020. Combined physical, chemical and biological clogging of managed aquifer recharge and the effect of biofilm on virus transport behavior: A column study. J. Water Process Eng. 33, 101115. https://doi.org/10.1016/j.jwpe.2019.101115

Rex, J., Dubé, S., Foord, V., 2013. Mountain pine beetles, salvage logging, and hydrologic change: Predicting wet ground areas. Water 5, 443–461

Reynolds, W.D., Lewis, J.K., 2012. A drive point application of the Guelph Permeameter method for coarse-textured soils. Geoderma 187–188, 59–66. https://doi.org/10.1016/j.geoderma.2012.04.004

Reynolds, W.D., 2008. Saturated hydraulic properties: ring infiltrometer. Carter MR Gregor. EG Eds Soil Sampl. Methods Anal. 2nd Ed CRC Press Boca Raton Pp 1043–1056

Reynolds, W.D., Bowman, B.T., Brunke, R.R., Drury, C.F., Tan, C.S., 2000. Comparison of tension infiltrometer, pressure infiltrometer, and soil core estimates of saturated hydraulic conductivity. Soil Sci. Soc. Am. J. 64, 478–484. https://doi.org/10.2136/sssaj2000.642478x

Reynolds, W.D., Elrick, D.E., 1990. Ponded Infiltration from a single ring: I. Analysis of steady flow. Soil Sci. Soc. Am. J. 54, 1233. https://doi.org/10.2136/sssaj1990.03615995005400050006x

Šařec, P., Novák, P., 2017. Influence of manure and activators of organic matter biological transformation on selected soil physical properties of Modal Luvisol. Agron. Res. 15, 565–575

Scarabeli, I.G.R., Tormena, C.A., Favilla, H.S., Figueiredo, G.C., 2018. Field-saturated hydraulic conductivity measured by two techniques and at different sampling positions relative to maize-crop rows and interrows. Semina Ciênc. Agrár. 39, 403–410

Servadio, P., Bergonzoli, S., Beni, C., 2016. Soil tillage systems and wheat yield under climate change scenarios. Agronomy 6, 43

Teng, J., Kou, J., Zhang, S., Sheng, D., 2019. Evaluating the influence of specimen preparation on saturated hydraulic conductivity using nuclear magnetic resonance technology. Vadose Zone J. 18, 180179. https://doi.org/10.2136/vzj2018.09.0179

Verhoef, A., Egea, G., 2013. Soil water and its management. Soil Cond. Plant Growth Blackwell Publ Chichester UK 269–322

Zeleke, T.B., Si, B.C., 2005. Parameter estimation using the falling head infiltration model: simulation and field experiment. Water Resour. Res. 41. https://doi.org/10.1029/2004WR003407

CHAPTER 3: Using single-ring infiltration methods to determine the soil hydraulic properties in a hydrological perspective

3.1. Introduction

Interpreting and simulating surface soil hydrological processes, such as rainfall excess generation, by physically based models requires determining the soil sorptivity, S (L $T^{-0.5}$) and the saturated soil hydraulic conductivity, K_s (L T^{-1}) (e.g., Touma et al., 2007). Soil sorptivity defines the ability of a soil to transmit water by capillarity and it varies with the initial and final soil water content and, when present, the depth of the water head at the soil surface. The saturated soil hydraulic conductivity represents the maximum rate of water flow due solely to gravity in a completely saturated soil. The S^2/K_s ratio allows calculation of the time to ponding during rainfall infiltration (White et al., 1989) and the scale parameter of the water retention curve, h_g (Lassabatere et al., 2006), and hence the macroscopic capillary length (Souza et al., 2014) that represents the relative magnitude of the capillarity and gravity forces which prevail during an infiltration process (Angulo-Jaramillo et al., 2016, 2019).

Many investigations have demonstrated that surface soil characteristics are highly dynamic and they can vary appreciably, even over short times such as during a rainfall event or between closely spaced rainstorms (Morin and Benyamini, 1977; Levy et al., 1986; Le Bissonnais and Singer, 1992; Fohrer et al., 1999; Torri et al., 1999; King and Bjorneberg, 2012). With reference to K_s, differences between altered and non-altered soil conditions by 47-291 times were reported by Ramos et al. (2000) and by 17-115 times by Assouline and Mualem (2002). The K_s values of different disturbed soils (0.35-6.2 mm/h in Ramos et al., 2000 and 0.42-1.3 mm/h in Assouline and Mualem, 2002) appeared to collapse towards a rather narrow range of small values, likely compatible with surface runoff formation in many instances. Instead, soil sorptivity seems to be less sensitive to soil disturbance (Somaratne and Smettem, 1993). However, the mentioned difference between S and K_s is not general since other investigations provided a different information. For example, in an investigation by Ndiaye et al. (2005), the influence of cumulative rainfall since tillage was more noticeable for K_s than S along a transect but not along another transect established on the same field. According to Assouline and Mualem (2006), surface soil conditions, and explicitly seal formation or the presence of a crust layer, need to be taken into account in the perspective to estimate runoff production.

Therefore, determining short term dynamics of soil properties is necessary to properly capture the general response of a porous medium in the context of the hydrological process of specific interest and hence to choose input parameters to physically based hydrological models that are appropriate for a particular application, soil and soil condition (Reynolds et al., 2000; Assouline and Mualem, 2002, 2006; Ndiaye et al., 2005).

Single-ring infiltration experiments appear an attractive alternative to more complex experiments, such as rainfall simulation, for investigating short term dynamics of soil hydraulic properties. Infiltrometer experiments are generally simple, parsimonious and rapid and consequently they are easier to perform in the field as compared with rainfall simulation experiments (Di Prima et al., 2017, 2018a). Moreover, the analysis of the single-ring infiltration data relies on robust physical theories.

The Simplified Falling Head (SFH) technique for determining K_s (Bagarello et al., 2004) and the Beerkan Estimation of Soil Transfer parameters (BEST) procedure of complete soil hydraulic characterization (Lassabatere et al., 2006; Yilmaz et al., 2010; Bagarello et al., 2014a) make use of this kind of experiment, frequently named beerkan infiltration run with reference to BEST, and they have the requirement of being reasonably rapid and easy to apply. With the SFH technique, a given, small water volume is applied on the soil surface and the time from the water application to the instant at which all water has infiltrated is used to determine K_s. With BEST, a given, small volume of water is poured in the cylinder at the start of the measurement and the elapsed time during the infiltration is measured. When the amount of water has completely infiltrated, an identical amount of water is poured into the cylinder, and the time needed for the water to infiltrate is logged. The procedure is

repeated until the difference in infiltration time between consecutive trials become negligible, signalling a practically steady state infiltration. Calculation of K_s by the SFH technique implies performing a falling-head, ponded and transient infiltration experiment. Steady-state condition is required in all three BEST alghoritms.The interest for the SFH and BEST techniques is evident in the scientific literature. For example, the SFH technique has been applied to monitor temporal changes in K_s, intensively characterize a clay soil at the plot scale, establish comparisons between pasture and forest soils, and detect low yielding zones in agricultural Swedish fields (Bagarello and Sgroi, 2007; Bagarello et al., 2010, 2012; Agnese et al., 2011; Keller et al., 2012). A more detailed assessment of the use that has been made of this technique in the past years is provided in the chapter 2, *Laboratory investigation on the Simplified Falling Head technique*, of this PhD thesis. BEST has been used to characterize temporal variability of soil hydraulic properties under high-frequency drip irrigation, review the soil hydraulic properties of a field sampled in the past, study the effect of sediment accumulation on the water infiltration capacity of two urban infiltration basins, analyse the spatial variability of the water retention and soil hydraulic conductivity curves in a small watershed, and determine the hydraulic properties of soils that are practically difficult to characterize with other laboratory and field experimental procedures (Mubarak et al., 2009a, 2010; Lassabatere et al., 2010; Gonzalez-Sosa et al., 2010; Bagarello et al., 2011). More details on the use of BEST methods until now are provided in the section *Applications of BEST methods* of this chapter.

Generally, single-ring infiltration runs are carried out by using rather small water volumes, even when steady-state methods of analysis of the infiltration data have to be employed. This circumstance has several advantages such as: i) transporting small water volumes in remote areas is easy (Bagarello et al., 2011); ii) many locations can be sampled with a limited water amount, which is important to improve confidence in the estimated mean value of a soil property (Kanso et al., 2018; Picciafuoco et al., 2019); and iii) the assumption of homogeneous soil and uniform initial water content, that is commonly made by infiltration models, is more realistic (Vandervaere et al., 2000). Moreover, using small amounts of water and hence performing relatively short duration runs is supported by the existing literature since attainment of quasi steady-state infiltration rates, that represent the necessary information for calculating the soil hydrodynamic parameters from the measured infiltration process in many circumstances, should generally be quite rapid in many field applications of the single-ring infiltration methods (Bagarello et al., 1999; Reynolds et al., 2000; Lassabatere et al., 2006, 2019; Stewart and Abou Najm, 2018; Xiao et al., 2019). For example, as a practical guideline, Lassabatere et al. (2006) suggested that eight to 15 water volumes, each establishing an initial ponded depth of water on the infiltration surface of nearly 1 cm, should be enough to detect near steady-state conditions. In many instances, emphasis is also put on the fact that obtaining reliable soil data by an infiltration method requires avoiding or at least reducing as much as possible any soil alteration due to the run. Consequently, small insertion depths of the ring are preferred, great care in ring insertion into the soil is recommended, compaction and shattering prone situations are suggested to be avoided, and the need to prevent or minimize disturbance of the infiltration surface when water is applied is emphasized (Reynolds, 2008; Angulo-Jaramillo et al., 2016; Khodaverdiloo et al., 2017; Lassabatere et al., 2019a).

However, there is some perplexity about the possibility to use ring infiltration methods to generally obtain usable soil hydraulic properties in hydrologically relevant contexts (e.g., Alagna et al., 2018, Dohnal et al., 2016, Votrubova et al., 2017). Perhaps, a reason could be a scepticism about the ability of infiltrometer techniques to capture in detail the dynamics of the soil properties given that, according to several investigations, these techniques could yield excessively high infiltration rates or K_s values in the perspective of explaining surface hydrological processes (Ben-Hur et al., 1987; Cerdà, 1996, 1997; van De Giesen et al., 2000; Bagarello et al., 2013). For example, Ben-Hur et al. (1987) suggested that predicting rainfall infiltration from double-ring infiltrometer data was not possible. The reason was that the structure of the bulk soil is the main factor controlling infiltration under water ponding conditions while the surface seal controls rainfall infiltration.

The infiltration rates measured by Cerdà (1996, 1999) in some Spanish sites by ring infiltrometers were 3-8 times greater than those obtained by rainfall simulation due to water depth pressure established in the rings and crust development under simulated rainfall. Working in Côte d'Ivoire, van de Giesen et al. (2000) obtained a too high K_s value, actually precluding runoff occurrence although runoff was measured. These authors explained this inconsistency by noting that, during tropical storms, massive air inclusion may block some larger pores and, more importantly, crust formation and associated particle sorting decreases overall permeability. A similar result was obtained in Sicily by Bagarello et al. (2013) on runoff plots established on a clay soil. The median K_s values obtained by intensively sampling the soil were not lower than 600 mm h^{-1} but runoff at the base of the plot was measured even with rainfall intensities of no more than 100 mm h^{-1}. These authors suggested that surface K_s decreased during the event due to soil compaction induced by rainfall impact and wetting induced soil swelling. More recently, Morbidelli et al. (2017) showed that the double-ring infiltrometer overestimated the areal value of K_s as compared with controlled rainfall-runoff experiments. Picciafuoco et al. (2019) concluded that the magnitude of the bias is still an open issue for any available device because of the difficulties related to the identification of a reference value of K_s. Therefore, the inability of ponded infiltrometer methods to yield data usable to model rainfall-runoff processes seems a more experimental than theoretical problem.

In fact, two factors have to be considered when soil characterization is aimed at simulating surface hydrological processes such as rainfall excess generation and runoff production: i) structure dependent soil properties have a dynamic nature and they can vary appreciably upon wetting due to, for example, aggregate breakdown by raindrop impact or weakening of interparticle bonds (Assouline, 2004; Dikinya et al., 2008; King and Bjorneberg, 2012; Chen et al., 2013); and ii) Hortonian surface runoff occurs as a consequence of prolonged and intense rainfall events (Assouline and Mualem, 2002, 2006; Wu et al., 2019). Therefore, in reality, a short and non-perturbing infiltration run could not represent the best choice to describe the hydrodynamic behaviour of a soil when surface runoff occurs. Instead, long runs and water application procedures that induce some surface soil alteration could yield more appropriate estimates of soil hydrodynamic properties to explain and simulate surface hydrological processes such as rainfall excess generation, although this approach could give rise to other perplexities such as that a longer and/or a soil perturbing experiment could imply a reduced homogeneity of the sampled soil volume, which instead is an assumption of the applied models to calculate soil hydraulic properties.

Moving from these premises, on 2014 the soil physics research group of the Agricultural, Food and Forest Sciences Department of the University of Palermo started a research activity with the general objective to improve our ability to use single-ring infiltration methods in a hydrological perspective (Bagarello et al., 2014b; Alagna et al., 2016a; Di Prima et al., 2017).

In a first investigation (Bagarello et al., 2014c), soil was sampled at four Sicilian sites with both the SFH technique and the BEST procedure and two heights of water application (0.03 and 1.5 m). The most appropriate BEST algorithm to analyse the data between BEST-slope (Lassabatere et al., 2006) and BEST-intercept (Yilmaz et al., 2010) was determined and the effect of the height of water pouring on the measured soil hydraulic properties was evaluated. The two considered BEST algorithms differed substantially given that 19 and 76 runs out of 80 were successful with BEST-slope and BEST-intercept, respectively, and only the latter algorithm was usable for low steady state infiltration rates. Therefore, BEST-intercept represented a practically important improvement as compared with the original BEST-slope algorithm. However, the characterization performed with BEST-intercept was expected to be rather approximate because the fitting quality of the infiltration model to the data was satisfactory only in a few cases. The height of water pouring did not affect significantly and/or appreciably the saturated soil hydraulic conductivity, K_s, measured with the SFH technique (differences between means varying with the site by a factor of 1.2-1.9) but it had an appreciable impact with BEST since low runs yielded higher means than the high ones by a factor of 11.5-35.2, depending on the sampled soil. The SFH and BEST techniques showed similarities at most of the sites for a low height of water application (differences by a factor of 1.2-9.3, not exceeding 1.5 at three sites).

With a great height of pouring, BEST yielded lower K_s values than the SFH technique by a factor of 12.6-80.8. All detected changes due to an increased height of water pouring were consistent with a pore size reduction, that was considered plausible since pore clogging and compaction phenomena were expected consequences of a high run. The different sensitivity of the two techniques to water application height was attributed to the fact that water was applied once with the SFH technique and several times with the BEST procedure. Each water application generally contributed to alter the soil surface, and the total energy of the applied water was an appropriate predictor of the changes in K_s when soil deterioration was not completed before concluding the infiltration run. This early investigation yielded several important suggestions. In particular, water height effects detected with a given technique cannot be considered of general validity, i.e. independent of the K_s measurement technique, for a particular soil. The choice of the methodology to be applied (SFH, BEST) and the height of water application (low, high) should vary with the intended use of the K_s data. If the objective of the field campaign is to obtain data usable to explain surface runoff generation phenomena during intense rainfall events, the most appropriate choice among the tested ones should be BEST with a high run, to mimic relatively prolonged rainfall effects on the soil surface. A low run is more appropriate to determine the saturated conductivity of a soil that is not directly impacted by rainfall, due for example to the presence of a mulching on the soil surface. In this case, the SFH and BEST techniques appeared to yield relatively equivalent results in sandy loam and clay soils, which suggested that the more rapid SFH technique should be applied if only K_s is the variable of interest. This technique should also be preferred when repeated water application is expected to also promote some soil disturbance, decreasing K_s, with a low application height.

The premise of the subsequent investigation by Alagna et al. (2016a) was that the soil water content at the start of the infiltration experiment, the height from which water is poured onto the soil surface and the duration of the infiltration run are factors possibly influencing determination of soil water transmission properties by an infiltrometer method. Therefore, a sandy-loam soil was sampled with the BEST procedure of soil hydraulic characterization and two heights of water pouring (0.03 and 1.5 m) under three different initial soil water content, θ_i ($0.12 \leq \theta_i \leq 0.20$ m^3m^{-3}), conditions. According to the BEST guidelines, relatively short infiltration runs (average run duration $\leq$ 1.5 hours, depending on both the date and the height from which water was poured) were carried out. However, three long infiltration runs (10 hours) were also carried out when θ_i was of 0.075 m^3m^{-3}. The saturated soil hydraulic conductivity, K_s, and the soil water sorptivity, S, were estimated for each infiltration run with the BEST-steady algorithm, developed by Bagarello et al. (2014a).

The mean values of K_s varied with the height of pouring of water and θ_i from 13 to 496 mm h^{-1}, and a low height from which water was poured yielded 13 to 27 times higher K_s means than a high height, depending on θ_i. High runs also had a homogenizing effect on the measured conductivity. An inverse relationship between K_s and θ_i was clearer with the low height of water pouring than the high one. The means of S varied from 35 to 126 mm $h^{-0.5}$, with the low runs yielding 2.3 to 2.8 times higher means than the high runs. The effects of the height from which water was poured were particularly noticeable for K_s probably because this property depends strongly on soil structure that is susceptible to alteration due to water application. Sorptivity was less affected by the height of pouring of water since this property depends more than K_s on soil matrix, which does not change with the water application procedure. The mean saturated hydraulic conductivity obtained with the long runs (15 mm h^{-1}) was close to the means of K_s obtained with the high and shorter runs (13-19 mm h^{-1}, depending on θ_i). The results of this investigation were considered to be useful to better explain the infiltration process at the field site. If water application does not perturb appreciably the exposed soil surface, initially wetter soil conditions lead to less infiltration due to the reduced ability of the soil to adsorb water but also because K_s decreases as the initial soil water content increases due to phenomena such as swelling, determining development of a less permeable soil volume.

Disturbing the soil surface by water pouring reduces in general infiltration and it also attenuates the effect of θ_i on this process. Long duration runs or runs carried out with a high height of pouring of water appear more appropriate than short duration runs with a low height of pouring of water to obtain data usable to explain surface runoff generation phenomena during intense rainfall events, especially

when the soil was relatively dry at the time of sampling. The application procedure of a given experimental method has to be considered a source of variability of the measured soil properties. Finally, the height from which water is poured can have a reduced impact on the measured soil properties in relatively wet soil conditions.

In the investigation by Di Prima et al. (2017), a link between rainfall simulation and ponding infiltrometer experiments was established for a Spanish sandy-loam soil. The height of water pouring for the infiltrometer run was chosen establishing a similarity between the gravitational potential energy of the applied water, E_p, and the simulated rainfall kinetic energy, E_k. To test the soundness of this procedure, the soil was sampled with the BEST procedure and two heights of water pouring (0.03 m, i.e. usual procedure, and 0.34 m, yielding $E_p = E_k$). Then, a comparison between experimental steady-state infiltration rates, i_{sR}, measured with rainfall simulation experiments determining runoff production and K_s values for the two water pouring heights was carried out in order to distinguish between theoretically possible ($i_{sR} \geq K_s$) and impossible ($i_{sR} < K_s$) situations. Physically possible K_s values were only obtained applying water at a relatively large distance from the soil surface. This result suggested the consistency between beerkan runs with a high height of water pouring and rainfall simulator experiments. Soil compaction and mechanical aggregate breakdown were the most plausible physical mechanisms determining reduction of K_s with height. Visually, the change in soil structure at surface was evident. In addition, some complementary experiments with the mini disk infiltrometer demonstrated that this change was responsible for a large decrease in hydraulic conductivity. This study confirmed that the height from which water is poured onto the soil surface is a key parameter in infiltrometer experiments and can be adapted to mimic the effect of high intensity rain on soil hydraulic properties.

At the end of this short overview of the main investigations carried out by the soil physics research group at the University of Palermo in the 2014 to 2017 years (Bagarello et al., 2014c; Alagna et al., 2016a; Di Prima et al., 2017), several improvements and developments could be delineated for future research.

In particular, the most logical continuation should be the assessment of the relationship between the water pouring height and the measured soil hydraulic conductivity with reference to other soils differing by their structural stability, that should also be evaluated by independent measurements. Soils should also differ by their initial soil moisture condition. In an attempt to generalize water height effects, soils in their natural status, that is not altered by smoothing and levelling actions before applying the infiltrometer, should also be sampled whenever possible.

The hypothesis that the height from which water is poured onto the soil surface is a parameter useful in infiltration experiments to mimic the effect of high intensity rain on the soil hydraulic properties needs specific experimental testing. At this aim, infiltration rates should also be measured during natural or simulated rainstorms.

Establishing which is the most appropriate BEST algorithm (BEST-slope, BEST-intecept, BEST-steady) to obtain soil data in a condition of possible soil properties alteration is another question to be solved.

A factor that has to be considered is that infiltration tests are commonly performed with constant boundary conditions at the soil surface. However, intensities are prone to time variation during a rainfall event, which implies that mechanisms of soil response to wetting may change during the event and between events. Therefore, recovery of soil hydraulic properties between two events should also be taken into account.

Establishing a similarity between the gravitational potential energy of the applied water, E_p, and the simulated rainfall kinetic energy, E_k, under different conditions appears necessary to better establish the physical link between the hydrological processes measured with rainfall simulation experiments and the proposed methodology for characterizing the soil.

The combined effects of the height of pouring of water and the run duration on the measured water transmission properties should be tested for different initial soil water conditions in other soils in an attempt to improve our ability to use measured soil properties for both interpreting and simulating hydrological processes, including runoff generation phenomena (Alagna et al., 2016a).

Starting from this experience, an intensive research activity was therefore planned and realized both in the laboratory and the field during this doctoral period, in an attempt to give a contribution towards an improved ability to obtain hydrologically relevant soil hydraulic properties by single-ring infiltration experimental methodologies.
In particular, three different investigations were carried out and the results were published in three papers on international scientific journals.
In short, the first investigation was carried out in the laboratory with the following objectives: i) measuring the effect of surface sealing on water infiltration of three bare soils with different textures exposed to the direct impact of raindrops; ii) evaluating the influence of the thickness of the upper layer of soil on seal formation and related impacts on water infiltration; iii) comparing ponded infiltrometer runs (beerkan runs) with rainfall simulation experiments in terms of saturated soil hydraulic conductivity for the case of soil sealing; and iv) establishing which BEST algorithm can satisfactorily be adopted to properly estimate K_s of the seal. The results of this investigation were reported in the paper by Di Prima S., Concialdi P., Lassabatere L., Angulo-Jaramillo R., Pirastru M., Cerdà A., Keesstra S. 2018a. Laboratory testing of Beerkan infiltration experiments for assessing the role of soil sealing on water infiltration. Catena, 167: 373-384.
The second investigation had the following objectives: i) checking the effects of the height of water pouring on the infiltration process in an initially near-saturated porous medium; ii) determining the impact of a pause in the infiltration run on the measured infiltration rates; and iii) determining the effect of the established ponded depth of water on the infiltration rates. The results were published in the paper: Alagna V., Bagarello V., Cecere N., Concialdi P., Iovino M. 2018. A test of water pouring height and run intermittence effects on single-ring infiltration rates. Hydrological Processes, 32: 3793-3804.
Finally, the objectives of the third investigation were to: i) verify water volume and pouring height effects on the established infiltration process; ii) establish if deterioration requires less water for a fine soil than a coarser one; and iii) compare soil hydrodynamic properties estimated with infiltration runs differing by both the number of poured water volumes and the height of water application. The results were reported in Auteri N., Bagarello V., Concialdi P., Iovino M. 2020. Testing an adapted beerkan infiltration run for a hydrologically relevant soil hydraulic characterization. Journal of Hydrology, 584, 12469714, 9 pp..
This chapter is organized into four sections and three appendices. In particular, after this introduction (3.1 section), the theory of the BEST methods is presented in the 3.2 section. An overview of the use that has been made of the BEST technique up to now is provided in the 3.3 section. The research activity on the BEST technique developed during the PhD course is briefly described in the 3.4 section. Finally, the **Appendices B, C** and **D** are the published papers by Di Prima et al. (2018), Alagna et al. (2018) and Auteri et al. (2020).

3.2. Theory

The BEST methods of soil hydraulic characterization focus specifically on the van Genuchten (1980) model with the Burdine (1953) condition for the water retention curve and the Brooks and Corey (1964) relationship for hydraulic conductivity:

$$\frac{\theta - \theta_r}{\theta_s - \theta_r} = \left[1 + \left(\frac{h}{h_g} \right)^n \right]^{-m} \quad (1)$$

$$m = 1 - \frac{2}{n} \quad (2)$$

$$\frac{K(\theta)}{K_s} = \left(\frac{\theta - \theta_r}{\theta_s - \theta_r} \right)^{\eta} \quad (3)$$

$$\eta = \frac{2}{mn} + 2 + p \quad (4)$$

where θ (L^3L^{-3}) is the volumetric soil water content, h (L) is the soil water pressure head, K ($L\ T^{-1}$) is the soil hydraulic conductivity, n, m and η are shape parameters, p is a tortuosity parameter, and h_g (L), that is proportional to the pressure head at the inflection point, θ_s (L^3L^{-3}), representing the saturated soil water content, θ_r (L^3L^{-3}), that is the residual soil water content (assumed to be zero in BEST) and K_s ($L\ T^{-1}$), that is the saturated soil hydraulic conductivity, are scale parameters related to soil structure.

BEST estimates shape parameters on the basis of particle size analysis and soil porosity determination:

$$P(D) = \left[1 + \left(\frac{D_g}{D} \right)^N \right]^{-M} \quad (5)$$

where $P(D)$ is the fraction by mass of particles passing a particular diameter, D (L); D_g (L) is a scale parameter and N and $M = 1 - 2/N$ are shape parameters. Fitting eq.(5) to the measured particle size distribution (PSD) allows us to calculate the shape index for PSD, p_M:

$$p_M = \frac{MN}{1 + M} \quad (6)$$

The m parameter of eq.(1) is calculated by:

$$m = \frac{1}{p_m} \left(\sqrt{1 + p^2{}_m} - 1 \right) \quad (7)$$

where:

$$p_m = p_M (1 + k)^{-1} \quad (8)$$

$$k = \frac{2s - 1}{2s(1 - s)} \quad (9)$$

$$(1 - f)^2 + f^{2s} = 1 \quad (10)$$

where f (L^3L^{-3}) is the soil porosity and s is the fractal dimension of the media, varying from 0.5 to 1. Minasny and McBratney (2007) proposed an alternative way to estimate the n parameter used in the BEST procedure from sand, *sa* (%, USDA classification), and clay, *cl* (%), percentages:

$$n = 2.18 + 0.11\left[48.087 - 44.954S(x_1) - 1.023S(x_2) - 3.896S(x_3)\right] \quad (11a)$$

where:

$$x_1 = 24.547 - 0.238sa - 0.082cl \quad (11b)$$

$$x_2 = -3.569 + 0.081sa \quad (11c)$$

$$x_3 = 0.694 - 0.024sa + 0.048cl \quad (11d)$$

$$S(x) = \frac{1}{1+\exp(-x)} \quad (11e)$$

For an infiltration experiment with zero water pressure head on a circular surface of radius, r (L), above a uniform soil with a uniform initial water content, θ_i (L^3L^{-3}), the three-dimensional cumulative infiltration, I (L), and the infiltration rate, i ($L\ T^{-1}$), can be approached by the following expressions proposed by Haverkamp et al. (1994):

$$I(t) = S\sqrt{t} + (AS^2 + BK_s)t \quad (12a)$$

$$i(t) = \frac{S}{2\sqrt{t}} + (AS^2 + BK_s) \quad (12b)$$

$$I_s(t) = (AS^2 + K_s)t + C\frac{S^2}{K_s} \quad (12c)$$

$$i_s(t) = AS^2 + K_s \quad (12d)$$

where t (T) is the time, S ($L\ T^{-0.5}$) is soil sorptivity, I_s (L) and i_s ($L\ T^{-1}$) are the asymptotic models for I and i for large times, and A (L^{-1}), B and C are constants having the following expressions:

$$A = \frac{\gamma}{r(\theta_s - \theta_i)} \quad (13a)$$

$$B = \frac{2-\beta}{3}\left[1 - \left(\frac{\theta_i}{\theta_s}\right)^{\eta}\right] + \left(\frac{\theta_i}{\theta_s}\right)^{\eta} \quad (13b)$$

$$C = \frac{1}{2(1-\beta)\left[1 - \left(\frac{\theta_i}{\theta_s}\right)^{\eta}\right]}\ln\left(\frac{1}{\beta}\right) \quad (13c)$$

where β and γ are infiltration constants that are commonly set at 0.6 and 0.75, respectively, for $\theta_i < 0.25\ \theta_s$ (Haverkamp et al., 1994).
In the BEST procedure, soil sorptivity is expressed as a function of the scale parameters and initial and final water contents using the approximation by Parlage (1975):

$$S^2(\theta_i,\theta_s) = -c_p(n,m,\eta)\theta_s K_s h_g\left(1-\frac{\theta_i}{\theta_s}\right)\left[1-\left(\frac{\theta_i}{\theta_s}\right)^{\eta}\right] \tag{14}$$

where:

$$c_p(n,m,\eta) = \Gamma\left(1+\frac{1}{n}\right)\left\{\frac{\Gamma\left(m\eta-\frac{1}{n}\right)}{\Gamma(m\eta)}+\frac{\Gamma\left(m\eta+m-\frac{1}{n}\right)}{\Gamma(m\eta+m)}\right\} \tag{15}$$

where Γ is the gamma function. The scale parameter, h_g, is derived from the estimated K_s and S values by the following relation obtained from eq.(14):

$$h_g = -\frac{S^2(\theta_i,\theta_s)}{c_p(n,m,\eta)(\theta_s-\theta_i)\left[1-\left(\frac{\theta_i}{\theta_s}\right)^{\eta}\right]K_s} \tag{16}$$

For the determination of K_s and S, three different BEST algorithms were proposed, namely BEST-slope, BEST-intercept and BEST-steady.
The original BEST-slope algorithm (Lassabatere et al., 2006) considers Eq.(12a) for modelling the transient cumulative infiltration data. Expressing the soil hydraulic conductivity as a function of sorptivity and experimental steady-state infiltration rate, i_s^{exp} (L T^{-1}). Eq.(12d) leads to:

$$K_s = i_s^{\exp} - AS^2 \tag{17}$$

which, when substituted into eq.(12a) yields:

$$I(t) = S\sqrt{t} + [A(1-B)S^2 + Bi_s^{\exp}]t \tag{18}$$

where i_s^{exp} is estimated as the slope of the regression line fitted to the last data points describing steady-state conditions on the I vs. t plot. Sorptivity, S, is estimated by fitting eq.(18) to the experimental data. The fit is performed by minimizing the classical objective function for cumulative infiltration:

$$f(S,K_s,k) = \sum_{i=1}^{k}[I_i^{\exp} - I(t_i)]^2 \tag{19}$$

where k is the number of data points considered for the transient state and I^{exp} and I are the measured and the estimated cumulative infiltration using Eq.(18), respectively. Once S is estimated, K_s is calculated by eq.(17). As the infiltration model is valid only for the transient state, the fit may not be valid for large values of k. Therefore, BEST fits data for a minimum of five points to a maximum of N_{tot} points, representing the whole dataset. For each data subset containing the first k points,

corresponding to a duration of the experiment equal to t_k, S and K_s are estimated and the time, t_{max} (T), defined as the maximum time for which the transient expression can be considered valid, is determined:

$$t_{\max} = \frac{1}{4(1-B)^2}\left(\frac{S}{K_s}\right)^2 \tag{20}$$

where $(S/K_s)^2$ corresponds to the gravity time defined by Philip (1969). Then, t_{max} is compared with the maximum time of the experimental dataset used for the fit, i.e. t_k. The values of S and K_s are not considered valid unless $t_k \leq t_{max}$. Among all values of S and K_s that fulfil this condition, the S and K_s values corresponding to the largest k (k_{max}) are retained since they are considered more precise.
Yilmaz et al. (2010) introduced a new BEST algorithm, named BEST-intercept. According to these authors, BEST-slope may lead to erroneous K_s values when $i_s \approx AS^2$. In particular, when the estimated AS^2 value exceeds the measured infiltration rate at the end of the experiment, the values obtained for K_s are negative. In the BEST-intercept algorithm, the constraint between S and K_s is defined by using the intercept of the asymptotic expansion in eq.(12c):

$$b_s^{\exp} \approx C\frac{S^2}{K_s} \tag{21}$$

Therefore, b_s^{exp} is estimated by linear regression analysis of the data describing steady-state conditions on the I vs. t plot, and the following relationship is applied to estimate K_s:

$$K_s = C\frac{S^2}{b_s^{\exp}} \tag{22}$$

Combining eqs.(12a) and (22) yields the following relationship to fit onto the transient phase of the experimental cumulative infiltration curve:

$$I(t) = S\sqrt{t} + \left[A + \frac{BC}{b_s^{\exp}}\right]S^2 t \tag{23}$$

Estimation of S follows the same procedure described for BEST-slope. Even in this case, the time validity of the transient infiltration model has to be checked through the calculation of t_{max}. The estimated sorptivity is then used to calculate K_s by eq.(22).
Bagarello et al. (2014a) proposed an alternative algorithm, named BEST-steady, that makes use of the intercept (b_s^{exp}) and the slope (i_s^{exp}) of the straight line fitted to the data describing the steady-state condition of the infiltration experiment. Combining eqs.(17) and (22) yields:

$$i_s^{\exp} = AS^2 + C\frac{S^2}{b_s^{\exp}} \tag{24}$$

and hence S can be calculated as:

$$S = \sqrt{\frac{i_s^{\exp}}{A + \frac{C}{b_s^{\exp}}}} \tag{25}$$

Then, K_s can be estimated using either eq.(17) or (22) or calculated as:

$$K_s = \frac{C i_s^{\exp}}{A b_s^{\exp} + C} \tag{26}$$

BEST-steady does not make any direct use of the data describing the transient state. However, monitoring this stage is necessary to establish when a steady-state condition begins (estimating i_s^{exp}) and how much water infiltrates the soil before reaching this condition (estimating b_s^{exp}) (Angulo-Jaramillo et al., 2016).
The adequacy of the transient infiltration model (eq.12) to fit the experimental data can be quantified by the relative error, E_r, according to the following relationship proposed by Lassabatere et al. (2006):

$$E_r = \sqrt{\frac{\sum_{i=1}^{k} [I^{\exp}(t_i) - I(t_i)]^2}{\sum_{i=1}^{k} [I^{\exp}(t_i)]^2}} \tag{27}$$

According to these authors an $E_r \leq 5.5\%$ denotes an acceptable error for transient cumulative infiltration.

3.3. Applications of BEST methods

The Elsevier's Scopus abstract and citation database of peer-reviewed literature (www.scopus.com) lists a total of 172 citations for Lassabatere et al. (2006), 62 citations for Yilmaz et al. (2010) and 37 citations for Bagarello et al. (2014a).
A summary of some applications of BEST methods is provided in **Table 3.1**. For each mentioned paper, the first column of this table reports the reference. The second column summarizes the main objectives of the investigation. The third column reports the land use. The used BEST algorithms are specified in the fourth column. Finally, the country where the investigation was made is given in the last column. In short, most of the mentioned investigations were carried out in France, Italy and Brazil.

Table 3.1 Investigations making use of the BEST procedure of soil hydraulic characterization

Reference	Aim of the investigation	Land-use	BEST Algorithms	Country
Mubarak et al. (2009b)	Assessing the temporal variability of the hydraulic properties caused by high frequency irrigation during a maize cropping season	Maize	Slope	France
Scalenghe and Ferraris (2009)	Studying pedogenesis processes after ecological engineering interventions	Unconsolidated, finely grained material	Slope	Italy/France
Xu et al. (2009)	Analyzing the vertical variation in soil hydraulic parameters of differently textured soils	Grassland	Slope	Ireland

Cannavo et al. (2010)	Characterizing the heterogeneity of sediment distribution in a stormwater retention/infiltration basin	Urban retention/infiltration basin	Slope	France
Gonzalez-Sosa et al. (2010)	Documenting the spatial variability of soil hydraulic properties linked to pedology and land use. Deriving of rules for the mapping of soil hydraulic properties	Pasture, crop, orchards, broad-leaved and coniferous forest, Small wood sometimes with ivy, clearing	Slope	France
Lassabatere et al. (2010)	Assessing the effect of sediment settlement on water infiltration at both the local and basin scales	Infiltration basins	Slope	France
Mubarak et al. (2010)	Studying variability of soil hydraulic properties with BEST and determining the sensitivity to the infiltration tests	Sorghum, soybean, sunflower, winter wheat, maize	Slope	France
Yilmaz et al. (2010)	Characterizing of the properties of BOF(basic oxygen furnace) slag using beerkan infiltration experiments	Anthropogenic materials	Slope and Intercept	France
Bagarello et al. (2011)	Hydraulic characterization and physical quality evaluation of some Burundian soils	Annual and perennial crops	Slope	Burundi
Nasta et al. (2012)	Studying the impact of p, β, and γ on the results obtained by the beerkan method for three experimental soils	Agricultural soil, sandy soil, and gravely deposit	Slope	France /Ukraine
Van Meir et al. (2012)	Description of an infiltration-drainage test carried out in Chernobyl Pilot Site	Little vegetation	Slope	Ukraine
Xu et al. (2012)	Studying performances of the BEST method and comparing the BEST and Wu methods	Grassland land cover	Slope and Intercept	Ireland
Alagna et al. (2013)	Developing and testing a simplified method to determine the hydrodinamic properties of the surface crust	Citrus orchard, vineyard	Slope	Italy
Goutaland et al. (2013)	Characterizing the in situ hydrodynamic properties of glaciofluvial lithofacies and understanding flow in the unsaturated zone	Stormwater infiltration basin	Slope	France
Yilmaz et al. (2013)	Investigating the hydraulic properties of basic oxygen furnace slag due to weathering and the mechanisms responsible for mineral alteration and their impact on the microstructure	Basic oxygen furnace slag	Intercept	France
Aiello et al. (2014)	Applicability of the BEST procedure in a sandy loam soil. Comparison between BEST and the Simplified Falling Head technique by Bagarello et al. (2004)	Citrus orchard	Slope and Intercept	Italy
Bagarello et al. (2014b)	Comparison between soil hydraulic parameters determined in the laboratory and the field	Citrus orchard, annual crops, vineyard, orchard, olive grove	Slope	Italy
Bagarello et al. (2014c)	Determining of the effect of the height of water application on the hydraulic properties obtained with the SFH technique and the BEST procedure	Citrus orchard and bare soil	Slope and Intercept	Italy
Bagarello et al. (2014d)	Using of the infiltration data to obtain an approximate determination of field-saturated soil hydraulic conductivity	Savanna with acacia trees, cereals, leguminosae, tuberose, banana and coffee trees	Slope	Burundi-Italy

Braud et al. (2014)	Understanding processes triggering flash floods	Vineyard, pasture	Slope	France
Gette-Bouvarot et al. (2014)	Determining the relative influence of sediment deposition and biofilm growth on degradation of the hydraulic properties of infiltration basins designed for groundwater recharge	Excavated infiltration basins filled with sand	Slope	France
Gonzalez-Merchan et al. (2014)	Evaluating the role of spontaneous vegetation on the clogging evolution of a urban infiltration basin	Layer of sediments mainly due to solids brought by stormwater	Slope	France
Marichal et al. (2014)	Studying effects of landscape changes and link between macrofauna and ecosystem services	Pastures, crops, tree plantations, forests	Slope	Colombia and Brazil
Montenegro et al. (2014)	Studying hydrological processes in the Mundau, Pajeú and Tapacurá basins in the State of Pernambuco, Brazil	Pasture	Slope	Brazil
Sales et al. (2014)	Identifying the behaviour of the infiltration capacity of the soil in a representative basin	Sugarcane, pineapple, and atlantic forest.	Slope	Brazil
Souza et al. (2014)	Effect of soil surface crusting on the mechanical and hydrodynamic properties of a cropped soil	Castor bean	Slope	Brazil
Canone et al. (2015)	Proposing a method for the calculation of border-irrigation efficiencies and evaluating the surface irrigation efficiency	Corn	Slope	Italy
Di Prima (2015)	Developing a compact infiltrometer for automatically collect infiltration data	Citrus orchard	Slope	Italy
Reyes Gómez et al. (2015)	Influence on hydraulic properties of different native and exotic plant species covers	E. lehmanniana, E. superba, B. gracilis, D. californica	Slope	Mexico
Siltecho et al. (2015)	Comparing unsaturated soil hydraulic properties obtained with different measurement methods (beerkan, disc infiltrometer, evaporation, pedotransfer function) under different land uses	Forest, ruzi grass, and rubber tree	Slope	Thailand
Alagna et al. (2016b)	Comparing saturated soil hydraulic conductivity, K_s, determined by different infiltrometer techniques	Spontaneous, sparse herbaceous vegetation	Slope, Intercept and Steady	Italy
Bièvre et al. (2016)	Relating variations in landslide velocities and geophysical properties to hydrogeological characteristics	Landslide	Slope	France
Castellini et al. (2016)	Assessing the effect of land use changes on two hillslopes of a Mediterranean catchment by indicators of soil physical quality quantitatively linked to soil hydraulic properties	Oak forest, mediterranean maquis and grassland	Slope and Intercept	Italy
Coutinho et al. (2016)	Hydraulic characterization and assessing the hydrological behavior of a permeable pavement	Pilot permeable pavement	Slope, Intercept and Steady	Brazil
Cullotta et al. (2016)	Testing the suitability of the BEST procedure to reproduce a laboratory based soil physical quality assessment	Holms and pubescent oaks forest and pasture	Steady	Italy
Di Prima et al. (2016)	Checking the usability of the device to automatize the beerkan infiltration experiment and analyzing the infiltration data to characterize soils	Citrus orchard, bare soil and an infiltration basin.	Slope, Intercept and Steady	Italy-France

Khaledian et al. (2016)	Identification of the effects of tillage on some soil properties	Small kiwi fruit garden under drip irrigation	Slope	Iran
Yang et al. (2016)	Assessing the effects of Napier grass management on soil hydrologic functions	Napier grass	Slope	China
Braud et al. (2017)	Mapping the variation in saturated soil hydraulic conductivity at regional scale	Forest and crops	Slope	France
Leite et al. (2017)	Comparing soil hydraulic properties and erosion for four different cover types	Abandoned pasture, forests	Steady	Brazil
Souza et al. (2017)	Assessing the soil physical quality and the spatial variability of physical and hydraulic soil properties	Fluvisol	Slope	Brazil
Castellini et al. (2018)	Testing applicability of the BEST procedure to estimate the water retention curve in four soils	Corn, durum wheat, citrus orchard	Slope, Intercept and Steady	Italy
Di Prima et al. (2018b)	Characterization of lateral preferential flow at the hillslope scale	Spontaneous grass	Steady	Italy
Di Prima et al. (2018c)	Investigating the impacts of conventional and organic farming management practices on soil physical quality under citrus crops	Orchards	Steady	Spain
Lozano-Baez et al. (2018)	Understanding the effect of forest restoration on K_s	Pasture, restored forest, and remnant forest	Steady	Brazil
Alagna et al. (2019)	Testing of the ability of BEST method to estimate saturated hydraulic conductivity of crusted and non-crusted soils	Mediterranean vineyard	Slope	Italy
Bagarello et al. (2019)	Improving knowledge of the factors that control variability of infiltration-based determinations of saturated hydraulic conductivity in clayey soils	Sowing and meadow-pasture	Steady	Italy
Batista et al. (2019)	Investigating the response of several physical properties and organic carbon in a sandy soil before and after grazing	Rain-fed continuous grazing system cultivated with Brachiaria decumbens	Steady	Brazil
Bouarafa et al. (2019)	Evaluating infiltration capacity and identifying possible malfunctioning of four urban stormwater management structures through the study of their hydrodynamic parameters	Grass-covered embankment, impervious parking lot, drainage ditch, vegetated hollow core slab	Slope, Intercept and Steady	France
Castellini et al. (2019a)	Assessing the impact of alternative soil management strategies on physical and hydraulic properties of fine textured soils	Durum wheat	Slope, Intercept and Steady	Italy
Castellini et al. (2019b)	Spatialization of soil hydraulic properties	Durum wheat	Steady	Italy
Cheik et al. (2019a)	Using X-ray CT to determine how soil macropores impact water infiltration.	Deciduous forest	Slope	Vietnam
Cheik et al. (2019b)	Determining how termite foraging activity impacts soil aggregation and water infiltration	Tropical dry-thorn forest.	Slope	India
Cheik et al. (2019c)	Determining whether termite foraging activity varies with the quality of the litter in a southern-Indian forest	Deciduous forest	Slope	India
Lassabatere et al. (2019b)	Developing a Beerkan Multi-Run (BMR) procedure for the simultaneous application of a set of 10 beerkan experiments	Quercus, Fagus	Slope, Intercept and Steady	Netherlands

Lassabatere et al. (2019c)	Introducing BEST-2K and testing it with both numerical and experimental data	Pasture, forest, orchard	Slope, Intercept and Steady	Italy
Silva Ursulino et al. (2019)	Combining Hydrus-1D with BEST method to estimate the temporal variability of soil moisture	Experimental river basin	Slope and Intercept	Brazil
Yilmaz et al. (2019)	Investigating the hydraulic properties of several technosols	Technosols	Slope, Intercept and Steady	France
Bagarello et al. (2020)	Checking short-term (hourly or daily) changes in soil structure-dependent hydraulic parameters associated with subsequent infiltration runs	Citrus orchard	Steady	Italy
Basant et al. (2020)	Testing the hypothesis that the drainage-woodlands are still subsidized by runoff generated from upslope areas following large rain events	Different species of woody plant and grass	Steady	Texas
Castellini et al. (2020)	Investigating the impact of tillage management on soil physical and hydraulic properties	Olive orchards	Steady	Italy
Di Prima et al. (2020)	Identifing the incidence and extent of preferential flow combining time-lapse of Ground-Penetrating Radar (GPR) surveys with automatized single-ring infiltration	Stormwater infiltration basin,	Slope, Intercept and Steady	France
Durand-Bessart et al. (2020)	Analyzing of interactions amongst shade trees, coffee plants, the coffee foliar disease complex and soil characteristics	Shade Trees and coffee plants	Slope	Nicaragua
Lavrnić et al. (2020)	Detecting modifications in hydrologic and hydraulic behavior in surface flow constructed wetland after 17 years of constant operation	Surface flow constructed wetland	Slope, Intercept and Steady	Italy
Lozano-Baez et al. (2020)	Comparing unsaturated and saturated soil hydraulic conductivity determined with simple and low-cost field infiltration methods (MDI and beerkan)	Pasture, 9-year-old restored forest, and remnant forest	Steady	Brazil
Palácio Filho et al. (2020)	Characterization of the hydrodynamic and hydrodispersive properties of an irrigated soil	Atriplex nummularia Lindl, secondary vegetation with shrubs and grasses, irrigated banana	Slope	Brazil

3.4. Characterization of non-rigid soils by single-ring infiltration experiments

Soil surface alteration is a major cause of decreased infiltration rates and increased surface runoff during a rainstorm. The general objective of the PhD research activity was to verify if single-ring infiltration experiments can be adapted in the perspective to obtain realistic soil data for simulation of hydrological processes such as rainfall excess generation. At this purpose, it was initially taken into account that the height of water application could be changed to simulate rainfall effects on soil surface and hence to explain surface runoff generation phenomena during intense rainfall events. In the past, BEST methods with different heights of water application appeared as good method to characterize soils in a hydrological perspective (Bagarello et al., 2014c, 2017; Alagna et al., 2016a; Di Prima et al., 2017). In particular, performing high runs, that is pouring water on the soil from a relatively high height with respect to the infiltration surface, determined a reduced ability of the soil to transmit water, which appears an expected phenomenon when rainfall excess is formed (Assouline and Mualem, 2002, 2006). Changes in soil surface were consistent with a pore size reduction, pore

clogging and compaction phenomena. According to the work performed in the past by the soil physics research group of the University of Palermo, the methodology to perform a single-ring infiltration experiment could be adapted to the hydrological process to be explained or simulated. In particular, the height of water application (low, high) should vary with the intended use of the K_s data. If the objective of the field campaign is to obtain data usable to explain surface runoff generation phenomena during intense rainfall events, the most appropriate choice should be performing BEST experiments with a high run because this procedure is expected to yield K_s values similar to those compatible with the occurrence of measurable runoff (Di Prima et al., 2017). A low run, that is water applied close to the infiltration surface, is more appropriate to determine the saturated conductivity of a soil that is not directly impacted by rainfall. The height from which water is poured could be expected to have more appreciable effects on K_s in initially dry soil conditions although the collected information was limited to a single soil (Alagna et al., 2016a). In any case, height effects appear also detectable in initially wet to very wet soil conditions (Bagarello et al., 2017).

A brief overview of the three developed lines of research during this PhD research activity is provided in the following. The published papers were reported in the **Appendices B, C** and **D**.

Soil surface sealing is a major cause of decreased infiltration rates and increased surface runoff during a rainstorm. The objective by Di Prima et al. (2018a) (**Appendix B**) was to quantify the effect of surface sealing on infiltration for three layered soils with different textures for the upper layer and investigate the capability of BEST procedure to catch the formation of the seal and related consequences on water infiltration. Rainfall experiments were carried out to induce the formation of the seal. beerkan infiltration runs were also carried out pouring water at different distances from the soil surface (BEST-H versus BEST-L runs, with High and Low water pouring heights, respectively) for the same type of layered soils. The saturated soil hydraulic conductivity, K_s, was determined from both rainfall simulation and beerkan infiltration experiments. Rainfall simulations carried out on soil layers having different depths allowed to demonstrate that infiltration processes were mainly driven by the seal and that K_s estimates were representative of the seal. Soil sealing induced an increase in soil bulk density by 38.7 to 42.1%, depending on the type of soil. Rainfall-deduced K_s data were used as target values and compared with those estimated by the beerkan runs. BEST-H runs proved to be more appropriate than BEST-L runs, those last triggering no seal formation. The predictive potential of the three BEST algorithms (BEST-slope, BEST-intercept and BEST-steady) to yield a proper K_s estimate for the seal was also investigated. BEST-slope yielded negative K_s values in 87% of the cases for BEST-H runs. Positive values were obtained in 100% of the cases with BEST-steady and BEST-intercept. However, poorer fits were obtained with the latter algorithm. The comparison of the K_s estimates with those deduced by rainfall simulation experiments allowed to identify the BEST-steady algorithm with BEST-H run as the best combination. More specifically, this algorithm limited the hydraulic characterization to the stabilized phase, i.e., when the seal was fully developed, avoiding uncertainties due to the seal formation during the early phase of the infiltration process. The other two algorithms that account for transient data were perturbed by the effect of the seal progressive formation and its related impacts on the infiltration. The repeated impact of water drops during a BEST-H run induced the formation of a seal layer having similar hydraulic properties with those obtained by the simulated storms. Infiltration was determined by the first few millimeters of the soil and the BEST-H runs had possibly accounted for the main physical features characterizing the phenomenon of induced soil sealing. The method proposed in this study could be used to easily measure the seal's saturated hydraulic conductivity of an initially undisturbed bare soil directly impacted by water with minimal experimental efforts, using small volumes of water and easily transportable equipment. In the future, the proposed methodology may be applied for different rainfall intensities and durations, taking into account that rainfall characteristics are among the major factors affecting the dynamics of seal formation.

The premises of the investigation by Alagna et al. (2018) (**Appendix C**) were that i) assessing how the infiltration process depends on the water impact energy improves interpretation of hydrological processes, ii) impact energies vary with the height of water pouring, i.e. the distance between the

water delivery point and the soil surface, and iii) the effects of the height of water pouring on infiltration in an initially near saturated soil can be tested in the field by two repeated beerkan infiltration runs separated by a short pause (minutes) and using both low (non-perturbing) and high (perturbing) heights of water application. The double two-stage beerkan run methodology was applied in two soils. The infiltration rate at the end of the perturbing stage of the experiment was 0.2-0.3 (sandy-loam soil) and 0.15 (loam soil) times that obtained with the initial, non-perturbing stage whereas, without any perturbing effect, infiltration rates at the end of the second run were 0.5 times those at the end of the first run. Therefore, the methodology distinguished between a decrease in infiltration rate due to water redistribution during the pause and that attributable to soil surface perturbation. Maintaining a small depth of water (10 mm) on the infiltration surface was not an alternative to the classical beerkan run for the non-perturbing stage of the experiment since two times higher infiltration rates were measured with a greater hydrostatic pressure. In conclusion, the relationship between infiltration into an initially near saturated soil and the energy of the applied water can be determined directly in the field at any time with a simple and parsimonious experiment. This circumstance could improve soil hydraulic characterization for interpreting and simulating hydrological processes. Taking into account that the measured infiltration rates are commonly used to estimate soil hydrodynamic parameters with a variety of methods, it is plausible to believe that the investigation by Alagna et al. (2018) could open some interesting perspective with reference to both interpretation and simulation of hydrological processes. In particular, it demonstrated that a simple experiment can be carried out directly in the field, i.e. in a real world situation, to establish a link between the energy of the applied water and the measured infiltration process in an initially near-saturated soil, i.e. in a condition particularly favorable to rainfall excess, and hence runoff, generation. Consequently, the collected experimental information could allow us to derive soil hydraulic properties that reflect the appropriate conditions for simulating a specific hydrological process even considering that, with the applied double two-stage beerkan run methodology, effects of different energy levels of the applied water can be tested by simply changing water pouring height. There are encouraging signs on the possibility to use the methodology to discriminate between soils. Spatial variability issues should be developed in the future to establish if a relatively small sample size for a given treatment, as suggested by this investigation, is generally appropriate to get reliable data.

In the investigation by Auteri et al. (2020 (**Appendix D**), beerkan infiltration runs carried out on a loam (AR) and a silty-clay (RO) soil were adapted in the perspective to obtain usable soil data to predict rainfall partition into infiltration and rainfall excess. In particular, the initially nearly dry soil was sampled with different water volumes (15 or 30) and heights of water application (low, L, 0.03 m, and high, H, 1.5 m), and the BEST-steady algorithm was applied to determine sorptivity, S, and K_s. The H runs altered the surface soil layer more than the L runs but the response of the two soils to disturbance was different. For the AR soil, deterioration of the surface layer was almost complete close to the end of the run while, for the RO soil, it was concluded after applying one third of the overall used water volume. The least soil perturbing experiment (15L), that was carried out with the commonly recommended experimental protocol, yielded high S (91-118 mm/h$^{0.5}$) and K_s (88-294 mm/h) values at the two sites, likely incompatible with formation of any rainfall excess. A soil perturbing experiment (30H) yielded significantly and substantially smaller S (26-40 mm/h$^{0.5}$) and K_s (4-6 mm/h) values, that appeared potentially compatible with formation of rainfall excess. The gravitational potential energy, E_p, of the water used for the infiltration run explained most of the variance of both K_s and S. In conclusion, the infiltration run can be adapted in an attempt to induce a soil disturbance likely similar to that expected for a rainfall producing runoff. In a relatively dry initial status, complete deterioration can require less water for a silty-clay soil than a loam soil. The saturated soil hydraulic conductivity is more sensitive than soil sorptivity to the applied experimental methodology. Finally, the gravitational potential energy of the applied water could be used to establish a link between the hydrological process that has to be explained and a soil hydraulic characterization appropriate to reach the desired objective. In a hydrological perspective, it also seems advisable to improve our knowledge on the short term modifications of K_s and S in an attempt to

verify if, under what experimental conditions and to what level they stabilize when a disturbing run is carried out. The lowest possible S and K_s values could be viewed as a sort of hydrologically relevant index since they describe the most favorable condition to runoff occurrence. According to this investigation, these developments should not be excessively demanding from an experimental point of view. An alternative method to characterize a soil in a runoff prone situation is to make the field campaign with common experimental protocols after a sealed layer has fully developed. Establishing a comparison between the two options (inducing disturbance, working on naturally altered soil) is obviously advisable although the latter option places constraints on the time when the experiment can be performed.

Appendix B:

Catena 167 (2018) 373–384

Contents lists available at ScienceDirect

Catena

journal homepage: www.elsevier.com/locate/catena

Laboratory testing of Beerkan infiltration experiments for assessing the role of soil sealing on water infiltration

S. Di Prima[a,*], P. Concialdi[b], L. Lassabatere[c], R. Angulo-Jaramillo[c], M. Pirastru[a], A. Cerdà[d], S. Keesstra[e]

[a] Agricultural Department, University of Sassari, Viale Italia, 39, 07100 Sassari, Italy
[b] Department of Agricultural, Food and Forest Sciences, University of Palermo, Viale delle Scienze, 90128 Palermo, Italy
[c] Université de Lyon, UMR5023 Ecologie des Hydrosystèmes Naturels et Anthropisés, CNRS, ENTPE, Université Lyon 1, 3 rue Maurice Audin, 69518 Vaulx-en-Velin, France
[d] Department of Geography, University of Valencia, Blasco Ibáñez, 28, 46010 València, Spain
[e] Team Soil Water and Land Use, Wageningen Environmental Research, Wageningen UR, Droevendaalsesteeg 3, 6700 AA Wageningen, The Netherlands

ARTICLE INFO

Keywords:
Soil sealing
Rainfall simulation
Beerkan infiltration experiment
BEST algorithms
Saturated soil hydraulic conductivity

ABSTRACT

Soil surface sealing is a major cause of decreased infiltration rates and increased surface runoff and erosion during a rainstorm. The objective of this paper is to quantify the effect of surface sealing on infiltration for 3 layered soils with different textures for the upper layer and investigate the capability of BEST procedure to catch the formation of the seal and related consequences on water infiltration. Rainfall experiments were carried out to induce the formation of the seal. Meanwhile, Beerkan infiltration runs were carried out pouring water at different distances from the soil surface (BEST-H versus BEST-L runs, with a High and Low water pouring heights, respectively) for the same type of layered soils. Then, we determined saturated soil hydraulic conductivity, K_s, values from rainfall simulation and Beerkan infiltration experiments. Rainfall simulations carried out on soil layers having different depths allowed to demonstrate that infiltration processes were mainly driven by the seal and that K_s estimates were representative of the seal. Mean K_s values, estimated for the late-phase, ranged from 13.9 to 26.2 mm h^{-1}. Soil sealing induced an increase in soil bulk density by 38.7 to 42.1%, depending on the type of soil. Rainfall-deduced K_s data were used as target values and compared with those estimated by the Beerkan runs. BEST-H runs proved more appropriate than BEST-L runs, those last triggering no seal formation. The predictive potential of the three BEST algorithms (BEST-slope, BEST-intercept and BEST-steady) to yield a proper K_s estimate for the seal was also investigated. BEST-slope yielded negative K_s values in 87% of the cases for BEST-H runs. Positive values were obtained in 100% of the cases with BEST-steady and BEST-intercept. However, poorer fits were obtained with the latter algorithm. The comparison of K_s estimates with rainfall-deduced estimates allowed to identify BEST-steady algorithm with BEST-H run as the best combination. The method proposed in this study could be used to easily measure the seal's saturated hydraulic conductivity of an initially undisturbed bare soil directly impacted by water with minimal experimental efforts, using small volumes of water and easily transportable equipment.

1. Introduction

Droplet impact during a rainfall event can modify surface soil structure and determines the splash erosion (e.g., Assouline and Mualem, 2002; Fernández-Raga et al., 2017). The compaction of fine material from the disrupted and dispersed aggregates may form a thin and highly dense layer (Mualem and Assouline, 1989). This surface sealing is a major cause of decreased infiltration rates and increased surface runoff and erosion during a rainstorm (Moldenhauer and Long, 1964). The formation of seals is dominated by a wide variety of factors involving soil properties, rainfall characteristics, and flow conditions (Assouline, 2004). The determination of seal hydraulic properties, as well as their evolution over time, is one of the key issues in properly describing water flow in soils (Augeard et al., 2007).

There are two main methodological approaches to measure the infiltration of the soil: rainfall simulations and water infiltration techniques using either ring or tension disk infiltrometers (Angulo-Jaramillo et al., 2016). Among the water infiltration techniques, the Beerkan

* Corresponding author.
E-mail address: sdiprima@uniss.it (S. Di Prima).

https://doi.org/10.1016/j.catena.2018.05.013
Received 16 October 2017; Received in revised form 11 May 2018; Accepted 14 May 2018
0341-8162/ © 2018 Elsevier B.V. All rights reserved.

method consists in infiltrating water through a ring under ponded conditions (Braud et al., 2005). Lassabatere et al. (2006) developed the BEST algorithm (Beerkan estimation of Soil pedoTransfer functions) to derive the whole set of soil hydraulic parameters related to water retention and unsaturated hydraulic conductivity curves from Beerkan experimental data. Ever since, three main algorithms were developed on the basis of this first version: BEST-slope (Lassabatere et al., 2006), BEST-intercept (Yilmaz et al., 2010) and BEST-steady (Bagarello et al., 2014a). The three algorithms make use of the same input data, but differ from the way they fit experimental data to the models for transient and steady states (Angulo-Jaramillo et al., 2016; Lassabatere et al., 2013). These differences allow one of the three methods to perform better according to the kind of soil. Beerkan runs and BEST calculations, also referred to as BEST procedure, are spread worldwide for the characterization of the hydraulic properties of uniform soils (Angulo-Jaramillo et al., 2016).

To study seal formation, most research studies in the last decades were performed with rainfall simulations, either during its dynamic stage or after it has already reached its final stage, when the seal layer is fully developed (e.g., Assouline, 2004; Baumhardt et al., 1990). Rainfall experiments are an attractive tool because the precision, accuracy and the possibility of high repetition rate offer a systematic approach to address the different factors that influence the studied processes (Iserloh et al., 2013). Besides, the use of water infiltration techniques for assessing soil sealing impacts on water infiltration is still largely unknown, notwithstanding that these methods have a noticeable practical interest (Bagarello et al., 2014b). Moreover, the use of ring or tension disk infiltrometers still presents a number of problems related both to theory and practice for data collected on heterogeneous layered soils (Angulo-Jaramillo et al., 2000); which is the case of sealed soils. Under such conditions, the steady-state water flow analysis based on usual analysis procedures are generally found to be inadequate (Logsdon and Jaynes, 1993). Besides, infiltrometer data are generally analyzed by assuming that the sampled porous medium is rigid, homogeneous, isotropic and uniformly unsaturated before the run (Alagna et al., 2013, 2017; Lassabatere et al., 2006, 2009; Reynolds and Elrick, 1990). However, when soil sealing occurs, the soil shifts from uniform to finely layered state. Lastly, the regular Beerkan runs that apply water at soil surface do not trigger any soil sealing; which fails to represent the real soil hydraulic behavior during intense rainfall events.

Recently, Di Prima et al. (2017) adapted the BEST infiltration procedure to mimic rainfall simulation experiments. These authors adapted the height of application of water (still maintaining ponding at surface) for mimicking the impacts of raindrops on soil surface. They demonstrated that both rainfall simulation experiments and modified Beerkan runs, carried out by applying water at a relatively large distance from the soil surface (BEST-H procedure), determine a similar degree of soil compaction and mechanical breakdown of aggregates, but the second ones are much easier to conduct. Moreover, the BEST-H procedure is easy to apply over large areas since the equipment to be transported is minimal and small volumes of water are enough to conduct an infiltration run. BEST-H runs can simply be replicated to develop a large number of sampling points, which means that intensive sampling over a large or relatively large areas is feasible (Gonzalez-Sosa et al., 2010). BEST procedures also allow to survey remote areas, which are difficult for other methods with heavy, expensive, time spending procedures and labor high costs (Bagarello et al., 2011). However, the comparison of BEST-H procedure with well tested methods for K_s estimation, such as rainfall simulation experiments, is necessary to experimentally assess the predictive performances of BEST for the case of soil sealing. Indeed, in the scientific literature there is no exhaustive testing of the relative performances of the BEST algorithms with regards to the specific case of layered and sealed soils.

The objectives of this research were to: (i) measure the effect of surface sealing on infiltration at the surface of three bare soils with different textures exposed to the direct impact of raindrops, (ii) evaluate the influence of the thickness of the upper layer of soil on seal formation and related impacts on water infiltration, (iii) compare ponded infiltrometer runs (Beerkan runs) with rainfall simulation experiments in terms of saturated soil hydraulic conductivity for the case of soil sealing, and (iv) investigate which BEST algorithm can be satisfactorily adopted to properly estimate K_s of the seal.

2. Material and methods

2.1. Soil sampling

Soil materials used in this study were taken from Ap horizons of three Sicilian sites with different physical properties (Bagarello et al., 2014a). According to the USDA classification, a sandy-loam (SL) soil and a clay-loam (CL) soil were sampled at the Department of Agricultural, Food and Forest Sciences of the Palermo University. A clay (C) soil was sampled at the experimental station for soil erosion measurement at Sparacia (University of Palermo), approximately 100 km south of Palermo. Particle size distribution (PSD) was determined following H_2O_2 pre-treatment to eliminate organic matter and clay deflocculation using sodium hexametaphosphate and mechanical agitation (Gee and Bauder, 1986). In particular, fine size fractions were determined by the hydrometer method, whereas the coarse fractions were obtained by mechanical dry sieving. The soil organic carbon content, OC (%), was determined by the Walkley–Black method (Nelson and Sommers, 1996). Then, the soil organic matter content, OM (%), was estimated using the van Bemmelen conversion factor of 1.724 (Van Bemmelen, 1890). Each soil was air-dried, ground to an aggregate or particle diameter slightly larger than 2 mm, and sieved through a 2-mm mesh (Bradford et al., 1987). The measured soil physical properties are summarized in Table 1.

2.2. Rainfall simulation experiments

Many laboratory as well as field studies have been conducted over more than five decades on the formation of seals at the surface of bare soils exposed to the direct impact of raindrops (e.g., Bradford et al., 1987; Lado et al., 2004; Tackett and Pearson, 1965; Touma et al., 2011). Laboratory experiments carried out on packed samples have the clear advantage to overcome the effects of soil heterogeneities and spatial variability on K_s measurements (Liu et al., 2011). In this investigation, we used the rainfall simulator of the Kraijenhoff van de Leur Laboratory for Water and Sediment Dynamics at Wageningen University, the Netherlands. A detailed description of the rainfall simulator is given in Lassu et al. (2015). A Lechler nozzle (nr. 460.788) was used to apply water from a 3.85-m height. In this study, a total of thirty storms were simulated at rainfall intensity $R = 60\ \mathrm{mm\ h^{-1}}$. The experiments were carried out on small rectangular soil plots encased in a transparent plexiglass box. The box set-up had two compartments: a soil compartment ($1.3 \times 10^{-2}\ \mathrm{m^2}$ plot area), and a runoff collection

Table 1
Coordinates, soil textural classification, clay (0–2 μm), silt (2–50 μm), and sand (50–2000 μm) content (in %) (USDA classification system) in the 0–10 cm depth range, soil organic matter (*OM* in %) content, dry soil bulk density (ρ_b in $\mathrm{g\ cm^{-3}}$), and initial volumetric soil water content (θ_0 in $\mathrm{cm^3\ cm^{-3}}$), for the three sampled soils. Standard deviations are indicated in parentheses.

Coordinates	33S 355,511 E 4,218,990 N	33S 355,341 E 4,219,012 N	33S 391,172 E 4,166,165 N
Textural classification	Sandy-loam	Clay-loam	Clay
Clay	17.6 (1.9)	29.9(2.8)	71.5 (1.8)
Silt	29.8 (2.8)	34.1(1.8)	23.6 (1.4)
Sand	52.6 (4.7)	36.0(1.2)	4.9 (0.8)
OM	3.9(0.7)	2.3(0.1)	1.1(0.6)
ρ_b	0.936 (0.008)	0.984 (0.018)	1.065 (0.029)
θ_0	0.062 (0.001)	0.039 (0.001)	0.059 (0.002)

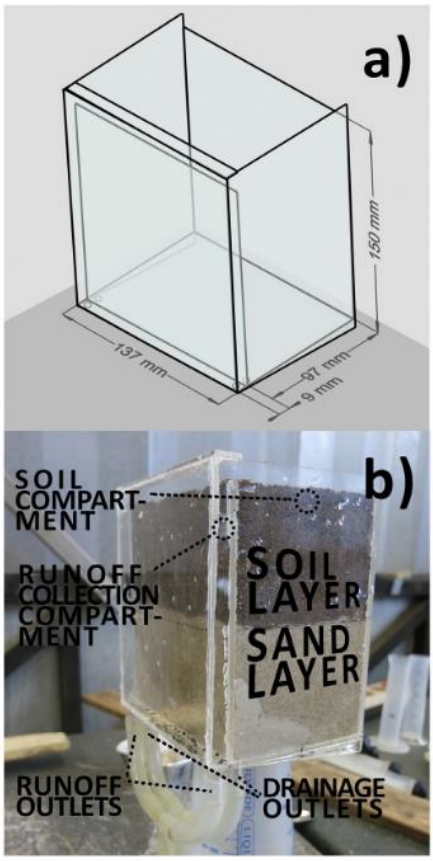

Fig. 1. (a) Schematic diagram and (b) set-up of the rainfall box.

compartment, which was covered to prevent direct access of rainfall (Fig. 1). This compartment was aimed at receiving runoff water over the soil. Each compartment had its own outlet to measure water runoff at surface and infiltration through the whole soil profile.

Following the procedure suggested by Bradford et al. (1987), the soil was compacted into the rainfall box and initial bulk density, determined from mass of soil and air-dried moisture content (Table 1). Soil material was added until the soil was levelled with the top of the box.

Then, the box was placed at a 9% slope under the laboratory simulator. Surface runoff from the runoff collection compartment was collected at 3 min intervals from the moment at which the runoff started to run out of the outlets until the differences in the measured runoff rates became negligible, signaling a steady-state process. The steady-state runoff rates, r (mm h^{-1}), were estimated considering the runoff rates of the last stage of the experiments, describing the steady-state phase of the process. Then, the infiltration curves were drawn by subtracting the runoff rates from the rainfall intensity (Di Prima et al., 2017). At steady state, when the soil surface is submitted to water ponding, the 1D vertical infiltration rate approaches the saturated soil hydraulic conductivity (Reynolds et al., 2000). Therefore, K_s was estimated from the rainfall simulation experiments as follows (White et al., 1989):

$$K_s = R - r \tag{1}$$

where R and r stand respectively for imposed rainfall rate and runoff rate. After each rainfall run the thickness of the seal layer was measured using a ruler.

Two different thicknesses of the soil layer were considered in this investigation. In particular, fifteen rainfall simulations (RS experiments), five for each soil, were carried out placing a 75-mm layer of soil over a 75-mm layer of sand in the soil compartment of the rainfall box (Fig. 1b). After visually evaluating the thickness of the seals formed during the RS experiments (Fig. 2), we settled up another fifteen rainfall simulations placing a thin (RS-T experiments) layer of soil (~1–2 mm deep) over a ~148–149 mm layer of sand. Those latter experiments were designed in order to obtain, at the end of the simulation, a fully developed seal made of the studied soil above the sand (Fig. 2). For this system, we consider that the contrast in hydraulic conductivity between the seal and the sand below is so high that the efficient hydraulic conductivity of the layered system approaches that of the seal alone, as already suggested for stratified media (e.g., Lassabatere et al., 2010; Slimene et al., 2017). In other words, the system seal above sand mimic perfectly the behavior of the seal alone.

This strategy has two advantages. Firstly, this strategy allowed the easily sampling of the seal for bulk density measurement. Before sampling, we visually verified that the seals formed over each studied soil and the sand were comparable and thus with similar physical and hydraulic properties. A sample of the seal layer was collected after each RS-T run using a 50-mm diameter ring. The risk of compaction or shattering of the sampled soil volume was minimized since the thin seal layer could be easily separated from the underlining sand layer, in opposite to the case of RS experiments. These samples were used to determine the dry bulk density of the seal layer. Moreover, this strategy was adopted in order to evaluate the influence of the seal at the late-phase of the infiltration process. In addition, we may expect that for any layered system, the efficient hydraulic properties may approach that of the seal, as soon as the seal is entirely formed and exhibits a much lower saturated hydraulic conductivity. In such case, final infiltration rates for both RS and RS-T experiments should be similar. The comparison of their values between RS and RS-T experiments allows the assessment of such hypothesis.

2.3. Concept of the BEST algorithms

BEST algorithms consider soil hydraulic properties follow van Genuchten (1980) model with Burdine (1953) condition for water retention curve and Brooks and Corey (1964) capillary function for hydraulic conductivity curve:

$$\frac{\theta - \theta_r}{\theta_s - \theta_r} = \left[1 + \left(\frac{h}{h_g}\right)^n\right]^{-m} \tag{2a}$$

$$m = 1 - \frac{1}{n} \tag{2b}$$

$$\frac{K(\theta)}{K_s} = \left(\frac{\theta - \theta_r}{\theta_s - \theta_r}\right)^{\eta} \tag{3a}$$

$$\eta = \frac{2}{m \times n} + 2 + p \tag{3b}$$

where θ (cm^3 cm^{-3}) is the volumetric soil water content, θ_r and θ_s are residual and saturated water contents, h (mm) is the water pressure head, h_g (mm) is the scale parameter for water pressure head, K (mm h^{-1}) is the soil hydraulic conductivity, K_s (mm h^{-1}) is the saturated hydraulic conductivity, n, m and η are shape parameters, and p is a tortuosity parameter taken equal to unity in agreement with Burdine condition (Lassabatere et al., 2006). BEST considers that residual water content is negligible, leading to $\theta_r \approx 0$. The three different BEST algorithms estimate the shape parameters n, m and η from the particle size distribution, using the same pedotransfer functions described in

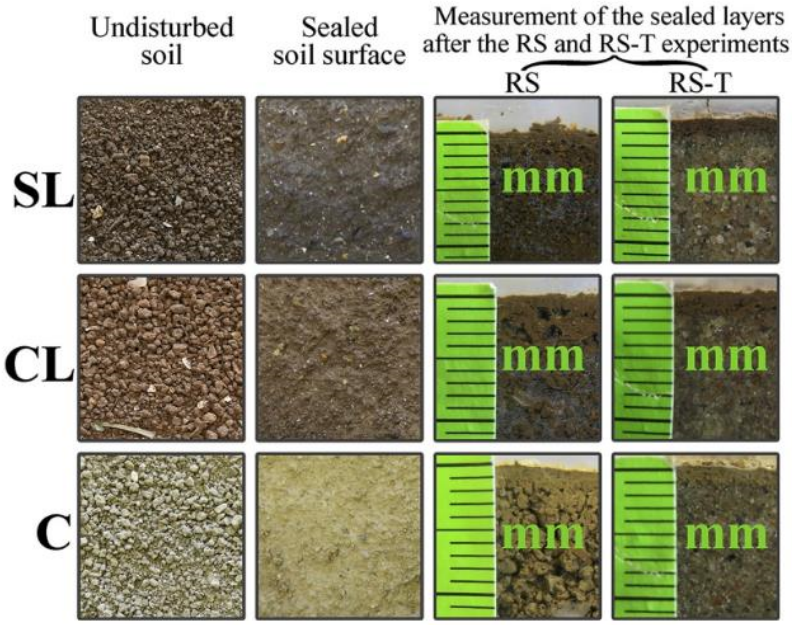

Fig. 2. Pictures of the undisturbed and sealed soil surfaces before and after the rainfall simulation experiments and measurement of the sealed layers after the rainfall simulation experiments carried out on thick (RS) and thin (RS-T) soil layers for the three soils (sandy-loam, SL, clay-loam, CL, and clay, C).

Lassabatere et al. (2006). And conversely, they differ from the way to estimate scale parameters h_g and K_s from cumulative infiltration data (see Appendix A). However, all the algorithms rely on the same mathematical framework for modelling Beerkan runs.

2.4. Beerkan infiltration runs and different heights of water pouring

A total of 30 Beerkan infiltration experiments were carried out, ten for each sampled soil, in laboratory plexiglass cylinders (200 mm diameter and 300 mm high). The cylinders were packed with the soil material following the same procedure adopted to fill the rainfall box. According to Bagarello et al. (2014a), a relatively small diameter of the ring (i.e., 50 mm) was chosen to detect more clearly the potential effects of soil disturbance due to water. Rings were gently inserted to a depth of 10 mm to prevent soil compaction and water leaking at surface. Following the BEST procedure suggested by Lassabatere et al. (2006), a known volume of water (17 mL) was poured in the ring at the start of the measurement and the elapsed time during the infiltration was measured. When the amount of water had completely infiltrated, an identical amount of water was poured into the ring, and the time needed for the water to infiltrate was logged. The procedure was repeated until the difference in infiltration time of the poured water volumes became negligible, signaling a practically steady-state infiltration. For each studied soil, five runs were carried out by pouring water at a small height above soil surface, i.e. at a height of 30 mm (Low, BEST-L runs). The energy was dissipated with the fingers, in an attempt to minimize soil disturbance due to water application, as commonly suggested (Reynolds, 1993). Water was applied from 250 mm height for the other 5 runs (High, BEST-H runs). In this case, the soil surface was not shielded to maximize possible damaging effects of water impact. For each infiltration run, cumulative infiltration, I (mm), was plotted against time, t (s), and a linear regression line was fitted to the last data points, describing the near steady-state conditions, in order to estimate the experimental steady-state infiltration rate, i_s (mm h^{-1}), and the associated intercept, b_s (mm). Then, the three alternative BEST algorithms were applied to estimate the saturated soil hydraulic conductivity, K_s (mm h^{-1}). θ_s was assumed to coincide with soil porosity, ε ($\theta_s = \varepsilon$), as usually suggested by many authors (e.g., Coutinho et al., 2016; Di Prima, 2015; Mubarak et al., 2010; Xu et al., 2009), since it is not expected to appreciably affect the BEST K_s predictions (Di Prima et al., 2017). For all calculations, the representative PSD, ρ_b, ε, θ_0 and θ_s values of each soil were obtained by averaging the individual determinations (Table 1).

2.5. Data analysis

According to the Lilliefors (1967) test, the hypothesis of normal distribution of the untransformed K_s data was not rejected for all the datasets. Therefore, K_s data were assumed to be normally distributed, and were summarized by calculating the mean, and the associated coefficient of variation, CV. Statistical comparison between two sets of data was conducted using a two-tailed t-test, whereas the Tukey Honestly Significant Difference test was applied to compare three or more sets of data. The related p-values were computed and compared to the level of significance of 0.05. Since a fitting of the infiltration model to the transient data is required with BEST-slope and BEST-intercept, the accuracy of these fits were assessed on the basis of the consistency of the model shape and the relative errors, as suggested by Lassabatere et al. (2006):

$$Er = \sqrt{\frac{\sum_{i=1}^{k} [I_{exp}(t_i) - I_{est}(t_i)]^2}{\sum_{i=1}^{k} I_{exp}(t_i)^2}} \quad (4)$$

where I_{exp} and I_{est} stand for experimental and estimated values for water infiltration.

Table 2
Minimum (Min), maximum (Max), mean, and coefficient of variation (CV, in %) of the saturated soil hydraulic conductivity, K_s (mm h^{-1}), values obtained by rainfall simulation experiments carried out on thick (RS) and thin (RS-T) soil layer for the three soils (sandy-loam, SL, clay-loam, CL, and clay, C) (sample size for each method, $N = 5$).

Site	Method	Min	Max	Mean	CV
SL	RS	21.4	31.9	25.5 a	18.1
	RS-T	24.2	27.7	26.2 a	5.4
CL	RS	15.6	22.3	18.8 b	14.0
	RS-T	18.9	21.8	20.8 b	5.9
C	RS	10.6	16.9	13.9 c	21.0
	RS-T	14.9	17.1	15.9 c	6.0

For a given soil, the values followed by the same lower case letter were not significantly different according to a two tailed *t*-test ($P < 0.05$). The values followed by a different lower case letter were significantly different.

3. Results and discussion

3.1. Rainfall simulation experiments and seal characterization

For the RS and RS-T experiments, experimental steady-state runoff rates, *r*, were reached before the end of all runs, so the saturated soil hydraulic conductivity, K_s, values were estimated considering the last data points of the infiltration curves (Table 2; Fig. 3). For the three studied soils, the mean K_s values of the RS and RS-T experiments ranged from 13.9 to 25.5 and from 15.9 to 26.2 mm h^{-1}, respectively. Visually, the change in soil structure at surface after the simulated storms was evident (Fig. 2). The compaction of fine material from the destroyed aggregates formed a thin (thickness of ~1 mm) and highly dense seal layer as already observed in previous studies (Assouline, 2004). The impact of rainfall on soil structure looked similar for both RS and RS-T experiments. We then deduced that the bulk densities of the seal layer were comparable for both RS and RS-T experiments. For these last experiments, the soil bulk density increased by 38.7–42.1%, depending on the soil, due to soil surface sealing of the initially undisturbed soils (Fig. 4).

For each soil, the mean K_s values differed at most by a negligible factor of 1.1 between RS and RS-T experiments, suggesting that considering different soil thicknesses did not appreciably affect the estimated K_s, in terms of average values. A lower variability of K_s was detected with the RS-T experiments, showing that a decrease in the soil thickness implied reduced uncertainties in the estimated mean values of K_s. The statistical irrelevance of the soil thickness on the estimated K_s implied that this parameter was representative of the hydraulic behavior of the least permeable layer (i.e., the seal layer), which controlled

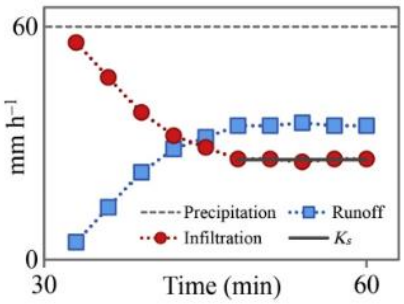

Fig. 3. Illustrative example of a simulated rainfall on a sandy-loam plot at 60 mm h^{-1} rainfall intensity. The infiltration curve was drawn by subtracting the runoff rate from the intensity. According to White et al. (1989), the saturated soil hydraulic conductivity, K_s (25.8 mm h^{-1}), was estimated by Eq. (1) considering the last five data points.

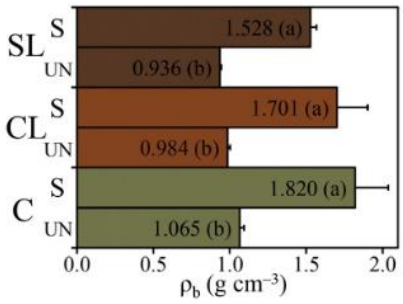

Fig. 4. Comparison between the mean bulk density, ρ_b (g cm^{-3}), values of the three undisturbed (UN) soils (sandy-loam, SL, clay-loam, CL, and clay, C) and of the sealed (S) layers sampled after the rainfall simulation experiments carried out on thin soil layers. Bars indicate standard deviation ($N = 5$).
For a given soil, the values followed by a different lower case letter were significantly different according to a two tailed *t*-test ($P < 0.05$).

the flow at the late-time of the process (Lassabatere et al., 2010). It also suggests that the same type of seal formed with similar saturated hydraulic conductivity, irrespective of the soil thickness. Briefly, water infiltration rates were progressively reduced by the formation of the seal resulting from the direct impact of the drops and tended towards the saturated hydraulic conductivity of the seal at its final stage of development.

3.2. Estimation of K_s of undisturbed soils with BEST algorithms

BEST-L and BEST-H runs obtained for the three undisturbed soils are depicted in Fig. 5. Experimental cumulative infiltrations clearly show the effect of soil sealing during the course of infiltration experiments. Indeed, the cumulative curves obtained for BEST-H runs follow those obtained for the BEST-L runs before deviating to the right. In other words, infiltration curves have similar concavity for shorter times with a more pronounced concavity for longer times (e.g., Fig. 5, SL BEST-H versus SL BEST-L, *I* data). Meanwhile, infiltration rates are comparable for shorter times but differ at longer times with infiltration rates that stabilizes for BEST-L runs whereas infiltration rates continue to decrease for BEST-H runs (e.g. Fig. 5, SL BEST-H versus SL BEST-L, *q* data). Cumulative infiltrations (*I*) and infiltration rates (*q*) obtained for BEST-H runs reveal the impact of soil sealing. At the beginning of experiments, the soil is not sealed at all and water infiltrates into the soil in the same way. Afterwards, when the amount of water applied to soil surface has been enough, the seal begins to form and to impede water infiltration, for BEST H runs. Such impediment reduces water infiltration rates (Fig. 5, BEST-H runs versus BEST-L runs, *q* data) and consequently increases the concavity of the cumulative infiltration curve (Fig. 5, BEST-H runs versus BEST-L runs, *I* data).

To explain these results, we must consider that BEST procedure assumes the idealized representation of a rigid porous medium (Lassabatere et al., 2013). During a BEST-L run, such condition is reasonably maintained since this procedure is expected to minimize soil surface alteration (Alagna et al., 2016a). Indeed, the structure of the soil is expected not to change appreciably during the experiment, approaching in practice the theoretical assumption of a rigid porous medium. On the other hand, under the exposure to the repeated impact of water volumes falling from a certain height, such as during a BEST-H run, structure dependent soil properties (e.g., hydraulic conductivity) may vary appreciably (Alagna et al., 2016b; Arya et al., 1998; Assouline, 2004; Ben-Hur et al., 2009; Dikinya et al., 2008; Ramos et al., 2000; van De Giesen et al., 2000). During a BEST-H run, the seal is progressively formed at the soil surface by the destruction of the soil aggregates exposed to the direct impact of the poured water volumes

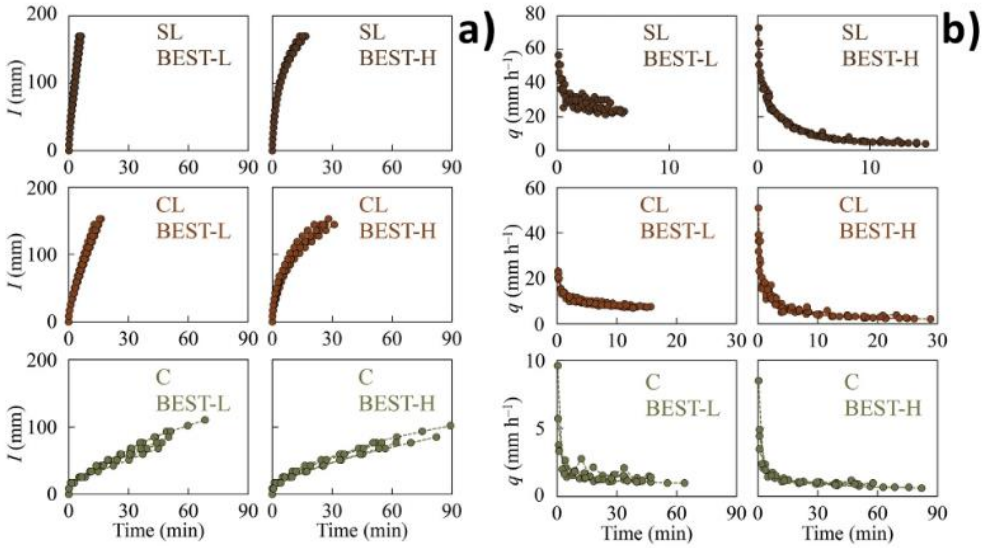

Fig. 5. (a) Cumulative infiltration, I (mm), and (b) infiltration rate, q (mm h^{-1}), for the three studied soils (sandy-loam, SL, clay-loam, CL, and clay, C) and different heights of water pouring (BEST-L and BEST-H runs).

(Di Prima et al., 2017). Therefore, it was expected that the dynamic of the seal formation relies on a decrease of saturated hydraulic conductivity of the soil during the exposure to the water drops (Assouline, 2004). As a consequence, the BEST-H runs exhibit a marked concave shape due to the progressive seal formation (Fig. 5).

The three BEST algorithms were used to treat the BEST-H and BEST-L runs carried out for the three initially unsealed soils. The treatment of the cumulative infiltration data with BEST algorithm may suffer from the impact of soil sealing on curve concavity. In a first step, we discuss the success rates obtained for the three algorithms. The BEST-slope algorithm yielded physically plausible estimates (i.e., positive K_s values) in 16 of 30 infiltration runs (53% of the cases), with the BEST-L procedure showing better results than BEST-H, yielding failure rate values of 7 and 87% respectively. The percentage of successful runs was of 100% with BEST-intercept. However, the fitting of the transient cumulative infiltration model on the data was less accurate for BEST-H than for BEST-L. With reference to the BEST-L runs, the BEST-intercept algorithm led to acceptable errors Er (i.e., $Er \leq 5\%$) for the SL and CL soils. On the other hand, critical Er values (i.e., $Er \gg 5\%$) were obtained for the BEST-H runs and for both BEST-L and BEST-H runs for the C soil (Fig. 6).

In addition to this effect on fit errors, soil sealing has also an impact on the quality of estimates for K_s with BEST-slope and BEST-intercept. These algorithms rely on infiltration models, i.e., Eqs. (7b) and (12), that do not account for such decrease in hydraulic conductivity and related strong curve concavity. Therefore, the hydraulic characterization carried out by these algorithms results in miss-estimation and poor performance at the same time. More specifically, the estimation of K_s by Eq. (7a) (BEST-slope) led to negative K_s values with $i_s < AS^2$ (Yilmaz et al., 2010). An illustrative example of K_s misestimation is reported in Fig. 7. Subpanel a depicts the case of a BEST-L run and the proper estimation of the K_s values by Eq. (7a). In this case the infiltration rate at the end of the experiment exceeds the estimated AS^2 values, leading to physically plausible and positive values for the saturated hydraulic conductivity. On the contrary, when the early- and late-time infiltration stages greatly differ in terms of infiltration rates as the result of the seal formation, the strong concavity of cumulative infiltration results in an over-estimation of soil sorptivity. Such overestimation results in too

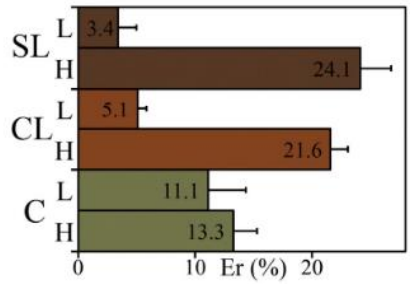

Fig. 6. Comparison between the mean relative error, Er (%), values (Eq. (4)) of the fitting of the BEST-intercept infiltration model (Eq. (12)) to the transient phase of the infiltration runs for the two heights of water pouring (low, L, and high, H), and for the three studied soils (sandy-loam, SL, clay-loam, CL, and clay, C). Bars indicate standard deviation ($N = 5$).

large values for the term AS^2 in Eq. (7a), resulting in negative values for K_s (Fig. 7b).

For the case of the BEST-H runs analyzed with the BEST-intercept algorithm the main problem was related to the poor fitting performance of the infiltration model with relative errors exceeding 5% (Fig. 6). Fig. 8a depicts the cumulative infiltration curve of a BEST-L run in which the infiltration model (Eq. (12)) fits accordingly to the transient infiltration data. Indeed, in this case the cumulative infiltration curve exhibits an usual shape, i.e., a gently concave part corresponding to the transient state and a linear part at the end of the curves related to the steady state (Di Prima et al., 2016). In the second case (Fig. 8b), the cumulative infiltration of the BEST-H run exhibits a marked concave shape due to the progressive seal formation. The marked concavity cannot be properly modelled by the infiltration model; which yields a poor fit of the infiltration model with a large value for relative error ($Er = 25.9\%$).

The inadaptability of BEST procedure to characterize sealed soils does not necessary occur if the seal is characterized a posteriori, i.e., once it is completely formed. For instance, Alagna et al. (in press)

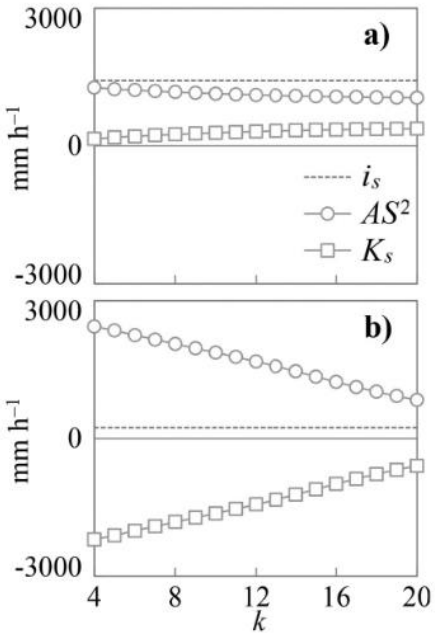

Fig. 7. Illustrative example of the estimation of K_s values by Eq. (7a) (BEST-slope) for different number of data points, k, (a) of a BEST-L run in which the infiltration rate at the end of the experiment (i_s) exceeds the estimated AS^2 values, leading to plausible values for the saturated hydraulic conductivity (positive K_s values), and (b) a BEST-H run in which $i_s < AS^2$, leading to erroneous K_s values ($K_s < 0$).

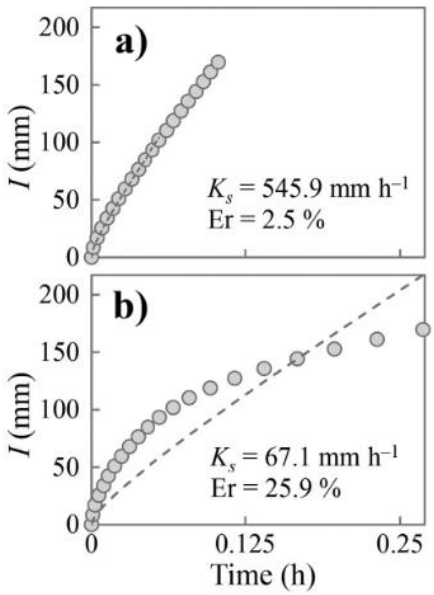

Fig. 8. Cumulative infiltration curve (a) of a BEST-L run in which Eq. (12) (dotted line; BEST-intercept) fits accordingly to the transient infiltration data yielding an *Er* value smaller than 5%, and (b) of a BEST-H run which exhibits a marked concave shape due to the progressive seal formation yielding a poor fit of the infiltration model (*Er* = 25.9%).

analyzed with the BEST-slope algorithm infiltration runs carried out using the BEST-L procedure on a crusted loamy soil in a Mediterranean vineyard (western Sicily, Italy). BEST-slope yielded positive K_s values in all cases. In addition, Eq. (7b) always yielded accurate fits with low relative errors. These authors concluded that the derived BEST-slope parameters were representative of the hydraulic behavior of the least permeable layer (i.e., the crust layer), which controlled the flow and consequently cumulative infiltration of the stratified medium, as proposed by Lassabatere et al. (2010) for layered soils.

Lastly, BEST-steady algorithm led to plausible values in 100% of the cases, thus proving more robust and efficient results than the other two BEST algorithms. However, even if BEST-steady appeared to be more robust than the other algorithms, additional information is needed to confirm that the target soil hydraulic parameters were accurately estimated. To overcome this lack, in the following section a comparison with independent K_s data estimated by rainfall simulation experiments was done in order to assess the adequacy of the three BEST algorithms.

We reported the averages of all the plausible estimates for both BEST-L and BEST-H runs for the three undisturbed soils in Table 3. As already discussed, BEST-H runs analyzed with the BEST-slope algorithm yielded a very high failure rate, leading to no values for SL and CL soils. BEST-intercept yielded poor fits and probably misestimated or overestimated values for K_s for the same soils and BEST-H runs (values highlighted in Table 3). In opposite, the case of BEST-L runs lead to proper BEST modelling and estimates. The comparison between BEST-H and BEST-L runs shows a significant decrease in K_s estimates from L to H. The height of water pouring had a strong impact with a clear decrease in estimates for K_s, probably due to seal formation during BEST-H runs.

The situation was different for the C soil. The discrepancy of BEST models and related erroneous values was less significant. For instance, estimates could be obtained with BEST-slope algorithm in all cases. The difference of height of water pouring did not yield a clear difference between BEST-L and BEST-H runs. Mean K_s values ranged between 6.8 and 27.6 mm h^{-1}. Differences between the two procedures were less noticeable than the other soils, with the BEST-L runs yielding higher

Table 3
Sample size, N, minimum, Min, maximum, Max, mean, and coefficient of variation, CV (%), of saturated soil hydraulic conductivity, K_s (mm h^{-1}), values obtained by the three BEST algorithms and low and high height of water pouring for the three soils (sandy-loam, SL, clay-loam, CL, and clay, C).

Soil	Height of water pouring	BEST algorithm	Statistic				
			N	Min	Max	Mean	CV
SL	High	Slope			$K_s < 0$		
		Intercept	5	64.8	78.7	71.7	8.5
		Steady	5	24.7	36.1	28.4	17.6
	Low	Slope	5	76.7	404.3	255.4	52.6
		Intercept	5	392.0	598.8	473.2	19.7
		Steady	5	343.8	553.5	430.2	20.8
CL	High	Slope			$K_s < 0$		
		Intercept	5	36.8	51.1	43.5	11.7
		Steady	5	18.2	23.3	21.1	9.2
	Low	Slope	5	17.7	66.7	43.0	45.7
		Intercept	5	135.6	156.4	144.1	6.2
		Steady	5	116.5	136.4	126.8	6.8
C	High	Slope	2	0.8	12.8	6.8	125.6
		Intercept	5	12.0	26.0	19.5	31.2
		Steady	5	7.6	22.1	15.2	39.2
	Low	Slope	4	2.8	17.0	9.5	65.7
		Intercept	5	17.5	33.5	27.6	22.6
		Steady	5	12.5	28.3	22.8	27.9

The underlined values indicated mean K_s values calculated with wrong estimations and unacceptable values for fit relative errors.

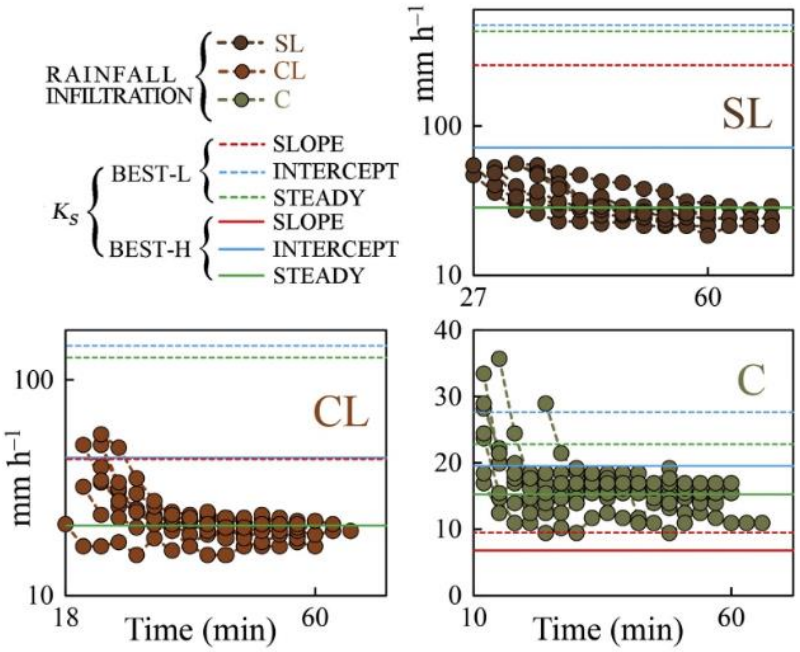

Fig. 9. Comparison between the mean K_s values obtained by the three BEST algorithms (BEST-slope, BEST-intercept and BEST-steady) and pouring water into the cylinder from two different heights (BEST-L and BEST-H runs), and infiltration rates of the rainfall simulation experiments for the three soils (sandy-loam, SL, clay-loam, CL, and clay, C).

means than BEST-H by a factor 1.4–1.5, depending on the algorithm. Such difference can be considered practically negligible for many hydrological applications (Elrick and Reynolds, 1992). We conclude that C soil showed a higher susceptibility to sealing in all cases (confirmed also by visual information), even if precautions were taken to minimize soil alteration (BEST-L runs). The susceptibility of this soil is not surprising, given its low organic matter content (1.1%) and the related absence of aggregates and soil structure (Reynolds et al., 2009). In addition, for this soil, clay dispersion is a possible additional mechanism responsible for the reduction of the hydraulic conductivity of saturated or near-saturated soil upon wetting (Bagarello et al., 2006).

3.3. Comparing K_s data estimated by contrasting infiltration techniques

In Fig. 9, all the infiltration rates obtained during the rainfall experiments are plotted against time. The data obtained for both the soil thickness (RS and RS-T experiments) were considered given the similarity of the collected experimental information in the two cases. The values of K_s obtained for the soils with BEST-H and BEST-L runs and for the three BEST algorithms are depicted on the same graph. As shown in Fig. 9, for the SL and CL soils, only the BEST-H procedure along with the BEST-steady algorithm yielded similar K_s values with those obtained by the rainfall simulation experiments. K_s values provided by BEST-L runs were much higher and inconsistent with RS and RS-T infiltration rates for soils SL and CL. Such discrepancy results from the absence of soil sealing for BEST-L runs and from the fact the K_s of undisturbed soils are much higher than that of the seal. For soil C, the difference for K_s estimates between BEST-L and BEST-H runs is less important. For the three soils, the estimates of K_s that are the most consistent with RS and RS-T infiltration rates are those obtained with BEST-H runs with BEST-steady algorithm. BEST-intercept and -slope lead to less consistent values. Note that BEST-slope provided no value for BEST-H runs and soils SL and CL (avoiding any comparison).

The result obtained with reference to the height of water pouring can be viewed as a confirmation of previous investigations (Alagna et al., 2016a; Bagarello et al., 2014a, 2017; Di Prima et al., 2017). More specifically, as already outlined by Di Prima et al. (2017), K_s data collected by ponding infiltrometer methods and usual experimental procedures, such as BEST-L runs, are generally expected to be unusable for interpreting field hydrological processes and particularly rainfall infiltration on bare soils prone to sealing. On the contrary, both rainfall simulation experiments and the BEST-H procedure determine a certain degree of compaction and mechanical breakdown of aggregates, accurately simulating processes during intense rainfall events. Therefore, K_s values estimated by these latter methodologies are more appropriate to explain surface runoff generation phenomena during intense storms.

A further objective of this investigation was to understand which BEST algorithm among BEST-slope, -intercept and -steady can be satisfactorily selected to properly estimate K_s for the specific case of an infiltration experiment implying an alteration of the soil surface. The K_s comparison carried out by applying different procedures to analyze the same infiltration run and independent rainfall simulation experiments allowed to identify BEST-steady as the most appropriate algorithm to estimate hydraulic properties from the BEST-H runs (Fig. 9). The statistical comparison reported in Fig. 10 supported the hypothesis that a characterization made with BEST-steady could be more appropriate to determine K_s data at the advanced stage of the seal formation of an initially undisturbed bare soil. Indeed, no statistical differences were detected between the mean K_s values obtained by the BEST-H procedure along with BEST-steady algorithm and by the rainfall simulation experiments. This result likely depends on the fact that BEST-steady considers exclusively the late phase of the infiltration process, i.e., when the seal is fully developed. Limiting the hydraulic characterization to the stabilized phase avoids the uncertainties due to specific shape of the cumulative infiltration and a no clear distinction between the early- and late-time infiltration process because of the progressive alteration of the soil surface (Bagarello et al., 2014b). Another implication of this result was that, with both methods, the formed seal layer ruled the late phase of the infiltration process and the estimated K_s values were representative of the seal (Fig. 10). In other words, the

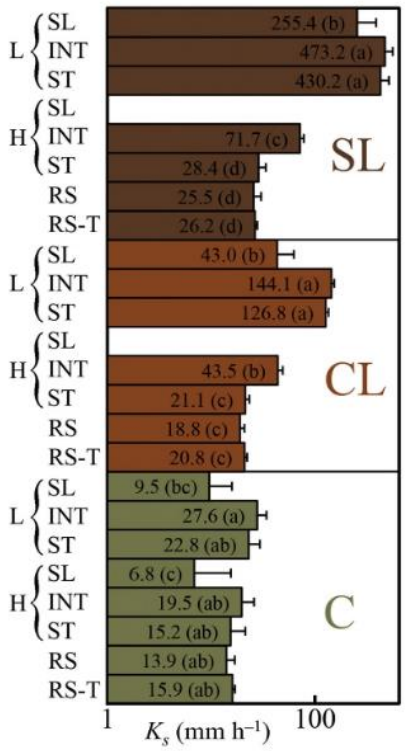

Fig. 10. Comparison between the mean K_s values obtained by the three BEST algorithms (BEST-slope, SL, BEST-intercept, INT, and BEST-steady, ST) and pouring water into the cylinder from two different heights (BEST-L, L, and BEST-H, H, runs) and by the rainfall simulation experiments carried out on thick (RS) and thin (RS-T) soil layer for the three soils (sandy-loam, SL, clay-loam, CL, and clay, C). Bars indicate standard deviation ($N = 5$).
For a given soil, the values followed by the same lower case letter were not significantly different according to the Tukey Honestly Significant Difference test ($P < 0.05$). The values followed by a different lower case letter were significantly different.

experiments presented in this study suggest that if any seal forms at the surface during a BEST-H infiltration test the BEST-steady estimates should proper characterize the hydraulic properties of the seal. We believe that this result has practical importance because, to our knowledge, this was the first time that a check of the BEST-H procedure and the three BEST algorithms with other well tested methods for K_s estimation was carried out to characterize sealing at the surface of several types of soils.

4. Summary and conclusions

In this study, we firstly used rainfall simulations to assess the effect of soil sealing on infiltration of three initially undisturbed bare soils with different textures, Clay, Clay Loam and Sandy Loam over a layer of sand. A system with the thickness of soil corresponding to the seal thickness (~2 mm) was tested versus 75 mm thickness for the upper soil layer. The results clearly pointed at similar processes and results for the large and small thickness of the upper layer. The formation of the seal appeared identical, irrespective of the upper layer thickness. The experimental data showed that soil sealing determined an increase in soil bulk density varying from 38.7 to 42.1%, depending on the soil. Such a decrease resulted in a significant drop in hydraulic conductivity with time. Water infiltration was governed mainly by seal formation and related decrease in saturated hydraulic conductivity. Under the conditions simulated here, the final infiltration rates were representative of the hydraulic behavior of the seal layer, which controlled the infiltration process at the late-phase of the rainfall simulations, irrespective of the upper soil layer thickness.

The potential of the BEST-H procedure, to simulate and assess the alteration of the soil surface, was then tested in conjunction with the three existing BEST algorithms, i.e., BEST-slope, BEST-intercept and BEST-steady, to derive saturated hydraulic conductivity. For each soil, the potential of the BEST-H procedure was tested comparing the K_s estimates with the corresponding target values, i.e., the K_s values estimated by rainfall simulation experiments. Among the existing BEST algorithms, BEST-steady allowed a proper estimation of K_s for all the studied soils. More specifically, this algorithm limited the hydraulic characterization to the stabilized phase, i.e., when the seal was fully developed, avoiding uncertainties due to the seal formation during the early phase of the infiltration process. The other two algorithms that account for transient data are too perturbed by the effect of the progressive formation of the seal and related impacts on the infiltration. BEST-H runs along with BEST-steady algorithm prove more appropriate for the characterization of sealed soils and the hydraulic conductivity of the seal. These low-cost techniques may be advantageous in comparison with more intensive techniques like rainfall simulations experiments.

Our findings demonstrated that the BEST-H procedure is suitable enough to properly characterize the seal layer formed during the repeated impact of the poured water volumes onto the initially unsealed soil surface. The repeated impact of water drops during a BEST-H run induced the formation of a seal layer having similar hydraulic properties with those obtained by the simulated storms. In other terms, the BEST-H runs had possibly accounted for the main physical features characterizing the phenomenon of induced soil sealing. We propose that the applied methodology here could be adopted as a simple tool in investigations aimed to study the impact of sealing on soil infiltration in situ and in the laboratory, particularly to explain surface runoff generation phenomena during intense storms, quantifying soil susceptibility to erosion, or investigating the effect of soil restoration strategies to improve the soil properties (Badalamenti et al., 2016; Pasta et al., 2012).

These findings also have direct implications in terms of our understanding of land management. The infiltration is determined by the first few millimeters of the soil. This shows the importance of soil surface management for the functioning of the soil in terms of the partitioning of the rainfall into infiltration and runoff, as well as the associated soil erosion and the movement of sediment and associated substances through the landscape. In the future, the proposed methodology may be applied for different rainfall intensities and durations. Indeed, rainfall characteristics are among the major factors affecting the dynamics of seal formation.

Acknowledgements

We acknowledge the Earth System Science and Environmental Management (ESSEM) COST Action ES1306 "Connecting European connectivity research" for the scholarship grant awarded to S. Di Prima. P. Concialdi helped to run the Beerkan infiltration experiments. S. Di Prima outlined the investigation, designed the rainfall box, performed the rainfall simulation experiments and analyzed the data. All authors contributed to discuss the results and write the manuscript. S.D.P. also thank H.M., P.R. and F.P.

Appendix A

For an infiltration experiment with zero pressure head on a circular surface of radius r_d (mm), the three-dimensional cumulative infiltration, I (mm), and infiltration rate, i (mm h^{-1}), can be approached by the following explicit transient [Eqs. (5a) and (5b)] and steady-state [Eqs. (5c) and (5d)] expansions (Haverkamp et al., 1994; Lassabatere et al., 2006):

$$I(t) = S\sqrt{t} + (AS^2 + BK_s)t \tag{5a}$$

$$i(t) = \frac{S}{2\sqrt{t}} + (AS^2 + BK_s) \tag{5b}$$

$$I_{+\infty}(t) = (AS^2 + K_s)t + C\frac{S^2}{K_s} \tag{5c}$$

$$i_s = AS^2 + K_s \tag{5d}$$

where t (h) is the time, S (mm h$^{-1/2}$) is soil sorptivity, and A (mm^{-1}), B and C are constants defined taking into account initial conditions as (Haverkamp et al., 1994):

$$A = \frac{\gamma}{r_d(\theta_s - \theta_0)} \tag{6a}$$

$$B = \frac{2-\beta}{3}\left[1 - \left(\frac{\theta_0}{\theta_s}\right)^{\eta}\right] + \left(\frac{\theta_0}{\theta_s}\right)^{\eta} \tag{6b}$$

$$C = \frac{1}{2\left[1-\left(\frac{\theta_0}{\theta_s}\right)^{\eta}\right](1-\beta)}\ln\left(\frac{1}{\beta}\right) \tag{6c}$$

where θ_0 (cm^3 cm^{-3}) is the initial volumetric water content, γ is a parameter for geometrical correction of the infiltration front shape (Castellini et al., 2018), and β is a parameter depending on the capillary diffusivity function (Angulo-Jaramillo et al., 2000). γ and β are commonly set at 0.75 and 0.6 for $\theta_0 < 0.25\ \theta_s$ (Haverkamp et al., 1994). Note that relations (6) apply only when residual water content is negligible and that these equations are sensitive to the estimation of saturated water content, which may be quite challenging under specific circumstances (Di Prima et al., 2017).

The three alternative BEST algorithms differ from the way they fit experimental data to the models defined by Eq. (5a). In particular, a fitting of the infiltration model to the transient data is required with BEST-slope and BEST-intercept, but these differ by the use of steady-state conditions described by i_s for the former algorithm and b_s for the latter one. Both of these last two terms are required by BEST-steady that does not need data fitting to the transient stage of the run but relies solely on the steady state. In the following, are presented the detailed descriptions of the three alternative BEST algorithms.

The BEST-slope algorithm by Lassabatere et al. (2006) considers Eq. (5a) for modelling the transient cumulative infiltration data. Eq. (5a) is modified with the replacement of hydraulic conductivity as a function of sorptivity and the experimental steady-state infiltration rate, i_s, using Eq. (5d), leading to:

$$K_s = i_s - AS^2 \tag{7a}$$

$$I(t) = S\sqrt{t} + [A(1-B)S^2 + Bi_s]t \tag{7b}$$

where i_s is estimated as the slope of regression line fitted to the last data points describing the steady-state conditions on the I vs. t plot. Eq. (7b) is fitted to experimental data to estimate S. Establishing a constraint like Eq. (7a) between the estimator for sorptivity and the one for saturated hydraulic conductivity and inverting cumulative infiltration data through optimizing only sorptivity avoids parameter non-uniqueness and increases the robustness of the inverse procedure (Lassabatere et al., 2013). The fit is performed by minimizing the classical objective function for cumulative infiltration:

$$f(S, K_s, k) = \sum_{i=1}^{k} [I_{exp}(t_i) - I_{est}(t_i)]^2 \tag{8}$$

where k is the number of data points considered for the transient state, I_{exp} is the experimental cumulative infiltration and I_{est} is the estimated cumulative infiltration using Eq. (7b). Once S is estimated, K_s is calculated by Eq. (7a). As the infiltration model is valid only at transient state, the fit may not be valid for large values of k. Therefore, BEST fits data for a minimum of two points to a maximum of N_{tot} points, representing the whole dataset. For each data subset containing the first k points, corresponding to a duration of the experiment equal to t_k, S and K_s are estimated and the time, t_{max} (h), defined as the maximum time for which the transient expression can be considered valid, is determined as follow:

$$t_{max} = \frac{1}{4(1-B)^2}\left(\frac{S}{K_s}\right)^2 \tag{9}$$

where $(S/K_s)^2$ is the gravity time defined by Philip (1969). Then, t_k is compared with t_{max}. The values of S and K_s are not considered valid unless t_k is lower than t_{max}. Among all values of S and K_s that fulfill this condition, the S and K_s values corresponding to the largest k (k_{step}) are retained since they are considered more precise.

The BEST-intercept algorithm by Yilmaz et al. (2010) defines the constraint between S and K_s by using the intercept of the asymptotic expansion in Eq. (5c):

$$b_s = \frac{CS^2}{K_s} \tag{10}$$

Therefore, b_s is estimated by linear regression analysis of the data describing steady-state conditions on the I vs. t plot, and the following relationship is applied to determine K_s:

$$K_s = C\frac{S^2}{b_s} \tag{11}$$

This procedure leads to the use of the division operator rather than the subtraction operator and thereby avoids obtaining negative values for the estimation of K_s. Combining Eqs. (5a) and (11) yields the following relationship to fit onto the transient state of the experimental cumulative infiltration:

$$I(t) = S\sqrt{t} + \left(AS^2 + BC\frac{S^2}{b_s}\right)t \tag{12}$$

Eq. (12), that is alternative to Eq. (7b), is applied to determine S by the same procedure described for BEST-slope, including the assessment of the time validity of the transient infiltration model by calculation of t_{max}. The estimated sorptivity is then used to calculate K_s by Eq. (11).

Finally, the BEST-steady procedure by Bagarello et al. (2014b) makes use of both the intercept (b_s) and the slope (i_s) of the straight line fitted to the data describing steady-state conditions on the I vs. t plot. With this algorithm, K_s can be directly calculated by the following equation (Di Prima et al., 2016):

$$K_s = \frac{Ci_s}{Ab_s + C} \tag{13}$$

Finally, the scale parameter for water pressure head can be computed from previous estimates of saturated hydraulic conductivity and sorptivity (Lassabatere et al., 2006). However, in this study, we focus mainly on the value of saturated hydraulic conductivity, K_s.

References

Alagna, V., Bagarello, V., Di Prima, S., Giordano, G., Iovino, M., 2013. A simple field method to measure the hydrodynamic properties of soil surface crust. J. Agric. Eng. 44, 74–79. http://dx.doi.org/10.4081/jae.2013.(s1):e14.

Alagna, V., Bagarello, V., Di Prima, S., Giordano, G., Iovino, M., 2016a. Testing infiltration run effects on the estimated water transmission properties of a sandy-loam soil. Geoderma 267, 24–33. http://dx.doi.org/10.1016/j.geoderma.2015.12.029.

Alagna, V., Bagarello, V., Di Prima, S., Iovino, M., 2016b. Determining hydraulic properties of a loam soil by alternative infiltrometer techniques. Hydrol. Process. 30, 263–275. http://dx.doi.org/10.1002/hyp.10607.

Alagna, V., Di Prima, S., Rodrigo-Comino, J., Iovino, M., Pirastru, M., Keesstra, S.D., Novara, A., Cerdà, A., 2017. The impact of the age of vines on soil hydraulic conductivity in vineyards in eastern Spain. Water 10, 14. http://dx.doi.org/10.3390/w10010014.

Alagna, V., Bagarello, V., Di Prima, S., Guaitoli, F., Iovino, M., Keesstra, S., Cerdà, A., 2018. Using beerkan experiments to estimate hydraulic conductivity of a crusted loamy soil in a Mediterranean vineyard. J. Hydrol. Hydromech (in press).

Angulo-Jaramillo, R., Vandervaere, J.-P., Roulier, S., Thony, J.-L., Gaudet, J.-P., Vauclin, M., 2000. Field measurement of soil surface hydraulic properties by disc and ring infiltrometers: a review and recent developments. Soil Tillage Res. 55, 1–29. http://dx.doi.org/10.1016/S0167-1987(00)00098-2.

Angulo-Jaramillo, R., Bagarello, V., Iovino, M., Lassabatère, L., 2016. Infiltration Measurements for Soil Hydraulic Characterization. Springer International Publishing.

Arya, L.M., Dierolf, T.S., Sofyan, A., Widjaja-Adhi, I., van Genuchten, M.T., 1998. Field measurement of the saturated hydraulic conductivity of a macroporous soil with unstable subsoil structure. Soil Sci. 163, 841–852.

Assouline, S., 2004. Rainfall-induced soil surface sealing. Vadose Zone J. 3, 570–591.

Assouline, S., Mualem, Y., 2002. Infiltration during soil sealing: the effect of areal heterogeneity of soil hydraulic properties. Water Resour. Res. 38, 1286. http://dx.doi.org/10.1029/2001WR001168.

Augeard, B., Assouline, S., Fonty, A., Kao, C., Vauclin, M., 2007. Estimating hydraulic properties of rainfall-induced soil surface seals from infiltration experiments and X-ray bulk density measurements. J. Hydrol. 341, 12–26. http://dx.doi.org/10.1016/j.jhydrol.2007.04.018.

Badalamenti, E., Gristina, L., Laudicina, V.A., Novara, A., Pasta, S., Mantia, T.L., 2016. The impact of Carpobrotus cfr. acinaciformis (L.) L. Bolus on soil nutrients, microbial communities structure and native plant communities in Mediterranean ecosystems. Plant Soil 409, 19–34. http://dx.doi.org/10.1007/s11104-016-2924-z.

Bagarello, V., Iovino, M., Palazzolo, E., Panno, M., Reynolds, W.D., 2006. Field and laboratory approaches for determining sodicity effects on saturated soil hydraulic conductivity. Geoderma 130, 1–13. http://dx.doi.org/10.1016/j.geoderma.2005.01.004.

Bagarello, V., Di Prima, S., Iovino, M., Provenzano, G., Sgroi, A., 2011. Testing different approaches to characterize Burundian soils by the BEST procedure. Geoderma 162, 141–150. http://dx.doi.org/10.1016/j.geoderma.2011.01.014.

Bagarello, V., Castellini, M., Di Prima, S., Iovino, M., 2014a. Soil hydraulic properties determined by infiltration experiments and different heights of water pouring. Geoderma 213, 492–501. http://dx.doi.org/10.1016/j.geoderma.2013.08.032.

Bagarello, V., Di Prima, S., Iovino, M., 2014b. Comparing alternative algorithms to analyze the Beerkan infiltration experiment. Soil Sci. Soc. Am. J. 78, 724. http://dx.doi.org/10.2136/sssaj2013.06.0231.

Bagarello, V., Cecere, N., Di Prima, S., Giordano, G., Iovino, M., 2017. Height of water pouring effects on infiltration runs carried out in an initially wet sandy-loam soil. In: Chemical Engineering Transactions, Chemical Engineering Transactions. Italian Association of Chemical Engineering - AIDIC, pp. 721–726. http://dx.doi.org/10.3303/cet1758121.

Baumhardt, R.L., Römkens, M.J.M., Whisler, F.D., Parlange, J.-Y., 1990. Modeling infiltration into a sealing soil. Water Resour. Res. 26, 2497–2505. http://dx.doi.org/10.1029/WR026i010p02497.

Ben-Hur, M., Yolcu, G., Uysal, H., Lado, M., Paz, A., 2009. Soil structure changes: aggregate size and soil texture effects on hydraulic conductivity under different saline and sodic conditions. Aust. J. Soil Res. 47, 688–696.

Bradford, J.M., Ferris, J.E., Remley, P.A., 1987. Interrill soil erosion processes: I. Effect of surface sealing on infiltration, runoff, and soil splash detachment. Soil Sci. Soc. Am. J. 51, 1566–1571.

Braud, I., De Condappa, D., Soria, J.M., Haverkamp, R., Angulo-Jaramillo, R., Galle, S., Vauclin, M., 2005. Use of scaled forms of the infiltration equation for the estimation of unsaturated soil hydraulic properties (the Beerkan method). Eur. J. Soil Sci. 56, 361–374. http://dx.doi.org/10.1111/j.1365-2389.2004.00660.x.

Brooks, R.H., Corey, T., 1964. Hydraulic Properties of Porous Media. Hydrol. Paper 3. Colorado State University, Fort Collins.

Burdine, N.T., 1953. Relative permeability calculation from pore size distribution data. Petr. Trans. Am. Inst. Min. Metall. Eng. 198, 71–77.

Castellini, M., Di Prima, S., Iovino, M., 2018. An assessment of the BEST procedure to estimate the soil water retention curve: a comparison with the evaporation method. Geoderma 320, 82–94. http://dx.doi.org/10.1016/j.geoderma.2018.01.014.

Coutinho, A.P., Lassabatere, L., Montenegro, S., Antonino, A.C.D., Angulo-Jaramillo, R., Cabral, J.J.S.P., 2016. Hydraulic characterization and hydrological behaviour of a pilot permeable pavement in an urban centre, Brazil. Hydrol. Process. 30, 4242–4254. http://dx.doi.org/10.1002/hyp.10985.

van De Giesen, N.C., Stomph, T.J., de Ridder, N., 2000. Scale effects of Hortonian overland flow and rainfall–runoff dynamics in a West African catena landscape. Hydrol. Process. 14, 165–175. http://dx.doi.org/10.1002/(SICI)1099-1085(200001)14:1<165::AID-HYP920>3.0.CO;2-1.

Di Prima, S., 2015. Automated single ring infiltrometer with a low-cost microcontroller circuit. Comput. Electron. Agric. 118, 390–395. http://dx.doi.org/10.1016/j.compag.2015.09.022.

Di Prima, S., Lassabatere, L., Bagarello, V., Iovino, M., Angulo-Jaramillo, R., 2016. Testing a new automated single ring infiltrometer for Beerkan infiltration experiments. Geoderma 262, 20–34. http://dx.doi.org/10.1016/j.geoderma.2015.08.006.

Di Prima, S., Bagarello, V., Lassabatere, L., Angulo-Jaramillo, R., Bautista, I., Burguet, M., Cerdà, A., Iovino, M., Prosdocimi, M., 2017. Comparing Beerkan infiltration tests with rainfall simulation experiments for hydraulic characterization of a sandy-loam soil. Hydrol. Process. 31, 3520–3532. http://dx.doi.org/10.1002/hyp.11273.

Dikinya, O., Hinz, C., Aylmore, G., 2008. Decrease in hydraulic conductivity and particle release associated with self-filtration in saturated soil columns. Geoderma 146, 192–200. http://dx.doi.org/10.1016/j.geoderma.2008.05.014.

Elrick, D.E., Reynolds, W.D., 1992. Methods for analyzing constant-head well permeameter data. Soil Sci. Soc. Am. J. 56, 320. http://dx.doi.org/10.2136/sssaj1992.03615995005600010052x.

Fernández-Raga, M., Palencia, C., Keesstra, S., Jordán, A., Fraile, R., Angulo-Martínez, M., Cerdà, A., 2017. Splash erosion: a review with unanswered questions. Earth Sci. Rev.

171, 463–477. http://dx.doi.org/10.1016/j.earscirev.2017.06.009.
Gee, G.W., Bauder, J.W., 1986. Particle-size analysis. In: Klute, A. (Ed.), SSSA Book Series. Methods of Soil Analysis, Part 1: Physical and Mineralogical Methods Soil Science Society of America, American Society of Agronomy, pp. 383–411.
van Genuchten, M.T., 1980. A closed-form equation for predicting the hydraulic conductivity of unsaturated soils. Soil Sci. Soc. Am. J. 44, 892–898.
Gonzalez-Sosa, E., Braud, I., Dehotin, J., Lassabatère, L., Angulo-Jaramillo, R., Lagouy, M., Branger, F., Jacqueminet, C., Kermadi, S., Michel, K., 2010. Impact of land use on the hydraulic properties of the topsoil in a small French catchment. Hydrol. Process. 24, 2382–2399. http://dx.doi.org/10.1002/hyp.7640.
Haverkamp, R., Ross, P.J., Smettem, K.R.J., Parlange, J.Y., 1994. Three-dimensional analysis of infiltration from the disc infiltrometer: 2. Physically based infiltration equation. Water Resour. Res. 30, 2931–2935. http://dx.doi.org/10.1029/94WR01788.
Iserloh, T., Ries, J.B., Arnáez, J., Boix-Fayos, C., Butzen, V., Cerdà, A., Echeverría, M.T., Fernández-Gálvez, J., Fister, W., Geißler, C., Gómez, J.A., Gómez-Macpherson, H., Kuhn, N.J., Lázaro, R., León, F.J., Martínez-Mena, M., Martínez-Murillo, J.F., Marzen, M., Mingorance, M.D., Ortigosa, L., Peters, P., Regüés, D., Ruiz-Sinoga, J.D., Scholten, T., Seeger, M., Solé-Benet, A., Wengel, R., Wirtz, S., 2013. European small portable rainfall simulators: a comparison of rainfall characteristics. Catena 110, 100–112. http://dx.doi.org/10.1016/j.catena.2013.05.013.
Lado, M., Ben-Hur, M., Shainberg, I., 2004. Soil wetting and texture effects on aggregate stability, seal formation, and erosion. Soil Sci. Soc. Am. J. 68, 1992–1999. http://dx.doi.org/10.2136/sssaj2004.1992.
Lassabatere, L., Angulo-Jaramillo, R., Soria Ugalde, J.M., Cuenca, R., Braud, I., Haverkamp, R., 2006. Beerkan estimation of soil transfer parameters through infiltration experiments—BEST. Soil Sci. Soc. Am. J. 70, 521. http://dx.doi.org/10.2136/sssaj2005.0026.
Lassabatere, L., Angulo-Jaramillo, R., Soria-Ugalde, J.M., Šimůnek, J., Haverkamp, R., 2009. Numerical evaluation of a set of analytical infiltration equations: evaluation infiltration. Water Resour. Res. 45http://dx.doi.org/10.1029/2009WR007941. (n/a-n/a).
Lassabatere, L., Angulo-Jaramillo, R., Goutaland, D., Letellier, L., Gaudet, J.P., Winiarski, T., Delolme, C., 2010. Effect of the settlement of sediments on water infiltration in two urban infiltration basins. Geoderma 156, 316–325. http://dx.doi.org/10.1016/j.geoderma.2010.02.031.
Lassabatere, L., Angulo-Jaramillo, R., Yilmaz, D., Winiarski, T., Caicedo, et al., 2013. BEST method: characterization of soil unsaturated hydraulic properties. In: Advances in Unsaturated Soils. CRC Press, London, pp. 527–532.
Lassu, T., Seeger, M., Peters, P., Keesstra, S.D., 2015. The Wageningen rainfall simulator: set-up and calibration of an indoor nozzle-type rainfall simulator for soil erosion studies. Land Degrad. Dev. 26, 604–612. http://dx.doi.org/10.1002/ldr.2360.
Lilliefors, H.W., 1967. On the Kolmogorov-Smirnov test for normality with mean and variance unknown. J. Am. Stat. Assoc. 62, 399–402. http://dx.doi.org/10.1080/01621459.1967.10482916.
Liu, H., Lei, T.W., Zhao, J., Yuan, C.P., Fan, Y.T., Qu, L.Q., 2011. Effects of rainfall intensity and antecedent soil water content on soil infiltrability under rainfall conditions using the run off-on-out method. J. Hydrol. 396, 24–32. http://dx.doi.org/10.1016/j.jhydrol.2010.10.028.
Logsdon, S.D., Jaynes, D.B., 1993. Methodology for determining hydraulic conductivity with tension infiltrometers. Soil Sci. Soc. Am. J. 57, 1426–1431.
Moldenhauer, W.C., Long, D.C., 1964. Influence of rainfall energy on soil loss and infiltration rates: I. Effect over a range of texture. Soil Sci. Soc. Am. J. 28, 813–817. http://dx.doi.org/10.2136/sssaj1964.03615995002800060036x.
Mualem, Y., Assouline, S., 1989. Modeling soil seal as a nonuniform layer. Water Resour. Res. 25, 2101–2108. http://dx.doi.org/10.1029/WR025i010p02101.
Mubarak, I., Angulo-Jaramillo, R., Mailhol, J.C., Ruelle, P., Khaledian, M., Vauclin, M., 2010. Spatial analysis of soil surface hydraulic properties: is infiltration method dependent? Agric. Water Manag. 97, 1517–1526. http://dx.doi.org/10.1016/j.agwat.2010.05.005.
Nelson, D.W., Sommers, L.E., 1996. Total carbon, organic carbon, and organic matter. In: Sparks, D.L. (Ed.), Methods of Soil Analysis, Part 3, Chemical Method. SSSA book series 5 Soil Science Society of America, Inc, Madison, WI, pp. 961–1010.
Pasta, S., Badalamenti, E., Mantia, T.L., 2012. Acacia cyclops A. Cunn. ex G. Don (Leguminosae) in Italy: first cases of naturalization. An. Jard. Bot. Madr. 69, 193–200. http://dx.doi.org/10.3989/ajbm.2314.
Philip, J.R., 1969. Theory of infiltration. Adv. Hydrosci. 5, 215–296.
Ramos, M., Nacci, S., Pla, I., 2000. Soil sealing and its influence on erosion rates for some soils in the Mediterranean area. Soil Sci. 165, 398–403.
Reynolds, W.D., 1993. Saturated hydraulic conductivity: field measurement. In: Carter, M.R. (Ed.), Soil Sampling and Methods of Analysis. 599–613 Canadian Society of Soil Science, Lewis Publishers, Boca Raton, FL.
Reynolds, W.D., Elrick, D.E., 1990. Ponded infiltration from a single ring: I. analysis of steady flow. Soil Sci. Soc. Am. J. 54, 1233. http://dx.doi.org/10.2136/sssaj1990.03615995005400050006x.
Reynolds, W.D., Bowman, B.T., Brunke, R.R., Drury, C.F., Tan, C.S., 2000. Comparison of tension infiltrometer, pressure infiltrometer, and soil core estimates of saturated hydraulic conductivity. Soil Sci. Soc. Am. J. 64, 478–484. http://dx.doi.org/10.2136/sssaj2000.642478x.
Reynolds, W.D., Drury, C.F., Tan, C.S., Fox, C.A., Yang, X.M., 2009. Use of indicators and pore volume-function characteristics to quantify soil physical quality. Geoderma 152, 252–263. http://dx.doi.org/10.1016/j.geoderma.2009.06.009.
Slimene, E.B., Lassabatere, L., Šimůnek, J., Winiarski, T., Gourdon, R., 2017. The role of heterogeneous lithology in a glaciofluvial deposit on unsaturated preferential flow – a numerical study. J. Hydrol. Hydromech. 65, 209–221. http://dx.doi.org/10.1515/johh-2017-0004.
Tackett, J., Pearson, R., 1965. Some characteristics of soil crusts formed by simulated rainfall. Soil Sci. 99, 407–413.
Touma, J., Raclot, D., Al-Ali, Y., Zante, P., Hamrouni, H., Dridi, B., 2011. In situ determination of the soil surface crust hydraulic resistance. J. Hydrol. 403, 253–260. http://dx.doi.org/10.1016/j.jhydrol.2011.04.004.
Van Bemmelen, J., 1890. Über die Bestimmung des Wassers, des Humus, des Schwefels, der in den colloïdalen Silikaten gebundenen Kieselsäure, des Mangans usw im Ackerboden. In: Die Landwirthschaftlichen Versuchs-Stationen. 37. pp. 279–290.
White, I., Sully, M.J., Melville, M.D., 1989. Use and hydrological robustness of time-to-incipient-ponding. Soil Sci. Soc. Am. J. 53, 1343–1346. http://dx.doi.org/10.2136/sssaj1989.03615995005300050007x.
Xu, X., Kiely, G., Lewis, C., 2009. Estimation and analysis of soil hydraulic properties through infiltration experiments: comparison of BEST and DL fitting methods. Soil Use Manag. 25, 354–361. http://dx.doi.org/10.1111/j.1475-2743.2009.00218.x.
Yilmaz, D., Lassabatere, L., Angulo-Jaramillo, R., Deneele, D., Legret, M., 2010. Hydrodynamic characterization of basic oxygen furnace slag through an adapted BEST method. Vadose Zone J. 9, 107. http://dx.doi.org/10.2136/vzj2009.0039.

Appendix C:

Received: 27 February 2018 | Accepted: 23 September 2018
DOI: 10.1002/hyp.13290

RESEARCH ARTICLE

WILEY

A test of water pouring height and run intermittence effects on single-ring infiltration rates

Vincenzo Alagna | Vincenzo Bagarello | Noemi Cecere | Paola Concialdi | Massimo Iovino

Department of Agricultural, Food and Forest Sciences, University of Palermo, Palermo, Italy

Correspondence
Vincenzo Alagna, Department of Agricultural, Food and Forest Sciences, University of Palermo, Viale delle Scienze, Palermo 90128, Italy.
Email: vincenzo.alagna01@unipa.it

Abstract

Assessing how the infiltration process depends on the water impact energy improves interpretation of hydrological processes. Impact energies vary with the height of water pouring; that is, the distance between the water delivery point and the soil surface. The effects of the height of water pouring on infiltration in an initially near saturated soil can be tested in the field by two repeated Beerkan infiltration runs separated by a short pause (30 min) and using both low (non-perturbing) and high (perturbing) heights of water application. The double two-stage Beerkan run methodology was applied in two soils. The infiltration rate at the end of the perturbing stage of the experiment was 0.2–0.3 (sandy-loam soil) and 0.15 (loam soil) times that obtained with the initial, nonperturbing stage whereas, without any perturbing effect, infiltration rates at the end of the second run were 0.5 times those at the end of the first run. Therefore, the methodology distinguished between a decrease in infiltration rate due to water redistribution during the pause and that attributable to soil surface perturbation. Maintaining a small depth of water (10 mm) on the infiltration surface was not an alternative to the classical Beerkan run for the non-perturbing stage of the experiment since two times higher infiltration rates were measured with a greater hydrostatic pressure. In conclusion, the relationship between infiltration into an initially near saturated soil and the energy of the applied water can be determined directly in the field at any time with a simple and parsimonious experiment. This circumstance could improve soil hydraulic characterization for interpreting and simulating hydrological processes.

KEYWORDS

Beerkan run, height of water pouring effects, infiltration, two-stage methodology

1 | INTRODUCTION

Single-ring infiltration techniques are widely used to determine soil hydrodynamic parameters directly in the field with limited resources and experimental efforts (Angulo-Jaramillo, Bagarello, Iovino, & Lassabatere, 2016). Consequently, they are attractive to characterize the soil when important and also complex hydrological processes have to be interpreted and simulated. Saturated hydraulic conductivity, K_s, of the surface soil layer is the most important soil parameter that influences rainfall partition into infiltration and surface runoff (Assouline & Mualem, 2002, 2006), and it can be determined with infiltrometer runs. However, the K_s data collected with these techniques could be thought to be unusable for hydrological studies since several investigations have shown that the K_s results were much higher than those obtained by other methods, or they were incompatible with any rainfall excess even if surface runoff was measured (Bagarello, Di Stefano, Iovino, & Sgroi, 2013; Cerdà, 1996, 1999; Morbidelli et al., 2017; van de Giesen, Stomph, & De Ridder, 2000; Williams & Bonell,

 © 2018 John Wiley & Sons, Ltd.

1988). This inconsistency can depend on different factors such as blocking of some large pores by massive air inclusion during natural events or crust formation and associated particle sorting decreasing overall permeability during the storm (Van de Giesen et al., 2000) but not, or not at the same rate, during the infiltration run. This last interpretation is a consequence of the fact that structure dependent soil properties have a dynamic nature, and they can vary appreciably upon wetting due to different phenomena such as aggregate breakdown promoted by raindrop impact or weakening of interparticle bonds (Assouline & Mualem, 2002, 2006; Chen, Sela, Svoray, & Assouline, 2013; Collis-George & Laryea, 1971). However, the inadequacy of infiltrometer data for hydrological investigations is not a general conclusion since an opposite information can also be found in the literature. For example, Di Prima, Marrosu, Lassabatere, Angulo-Jaramillo, and Pirastru (2018) recently concluded that single-ring infiltration measurements yielded plausible estimations of the matrix K_s in an investigation on lateral preferential flow at the hillslope scale.

Presumably, additional checks of the factors controlling in the field a single-ring infiltration process will improve our ability to make predictions on the hydrological relevance of the collected data. In a hydrological perspective, the height of water pouring and the temporary interruption of the run are two relevant factors.

The height of water pouring has to be considered because, for a given water volume, the energy of the applied water changes with the distance between the soil surface and the water application point (Bagarello, Castellini, Di Prima, & Iovino, 2014), and there are many evidences of the importance of the water impact energy on the surface soil characteristics. For example, increasing the water impact energy was found to reduce both the final infiltration rate and cumulative infiltration in an unstable sandy-loam soil (Smith, Levy, & Shainberg, 1990). In an investigation by Ramos, Nacci, and Pla (2000), the saturated hydraulic conductivity of a 1-cm thick soil layer decreased by 47 to 291 times, depending on the soil characteristics, when the energy of the applied water for the run increased. Establishing height of water pouring effects on initially saturated or near-saturated soil is particularly important since this is the most favourable condition for rainfall excess generation.

A temporary interruption of the run should be considered since it can be viewed as a means to mimic intra-event intermittence of natural rainfall events that typically include rain and no-rain periods (Dunkerley, 2015), also considering that the infiltrometer establishes a three-dimensional process whereas rain infiltration is essentially a one-dimensional process. The temporary interruption of the run could have implications on the single-ring infiltration process since achieving steadiness conditions requires time (Reynolds & Elrick, 2002), and the interruption that could occur either before or after reaching steady-state, induces some water redistribution during the pause. Therefore, interrupting water application for a given time period could be a way to compare the infiltration process under different initial soil water content conditions; that is, presumably homogeneous at the beginning of the run but maybe not when the process starts again. Moreover, a first steady-state infiltration rate higher than the subsequent one can be expected when the first stage of a two-stage infiltration rate is carried out on an initially drier soil than the second one (Císlerová, Šimůnek, & Vogel, 1988), or as a consequence of weakening of particle bonds and particle clogging phenomena that are expected to be more noticeable for a longer run (Dikinya, Hinz, & Aylmore, 2008).

Bagarello et al. (2014) and Alagna, Bagarello, Di Prima, Giordano, and Iovino (2016a) suggested that the Beerkan infiltration run (Lassabatère et al., 2006) is usable for checking water energy impact effects on hydrodynamic parameters of the surface soil layer directly in the field. In particular, the suggested method establishes a comparison between infiltration runs carried out with different heights of water pouring. With the so-called L (low) runs, water is applied at a small distance from the infiltration surface; that is, approximately at a height, h_w, of 0.03 m, in an attempt to minimize soil disturbance due to water application. Water is applied from h_w = 1.5 m at other sampling points (high, H, runs) to induce damaging effects of water impact. Using rainfall simulation experiments, Di Prima et al. (2017) demonstrated that the height from which water is poured onto the soil surface with a Beerkan run is a useful parameter in infiltration experiments to mimic the effect of high intensity rain on surface soil hydraulic properties.

The L and H infiltration runs can in principle be carried out under any antecedent soil water condition. However, sampling in the field, a naturally saturated or quasi-saturated soil can be quite difficult because close to saturation conditions can be rare, and soils can remain saturated or quasi-saturated for too much short times. Therefore, the time of sampling appears unpredictable and, in any case, it should be extremely timely.

To practically solve this problem, Bagarello, Cecere, Di Prima, Giordano, and Iovino (2017a) recently developed a methodology to establish water impact energy effects on infiltration rates for an almost initially near saturated soil. Two types of two-stage infiltration runs are carried out, namely, L1L2 and L1H2. In the former case, water is first applied by an L procedure, and then the sampled soil is allowed to drain for no more than a few dozens of minutes. Subsequently, the L procedure is used again to pour other water. With the L1H2 run, an H procedure is used for the second stage of the infiltration experiment. A comparison between the infiltration processes for the second stage of the run is then carried out. Performing recurrent water application experiments is a common way to prewet the soil and explore soil surface dynamics under wetting and drying conditions both in the field (Bagarello, Iovino, & Tusa, 2000; Císlerová et al., 1988; Dohnal, Vogel, Dusek, Votrubova, & Tesar, 2016) and the laboratory (Fohrer, Berkenhagen, Hecker, & Rudolph, 1999; King & Bjorneberg, 2012; Le Bissonnais & Singer, 1992; Levy, Shainberg, & Morin, 1986). The data collected by the developed protocol allow to simultaneously establish what happens when (a) a given water amount is applied on an initially near-saturated soil with different energy levels, and (b) the infiltration run is temporarily interrupted.

A point needing consideration is that, according to Bagarello et al. (2017a), the Beerkan methodology has to be applied for the H stage of the run since this methodology permits exposing the soil surface to the beating action of the applied water, as desired. For the L stage, a very small (i.e., a few millimetres) ponding depth of water could steadily be maintained by using, for example, the device developed by Di Prima (2015) instead of successively pouring water. Following Gonzalez-Sosa et al. (2010), another alternative way to perform an L-type run could be establishing some kind of falling head infiltration process with a relatively small (i.e., a few centimetres in this case)

initial ponded depth of water. The different ways to perform the L part of the run are equivalent if they can be expected to yield a similar experimental information. It is still necessary to experimentally check the similarity of the possible alternative methodologies for an L run, even because hydrostatic pressure effects on infiltration rates could not be negligible (Reynolds, Elrick, & Youngs, 2002a). Another reason for making this check is that some methods of analysis of the infiltration data, such as the Beerkan Estimation of Soil Transfer parameters (BEST) procedure of soil hydraulic characterization (Lassabatère et al., 2006), yield estimates of soil structure dependent parameters, including K_s, by assuming a null pressure head on the infiltration surface. Obtaining reliable estimates of these parameters requires an experimental infiltration process consistent with the theory or a negligible effect of the ponded depth of water on the measured infiltration.

The general objective of this investigation was to improve our knowledge of the physical factors that influence single-ring infiltration in the field. The specific objective was to check the effects of the following factors on the infiltration rates for a sandy-loam and a loam soil: (a) height of water pouring on the initially near-saturated porous medium, (b) pause in the infiltration run, and (c) established ponded depth of water on the infiltration surface.

2 | MATERIALS AND METHODS

2.1 | Field sites

The field experiments were carried out at the so-called AR (Aranceto) and OR (Orleans) sites that were established at the Department of Agricultural, Food and Forestry Sciences of the Palermo (Italy) University (Table 1). An approximately 150 m^2 flat area of a citrus orchard, with trees spaced 4 m × 4 m apart, was selected at the AR site. The soil had a relatively high sand and gravel content. The soil texture of the upper part of the profile, 0.1 m thick, was sandy-loam according to the USDA classification (Alagna, Bagarello, Di Prima, Giordano, & Iovino, 2016a). An area of approximately the same size, supporting a meadow, was selected at the OR site. The soil texture at the surface was loam in this case (Alagna, Bagarello, Di Prima, & Iovino, 2016b).

2.2 | Infiltration experiments

Field infiltration experiments of the Beerkan type (Lassabatère et al., 2006) were carried out on selected dates during the months of June and July 2017. The main features of these experiments were as follows:

- Insertion of 0.08 m diametre rings to a depth of 0.01 m. The rings were particularly small to more clearly detect possible effects of soil disturbance due to water application;
- Filling plastic glasses with 57 ml of water for each glass;
- Infiltration runs carried out by successively pouring the water contained in a glass on the confined infiltration surface. In particular, a given volume of water was poured in the ring in approximately 3 s at the start of the measurement, and the elapsed time during the infiltration was measured. When the amount of water had completely infiltrated, an identical amount of water was poured into the ring, and the time needed for the water to infiltrate was logged. The procedure was repeated 15 times, according to the existing guidelines (Lassabatère et al., 2006), but 30 water volumes were applied for some runs. In some cases, a constant depth of ponding of 0.01 m was maintained during the Beerkan type run on the infiltration surface;

TABLE 1 General information on the sampled field sites and statistics (*N* = sample size; *CV* = coefficient of variation) of dry soil bulk density, ρ_b, and antecedent gravimetric, w_i, and volumetric, θ_i, soil water content

Characteristic factor	statistic	Values or class	
		AR site	OR site
Coordinates		38°06′24″N 13°21′06″E	38°06′26.6″N 13°20′60.0″E
Size of the experimental area (m^2)		150	150
Clay (%)		17.6	31.3
Silt (%) (USDA classification)		29.8	42.2
Sand (%)		52.6	40.7
Gravel (%)		13.0	-
Soil textural class		Sandy-loam	Loam
ρ_b (g cm^{-3}) (L1L2, L1H2, L and LP runs)	N Mean CV (%)	20 1.117 6.2	20 1.121 7.8
w_i (g g^{-1}) (L1L2, L1H2, L and LP runs)	N Mean CV (%)	20 0.071 15.6	20 0.053 19.5
θ_i (m^3m^{-3}) (L1L2, L1H2, L and LP runs)	N Mean CV (%)	20 0.080 16.2	20 0.060 21.8
w_i (g g^{-1}) (L1L2W runs)	N Mean CV (%)	5 0.177 6.4	5 0.178 19.6

Note. AR site: Aranceto site; OR site: Orleans site.

- Low (L) infiltration runs, carried out by applying water at a small distance from the infiltration surface; that is, approximately at a height, h_w, of 0.03 m, and dissipating its energy on the fingers of the hand; and
- High (H) infiltration runs, meaning that water was applied from h_w = 1.5 m, and the soil surface was not shielded. To ensure flow verticality and prevent wind effects, the device developed by Bagarello et al. (2014) and Alagna, Bagarello, Di Prima, Giordano, and Iovino (2016a) was used to pour water on the confined infiltration surface.

Two types of two-stage infiltration runs were carried out, namely, L1L2 and L1H2. In the former case, 15 volumes of water were applied by the L procedure, and then the sampled soil was allowed to drain for half an hour. The aim of a short pause was to give time to the previously infiltrated water to redistribute while maintaining near-saturated conditions at the beginning of the subsequent infiltration run. Subsequently, the L procedure was used to pour other 15 volumes of water. In the latter case, the H procedure was used for the second stage of the infiltration run. For each soil, five L1L2 runs and five L1H2 runs were carried out at 10 randomly selected sampling points. An L1L2 run and an L1H2 run were carried out relatively close to one another and almost simultaneously on each sampling occasion to sample a soil having presumably similar characteristics in terms of dry soil bulk density, ρ_b (g cm^{-3}), and volumetric soil water content at the time of the run, θ_i (m^3 m^{-3}). In particular, two rings were inserted at a distance of 1.0–1.5 m each other, and two undisturbed soil cores (0.05 m in height by 0.05 m in diameter) were collected at the 0 to 0.05 m and 0.05 to 0.10 m depths at an intermediate distance between the two rings. These cores were used to determine ρ_b and the gravimetric soil water content, w_i (g g^{-1}), and hence θ_i, in the laboratory. Five L runs were also carried out at other randomly selected points by successively pouring 30 volumes of water. Five additional runs, indicated by the acronym LP, were carried out by steadily maintaining a small depth of ponding, equal to 0.01 m, on the soil surface during application of the 30 water volumes with the Beerkan procedure. Following Reynolds, Elrick, and Youngs (2002b), the level corresponding to a ponding depth of 0.01 m was marked on the cylinder wall and the pre-established water volume was added whenever the water level in the ring reached the mark. The L1L2, L1H2, L, and LP runs were carried out at the natural antecedent soil water content (Table 1). Other five runs of the L1L2 type, indicated by the acronym L1L2W (W = wet) were carried out a day after plenty prewetting the soil. In particular, small circular areas (each of approximately 0.5 m^2) were delimited by small levees and 25 L of water were poured on each delimited soil surface. Only w_i was determined immediately before the infiltration run in this case (Table 1) since the very wet antecedent soil conditions suggested that there was the risk to excessively compact the soil during ring insertion for 0.05 m.

A sample size of N = 5 for a given treatment was chosen since a small area in the field is better characterized by averaging a few closely spaced replicated measurements rather than by a single measurement due to spatial variability of soil hydrodynamic parameters (Fodor, Sándor, Orfanus, Lichner, & Rajkai, 2011; Nano, Nicolardot, & Ubertosi, 2015).

2.3 | Data analysis

Each stage of the two-stage infiltration runs (L1L2, L1H2, L1L2W) and also the single stage for the L and LP runs were characterized in terms of final infiltration rate, *FIR* (mm s^{-1}), that was obtained by linear regression analysis of the last three cumulative infiltration, I, vs. time, t, data points, and total duration, d (s). Calculation of *FIR* and d was also made considering the first half (i.e., first 15 water volumes) of the L runs with the aim to establish a comparison with the results of the L1 runs, applied water volumes being equal. Working with final rates implies that all possible disturbance effects due to water application have occurred, and it represents a rather common choice in the investigations dealing with recurrent water applications (e.g., Dohnal et al., 2016; Le Bissonnais & Singer, 1992; Levy et al., 1986). Run duration was also considered since it was a good indicator of soil disturbance phenomena in previous investigations (Alagna, Bagarello, Di Prima, Giordano, & Iovino, 2016a; Bagarello et al., 2014). Moreover, changes at the soil surface are expected to occur soon after the start of water application (Thompson & James, 1985), and therefore a given volume of water should take a longer time to infiltrate if these phenomena occur.

Due to the small sample sizes for each treatment, the statistical distribution of the data was not checked, and both *FIR* and d were assumed to be ln-normally distributed since this distribution is frequently found to be appropriate for saturated soil hydrodynamic parameters (Coutinho et al., 2016; Lee, Reynolds, Elrick, & Clothier, 1985; Sisson & Wierenga, 1981). Consequently, the geometric mean and the associated coefficient of variation, *CV*, were calculated to summarize the data (Lee et al., 1985). Two tailed t tests (P = 0.05) were carried out on the ln-normally transformed data to compare two datasets.

3 | RESULTS

3.1 | Beerkan infiltration runs

Each individual Beerkan infiltration run was visually checked by plotting the data on an infiltration rate, i_r, vs. time, t, plot. Data for all runs were then summarized on an i_r vs. cumulative infiltration, I, plot (Figure 1) according to other authors such as Morin and Benyamini (1977) and Assouline (2013), since durations changed from run to run, making presentation of all data on a single i_r vs. t plot rather confuse.

For the L1L2, L1H2, and L1L2W runs, and for both soils, i_r decreased as t, and consequently I, increased during the first stage of the two-stage infiltration run, as expected (Elrick & Reynolds, 1992). Moreover, the *FIR* for the second stage, FIR_{II}, was always smaller than the *FIR* for the first stage, FIR_I (Table 2).

Even for the L and LP runs, the infiltration rates declined with time, and they approached a near constant value (Figure 1). In the sandy-loam soil, however, one of the five infiltration curves for the L runs (dashed line in the figure) showed a clear and noticeable deviation from the other ones. Perhaps, this anomalous behaviour was due to the presence of a relatively large stone close to the infiltration

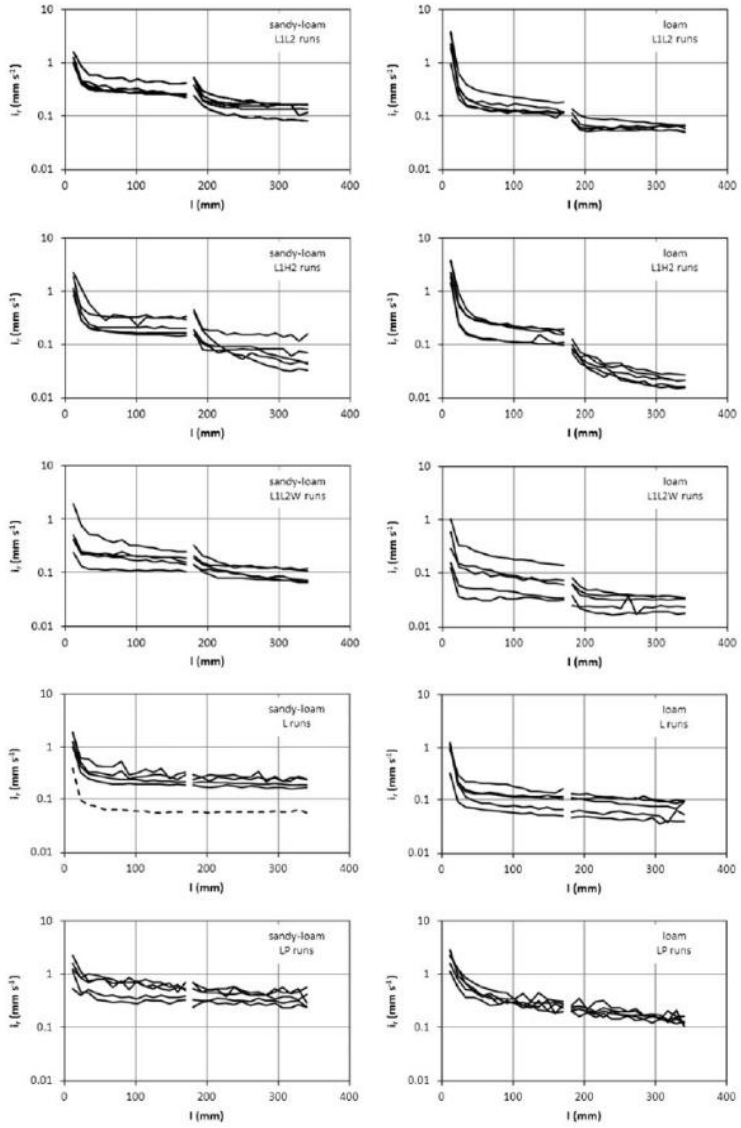

FIGURE 1 Individual infiltration rate, *ir*, vs. cumulative infiltration, *I*, curves for the two sampled soils and each type of infiltration run. For the L and LP runs, the interruption in the plot between the first and second part of the process simplifies visual comparison with the other infiltration runs

surface. Prudentially, this run was not considered in the subsequent analysis of the data.

3.2 | Effects of water pouring height

The first stage of the L1L2 and L1H2 runs yielded not statistically significant differences for FIR_I and d_I in both soils (Table 2). Consequently, the second stage results for the L1L2 and L1H2 runs were directly comparable. The L1H2 runs yielded significantly smaller FIR_{II} values and significantly greater d_{II} values than the L1L2 runs in both soils. In particular, the final infiltration rate was 2.1 times smaller, and the infiltration process was 1.9 times longer with the L1H2 runs than the L1L2 ones in the sandy-loam soil. For the loam soil, the L1H2 runs yielded 3.0 times smaller FIR_{II} values and 2.2 greater d_{II} values than the L1L2 runs. In both soils, lower FIR_{II}/FIR_I values and higher d_{II}/d_I values were obtained with the L1H2 runs than the L1L2 ones but differences between the two types of run were statistically significant only for the loam soil.

Therefore, an effect of the water pouring height on the infiltration process was recognized for both soils, and it was particularly clear;

TABLE 2 Mean and coefficient of variation, CV (%), of final infiltration rates and run durations for the L1L2, L1H2, L1L2W, and L runs

	Sandy-loam						Loam					
	L1L2		L1H2		L1L2W		L1L2		L1H2		L1L2W	
Variable	mean	CV	mean	CV	mean	CV	mean	CV	mean	CV	mean	CV
FIR_I (mm s^{-1})	0.276 a (b) c	23.0	0.218 a	36.7	0.163 (b)	30.9	0.127 d (e) f	21.4	0.143 d	30.3	0.059 (e)	67.2
d_I (s)	497 a (b) c	23.5	670 a	35.6	845 (b)	41.8	1,019 d (e) f	27.4	873 d	36.7	2,190 (e)	77.3
FIR_{II} (mm s^{-1})	0.127 (a) (b) (c)	30.6	0.060 (a)	57.4	0.083 (b)	26.4	0.060 (d) (e) f	12.5	0.020 (d)	24.2	0.028 (e)	31.5
d_{II} (s)	1,092 (a) (b) c	25.1	2,096 (a)	46.7	1,669 (b)	25.0	2,642 (d) (e) f	15.1	5,908 (d)	24.0	5,569 (e)	35.4
FIR_{II}/FIR_I	0.46 a b (c)	41.3	0.27 a	52.3	0.51 b	17.1	0.47 (d) e (f)	18.7	0.14 (d)	27.7	0.47 e	39.6
d_{II}/d_I	2.20 a b(c)	30.3	3.13 a	42.5	1.97 b	25.3	2.59 (d) e (f)	16.6	6.77 (d)	32.6	2.54 e	39.6

	L	
Variable	mean	CV
FIR_I (mm s^{-1})	0.236 c	21.8
d_I (s)	600 c	25.4
FIR_{II} (mm s^{-1})	0.206 (c)	20.9
d_{II} (s)	794 c	19.9
FIR_{II}/FIR_I	0.87 (c)	6.0
d_{II}/d_I	1.32 (c)	7.4
	0.090 f	44.9
	1.503 f	44.4
	0.069 f	38.9
	2.284 f	42.2
	0.76 (f)	13.6
	1.52 (f)	12.5

For a given variable, a statistical comparison (two-tailed *t* test at $P = 0.05$) was carried out between two means followed by the same lower case letter. Differences between means followed by a letter enclosed in parenthesis were statistically significant. Differences between means followed by a letter not enclosed in parenthesis were not statistically significant. FIR_I and d_I = final infiltration rate and duration, respectively, for the first stage of the L1L2, L1H2, and L1L2W runs or the first half (first 15 water volumes) of the L runs. FIR_{II} and d_{II} = final infiltration rate and duration, respectively, for the second stage of the L1 L2, L1H2 and L1 L2W runs or the second half (second set of 15 water volumes) of the L runs.

that is, statistically supported for all considered variables, for the loam soil. Due to this effect, the duration of the second stage of the two-stage infiltration experiment approximately doubled in both soils, and the infiltration rate at the end of the run decreased by two times in the sandy-loam soil and three times in the loam soil. Therefore, the loam soil was 1.5 times more sensitive to height effects than the sandy-loam soil.

3.3 | Pause in water application

The L1L2 vs. L runs comparison revealed a similarity of the first stage of the infiltration process (i.e., application of the first 15 water volumes) both in terms of *FIR* and *d* for both soils (Table 2). With the L runs, the application of other 15 volumes of water determined a decrease of *FIR* by 1.1 and 1.3 times for the sandy-loam and the loam soils, respectively, and an associated increase of the duration of the process by 1.3 and 1.5 times. The corresponding ratios for the L1L2 runs were 2.2 and 2.1 for *FIR* and 2.2 and 2.6 for *d*. In the sandy-loam soil, statistical differences between the two types of run were detected for FIR_{II} (1.6 times lower for the L1L2 runs than the L runs), FIR_{II}/FIR_I (1.9 times lower for the L1L2 runs), and d_{II}/d_I (1.7 times greater for the L1L2 runs). In the loam soil, differences were statistically significant for FIR_{II}/FIR_I (1.6 times lower for the L1L2 runs) and d_{II}/d_I (1.7 times greater for the L1L2 runs).

Therefore, in the absence of any break in the water application sequence, the infiltration process occurred according to theory (Elrick & Reynolds, 1992). The pause in water application for half an hour determined a slowdown of the process when it started again, implying that a given water volume infiltrated the soil more slowly. A ratio-based comparison of the data (FIR_{II}/FIR_I and d_{II}/d_I) allowed to detect effects that were less clear (i.e., numerically perceivable but not always statistically supported) by establishing a comparison between FIR_{II} and d_{II} values for the two types of run. This discrepancy was not surprising because the reasoning in terms of slowdown required a preliminary comparison between the two stages of the run, while the reasoning in terms of second stage results implied neglecting the first stage of the run. In other terms, the two approaches differed by the used experimental information.

At both sites, prewetting the soil (L1L2W dataset) implied significantly smaller infiltration rates and longer runs in both stages of the two-stage infiltration run as compared with the non prewetted condition (L1L2 dataset; Table 2). In particular, in the comparison between the L1L2 and L1L2W runs for the sandy-loam soil, the *FIR* and *d* values of the first stage were 1.7 times higher and smaller, respectively, under the initially drier conditions and this factor decreased to 1.5 during the second stage. For the loam soil, the factor of difference was of 2.1–2.2 depending on the considered variable and stage. For both soils, the FIR_{II}/FIR_I and d_{II}/d_I values did not differ significantly between the two run types. In the passage from the first run to the second one, the *FIR* value decreased approximately by a factor of two in both soils, regardless of the initial soil water content. The *d* value increased by 2.0–2.2 times in the sandy-loam soil and slightly more; that is, by 2.5–2.6 times, in the loam soil. Therefore, the slowdown of the infiltration process attributable to the pause in water application was independent of the initial soil water content.

3.4 | Effects of ponding depth

For both sampled soils, visual inspection of the infiltration rate curves (Figure 2) clearly suggested that steadily maintaining a ponded depth of water of 0.01 m on the infiltration surface (LP runs) yielded higher infiltration rates as compared with those measured by strictly applying the Beerkan run infiltration procedure (L runs). The statistical analysis of the data supported this suggestion (Table 3). In particular, the LP runs were 1.8 times faster and yielded a 1.7 times higher estimate of *FIR* as compared with the L runs in the sandy-loam soil. For the loam soil, the factors of difference were equal to 2.0 and 2.6 for *FIR* and *d*, respectively.

Therefore, the two types of runs were not equivalent. In particular, even a small, steadily maintained, depth of ponding on the infiltration surface during the run was enough to influence the process. In this experiment, the presence of this small ponding depth of water implied detection of approximately two times higher final infiltration rates and 2.0–2.5 times shorter durations of the process. Differences between the two types of runs were slightly more noticeable for the loam soil than the sandy-loam one.

4 | DISCUSSION

4.1 | Effects of water pouring height

More water impact energy is expected to determine more alteration of the soil surface (Thompson & James, 1985), lower infiltration rates (Assouline & Mualem, 2002, 2006), and smaller saturated soil hydraulic conductivity values (Alagna, Bagarello, Di Prima, Giordano, & Iovino, 2016a; Bagarello et al., 2014; Ramos et al., 2000). Therefore, changes in *FIR* and *d* between the two stages of the run were more noticeable for the L1H2 experiment than the L1L2 one since, in the second stage of the infiltration run, more energy was supplied to the soil with the former experiment than the latter one. This result suggested that the used sample size was enough to obtain a qualitatively expected information, and it supported the conclusion by Bagarello, Cecere, et al. (2017a) that the impact of water pouring height on both *FIR* and *d* is detectable in initially very wet soil conditions.

The loam soil was more sensitive to height effects than the sandy-loam soil although the former soil had more clay than the latter one (Table 1), and an increase in clay content should improve aggregate stability (Le Bissonnais, 1996; Moutier, Shainberg, & Levy, 1998). However, the loam soil was appreciably poorer in sand as compared with the sandy-loam soil. A higher percentage of coarse particles could suggest a certain rigidity of the porous medium, and hence a reduced sensitivity to disturbance due to wetting (Alagna, Bagarello, Di Prima, Giordano, & Iovino, 2016a). Moreover, less sand implies a higher content of smaller particles and hence a higher possibility that particle detachment and clogging of the largest pores occur when the applied water has a high impact energy.

From a methodological point of view, this experiment was similar to that carried out in the same sandy-loam soil by Bagarello, Cecere, et al. (2017a) on March to May 2015. In particular, experimental differences were small and presumably negligible since they included a slight difference in the pause between the two water application stages (16–62 min, depending on the run, in the previous experiment), and the fact that *FIR* was set equal to the last measured i_r value. The initial soil water content was 0.08 $m^3\ m^{-3}$ in this investigation and approximately 0.18 $m^3\ m^{-3}$ in the investigation by Bagarello, Cecere, et al. The data collected in the previous experiment were similar to those of this investigation. In particular, the two experiments consistently suggested that the infiltration rate at the end of the second stage was 0.5–0.6 times that at the end of the first stage with a non-perturbing run and 0.2–0.3 times with a soil perturbing run. This result can be viewed not only as a suggestion of the robustness of the applied methodology but also as an indication of temporal stability of the tested height effects. More sampling dates are advisable to draw more general conclusions.

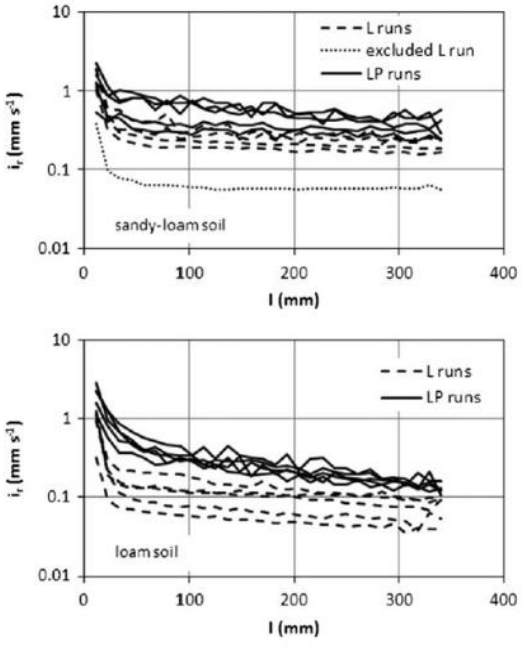

FIGURE 2 Individual infiltration rate, *ir*, vs. cumulative infiltration, *I*, curves for the two sampled soils and each L and LP infiltration run

4.2 | Pause in water application

The data for the L runs clearly suggested that the infiltration process did not stabilize after application of 15 water volumes, especially in the finer textured soil. This result was consistent with the physics of the process since attainment of steady-state infiltration rates is expected to be slow, especially in fine-textured soils (Elrick & Reynolds, 1992; Reynolds, 1993). An implication of this result is that using a priori 15 water volumes with the BEST procedure of soil hydraulic characterization (Angulo-Jaramillo et al., 2016; Lassabatère et al., 2006) could not always be the best choice to derive reliable estimates of soil hydraulic parameters. All BEST algorithms make use of steady-state infiltration rates for the calculations (Angulo-Jaramillo et al., 2016), and with 15 water volumes, the risk to believe that transient infiltration data are

TABLE 3 Mean and coefficient of variation, *CV* (%), of final infiltration rates, *FIR*, and run durations, *d*, for the L and LP runs

	Sandy-loam				Loam			
	L		LP		L		LP	
Variable	mean	CV	mean	CV	mean	CV	mean	CV
FIR ($mm\ s^{-1}$)	0.206 (a)	20.9	0.345 (a)	28.4	0.069 (b)	38.9	0.137 (b)	9.7
d (s)	1,394 (a)	22.0	758 (a)	30.9	3,793 (b)	42.4	1,453 (b)	14.4

For a given variable, a statistical comparison (two-tailed t test at $P = 0.05$) was carried out between two means followed by the same lower case letter. Differences between means followed by a letter enclosed in parenthesis were statistically significant.

indicative of a steady condition cannot be excluded. Instead, when performing the test, it could be advisable to compute infiltration rates and continue the experiment until steady-state is reached, although the criteria that can be applied to detect steadiness conditions are approximate and alternative criteria could be expected to yield different estimates of steady-state infiltration rates.

For a given volume of infiltrated water, a pause in the water application sequence for half an hour determined a slowdown of the infiltration process when it reinitiated. The decrease of *FIR* and the increase of *d* between the two stages of the nonperturbing run did not change with the initial soil water conditions although infiltration was generally slower in the initially wetter soil.

In order to explain these results, it was considered that, at the end of the first stage of the run, the soil volume close to the infiltration surface is field-saturated, and it is more or less dry outside the wetting zone. Therefore, soil water redistribution processes occur during the pause. The second stage of the run can be viewed as a new infiltration process that occurs in an initially wetter soil as compared with the first stage and therefore with smaller expected infiltration rates. This reasoning could also explain why the second stage of the run was faster in the initially drier soil. In particular, redistribution processes during the pause should be more noticeable in an initially drier soil since pressure head gradients are higher in this case. Therefore, the soil was likely drier for the L1L2 runs than the L1L2W ones at the beginning of the second stage.

The effect of the initial soil water content on transient infiltration rates can also be discussed, in a more formal way, using 3D infiltration models. In the BEST procedure (Lassabatère et al., 2006), transient, $i_r(t)$ ($L\ T^{-1}$), and steady-state, i_s ($L\ T^{-1}$), infiltration rates are modelled as follows:

$$i_r(t) = \frac{S}{2\sqrt{t}} + \left(A\ S^2 + B\ K_s\right) \tag{1}$$

$$i_s = A\ S^2 + K_s \tag{2}$$

where t (T) is the time, S ($L\ T^{-1/2}$) is soil sorptivity, K_s ($L\ T^{-1}$) is saturated soil hydraulic conductivity, and the A (L^{-1}) and B constants are defined for the specific case of a Brooks and Corey (1964) relationship as follows:

$$A = \frac{\gamma}{r\ (\theta_s - \theta_i)} \tag{3}$$

$$B = \frac{2-\beta}{3}\left[1 - \left(\frac{\theta_i}{\theta_s}\right)^{\eta}\right] + \left(\frac{\theta_i}{\theta_s}\right)^{\eta} \tag{4}$$

where r (L) is the radius of the source, θ_i (L^3L^{-3}) is the initial soil water content, θ_s (L^3L^{-3}) is the saturated soil water content, η is the shape parameter of the Brooks and Corey hydraulic conductivity function, and β and γ are coefficients that are commonly set at 0.6 and 0.75, respectively, for $\theta_i < 0.25 \times \theta_s$ (Haverkamp, Ross, Smettem, & Parlange, 1994; Smettem, Parlange, Ross, & Haverkamp, 1994). Soil sorptivity decreases as θ_i increases but A increases with θ_i. For θ_i varying between 0 and $0.25 \times \theta_s$, it is possible to show that B is practically independent of θ_i. Therefore, the effect of θ_i on i_r is not immediately predictable since the decrease of S as θ_i increases suggests lower expected infiltration rates, but the associated increase of A could indicate higher expected i_r values. However, according to Reynolds and Elrick (1990), steady-state 3D infiltration rate is given by:

$$i_s = \frac{(K_s H + \phi_m)}{\pi r G} + K_s \tag{5}$$

where H (L) is the steady depth of ponding on the infiltration surface, ϕ_m (L^2T^{-1}) is the matric flux potential (Gardner, 1958), and G is a shape factor that can be estimated on the basis of the ring radius and its depth of insertion into the soil. Equation (5) was developed for $H > 0$, but it was found to also be usable for $H = 0$ (Bagarello, Di Prima, & Iovino, 2017b). The matric flux potential is defined as follows:

$$\phi_m = \int_{h_i}^{0} K(h)dh \quad h_i \le h \le 0 \tag{6}$$

where h (L) is soil water pressure head, h_i (L) is the initial value of h, and K ($L\ T^{-1}$) is the soil hydraulic conductivity. Equations 5 and 6 establish that i_s decreases as θ_i increases since ϕ_m decreases. For consistency between Equations 2 and 5, the term $A \times S^2$ in Equations 1 and 2 has to decrease as θ_i increases. Consequently, infiltration rates during the transient phase of the 3D infiltration process have to decrease as θ_i increases.

Another possible explanation of the detected slowdown of the infiltration process in the passage between the two stages is related to soil particle mobilization, since enhanced weakening of particle bonds is expected with longer infiltration runs (Dikinya et al., 2008). Even this interpretation seems consistent with a decrease of *FIR* and an increase of *d* that do not change with the initial soil water content. At the beginning of the second stage of the run, weakening of particle bonds is probably similar for the L1L2 and L1L2W runs because the soil is field-saturated at the end of the first stage, and the pause in water application has the same duration in both cases. Consequently,

when the run starts again, the possibility that soil particle detachment and mobilization processes occurs is similar for the two types of run.

Following Císlerová et al. (1988), Dohnal et al. (2016), and Votrubova et al. (2017), in recurrent one-dimensional and three-dimensional ponding infiltration experiments, even a short pause between two water applications can result in a sharp decrease of the steady-state infiltration rate in the next run as a consequence of air entrapment. According to Císlerová et al., (1988) the decrease in steady infiltration rate in recurrent ponding infiltration experiments is high when the soil is initially dry, and it may not occur if the soil is saturated from the beginning of the experiment. In other terms, the relevance of the phenomenon should be expected to depend on the soil water content at the beginning of the infiltration process. The interpretation by Císlerová et al., (1988) was not considered to explain the decrease in the final infiltration rate between two non-perturbing stages of the run since it was independent of the initial soil water content. However, this conclusion needs testing since the soil was never saturated from the beginning of the experiment in this investigation.

4.3 | Effects of ponding depth

A faster infiltration process under ponding (LP runs) than that established with strictly the Beerkan procedure (L runs) could have different explanations. One is that, in the former case, the hydrostatic pressure on the infiltration surface increases and gradients of the hydraulic potential during the infiltration process are consequently higher. Air entrapment could be another factor affecting the L vs. LP runs comparison (e.g., Reynolds, 1993). In the case of a Beerkan infiltration run, in which water is applied when all the previously poured water volume has disappeared, the infiltration surface is repeatedly in direct contact with the atmosphere, but this contact is totally avoided when an even small ponding depth of water is maintained on the infiltration surface. Therefore, the opportunities to entrap air in the sampled soil volume could be thought to increase at each water application in the former case. On the other hand, maintaining soil saturation conditions even with the classical Beerkan run could suggest that differences between the L and LP runs cannot be explained by air entrapment. It has also to be considered that the soil water content close to the infiltration surface is high for the entire duration of the infiltration run, and particle bonds are expected to be weakened by wetting (Dikinya et al., 2008). Therefore, each water pouring during the Beerkan run could have some soil perturbing effect that implies a decrease in infiltration rates, notwithstanding that water is applied with care.

Attempting to explain differences between the L and LP runs, the geometric mean values of i_r were calculated for each applied water volume and the differences between the experimental infiltration rates, both in absolute (mean of i_r for the LP run–mean of i_r for the L run) and relative (the above mentioned difference divided by the mean of i_r for the L run) terms, were plotted against I (Figure 3). For both soils, the L and LP data similarity tended in general to increase at later stages of the infiltration process since both the absolute and the relative i_r differences were greater than 0 but steadily decreasing as I increased. This kind of behaviour was physically plausible. In particular, the wetted soil volume close to the infiltration surface is expected to increase in size as the process proceeds (Elrick & Reynolds, 1992) and consequently, the gradients in the hydraulic potential, representing the driving force for water movement, tend to become more similar for the L and LP runs.

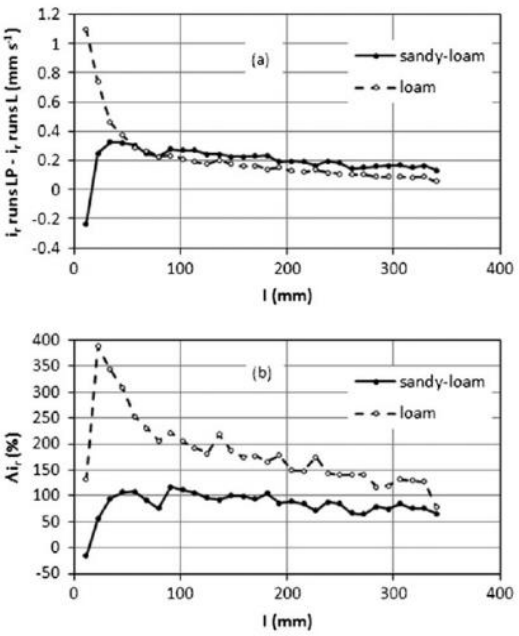

FIGURE 3 Differences between infiltration rates, *ir*, for the LP and L runs plotted against cumulative infiltration, I [$\Delta i_r = 100 \times (i_{r,\text{ runs LP}} - i_{r,\text{ runs L}})/i_{r,\text{ runs L}}$]

The ponding depth effects during the transient infiltration process can theoretically be discussed by considering that the BEST infiltration model (Lassabatère et al., 2006) was also used by Hinnell, Lazarovitch, and Warrick (2009) in conjunction with the approximation for sorptivity under ponding conditions, $S(H)$, by Green and Ampt (1911) as follows:

$$S(H) \approx \sqrt{2K_s(\theta_s - \theta_i)(H - h_f)} \tag{7}$$

where h_f (L) is the pressure head at the wetting front. For a ponded depth of water, $H = H_1$, $S = S(H_1)$, and the corresponding transient infiltration rates are denoted by the symbol i_{r1}. For $H = H_2$ ($<H_1$), $S = S(H_2) < S(H_1)$ and the i_{r2} symbol is used for the infiltration rates. According to Equation (1), the difference between i_{r1} and i_{r2} at a given time is given by:

$$i_{r1} - i_{r2} = \frac{[S(H_1) - S(H_2)]}{2\sqrt{t}} + A\left[S(H_1)^2 - S(H_2)^2\right] \tag{8}$$

The first addend on the right side of Equation (8) decreases as t increases. Therefore, $i_{r1}-i_{r2}$ is expected to decrease with time and also to approach a constant value that depends on the two sorptivity values and hence the established ponded depths of water. Checking the suggested interpretation appears advisable also because there are indications in the literature that the infiltration process does not

depend appreciably on the ponding depth of water, at least when these depths are small (Touma, Voltz, & Albergel, 2007).

Progressive air entrapment and additional surface disturbance at each water pouring for the L runs were less likely factors affecting the L vs. LP runs comparison since these phenomena should determine larger infiltration rate differences at later stages of the run.

5 | CONCLUSIONS

This investigation showed that a simple and parsimonious double two-stage Beerkan run methodology can be applied in the field to simultaneously (a) enucleate the effects of water pouring height on the measured infiltration rates in initially near-saturated conditions and (b) establish the influence of a short pause in the run on the measured infiltration. Small changes in the method to perform a non-perturbing run, yielding the necessary information to characterize the practically null height of water pouring condition, can influence the quantitative assessment of the mentioned effects.

According to the developed analysis, height of water pouring effects on infiltration rates can be noticeable, and a loam soil should be expected to be 1.5 times more sensitive to disturbance effects induced by a high height of pouring than a sandy-loam soil.

In the absence of any intentional soil disturbance, the slowdown of the infiltration process in the second stage of the run can be explained by the water redistribution processes during the pause between the two stages of the run. Therefore. the second part of the experiment can be viewed as a new infiltration process into an unsaturated, but close to saturation, soil.

The decrease of the final infiltration rate and the increase of the infiltration duration during the second stage of the run as compared with the first stage do not seem to change appreciably with the antecedent soil water content, regardless of the fact that the second stage is or is not perturbing.

The infiltration process established with the classical Beerkan run; that is, by repeatedly pouring small volumes of water on the soil surface, should not be compared with that measured by steadily maintaining a small (10 mm) ponding depth of water on the infiltration surface. In particular, the infiltration rates can be expected to be more similar as infiltration proceeds. The differences between the two ways to perform a non-perturbing infiltration run appear to depend on a different contribution of the hydrostatic pressure component on total flow.

Taking into account that the measured infiltration rates are usable to estimate soil hydrodynamic parameters with a variety of methods, it is plausible to believe that this investigation could open some interesting perspective with reference to both interpretation and simulation of hydrological processes. In particular, it demonstrated that a simple experiment can be carried out directly in the field; that is, in a real world situation, to establish a link between the energy of the applied water and the measured infiltration process in an initially near-saturated soil; that is, in a condition particularly favourable to rainfall excess, and hence runoff, generation. Consequently, the collected experimental information could allow us to derive soil hydraulic properties that reflect the appropriate conditions for simulating a specific hydrological process even considering that, with the applied double two-stage Beerkan run methodology, effects of different energy levels of the applied water can be tested by simply changing water pouring height. There are encouraging signs on the possibility to use the methodology to discriminate between soils. More data should be collected to make conclusions of general validity. In particular, a point needing additional investigation is the influence of the antecedent soil water content on the results of the two stage infiltration run. The current suggestion is that this influence is negligible, but it was based on a still limited experimental information. Spatial variability issues should also be developed in the future to establish if a relatively small sample size for a given treatment, as suggested by this investigation, is generally appropriate to get reliable data.

ORCID

Vincenzo Alagna http://orcid.org/0000-0002-0936-2652
Massimo Iovino http://orcid.org/0000-0002-3454-2030

REFERENCES

Alagna, V., Bagarello, V., Di Prima, S., Giordano, G., & Iovino, M. (2016a). Testing infiltration run effects on the estimated water transmission properties of a sandy-loam soil. *Geoderma*, *267*, 24–33. https://doi.org/10.1016/j.geoderma.2015.12.029

Alagna, V., Bagarello, V., Di Prima, S., & Iovino, M. (2016b). Determining hydraulic properties of a loam soil by alternative infiltrometer techniques. *Hydrological Processes*, *30*, 263–275. https://doi.org/10.1002/hyp.10607

Angulo-Jaramillo, R., Bagarello, V., Iovino, M., & Lassabatere, L. (2016). *Infiltration measurements for soil hydraulic characterization* (p. 386). Switzerland, ISBN 978-3-319-31786-1, 978-3-319-31788-5 (eBook), doi: https://doi.org/10.1007/978-3-319-31788-5: Springer International Publishing.

Assouline, S. (2013). Infiltration into soils: Conceptual approaches and solutions. *Water Resources Research*, *49*(4), 1755–1772. https://doi.org/10.1002/wrcr.20155

Assouline, S., & Mualem, Y. (2002). Infiltration during soil sealing: The effect of areal heterogeneity of soil hydraulic properties. *Water Resources Research*, *38*(12), 22-1–22-9. https://doi.org/10.1029/2001WR001168

Assouline, S., & Mualem, Y. (2006). Runoff from heterogeneous small bare catchments during soil surface sealing. *Water Resources Research*, *42*, W12405, 11 pp. https://doi.org/10.1029/2005WR004592

Bagarello, V., Castellini, M., Di Prima, S., & Iovino, M. (2014). Soil hydraulic properties determined by infiltration experiments and different heights of water pouring. *Geoderma*, *213*, 492–501. https://doi.org/10.1016/j.geoderma.2013.08.032

Bagarello, V., Cecere, N., Di Prima, S., Giordano, G., & Iovino, M. (2017a). Height of water pouring effects on infiltration runs carried out in an initially wet sandy-loam soil. *Chemical Engineering Transactions*, *58*, 721–726. https://doi.org/10.3303/CET1758121

Bagarello, V., Di Prima, S., & Iovino, M. (2017b). Estimating saturated soil hydraulic conductivity by the near steady-state phase of a Beerkan infiltration test. *Geoderma*, *303*, 70–77. https://doi.org/10.1016/j.geoderma.2017.04.030

Bagarello, V., Di Stefano, C., Iovino, M., & Sgroi, A. (2013). Using a transient infiltrometric technique for intensively sampling field-saturated hydraulic conductivity of a clay soil in two runoff plots. *Hydrological Processes*, *27*(24), 3415–3423. https://doi.org/10.1002/hyp.9448

Bagarello, V., Iovino, M., & Tusa, G. (2000). Factors affecting measurement of the near saturated soil hydraulic conductivity. *Soil Science Society of America Journal*, *64*, 1203–1210. https://doi.org/10.2136/sssaj2000.6441203x

Brooks, R.H., & Corey, T. (1964). Hydraulic properties of porous media. *Hydrology Paper*, Vol. 3 Colorado State University, Fort Collins. 24 pp.

Cerdà, A. (1996). Seasonal variability of infiltration rates under contrasting slope conditions in southeast Spain. *Geoderma*, *69*(3–4), 217–232. https://doi.org/10.1016/0016-7061(95)00062-3

Cerdà, A. (1999). Seasonal and spatial variations in infiltration rates in badland surfaces under Mediterranean climatic conditions. *Water Resources Research*, *35*(1), 319–328. https://doi.org/10.1029/98WR01659

Chen, L., Sela, S., Svoray, T., & Assouline, S. (2013). The role of soil-surface sealing, microtopography, and vegetation patches in rainfall-runoff processes in semiarid areas. *Water Resources Research*, *49*(9), 5585–5599. https://doi.org/10.1002/wrcr.20360

Císlerová, M., Šimůnek, J., & Vogel, T. (1988). Changes of steady-state infiltration rates in recurrent ponding infiltration experiments. *Journal of Hydrology*, *104*, 1–16. https://doi.org/10.1016/0022-1694(88)90154-0

Collis-George, N., & Laryea, K. B. (1971). Infiltration behaviour of structurally unstable soils under ponded and non-ponded conditions. *Soil Research*, *9*(1), 7–20. https://doi.org/10.1071/SR9710007

Coutinho, A. P., Lassabatere, L., Montenegro, S., Antonino, A. C. D., Angulo-Jaramillo, R., & Cabral, J. J. (2016). Hydraulic characterization and hydrological behaviour of a pilot permeable pavement in an urban centre, Brazil. *Hydrological Processes*, *30*(23), 4242–4254.

Di Prima, S. (2015). Automated single ring infiltrometer with a low-cost microcontroller circuit. *Computers and Electronics in Agriculture*, *118*, 390–395. https://doi.org/10.1016/j.compag.2015.09.022

Di Prima, S., Bagarello, V., Lassabatere, L., Angulo-Jaramillo, R., Bautista, I., Burguet, M., … Prosdocimi, M. (2017). Comparing Beerkan infiltration tests with rainfall simulation experiments for hydraulic characterization of a sandy-loam soil. *Hydrological Processes*, *31*, 3520–3532. https://doi.org/10.1002/hyp.11273

Di Prima, S., Marrosu, R., Lassabatere, L., Angulo-Jaramillo, R., & Pirastru, M. (2018). In situ characterization of preferential flow by combining plot- and point-scale infiltration experiments on a hillslope. *Journal of Hydrology*, *563*, 633–642. https://doi.org/10.1016/j.jhydrol.2018.06.033

Dikinya, O., Hinz, C., & Aylmore, G. (2008). Decrease in hydraulic conductivity and particle release associated with self-filtration in saturated soil columns. *Geoderma*, *146*, 192–200. https://doi.org/10.1016/j.geoderma.2008.05.014

Dohnal, M., Vogel, T., Dusek, J., Votrubova, J., & Tesar, M. (2016). Interpretation of ponded infiltration data using numerical experiments. *Journal of Hydrology and Hydromechanics*, *64*(3), 289–299. https://doi.org/10.1515/johh-2016-0020

Dunkerley, D. (2015). Intra-event intermittency of rainfall: An analysis of the metrics of rain and no-rain periods. *Hydrological Processes*, *29*(15), 3294–3305.

Elrick, D. E., & Reynolds, W. D. (1992). Methods for analyzing constant-head well permeameter data. *Soil Science Society of America Journal*, *56*, 320–323. https://doi.org/10.2136/sssaj1992.03615995005600010052x

Fodor, N., Sándor, R., Orfanus, T., Lichner, L., & Rajkai, K. (2011). Evaluation method dependency of measured saturated hydraulic conductivity. *Geoderma*, *165*(1), 60–68. https://doi.org/10.1016/j.geoderma.2011.07.004

Fohrer, N., Berkenhagen, J., Hecker, J. M., & Rudolph, A. (1999). Changing soil and surface conditions during rainfall. Single rainstorm/subsequent rainstorm. *Catena*, *37*, 355–375.

Gardner, W. (1958). Some steady-state solutions of the unsaturated moisture flow equation with application to evaporation from a water table. *Soil Science*, *85*, 228–232. https://doi.org/10.1097/00010694-195804000-00006

Gonzalez-Sosa, E., Braud, I., Dehotin, J., Lassabatère, L., Angulo-Jaramillo, R., Lagouy, M., … Michel, K. (2010). Impact of land use on the hydraulic properties of the topsoil in a small French catchment. *Hydrological Processes*, *24*, 2382–2399. https://doi.org/10.1002/hyp.7640

Green, W. H., & Ampt, G. A. (1911). Studies in soil physics. I. The flow of air and water through soils. *The Journal of Agricultural Science*, *4*, 1–24.

Haverkamp, R., Ross, P. J., Smettem, K. R. J., & Parlange, J. Y. (1994). Three-dimensional analysis of infiltration from the disc infiltrometer: 2. Physically based infiltration equation. *Water Resources Research*, *30*(11), 2931–2935. https://doi.org/10.1029/94WR01788

Hinnell, A. C., Lazarovitch, N., & Warrick, A. W. (2009). Explicit infiltration function for boreholes under constant head conditions. *Water Resources Research*, *45*, W10429. 9 pp

King, B. A., & Bjorneberg, D. L. (2012). Infiltration characteristics of bare soil under sequential water application events. *Proceedings of Irrigation Association Conference*, November 4–8, Orlando, Florida. 9 pp.

Lassabatère, L., Angulo-Jaramillo, R., Soria Ugalde, J. M., Cuenca, R., Braud, I., & Haverkamp, R. (2006). Beerkan estimation of soil transfer parameters through infiltration experiments—BEST. *Soil Science Society of America Journal*, *70*, 521–532. https://doi.org/10.2136/sssaj2005.0026

Le Bissonnais, Y. (1996). Aggregate stability and assessment of soil crustability and erodibility: I. Theory and methodology. *European Journal of Soil Science*, *47*, 425–437. https://doi.org/10.1111/j.1365-2389.1996.tb01843.x

Le Bissonnais, Y., & Singer, M. J. (1992). Crusting, runoff, and erosion response to soil water content and successive rainfalls. *Soil Science Society of America Journal*, *56*, 1898–1903. https://doi.org/10.2136/sssaj1992.03615995005600060042x

Lee, D. M., Reynolds, W. D., Elrick, D. E., & Clothier, B. E. (1985). A comparison of three field methods for measuring saturated hydraulic conductivity. *Canadian Journal of Soil Science*, *65*, 563–573. https://doi.org/10.4141/cjss85-060

Levy, G., Shainberg, I., & Morin, J. (1986). Factors affecting the stability of soil crusts in subsequent storms. *Soil Science Society of America Journal*, *50*, 196–201. https://doi.org/10.2136/sssaj1986.03615995005000010037x

Morbidelli, R., Saltalippi, C., Flammini, A., Cifrodelli, M., Picciafuoco, T., Corradini, C., & Govindaraju, R. S. (2017). In situ measurements of soil saturated hydraulic conductivity: Assessment of reliability through rainfall–runoff experiments. *Hydrological Processes*, *31*(17), 3084–3094. https://doi.org/10.1002/hyp.11247

Morin, J., & Benyamini, Y. (1977). Rainfall infiltration into bare soils. *Water Resources Research*, *13*(5), 813–817. https://doi.org/10.1029/WR013i005p00813

Moutier, M., Shainberg, I., & Levy, G. J. (1998). Hydraulic gradient, aging, and water quality effects on hydraulic conductivity of a vertisol. *Soil Science Society of America Journal*, *62*(6), 1488–1496. https://doi.org/10.2136/sssaj1998.03615995006200060003x

Nano, C. U., Nicolardot, B., & Ubertosi, M. (2015). Near-saturated hydraulic conductivity measured on a swelling silty clay loam for three integrated weed management based cropping systems. *Soil and Tillage Research*, *150*, 192–200. https://doi.org/10.1016/j.still.2015.02.003

Ramos, M. C., Nacci, S., & Pla, I. (2000). Soil sealing and its influence on erosion rates for some soils in the Mediterranean area. *Soil Science*, *165*(5), 398–403. https://doi.org/10.1097/00010694-200005000-00003

Reynolds, W. D. (1993). Chapter 56 saturated hydraulic conductivity: Field measurement. In M. R. Carter (Ed.), *Soil sampling and methods of analysis. Canadian Society of Soil Science* (pp. 599–613). Boca Raton, FL: Lewis Publishers.

Reynolds, W. D., & Elrick, D. E. (1990). Ponded infiltration from a single ring: I. Analysis of steady flow. *Soil Science Society of America Journal*, *54*, 1233–1241. https://doi.org/10.2136/sssaj1990.03615995005400050006x

Reynolds, W. D., & Elrick, D. E. (2002). 3.4.3.2.B pressure infiltrometer. In J. H. Dane, & G. C. Topp (Eds.), *Methods of soil analysis, physical methods, part 4 3rd edition. Soil Science Society of America* (pp. 826–836). Madison, WI.

Reynolds, W. D., Elrick, D. E., & Youngs, E. G. (2002a). 3.4.3.2 ring or cylinder infiltrometers (vadose zone). In J. H. Dane, & G. C. Topp (Eds.), *Methods of soil analysis, physical methods, part 4. Soil Science Society of America* (pp. 818–820). Madison, WI.

Reynolds, W. D., Elrick, D. E., & Youngs, E. G. (2002b). 3.4.3.2.A single-ring and double- or concentric-ring infiltrometers. In J. H. Dane, & G. C. Topp (Eds.), *Methods of soil analysis, physical methods, part 4. Soil Science Society of America* (pp. 821–826). Madison, WI.

Sisson, J. B., & Wierenga, P. J. (1981). Spatial variability of steady-State infiltration rates as a stochastic process 1. *Soil Science Society of America Journal*, *45*(4), 699–704. https://doi.org/10.2136/sssaj1981.03615995004500040005x

Smettem, K. R. J., Parlange, J. Y., Ross, J. P., & Haverkamp, R. (1994). Three-dimensional analysis of infiltration from disc infiltrometer. 1. A capillary-based theory. *Water Resources Research*, *30*, 2925–2929. https://doi.org/10.1029/94WR01787

Smith, H. J. C., Levy, G. J., & Shainberg, I. (1990). Water-droplet energy and soil amendments: Effect on infiltration and erosion. *Soil Science Society of America Journal*, *54*, 1084–1087. https://doi.org/10.2136/sssaj1990.03615995005400040026x

Thompson, A. L., & James, L. G. (1985). Water droplet impact and its effect on infiltration. *Transactions of ASAE*, *28*(5), 1506–1510. 1520, https://doi.org/10.13031/2013.32468

Touma, J., Voltz, M., & Albergel, J. (2007). Determining soil saturated hydraulic conductivity and sorptivity from single ring infiltration tests. *European Journal of Soil Science*, *58*(1), 229–238. https://doi.org/10.1111/j.1365-2389.2006.00830.x

Van de Giesen, N. C., Stomph, T. J., & De Ridder, N. (2000). Scale effects of Hortonian overland flow and rainfall–runoff dynamics in a West African catena landscape. *Hydrological Processes*, *14*(1), 165–175. https://doi.org/10.1002/(SICI)1099-1085(200001)14:1<165::AID-HYP920>3.0.CO;2-1

Votrubova, J., Dohnal, M., Vogel, T., Tesar, M., Jelinkova, V., & Cislerova, M. (2017). Ponded infiltration in a grid of permanent single-ring infiltrometers: Spatial versus temporal variability. *Journal of Hydrology and Hydromechanics*, *65*(3), 244–253. https://doi.org/10.1515/johh-2017-0015

Williams, J., & Bonell, M. (1988). The influence of scale of measurement on the spatial and temporal variability of the Philip infiltration parameters—An experimental study in an Australian savannah woodland. *Journal of Hydrology*, *104*(1–4), 33–51. https://doi.org/10.1016/0022-1694(88)90156-4

How to cite this article: Alagna V, Bagarello V, Cecere N, Concialdi P, Iovino M. A test of water pouring height and run intermittence effects on single-ring infiltration rates. *Hydrological Processes*. 2018;1–12. https://doi.org/10.1002/hyp.13290

Appendix D:

Journal of Hydrology 584 (2020) 124697

Contents lists available at ScienceDirect

Journal of Hydrology

journal homepage: www.elsevier.com/locate/jhydrol

Research papers

Testing an adapted beerkan infiltration run for a hydrologically relevant soil hydraulic characterization

N. Auteri, V. Bagarello*, P. Concialdi, M. Iovino

University of Palermo, Department of Agricultural, Food and Forest Sciences, Italy

ARTICLE INFO

"This manuscript was handled by Corrado Corradini-in-Chief, with the assistance of Wei Hu, Associate Editor".

Keywords:
Soil hydraulic properties
Surface hydrological processes
BEST procedure
Experimental methods

ABSTRACT

Literature raises doubts about the usability of infiltrometer methods to characterize soils in a hydrological perspective since these methods often yield excessively high infiltration rates or saturated soil hydraulic conductivity, K_s, values. For a loam (AR) and a silty-clay (RO) soil, beerkan infiltration runs were adapted in the perspective to obtain usable soil data to predict rainfall partition into infiltration and rainfall excess. In particular, the initially nearly dry soil was sampled with different water volumes (15 or 30) and heights of water application (low, L, 0.03 m, and high, H, 1.5 m), and the BEST-steady algorithm was applied to determine sorptivity, S, and K_s. The H runs altered the surface soil layer more than the L runs but the response of the two soils to disturbance was different. For the AR soil, deterioration of the surface layer was almost complete close to the end of the run while, for the RO soil, it was concluded after applying one third of the overall used water volume. The least soil perturbing experiment (15L), that was carried out with the commonly recommended experimental protocol, yielded high S (91–118 mm/h$^{0.5}$) and K_s (88–294 mm/h) values at the two sites, likely incompatible with formation of any rainfall excess. A soil perturbing experiment (30H) yielded significantly and substantially smaller S (26–40 mm/h$^{0.5}$) and K_s (4–6 mm/h) values, that appeared potentially compatible with formation of rainfall excess. The gravitational potential energy, E_p, of the water used for the infiltration run explained most of the variance of both K_s and S. In conclusion, the infiltration run can be adapted in an attempt to induce a soil disturbance likely similar to that expected for a rainfall producing runoff. In a relatively dry initial status, complete deterioration can require less water for a silty-clay soil than a loam soil. The saturated soil hydraulic conductivity is more sensitive than soil sorptivity to the applied experimental methodology. Finally, the gravitational potential energy of the applied water could be used to establish a link between the hydrological process that has to be explained and a soil hydraulic characterization appropriate to reach the desired objective.

1. Introduction

Explaining and simulating rainfall partition into infiltration and surface runoff, which is a central topic in hydrology of arid and semi-arid areas (Assouline and Mualem, 2002, 2006; Chen et al., 2013; Wu et al., 2019), requires determining sorptivity, S, and saturated hydraulic conductivity, K_s, of the surface soil layer (Touma et al., 2007). Due to their dependence on soil structure, these properties frequently show a noticeable spatial and temporal variability (Prieksat et al., 1994; Logsdon and Jaynes, 1996). Therefore, soil should be sampled intensively to characterize an area of interest (Bagarello et al., 2013). Working directly in the field is preferred to obtain reliable data since the functional connection of the sampled soil volume with the surrounding porous medium is maintained in this case (Bouma, 1982). Experimental methods to determine the soil hydraulic properties in the field should be cheap, simple, parsimonious and rapid.

Ponding single-ring infiltration methods generally have these requirements (Reynolds, 2008). Moreover, they are based on robust theories, have been extensively tested and can also yield a complete soil hydraulic characterization. This is the case of the so-called BEST (Beerkan Estimation of Soil Transfer parameters) method (Lassabatere et al., 2006; Yilmaz et al., 2010; Bagarello et al., 2014a; Angulo-Jaramillo et al., 2016, 2019) which estimates water retention and hydraulic conductivity curves by a three-dimensional field infiltration experiment at theoretically zero pressure head and the infiltration model by Haverkamp et al. (1994).

However, the literature raises doubts about the usability of infiltrometer methods to explain surface hydrological processes since a

* Corresponding author.
E-mail address: vincenzo.bagarello@unipa.it (V. Bagarello).

https://doi.org/10.1016/j.jhydrol.2020.124697
Received 15 October 2019; Received in revised form 10 February 2020; Accepted 14 February 2020
Available online 17 February 2020
0022-1694/ © 2020 Elsevier B.V. All rights reserved.

tendency of these methods to yield excessively high infiltration rates or K_s values has been reported by many authors. For example, Ben-Hur et al. (1987) suggested that predicting rainfall infiltration from double-ring infiltrometer data was not possible. The reason was that the structure of the bulk soil is the main factor controlling infiltration under water ponding conditions while the surface seal controls rainfall infiltration. The infiltration rates measured by Cerdà (1996, 1999) in some Spanish sites by ring infiltrometers were 3–8 times greater than those obtained by rainfall simulation due to water depth pressure established in the rings and crust development under simulated rainfall. Working in Côte d'Ivoire, van de Giesen et al. (2000) obtained a too high K_s value, actually precluding runoff occurrence although runoff was measured. These authors explained this inconsistency by noting that, during tropical storms, massive air inclusion may block some larger pores and, more importantly, crust formation and associated particle sorting decreases overall permeability. A similar result was obtained in Sicily by Bagarello et al. (2013) on runoff plots established on a clay soil. The median K_s values obtained by intensively sampling the soil were not lower than 600 mm/h but runoff at the base of the plot was measured even with rainfall intensities of no more than 100 mm/h. These authors suggested that surface K_s decreased during the event due to soil compaction induced by rainfall impact and wetting induced soil swelling. Recently, Morbidelli et al. (2017) showed that the double-ring infiltrometer overestimated the areal value of K_s as compared with controlled rainfall-runoff experiments. Picciafuoco et al. (2019) concluded that the magnitude of the bias is still an open issue for any available device because of the difficulties related to the identification of a reference value of K_s. Therefore, the inability of ponded infiltrometer methods to yield data usable to model rainfall-runoff processes seems a more experimental than theoretical problem.

Generally, single-ring infiltration runs make use of rather small water volumes. This circumstance has several advantages such as: i) transporting small water volumes in remote areas is easy (Bagarello et al., 2011); ii) many locations can be sampled with a limited water amount, which is important to improve confidence in the estimated mean value of a soil property (Kanso et al., 2018; Picciafuoco et al., 2019); and iii) the assumption of homogeneous soil and uniform initial water content, that is commonly made by infiltration models, is more realistic (Vandervaere et al., 2000). Moreover, using small amounts of water and hence performing relatively short duration runs is supported by the existing literature since attainment of quasi steady-state infiltration rates should be quite rapid in many circumstances (Bagarello et al., 1999; Reynolds et al., 2000; Lassabatere et al., 2006, 2019; Stewart and Abou Najm, 2018; Xiao et al., 2019). In many instances, emphasis is also put on the fact that obtaining reliable soil data by an infiltration method requires avoiding or at least reducing as much as possible any soil alteration due to the run. Consequently, small insertion depths of the ring are preferred, great care in ring insertion into the soil is recommended, compaction and shattering prone situations are suggested to impede or compromise ring insertion into the soil, and the need to prevent or minimize disturbance of the infiltration surface when water is applied is emphasized (Reynolds, 2008; Angulo-Jaramillo et al., 2016; Khodaverdiloo et al., 2017; Lassabatere et al., 2019).

However, two factors have to be considered in the perspective to characterize the soil for simulating surface hydrological processes: i) structure dependent soil properties have a dynamic nature and they can vary appreciably upon wetting due to, for example, aggregate breakdown by raindrop impact or weakening of interparticle bonds (Assouline, 2004; Dikinya et al., 2008; King and Bjorneberg, 2012; Chen et al., 2013); and ii) Hortonian surface runoff occurs as a consequence of prolonged and intense rainfall events (Assouline and Mualem, 2002, 2006; Wu et al., 2019). Therefore, in reality, a short and non-perturbing infiltration run could not represent the best choice to describe the hydrodynamic behavior of a soil when surface runoff occurs. Instead, long runs and water applications that induce some surface soil alteration could yield more appropriate estimates of soil hydrodynamic properties to explain and simulate surface hydrological processes.

Starting from this premise, Bagarello et al. (2014b) and Alagna et al. (2016, 2018) tested the effect of the height of water pouring for a single-ring infiltration experiment on the detectable soil response, in an attempt to distinguish between the theoretically expected decrease of infiltration rates during the run (Elrick and Reynolds, 1992) and that specifically due to mechanical disturbance of the infiltration surface. With the beerkan infiltration experiment and BEST methodologies of data analysis, low runs (L, height of water pouring, h_w = 0.03 m) yielded higher mean values of K_s than high (H, h_w = 1.5 m) runs by a factor of 11–35, depending on the sampled site, whereas height effects were less appreciable for sorptivity, in agreement with a similar finding by Somaratne and Smettem (1993). A relatively coarse textured soil was more sensitive to mechanical disturbance in initially drier conditions, in agreement with other investigations suggesting a greater rainfall induced soil disturbance in these conditions (Truman et al., 1990; Fohrer et al., 1999). Deterioration of the soil surface due to the higher height of water pouring was practically completed by the end of the run for the fine textured soils but not for the relatively coarse textured ones, and it is still unclear if this result was fortuitous. The usability of the beerkan run methodology and the BEST procedure to obtain soil data specifically representative of the altered soil surface layer was later demonstrated by Di Prima et al. (2017, 2018) and Alagna et al. (2019).

All the available information on the L and H infiltration runs methodology was collected by a standard protocol that yields an experimental cumulative infiltration curve by pouring a sequence of 15 water volumes, each establishing an initial water depth of nearly 1 cm on the infiltration surface. This protocol, that is largely applied (Angulo-Jaramillo et al., 2016, 2019; Lassabatere et al., 2019), was introduced in the first BEST paper (Lassabatere et al., 2006), probably because it was considered a reasonable compromise between the need to reach a near steady-state infiltration rate at the end of the run and that to use as small water volumes as possible for field campaigns. However, a longer infiltration process could promote a weakening of inter-particle bonds affecting the comparison between the L and H runs to an unpredictable extent. Indeed, either more similar or dissimilar results between the two types of runs can be expected in comparison with the standard (i.e., 15 water volumes) infiltration test. The former result could be the consequence of a progressive soil structure deterioration also occurring with the least soil perturbing runs. The latter result could occur since structure deterioration is easier and more complete with the perturbing runs due to the greater propensity of soil particles to be displaced. Therefore, the effect of the applied water volume should be established experimentally given that it was never tested before.

The objective of this investigation was to verify if performing a beerkan infiltration run with more water than that corresponding to the standard experimental protocol could make sense in the perspective to obtain realistic soil data for simulation of hydrological processes. In particular, a loam and a silty-clay soil were sampled by L and H runs using for the first time a relatively large number of water volumes to i) verify water volume and pouring height effects on the established infiltration process; ii) establish if deterioration requires less water for the finer soil than the coarser one; and iii) compare soil hydrodynamic properties estimated with infiltration runs differing by both the number of poured water volumes and the height of water application.

2. Materials and methods

2.1. Field sites

Two Sicilian soils with different physical properties were chosen for this investigation (Table 1). Disturbed soil samples were collected from

Table 1
Coordinates, land use, management practices, clay (*cl* in %), silt (*si* in %), and sand (*sa* in %) content (USDA classification system) in the 0–0.1 m depth range, soil textural classification, organic carbon content (*OC* in %), dry soil bulk density (ρ_b in kg/m^3), and initial volumetric soil water content (θ_i in m^3/m^3), for the sampled soils at the AR (Palermo) and RO (Roccamena) sites. Coefficients of variations in % are indicated in parentheses (sample sizes, $N = 4$ for *cl*, *si* and *sa*, *2* for OC and 10 for ρ_b and θ_i).

Variable	AR	RO
Coordinates	38.107282N 13.351922E	37.840178N 13.152530E
Land use	Citrus orchard	Fruit orchard
Management practices	No tillage	No tillage
cl	15.4 (6.5)	46.7 (2.5)
si	36.2 (0.2)	41.0 (2.4)
sa	48.4 (2.1)	12.4 (3.3)
Textural classification	loam	silty clay
OC	3.14 (0.5)	1.65 (0.4)
ρ_b	1064 (5.5)	998 (7.1)
θ_i	0.158 (21.8)	0.184 (16.1)

the upper 0.10 m of the profile to determine the soil particle size distribution (PSD). The PSD was determined using conventional methods following H_2O_2 pre-treatment to eliminate organic matter and clay deflocculation using sodium hexametaphosphate and mechanical agitation (Gee and Bauder, 1986). Soil organic carbon content, *OC* (%), was also determined by the Walkley-Black method. The risk of structural degradation of the sampled soils was then estimated by the structural stability index, *SI* (Pieri, 1992):

$$SI = \frac{1.724 \times OC}{silt + clay} \times 100$$

with *OC*, silt and clay contents expressed in percentage.

According to the USDA classification, a loam soil (AR site) was located at the Department of Agricultural, Food and Forest Sciences of the Palermo (Italy) University, at a few tens of meters from the sandy-loam soil sampled by Bagarello et al. (2014b). A silty-clay soil (RO site) was located near Roccamena, approximately 70 km south of Palermo. These two soils had a similar silt percentage (36–41%) but the AR soil had a 3.9 times higher sand content and a 3.0 times lower clay content than the RO soil. Therefore, the former soil was appreciably coarser than the latter one, which represented a favorable condition to verify a possible soil texture effect on the response to the infiltration run (Bagarello et al., 2014b). The two soils also differed in terms of structural stability since *SI* was equal to 10.5% for the AR soil, which denotes a stable structure (Pieri, 1992; Reynolds et al., 2009), and 3.2% for the RO soil, that indicates a structurally degraded soil.

Land use and management practices at each site were summarized in Table 1. An area of approximately 150 m^2 was selected at each site and the sampled soil surface was gently levelled and smoothed by manual implements. Bare areas were sampled at both sites.

2.2. Experimental field methods

Small diameter ($D = 0.08$ m) rings were inserted on the soil surface to a depth of 0.01 m for the beerkan infiltration runs (Lassabatere et al., 2006). Ring insertion was conducted manually or by gently using a rubber hammer and ensuring that the upper rim of the ring remained horizontal during insertion. The rings were particularly small to more clearly detect possible effects of soil disturbance due to water application. A total of 20 infiltration runs were carried out at randomly selected locations at a site. For each run, 30 water volumes, each of 57 mL, were successively poured in approximately 3 s on the confined infiltration surface. For each water volume (1st, 2nd, …, 30th), the infiltration time was measured from water application to disappearance of all water, when the subsequent water volume was poured on the infiltration surface. Despite other choices could have been made to establish when adding a new volume of water (Smith, 1999), waiting for complete disappearance of water from the infiltration surface was preferred to reduce operator's subjectivity when the infiltration surface was disturbed as a consequence of repeated, soil perturbing water pours. Ten runs were carried out by applying water at a small distance from the infiltration surface, i.e. approximately at a height, h_w, of 0.03 m. Water energy was dissipated on the fingers of the hand in an attempt to minimize soil disturbance due to water application (low, L, runs). Water was applied from $h_w = 1.5$ m at the other 10 sampling points (high, H, runs). The soil surface was not shielded in this case to maximize possible disruptive effects of water impact. To ensure flow verticality and prevent wind effects, the device developed by Bagarello et al. (2014b) and Alagna et al. (2016) was used.

At least one L and one H run were carried out on a given day at a distance of no more than 1.5–2.0 m from each other. In an intermediate position between the two sampling points for infiltration, two undisturbed soil cores (0.05 m in height by 0.05 m in diameter) were collected at the 0 to 0.05 m and 0.05 to 0.10 m depths, in accordance with other investigations (e.g., Lassabatere et al., 2019). These cores were used to determine the dry soil bulk density, ρ_b, and the antecedent volumetric soil water content, θ_i. The soil porosity, f, was calculated from ρ_b assuming a soil particle density of 2650 kg/m^3. According to other investigations, the field saturated soil water content, θ_s, was assumed to coincide with f (Mubarak et al., 2009; Bagarello et al., 2011; Angulo-Jaramillo et al., 2016, 2019). The data were averaged over the two depths and they were associated with the couple of L and H runs performed in the vicinity of the soil sampling location. A nearly uniform vertical profile of θ_i was assumed because the two soils were not irrigated and no rainfall occurred for several weeks before sampling. A summary of both ρ_b and θ_i for the two sampling sites was reported in Table 1.

This field experiment was carried out in the spring months of 2019, that is in a similar period of the year to that of the experiment by Bagarello et al. (2014b). The antecedent soil water conditions did not differ much between this investigation ($\theta_i = 0.16$ and 0.18 m^3/m^3 for the coarser and the finer soil, respectively, Table 1) and the previous one ($\theta_i = 0.12$–0.14 and 0.19–0.25 m^3/m^3 for the coarser and the finer soils, respectively). Therefore, this new experiment appeared usable to test the suggestion by Bagarello et al. (2014b) that, in initially dry or relatively dry conditions, complete soil disturbance due to height effects requires less water for fine than relatively coarse textured soils.

2.3. Calculations and data analysis

Infiltration data were plotted on cumulative infiltration, I (L), vs. time, t (T), and infiltration rate, i_r (L/T), vs. I plots to take an initial look at the general response of the two types of experiments (L and H) for the two sites. The i_r vs. I plot was used since durations changed from run to run, making presentation of all data on a single i_r vs. t plot confuse. The mean infiltration time of each applied water volume (1st, 2nd, …, 30th) was also calculated for both the low, Δt_L (T), and the high, Δt_H (T), runs. The $\Delta t_H/\Delta t_L$ ratio was then plotted against the number of the applied water volumes to detect the effect of the height of water pouring on infiltration.

For each run, the BEST-steady algorithm (Bagarello et al., 2014a) was applied to calculate soil sorptivity, S (L/T$^{0.5}$), and saturated soil hydraulic conductivity, K_s (L/T), from the experimentally determined intercept, b_s (L), and slope, i_s (L/T), of the straight line fitted to the data describing steady-state conditions on the I vs. t plot. Calculation of S and K_s was described in detail elsewhere (Bagarello et al., 2014a; Angulo-Jaramillo et al., 2016, 2019) and it was not repeated here for brevity reasons. BEST-steady was preferred to BEST-slope (Lassabatere et al., 2006) and BEST-intercept (Yilmaz et al., 2010) because it was the only algorithm that, in another investigation, allowed a successful treatment of runs involving soil alteration and led to K_s values close to those obtained by rainfall simulation (Di Prima et al., 2018). In

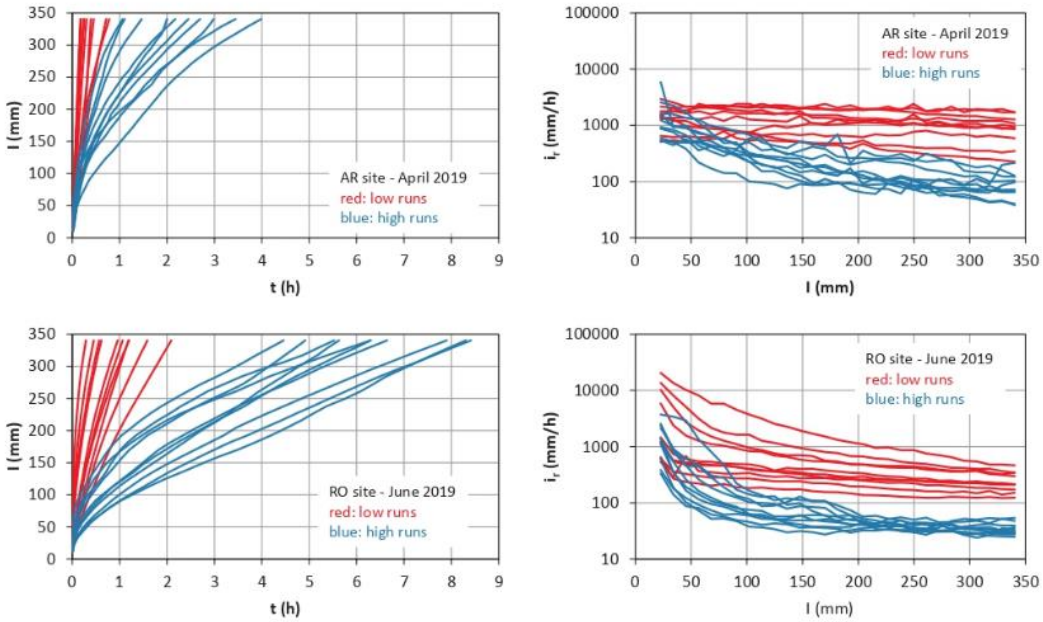

Fig. 1. Cumulative infiltration, I, vs. time, t, and infiltration rates, i_f, vs. I at the AR and RO sites for the two heights of water pouring (sample size, $N = 10$ for each site and type of run).

particular, these last authors suggested that, if any seal forms at the soil surface during a perturbing infiltration test, the BEST-steady estimates should properly characterize the hydraulic properties of the seal. The ability of the BEST methodology of soil hydraulic characterization to yield reliable estimates of the hydrodynamic parameters of the altered surface soil layer was also demonstrated by Alagna et al. (2019) with a field experiment and numerical simulation for a loam soil.

Two S and K_s values were determined for each infiltration run. In particular, an estimate of these parameters was obtained by considering a run with 15 water volumes, that represents the standard number of water volumes for a beerkan experiment and was used in previous investigations on height effects (Lassabatere et al., 2006; Bagarello et al., 2014b; Alagna et al., 2016). Another estimate of S and K_s was obtained for a run with 30 water volumes, that is using the complete experimental information. This procedure was applied for both the L and H runs. Consequently, four different experimental methodologies were considered to calculate S and K_s: 15L (15 water volumes and low height of water pouring), 30L (30 water volumes, L runs), 15H (15 water volumes and high height of water pouring) and 30H (30 water volumes, H runs). For each experimental methodology, the gravitational potential energy, E_p (J/m^2), of the water used for the infiltration run was calculated taking into account that both the mass of water and the height of fall were known. For example, 15 water volumes, each of 57 mL, correspond to a mass of water $m = 0.855$ kg, assuming a water density of 1000 kg/m^3. If the height of water pouring is $h = 1.5$ m and the infiltration surface is $A = \pi D^2/4 = 0.00503$ m^2, $E_p = mgh/A = 2502.1$ J/m^2 is obtained, g (m/s^2) being the acceleration due to gravity.

Each dataset was summarized by calculating the mean, M, and the associated coefficient of variation, CV. The arithmetic mean and the associated CV were calculated for cl, si, sa, OC, ρ_b and θ_i. For S and K_s, the statistical frequency distribution of the data was assumed to be ln-normal and geometric means and associated CVs were calculated using the appropriate ln-normal equations (Lee et al., 1985).

For each soil, comparisons were established between the hydrodynamic parameters estimated by different experimental methodologies. In particular, differences in K_s and S between the least (15L) and the most (30H) soil altering experiments were checked. The dependence of these differences on the two experimental factors that were allowed to vary was then determined by comparing the 15 L and 30 L (water volume) and the 30 L and 30 H (height of pouring) methodologies.

Subsequently, a comparison between the two soils was carried out with reference to the four experimental methodologies. The 15 L methodology was considered because it represents the standard beerkan infiltration experiment. The 30L methodology was perhaps more reliable with respect to attainment of steady-state infiltration rates. The 15H methodology was the most soil perturbing methodology in previous investigations on height effects. The 30H methodology had the most perturbing character in this investigation.

The relationship between the mean values of both K_s and S obtained with the four experimental methodologies and E_p was then tested to verify if the energy of the water used for the infiltration experiment explained changes in the two hydrodynamic parameters. Exponential, linear, logarithmic and power relationships were considered and the relationship having the highest coefficient of determination, R^2, was retained for further analysis.

Two-tailed t tests ($P < 0.05$) were carried out on ln-transformed S and K_s values to compare two datasets. A two-tailed t test was also used to establish the statistical significance of the fitted regression line to the data (Glantz, 2012).

3. Results

3.1. Infiltration process

Both the cumulative infiltration (I vs. t) and the infiltration rate (i_f vs. I) curves signaled that, at both sites, the infiltration processes was

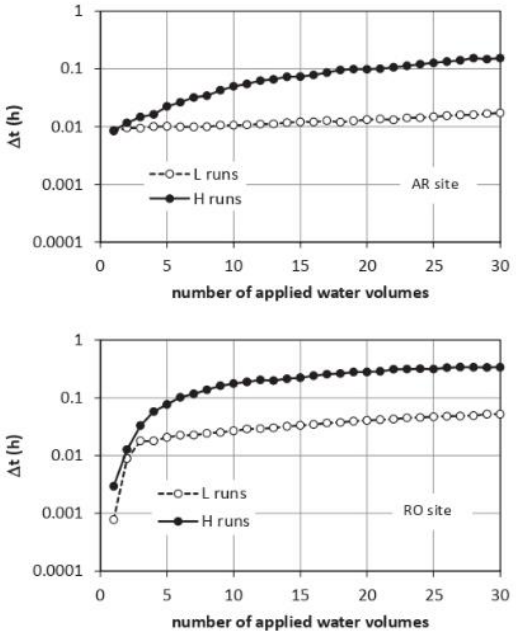

Fig. 2. Mean infiltration time, Δt, of each applied water volume for the two types of runs (low, L, and high, H) and the AR and RO sites (each data point in the graphs is the mean of 10 individual Δt values).

generally consistent with theory (Fig. 1). In particular, the concavity of the I vs. t curves was generally facing downwards and the infiltration rates decreased during the run. In some cases, the I vs. t relationship was nearly linear, indicating a practically steady-state infiltration process from the beginning of the run. In a single case (AR site, L10 run), i_f increased during part of the run and therefore the concavity of the cumulative infiltration curve was faced upwards.

Infiltration rates were greater for the L runs than the H ones at both sites and, consequently, the former runs (mean infiltration time = 0.57 h, CV = 59.9%, at the AR site and 1.00 h, CV = 55.3%, at the RO site) were shorter than the latter ones (mean infiltration time = 2.34 h, CV = 41.7%, at the AR site and 6.44 h, CV = 21.5%, at the RO site). Both types of runs were more rapid at the AR than the RO site. Relative variability of total run duration was smaller for the H runs than the L runs at both sites, suggesting a more homogeneous response of the sampled sites with the most perturbing runs.

At both sites and for both types of run, the mean infiltration time of a given water volume increased during the run (Fig. 2). However, Δt_H was greater than Δt_L from the beginning of the process, suggesting that soil perturbation had an immediate influence on infiltration. The graphs of Fig. 2 also suggested that Δt became nearly constant for the last 3–5 water volumes, depending on the site and the height of water pouring, denoting a near stabilization of infiltration rates close to the end of the experiment.

The $\Delta t_H/\Delta t_L$ ratio was always greater than one and it increased, for at least a part of the run, with the number of applied water volumes (Fig. 3). In particular, at the AR site, the relationship between $\Delta t_H/\Delta t_L$ and the number of applied water volumes showed an increasing trend for almost the whole duration of the run although the results for the last four water volumes could also be viewed as suggesting a final stabilization of $\Delta t_H/\Delta t_L$. Three particularities were detectable at the RO site: i) the first water volume determined an appreciably slower infiltration process when it was applied with the H procedure as compared with the

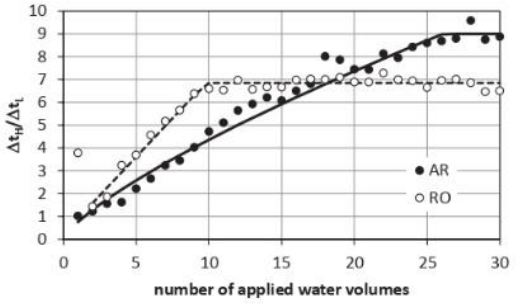

Fig. 3. Ratio between the mean infiltration time for a water application height of 1.5 m (Δt_H) and 0.03 m (Δt_L) during the beerkan runs plotted against the number of the applied volumes of water for the AR and RO sites.

L one ($\Delta t_H/\Delta t_L$ = 3.8); ii) $\Delta t_H/\Delta t_L$ was appreciably smaller (1.4) with the second water application but it then increased with the number of the applied water volumes; and iii) $\Delta t_H/\Delta t_L$ stabilized after applying ten volumes of water. The highest values of $\Delta t_H/\Delta t_L$ were detected on the coarser soil ($\Delta t_H/\Delta t_L \leq$ 9.6 and 7.3 at the AR and RO sites, respectively).

At the AR site, $\Delta t_H/\Delta t_L$ increased for almost all the run, suggesting a progressive deterioration of the surface soil layer that, however, seemed almost complete close to the end of the run since $\Delta t_H/\Delta t_L$ did not change much in this last phase. Soil deterioration was concluded by the end of the run at the RO site since $\Delta t_H/\Delta t_L$ stabilized early, that is after pouring one third of the overall used water volume.

In general, a higher $\Delta t_H/\Delta t_L$ value indicates a greater difference between infiltration with low and high runs. The number of the applied water volumes influenced the comparison between the two soils with respect to the relevance of height of pouring on infiltration. In particular, this effect was greater at the RO site than the AR site for $\leq$17 volumes. The opposite was true for 20 or more water volumes, and the two soils yielded a similar response with 18–19 water volumes. Therefore, the information collected with a small number of water volumes was not representative for the late phase of the run.

3.2. Soil hydrodynamic parameters

Valid calculations of K_s and S were obtained for seven L runs and nine H runs at the AR site and for nine L runs and 10 H runs at the RO site. Invalid calculations occurred as a consequence of a negative estimate of b_s for the nearly linear or concave upwards cumulative infiltration curves.

At both sites, the highest and the lowest K_s and S values were obtained with the experiments that induced the lowest (15 L) and the highest (30 H) soil disturbance, respectively, and all differences between two extreme mean values were statistically significant (Table 2). Therefore, the applied experimental methodology had a statistically detectable impact on determination of both soil hydrodynamic parameters. The changes of K_s were more noticeable at the AR site (decrease by 46.6 times from the 15 L to the 30 H experiment) than the RO site (22.1 times). The opposite result was obtained for S but in this case the two soils yielded a similar response (decrease by 2.9 and 3.4 times at the AR and RO sites, respectively).

Therefore, K_s was more affected than S by the applied experimental methodology, in agreement with previous findings (Somaratne and Smettem, 1993; Bagarello et al., 2014b). This result confirmed that K_s is a sentinel property since it is highly sensitive to the applied experimental methodology (Reynolds et al., 2000).

The saturated conductivity decreased by 3.5 times at both sites for increasing water volumes (comparison between 15 L and 30 L methodologies) and by 13.3 (AR site) and 6.3 (RO site) times for increasing

Table 2
Summary statistics of the saturated soil hydraulic conductivity, K_s, and sorptivity, S, values obtained at the two sampling sites with different experimental methodologies.

Variable	Experimental methodology	Statistic	AR site	RO site
K_s (mm/h)	15L	Mean	293.8 (a)(c)	88.4 (b)(c)
		CV (%)	107.6	48.0
	30L	Mean	83.8 (d)	25.2 (d)
		CV (%)	88.9	27.0
	15H	Mean	31.0 (e)	9.8 (e)
		CV (%)	95.4	46.1
	30H	Mean	6.3 (a)f	4.0 (b)f
		CV (%)	67.6	60.8
S (mm/h$^{0.5}$)	15L	Mean	118.3 (a)c	91.0 (b)c
		CV (%)	25.2	36.8
	30L	Mean	113.2 (d)	72.1 (d)
		CV (%)	32.1	21.6
	15H	Mean	58.7 (e)	33.1 (e)
		CV (%)	32.0	22.8
	30H	Mean	40.3 (a)(f)	26.5 (b)(f)
		CV (%)	25.4	13.3

15L and 30L: 15 and 30 water volumes, respectively, and low height of water pouring. 15H and 30H: 15 and 30 water volumes, respectively, and high height of water pouring. For a given variable, means followed by the same letter enclosed in parenthesis were significantly different at $P = 0.05$ according to a two-tailed t test. Means followed by the same letter not enclosed in parenthesis were not significantly different.

height of water pouring (30 L vs. 30 H methodologies; Table 2). More water determined a decrease of S by 1.1 and 1.3 times at the AR and RO sites, respectively, whereas S decreased by 2.8 times at the AR site and 2.7 times at the RO site with a higher height of water pouring.

With the standard beerkan infiltration run (15 L), the AR soil had a 3.3 times greater K_s value and a similar S value as compared with the RO soil (Table 2). Using more water for the run (30L) or increasing its perturbing character (15H) did not modify the K_s results (soil differences by 3.2–3.3 times) but it induced a difference for S that was 1.6–1.8 times higher at the former site than the latter one. Using more water for the run and increasing its perturbing character (30H) made the two soils statistically similar with reference to K_s but the AR soil was 1.5 times more sorptive than the RO soil.

At both sites, the gravitational potential energy, E_p, of the water used for the infiltration run explained much of the variance in both K_s and S (Fig. 4). The effect of E_p was stronger for S than K_s and, for the latter soil parameter, the fitted relationship for the RO site was significant at $P = 0.10$ instead of $P = 0.05$ as in all the other cases. However, the R^2 differences between the two soils were minimal.

With reference to the mean K_s values for the AR site, Fig. 5 shows the fitted relationship obtained by considering simultaneously the data collected in this investigation and those obtained by Bagarello et al. (2014b). Even in this case, the R^2 value was significant and also rather high (0.86), notwithstanding the differences in the applied experimental methods, given that Bagarello et al. (2014b) used BEST-intercept (Yilmaz et al., 2010) and the one-dimensional simplified falling-head technique (Bagarello et al., 2004). The fact that even in this case it was possible to fit a unique relationship to the data suggested that the energy of the applied water for the experiment had a major impact on the results of the field campaign. According to the relationship of Fig. 5, the soil maintains its permeability characteristics for an E_p value that does not exceed approximately 1000 J/m^2 but it decreases even appreciably for higher E_p values.

4. Discussion

The environmental conditions of this investigation were similar to those reported by Bagarello et al. (2014b). In particular, they were typical of the spring period in the Mediterranean area, that is persistently dry and occasionally hot. Before sampling, the soil had time enough to dry out after the winter period but not to become extremely dry as could occur in summer months. According to this investigation, a soil structure explanation (Pieri, 1992; Reynolds et al., 2009) could be invoked to explain the detected soil effect on the dynamics of the alteration process (Bagarello et al., 2014b). In particular, degradation is more impulsive (fast occurrence and rapid stabilization) in a structurally less resilient soil than in a more resilient medium.

Development of a structural seal layer at the soil surface is a dynamic process which depends on many factors and has a very large impact on infiltration (Fohrer et al., 1999; Assouline and Mualem, 2002; Assouline, 2004). According to this investigation, a simple methodology that makes use of two different heights of water pouring (≤ 1.5 m) and less than 2 L of water can be applied in the field to check changes in the infiltration process under development of an altered layer at the soil surface.

A greater K_s stability was detected for the silty-clay soil than the loam soil (Table 2), in agreement with other investigations. For example, Assouline and Mualem (2002) reported a saturated conductivity of the seal layer lower than that of the underlying undisturbed soil by 17 times for a relatively fine textured (silty-clay-loam) soil and by 79–115 times for two coarser (loam and sandy-loam) soils. This similarity supports the usability of an adapted infiltration run for a hydrologically relevant soil hydraulic characterization. In particular, a soil can be characterized under different conditions, ranging from a nearly undisturbed situation (relatively short and non-perturbing run) to heavily disturbed (long and perturbing run).

A run making use of more water (30 L instead of 15 L) can be expected to yield smaller infiltration rates at the end of the process for different reasons. The most obvious is a closer attainment of nearly steady-state conditions with the longer run (Reynolds and Elrick, 2002). Fig. 2 gave some weak support to this interpretation but the estimated i_s values were characterized by R^2 values of the near steady-state phase of the process varying between 0.997 and 1.0 for the 15L runs, denoting a stabilization of the infiltration process with the shorter run. Therefore, attainment of steady-state was probably a minor factor influencing the established comparison. More water implies larger sampled volumes (Elrick and Reynolds, 1992) which could suggest that the different response of the two types of run was a consequence of small scale spatial variability of soil hydraulic properties (Price and Bauer, 1984; Mallants et al., 1996). However, each individual 30L run yielded a smaller K_s value than the corresponding 15L run and it was unlikely that each smaller soil bulb was systematically embedded in a less permeable bulb. A more plausible explanation was that more water promoted soil structural changes (Or, 1996; Bagarello and Sgroi, 2004; Lado et al., 2004; Dikinya et al., 2008). The infiltration run was longer and therefore there was more time for a weakening of the bonds between soil particles and more chances that detached soil particles were transported, with a subsequent modification of the soil pore system.

Applying water from a higher height (30 H instead of 30 L) can be expected to yield smaller infiltration rates as a consequence of mechanical effects on the soil surface, such as compaction and vertical displacement of detached soil particles and small aggregates. Vertical heterogeneity of soil hydraulic properties was not considered to explain the detected differences between the 30L and 30H runs since the same water volume was used for these runs. Areal heterogeneity was also viewed as an unlikely explanation because the sampled area was rather small and the number of replications was relatively large.

Therefore, most of the decrease in the soil hydrodynamic parameters detected in the passage from the 15 L to 30 H runs occurred because water was poured from a high height. Structural changes due to prolonged wetting contributed to make the decrease of S and K_s more noticeable. Likely, changing the experimental method implied passing from a process mainly governed by an unstable structural macroporosity (Watson and Luxmoore, 1986; Jarvis and Messing, 1995; Jarvis et al., 2013) to a process that was more controlled by the soil matrix. In

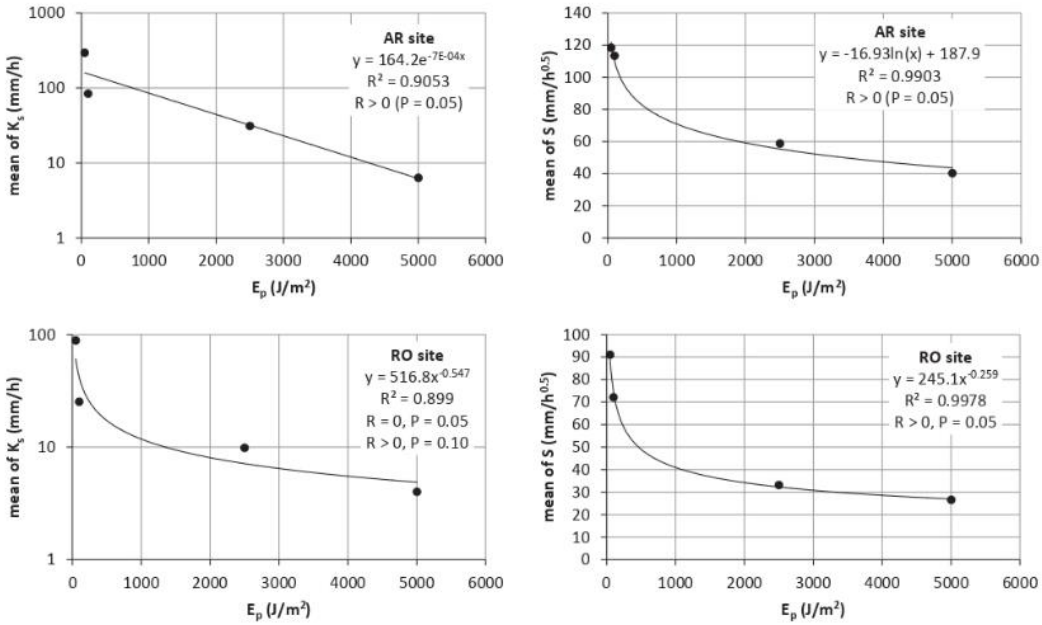

Fig. 4. Mean saturated soil hydraulic conductivity, K_s, and sorptivity, S, values vs. gravitational potential energy, E_p, of the applied water for the AR and RO sampling sites.

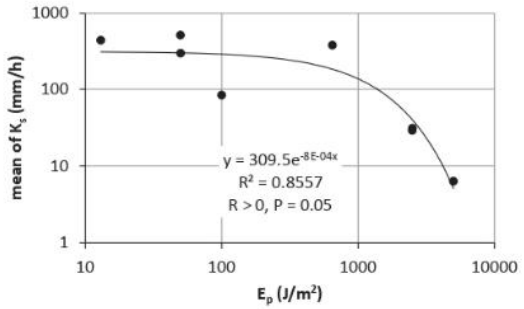

Fig. 5. Relationship between the mean saturated soil hydraulic conductivity, K_s, and the gravitational potential energy, E_p, of the applied water obtained by considering simultaneously the data collected in this investigation and in that by Bagarello et al. (2014b).

such a situation, a greater S value for the AR soil than the RO one was consistent with less dissipation for the coarsest soil (Stewart et al., 2013).

A decline of the soil hydrodynamic properties can occur at the seasonal temporal scale (Hu et al., 2009) and, according to this investigation, it can also have a nearly abrupt character. The decrease of S and K_s induced by the perturbing run in a situation of no-tillage management practice (Table 1) could also be viewed as a suggestion that soil recovery processes occurred after previous damaging (Hu et al., 2012, 2018; Bagarello et al., 2020).

Rainfall energy is known to influence infiltration since it controls development of a structural seal layer at the soil surface (Thompson and James, 1985; Smith et al., 1990; Schiettecatte et al., 2005; King and Bjorneberg, 2012). According to investigation, the energy of the applied water by a beerkan infiltration run could be used to establish a link between the hydrological process that has to be simulated and a soil hydraulic characterization appropriate to reach the desired objective. However, it will be necessary to take into account that the same total energy can be obtained with different intensities and durations (rainfall) and with different water volumes and heights of pouring (infiltration run). Moreover, it should also be considered that, in natural conditions, part of the energy could be dissipated by the vegetation covering the soil whereas, according to the experimental protocol for a beerkan infiltration run (Lassabatere et al., 2006), the surface vegetation has to be removed from the area to be sampled. Even in this case, an effect of the vegetation on the response of the L and H runs cannot be excluded because the roots remain in situ and they could reinforce the soil (Cislaghi et al., 2017).

Predicting areal infiltration and runoff from small bare catchments in arid and semiarid areas needs considering areal heterogeneity of soil hydraulic properties, and particularly of K_s, as well as the presence of a sealed layer at the soil surface (Assouline and Mualem, 2002, 2006). Obtaining in the field the effective soil hydraulic properties by considering that soil structure deteriorates as a consequence of raindrop impact is still a challenge. This investigation could open some new perspective to approach this objective by adapting common single-ring infiltration methods. A non-perturbing infiltration experiment provides the necessary information to characterize the nearly undisturbed soil whereas the perturbing infiltration experiment characterizes the upper altered soil layer (Di Prima et al., 2018). The experiments are simple and rather parsimonious in terms of both equipment and required water amounts, which means that many replicated infiltration runs can be carried out to characterize areal variability of soil hydraulic properties. In the future, the actual potential of this methodological suggestion could perhaps be checked by establishing a link between hydrological data and alternative soil hydraulic characterizations. As an example for the RO soil, Fig. 6 shows the relationship between the time to ponding, t_p, and the rainfall intensity, i_{rain}, developed according to White et al. (1989) for each of the four experimental scenarios of this investigation.

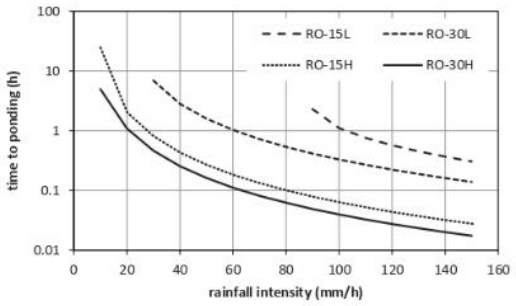

Fig. 6. Relationship between the time to ponding according to White et al. (1989) and the rainfall intensity for different experimental methodologies of soil hydraulic characterization at the RO site.

If at least a few t_p values can experimentally be determined, the closeness of the t_p data to the predicted $t_p(i_{rain})$ relationships could represent a criterion to establish what is the most appropriate soil sampling methodology. This kind of check could yield a more robust information as compared with that obtained by comparing different methods to measure soil hydraulic properties. The reason is that, especially with reference to K_s, different methods can be expected to yield dissimilar results and there is no independent K_s datum or benchmark upon which evaluations and judgments can be made (Reynolds et al., 2000; Picciafuoco et al., 2019).

5. Conclusions

This investigation showed that the single-ring beerkan infiltration run can be adapted in an attempt to induce a soil disturbance that is likely similar to the one expected when a rainfall event produces runoff. In particular, using much water for the experiment and applying water from a relatively high height on the infiltration surface determined an appreciable decrease of sorptivity, S and, particularly, of saturated soil hydraulic conductivity, K_s, as compared with the standard beerkan run. These data seem more hydrologically relevant than those obtained with standard experimental methodologies since they were obtained in a soil condition that is closer to that expected when runoff is formed.

The investigation also showed that, in an initially relatively dry soil, deterioration effects attributable to the mechanical impact of the water required less water for a silty-clay soil than a loam soil.

The gravitational potential energy, E_p, of the water used for the infiltrometer experiment explained much of the variance of the K_s and S values obtained by different experimental methodologies.

In conclusion, an infiltrometer experiment can be carried out in such a way to mimic what happens in real situations when rainfall produces Hortonian runoff. Soil disturbance can be controlled by changing the water volume used for the run and the height of water pouring. The field experiment remains rather simple and consequently the attractiveness of infiltrometer methods is not reduced by adapting the run to a hydrologically representative situation. The few encouraging signs about the reliability of the proposed method to estimate soil hydraulic properties relevant for simulating runoff deserve stronger confirmation.

In a hydrological perspective, it also seems advisable to improve our knowledge on the short term modifications of K_s and S in an attempt to verify if, under what experimental conditions and to what level they stabilize when a disturbing run is carried out. The lowest possible S and K_s values could be viewed as a sort of hydrologically relevant index since they describe the most favorable condition to runoff occurrence. According to this investigation, these developments should not be excessively demanding from an experimental point of view. An alternative method to characterize a soil in a runoff prone situation is to make the field campaign with common experimental protocols after a sealed layer has fully developed. Establishing a comparison between the two options (inducing disturbance, working on naturally altered soil) is obviously advisable although the latter option places constraints on the time when the experiment can be performed.

Funding

This research did not receive any specific grant from funding agencies in the public, commercial, or not-for-profit sectors.

CRediT authorship contribution statement

N. Auteri: Investigation, Writing - original draft. **V. Bagarello:** Conceptualization, Methodology, Formal analysis, Writing - original draft, Writing - review & editing, Supervision. **P. Concialdi:** Formal analysis, Investigation, Writing - original draft. **M. Iovino:** Conceptualization, Methodology, Writing - original draft, Writing - review & editing, Supervision.

Declaration of Competing Interest

The authors declare that they have no known competing financial interests or personal relationships that could have appeared to influence the work reported in this paper.

References

Alagna, V., Bagarello, V., Di Prima, S., Giordano, G., Iovino, M., 2016. Testing infiltration run effects on the estimated water transmission properties of a sandy-loam soil. Geoderma 267, 24–33. https://doi.org/10.1016/j.geoderma.2015.12.029.

Alagna, V., Bagarello, V., Cecere, N., Concialdi, P., Iovino, M., 2018. A test of water pouring height and run intermittence effects on single-ring infiltration rates. Hydrol. Process. 32, 3793–3804. https://doi.org/10.1002/hyp.13290.

Alagna, V., Bagarello, V., Di Prima, S., Guaitoli, F., Iovino, M., Keesstra, S., Cerdà, A., 2019. Using Beerkan experiments to estimate hydraulic conductivity of a crusted loamy soil in a Mediterranean vineyard. J. Hydrol. Hydromechan. 67 (2), 191–200. https://doi.org/10.2478/johh-2018-0023.

Angulo-Jaramillo, R., Bagarello, V., Iovino, M., Lassabatere, L., 2016. Infiltration Measurements for Soil Hydraulic Characterization. Springer International Publishing, Switzerland, pp. 386 ISBN 978-3-319-31786-1, 978-3-319-31788-5 (eBook), doi: 10.1007/978-3-319-31788-5.

Angulo-Jaramillo, R., Bagarello, V., Di Prima, S., Gosset, A., Iovino, M., Lassabatere, L., 2019. Beerkan Estimation of Soil Transfer parameters (BEST) across soils and scales. Invited Review Paper. J. Hydrol. 576, 239–261. https://doi.org/10.1016/j.jhydrol.2019.06.007.

Assouline, S., 2004. Rainfall-induced soil surface sealing: a critical review of observations, conceptual models, and solutions. Vadose Zone J. 3, 570–591.

Assouline, S., Mualem, Y., 2002. Infiltration during soil sealing: The effect of areal heterogeneity of soil hydraulic properties. Water Resour. Res. 38 (12), 1286. https://doi.org/10.1029/2001WR001168.

Assouline, S., Mualem, Y., 2006. Runoff from heterogeneous small bare catchments during soil surface sealing. Water Resour. Res. 42 (12), W12405. https://doi.org/10.1029/2005WR004592.

Bagarello, V., Sgroi, A., 2004. Using the single-ring infiltrometer method to detect temporal changes in surface soil field-saturated hydraulic conductivity. Soil Tillage Res. 76, 13–24.

Bagarello, V., Iovino, M., Reynolds, W.D., 1999. Measuring hydraulic conductivity in a cracking clay soil using the Guelph permeameter. Trans. ASAE 42 (4), 957–964.

Bagarello, V., Iovino, M., Elrick, D., 2004. A simplified falling-head technique for rapid determination of field-saturated hydraulic conductivity. Soil Sci. Soc. Am. J. 68, 66–73.

Bagarello, V., Di Prima, S., Iovino, M., Provenzano, G., Sgroi, A., 2011. Testing different approaches to characterize Burundian soils by the BEST procedure. Geoderma 162, 141–150. https://doi.org/10.1016/j.geoderma.2011.01.014.

Bagarello, V., Di Stefano, C., Iovino, M., Sgroi, A., 2013. Using a transient infiltrometric technique for intensively sampling field-saturated hydraulic conductivity of a clay soil in two runoff plots. Hydrol. Process. 27, 3415–3423. https://doi.org/10.1002/hyp.9448.

Bagarello, V., Di Prima, S., Iovino, M., 2014a. Comparing alternative algorithms to analyze the beerkan infiltration experiment. Soil Sci. Soc. Am. J. 78, 724–736. https://doi.org/10.2136/sssaj2013.06.0231.

Bagarello, V., Castellini, M., Di Prima, S., Iovino, M., 2014b. Soil hydraulic properties determined by infiltration experiments and different heights of water pouring. Geoderma 213, 492–501. https://doi.org/10.1016/j.geoderma.2013.08.032.

Bagarello V., Cecere N., David S.M., Di Prima S. 2020. Determining short-term changes of the hydraulic properties of a sandy-loam soil by a three-run infiltration experiment.

In press on Hydrol. Sci. J. (accepted on December 20, 2019).
Ben-Hur, M., Shainberg, I., Morin, J., 1987. Variability of infiltration in a field with surface-sealed soil. Soil Sci. Soc. Am. J. 51, 1299–1302.
Bouma, J., 1982. Measuring the hydraulic conductivity of soil horizons with continuous macropores. Soil Sci. Soc. Am. J. 46, 438–441.
Cerdà, A., 1996. Seasonal variability of infiltration rates under contrasting slope conditions in southeast Spain. Geoderma 69, 217–232.
Cerdà, A., 1999. Seasonal and spatial variations in infiltration rates in badland surfaces under Mediterranean climatic conditions. Water Resour. Res. 35 (1), 319–328.
Chen, L., Sela, S., Svoray, T., Assouline, S., 2013. The role of soil-surface sealing, microtopography, and vegetation patches in rainfall–runoff processes in semiarid areas. Water Resour. Res. 49 (9), 5585–5599. https://doi.org/10.1002/wrcr.20360.
Cislaghi, A., Bordoni, M., Meisina, C., Bischetti, G.B., 2017. Soil reinforcement provided by the root system of grapevines: Quantification and spatial variability. Ecol. Eng. 109 (Part B), 169–185.
Dikinya, O., Hinz, C., Aylmore, G., 2008. Decrease in hydraulic conductivity and particle release associated with self-filtration in saturated soil columns. Geoderma 146 (1–2), 192–200. https://doi.org/10.1016/j.geoderma.2008.05.014.
Di Prima, S., Bagarello, V., Lassabatere, L., Angulo-Jaramillo, R., Bautista, I., Burguet, M., Cerdà, A., Iovino, M., Prosdocimi, M., 2017. Comparing Beerkan infiltration tests with rainfall simulation experiments for hydraulic characterization of a sandy-loam soil. Hydrol. Process. 31, 3520–3532. https://doi.org/10.1002/hyp.11273.
Di Prima, S., Concialdi, P., Lassabatere, L., Angulo-Jaramillo, R., Pirastru, M., Cerdà, A., Keesstra, S., 2018. Laboratory testing of Beerkan infiltration experiments for assessing the role of soil sealing on water infiltration. Catena 167, 373–384. https://doi.org/10.1016/j.catena.2018.05.013.
Elrick D.E., Reynolds W.D. 1992. Infiltration from constant-head well permeameters and infiltrometers. In G.C. Topp, W.D. Reynolds and R.E. Green (eds.), Advances in Measurement of Soil Physical Properties: Bringing Theory into Practice, SSSA Special Publication no. 30, Madison, WI, USA. pp.1–24.
Fohrer, N., Berkenhagen, J., Hecker, J.-M., Rudolph, A., 1999. Changing soil and surface conditions during rainfall: Single rainstorm/subsequent rainstorms. Catena 37 (3–4), 355–375. https://doi.org/10.1016/S0341-8162(99)00026-0.
Gee, G.W., Bauder, J.W., 1986. Particle-size Analysis. In SSSA Book SeriesSoil Science Society of America. American Society of Agronomy, pp. 383–411.
Glantz, S.A., 2012. Primer of Biostatistics, 7th ed. The McGraw-Hill Companies.
Haverkamp, R., Ross, P.J., Smettem, K.R.J., Parlange, J.Y., 1994. Three-dimensional analysis of infiltration from the disc infiltrometer: 2. Physically based infiltration equation. Water Resour. Res. 30 (11), 2931–2935.
Hu, W., Shao, M., Wang, Q., Fan, J., Horton, R., 2009. Temporal changes of soil hydraulic properties under different land uses. Geoderma 149, 355–366.
Hu, W., Shao, M.A., Si, B.C., 2012. Seasonal changes in surface bulk density and saturated hydraulic conductivity of natural landscapes. Eur. J. Soil Sci. 63, 820–830.
Hu, W., Tabley, F., Beare, M., Tregurtha, C., Gillespie, R., Qiu, W., Gosden, P., 2018. Short-term dynamics of soil physical properties as affected by compaction and tillage in a silt loam soil. Vadose Zone J. 17, 180115. https://doi.org/10.2136/vzj2018.06.0115.
Jarvis, N.J., Messing, I., 1995. Near-saturated hydraulic conductivity in soils of contrasting texture measured by tension infiltrometers. Soil Sci. Soc. Am. J. 59, 27–34.
Jarvis, N., Koestel, J., Messing, I., Moeys, J., Lindahl, A., 2013. Influence of soil, land use and climatic factors on the hydraulic conductivity of soil. Hydrol. Earth Syst. Sci. 17 (12), 5185–5195. https://doi.org/10.5194/hess-17-5185-2013.
Kanso, T., Tedoldi, D., Gromaire, M.-C., Ramier, D., Saad, M., Chebbo, G., 2018. Horizontal and vertical variability of soil hydraulic properties in roadside sustainable drainage systems (SuDS) – Nature and implications for hydrological performance evaluation. Water 10, 987. https://doi.org/10.3390/w10080987.
Khodaverdiloo, H., Cheraghabdal, H.K., Bagarello, V., Iovino, M., Asgarzadeh, H., Dashtaki, S.G., 2017. Ring diameter effects on determination of field-saturated hydraulic conductivity of different loam soils. Geoderma 303, 60–69. https://doi.org/10.1016//j.geoderma.2017.04.031.
King, B.A., Bjorneberg, D.L., 2012. Transient soil surface sealing and infiltration model for bare soil under droplet impact. Trans. ASABE 55 (3), 937–945.
Lado, M., Paz, A., Ben-Hur, M., 2004. Organic matter and aggregate size interactions in infiltration, seal formation, and soil loss. Soil Sci. Soc. Am. J. 68, 935–942.
Lassabatere, L., Angulo-Jaramillo, R., Soria Ugalde, J.M., Cuenca, R., Braud, I., Haverkamp, R., 2006. Beerkan estimation of soil transfer parameters through infiltration experiments – BEST. Soil Sci. Soc. Am. J. 70, 521–532. https://doi.org/10.2136/sssaj2005.0026.
Lassabatere, L., Di Prima, S., Angulo-Jaramillo, R., Keesstra, S., Salesa, D., 2019. Beerkan multi-runs for characterizing water infiltration and spatial variability of soil hydraulic properties across scales. Hydrol. Sci. J. 64 (2), 165–178. https://doi.org/10.1080/02626667.2018.1560448.
Lee, D.M., Reynolds, W.D., Elrick, D.E., Clothier, B.E., 1985. A comparison of three field methods for measuring saturated hydraulic conductivity. Can. J. Soil Sci. 65, 563–573.
Logsdon, S.D., Jaynes, D.B., 1996. Spatial variability of hydraulic conductivity in a cultivated field at different times. Soil Sci. Soc. Am. J. 60, 703–709.
Mallants, D., Mohanty, B.P., Jacques, D., Feyen, J., 1996. Spatial variability of hydraulic properties in a multi-layered soil profile. Soil Sci. 161 (3), 167–181.
Morbidelli, R., Saltalippi, C., Flammini, A., Cifrodelli, M., Picciafuoco, T., Corradini, C., Govindaraju, R.S., 2017. In situ measurements of soil saturated hydraulic conductivity: assessment of reliability through rainfall–runoff experiments. Hydrol. Process. https://doi.org/10.1002/hyp.11247.
Mubarak, I., Mailhol, J.C., Angulo-Jaramillo, R., Ruelle, P., Boivin, P., Khaledian, M., 2009. Temporal variability in soil hydraulic properties under drip irrigation. Geoderma 150 (1–2), 158–165. https://doi.org/10.1016/j.geoderma.2009.01.022.
Or, D., 1996. Wetting-induced soil structural changes: the theory of liquid phase sintering. Water Resour. Res. 32 (10), 3041–3049.
Picciafuoco, T., Morbidelli, R., Flammini, A., Saltalippi, C., Corradini, C., Strauss, P., Blöschl, G., 2019. On the estimation of spatially representative plot scale saturated hydraulic conductivity in an agricultural setting. J. Hydrol. 570, 106–117. https://doi.org/10.1016/j.jhydrol.2018.12.044.
Pieri, C.J.M.G., 1992. Fertility of SOILS: A FUTURE FOR FARMING IN THE West African Savannah. Springer-Verlag, Berlin, Germany.
Price, A.G., Bauer, B.O., 1984. Small-scale heterogeneity and soil-moisture variability in the unsaturated zone. J. Hydrol. 70 (1–4), 277–293.
Prieksat, M.A., Kaspar, T.C., Ankeny, M.D., 1994. Positional and temporal changes in ponded infiltration in corn field. Soil Sci. Soc. Am. J. 58, 181–184.
Reynolds, W.D., 2008. Chapter 77. Saturated hydraulic properties: ring infiltrometer. In: Carter, M.R., Gregorich, E.G. (Eds.), Soil Sampling and Methods of Analysis, 2nd. Canadian Society of Soil Science, Boca Raton, FL, USA, pp. 1043–1056.
Reynolds W.D., Elrick D.E. 2002. 3.4.3.2.b Pressure infiltrometer. In: J.H. Dane and G.C. Topp (eds.), Methods of Soil Analysis, Part 4, Physical Methods, Number 5 in the Soil Science Society of America Book Series, Soil Science Society of America, Inc., Madison, WI, USA. pp. 826–836.
Reynolds, W.D., Bowman, B.T., Brunke, R.R., Drury, C.F., Tan, C.S., 2000. Comparison of tension infiltrometer, pressure infiltrometer, and soil core estimates of saturated hydraulic conductivity. Soil Sci. Soc. Am. J. 64, 478–484.
Reynolds, W.D., Drury, C.F., Tan, C.S., Fox, C.A., Yang, X.M., 2009. Use of indicators and pore volume-function characteristics to quantify soil physical quality. Geoderma 152, 252–263. https://doi.org/10.1016/j.geoderma.2009.06.009.
Schiettecatte, W., Jin, K., Yao, Y., Cornelis, W.M., Lu, J., Wu, H., Verbist, K., Cai, D., Gabriels, D., Hartmann, R., 2005. Influence of simulated rainfall on physical properties of a conventionally tilled loess soil. Catena 64, 209–221.
Smith, R.E., 1999. Technical note: Rapid measurement of soil sorptivity. Soil Sci. Soc. Am. J. 63, 55–57.
Smith, H.J.C., Levy, G.J., Shainberg, I., 1990. Water-droplet energy and soil amendments: effect on infiltration and erosion. Soil Sci. Soc. Am. J. 54, 1084–1087.
Somaratne, N.M., Smettem, K.R.J., 1993. Effect of cultivation and raindrop impact on the surface properties of an Alfisol under wheat. Soil Tillage Res. 26, 115–125.
Stewart, R.D., Rupp, D.E., Abou Najm, M.R., Selker, J.S., 2013. Modeling effect of initial soil moisture on sorptivity and infiltration. Water Resour. Res. 49, 7037–7047. https://doi.org/10.1002/wrcr.20508.
Stewart, R.D., Abou Najm, M.R., 2018. A comprehensive model for single ring infiltration. I: initial water content and soil hydraulic properties. Soil Sci. Soc. Am. J. 82, 548–557. https://doi.org/10.2136/sssaj2017.09.0313.
Thompson, A.L., James, L.G., 1985. Water droplet impact and iys effect on infiltration. Trans. ASAE 1506–1510, 1520.
Touma, J., Voltz, M., Albergel, J., 2007. Determining soil saturated hydraulic conductivity and sorptivity from single ring infiltration tests. Eur. J. Soil Sci. 58 (1), 229–238. https://doi.org/10.1111/j.1365-2389.2006.00830.x.
Truman, C.C., Bradford, J.M., Ferris, J.E., 1990. Antecedent water content and rainfall energy influence on soil aggregate breakdown. Soil Sci. Soc. Am. J. 54, 1385–1392.
van de Giesen, N.C., Stomph, T.J., de Ridder, N., 2000. Scale effects of Hortonian overland flow and rainfall-runoff dynamics in a West African catena landscape. Hydrol. Process. 14, 165–175.
Vandervaere, J.P., Vauclin, M., Elrick, D.E., 2000. Transient flow from tension infiltrometers: I. The two-parameter equation. Soil Sci. Soc. Am. J. 64, 1263–1272.
Watson, K.W., Luxmoore, R.J., 1986. Estimating macroporosity in a forest watershed by use of a tension infiltrometer. Soil Sci. Soc. Am. J. 50, 578–582.
White, I., Sully, M.J., Melville, M.D., 1989. Use and hydrological robustness of time-to-incipient-ponding. Soil Sci. Soc. Am. J. 29, 1343–1346.
Wu, S., Chen, L., Wang, N., Xu, S., Bagarello, V., Ferro, V., 2019. Variable power-law scaling of hillslope Hortonian rainfall-runoff processes. Hydrol. Process. https://doi.org/10.1002/hyp.13538.
Xiao, B., Sun, F., Hu, K., Kidron, G.J., 2019. Biocrusts reduce surface soil infiltrability and impede soil water infiltration under tension and ponding conditions in dryland ecosystems. J. Hydrol. 568, 792–802. https://doi.org/10.1016/j.jhydrol.2018.11.051.
Yilmaz, D., Lassabatere, L., Angulo-Jaramillo, R., Deneele, D., Legret, M., 2010. Hydrodynamic characterization of basic oxygen furnace slag through an adapted BEST method. Vadose Zone J. 9, 1–10.

References

Aiello, R., Bagarello, V., Barbagallo, S., Consoli, S., Di Prima, S., Giordano, G., Iovino, M., 2014. An assessment of the beerkan method for determining the hydraulic properties of a sandy loam soil. Geoderma 235–236, 300–307. https://doi.org/10.1016/j.geoderma.2014.07.024

Agnese, C., Bagarello, V., Baiamonte, G., Iovino, M., 2011. Comparing physical quality of forest and pasture soils in a Sicilian watershed. Soil Sci. Soc. Am. J. 75, 1958. https://doi.org/10.2136/sssaj2011.0044

Alagna, V., Bagarello, V., Di Prima, S., Guaitoli, F., Iovino, M., Keesstra, S., Cerdà, A., 2019. Using beerkan experiments to estimate hydraulic conductivity of a crusted loamy soil in a Mediterranean vineyard. J. Hydrol. Hydromech. 67. https://doi.org/10.2478/johh-2018-0023

Alagna, V., Bagarello, V., Cecere, N., Concialdi, P., Iovino, M., 2018. A Test of water pouring height and run intermittence effects on single-ring infiltration rates. Hydrol. Process. https://doi.org/10.1002/hyp.13290

Alagna, V., Bagarello, V., Di Prima, S., Giordano, G., Iovino, M., 2016a. Testing infiltration run effects on the estimated water transmission properties of a sandy-loam soil. Geoderma 267, 24–33. https://doi.org/10.1016/j.geoderma.2015.12.029

Alagna, V., Bagarello, V., Di Prima, S., Iovino, M., 2016b. Determining hydraulic properties of a loam soil by alternative infiltrometer techniques. Hydrol. Process. 30, 263–275. https://doi.org/10.1002/hyp.10607

Alagna, V., Bagarello, V., Di Prima, S., Giordano, G., Iovino, M., 2013. A simple field method to measure the hydrodynamic properties of soil surface crust. J. Agric. Eng. 44, 74–79. https://doi.org/10.4081/jae.2013.(s1):e14

Angulo-Jaramillo, R., Bagarello, V., Di Prima, S., Gosset, A., Iovino, M., Lassabatere, L., 2019. Beerkan Estimation of Soil Transfer parameters (BEST) across soils and scales. J. Hydrol. 576, 239–261. https://doi.org/10.1016/j.jhydrol.2019.06.007

Angulo-Jaramillo, R., Bagarello, V., Iovino, M., Lassabatere, L., 2016. Unsaturated soil hydraulic properties, in: Infiltration measurements for soil hydraulic characterization. Springer International Publishing, pp. 181–287.

Assouline, S., Mualem, Y., 2006. Runoff from heterogeneous small bare catchments during soil surface sealing. Water Resour. Res. 42, W12405. https://doi.org/10.1029/2005WR004592

Assouline, S., 2004. Rainfall-induced soil surface sealing. Vadose Zone J. 3, 570–591

Assouline, S., Mualem, Y., 2002. Infiltration during soil sealing: The effect of areal heterogeneity of soil hydraulic properties. Water Resour. Res. 38, 1286. https://doi.org/10.1029/2001WR001168

Auteri, N., Bagarello, V., Concialdi, P., Iovino, M., 2020. Testing an adapted beerkan infiltration run for a hydrologically relevant soil hydraulic characterization. J. Hydrol. 584, 124697. https://doi.org/10.1016/j.jhydrol.2020.124697

Bagarello, V., Cecere, N., David, S.M., Prima, S.D., 2020. Determining short-term changes in the hydraulic properties of a sandy-loam soil by a three-run infiltration experiment. Hydrol. Sci. J.

Bagarello, V., Baiamonte, G., Caia, C., 2019. Variability of near-surface saturated hydraulic conductivity for the clay soils of a small Sicilian basin. Geoderma 340, 133–145. https://doi.org/10.1016/j.geoderma.2019.01.008

Bagarello, V., Cecere, N., Prima, S.D., Giordano, G., Iovino, M., 2017. Height of water pouring effects on infiltration runs carried out in an initially wet sandy-loam soil. Chem. Eng. Trans. 721–726. https://doi.org/10.3303/CET1758121

Bagarello, V., Di Prima, S., Iovino, M., 2014a. Comparing alternative algorithms to analyze the beerkan infiltration experiment. Soil Sci. Soc. Am. J. 78, 724. https://doi.org/10.2136/sssaj2013.06.0231

Bagarello, V., Di Prima, S., Giordano, G., Iovino, M., 2014b. A test of the Beerkan Estimation of Soil Transfer parameters (BEST) procedure. Geoderma 221–222, 20–27. https://doi.org/10.1016/j.geoderma.2014.01.017

Bagarello, V., Castellini, M., Di Prima, S., Iovino, M., 2014c. Soil hydraulic properties determined by infiltration experiments and different heights of water pouring. Geoderma 213, 492–501. https://doi.org/10.1016/j.geoderma.2013.08.032

Bagarello, V., Di Prima, S., Iovino, M., Provenzano, G., 2014d. Estimating field-saturated soil hydraulic conductivity by a simplified beerkan infiltration experiment. Hydrol. Process. 28, 1095–1103. https://doi.org/10.1002/hyp.9649

Bagarello, V., Di Stefano, C., Iovino, M., Sgroi, A., 2013. Using a transient infiltrometric technique for intensively sampling field-saturated hydraulic conductivity of a clay soil in two runoff plots. Hydrol. Process. 27, 3415–3423. https://doi.org/10.1002/hyp.9448

Bagarello, V., D'Asaro, F., Iovino, M., 2012. A field assessment of the Simplified Falling Head technique to measure the saturated soil hydraulic conductivity. Geoderma 187–188, 49–58. https://doi.org/10.1016/j.geoderma.2012.04.008

Bagarello, V., Di Prima, S., Iovino, M., Provenzano, G., Sgroi, A., 2011. Testing different approaches to characterize Burundian soils by the BEST procedure. Geoderma 162, 141–150. https://doi.org/10.1016/j.geoderma.2011.01.014

Bagarello, V., Stefano, C.D., Ferro, V., Iovino, M., Sgroi, A., 2010. Physical and hydraulic characterization of a clay soil at the plot scale. J. Hydrol. 387, 54–64. https://doi.org/10.1016/j.jhydrol.2010.03.029

Bagarello, V., Sgroi, A., 2007. Using the simplified falling head technique to detect temporal changes in field-saturated hydraulic conductivity at the surface of a sandy loam soil. Soil Tillage Res. 94, 283–294. https://doi.org/10.1016/j.still.2006.08.001

Bagarello, V., Iovino, M., Elrick, D., 2004. A Simplified Falling-Head technique for rapid determination of field-saturated hydraulic conductivity. Soil Sci. Soc. Am. J. 68, 66. https://doi.org/10.2136/sssaj2004.6600

Bagarello, V., Iovino, M., Reynolds, W.D., 1999. Measuring hydraulic conductivity in a cracking clay soil using the Guelph permeameter. Trans. ASAE 42.

Basant, S., Wilcox, B.P., Leite, P.M., Morgan, C.L., 2020. When savannas recover from overgrazing, ecohydrological connectivity collapses. Environ. Res. Lett. 15, 054001. https://doi.org/10.1088/1748-9326/ab71a1

Batista, P.H.D., Almeida, G.L.P. de, Pandorfi, H., Tavares, U.E., Melo, A.A.S. de, Guiselini, C., 2019. Spatial variability of soil physical-hydric attributes under bovine trampling in agreste of Pernambuco State, Brazil. Acta Sci. Agron. 41. https://doi.org/10.4025/actasciagron.v41i1.39594

Ben-Hur, M., Shainberg, I., Morin, J., 1987. Variability of infiltration in a field with surface-sealed Soil. Soil Sci. Soc. Am. J. 51, 1299-1302.https://doi.org/10.2136/sssaj1987.03615995005100050037x

Bièvre, G., Jongmans, D., Goutaland, D., Pathier, E., Zumbo, V., 2016. Geophysical characterization of the lithological control on the kinematic pattern in a large clayey landslide (Avignonet, French Alps). Landslides 13, 423–436. https://doi.org/10.1007/s10346-015-0579-0

Bouarafa, S., Lassabatere, L., Lipeme-Kouyi, G., Angulo-Jaramillo, R., 2019. Hydrodynamic characterization of sustainable urban drainage systems (SuDS) by using beerkan infiltration experiments. Water 11, 660. https://doi.org/10.3390/w11040660

Braud, I., Desprats, J.-F., Ayral, P.-A., Bouvier, C., Vandervaere, J.-P., 2017. Mapping topsoil field-saturated hydraulic conductivity from point measurements using different methods. J. Hydrol. Hydromech. 65. https://doi.org/10.1515/johh-2017-0017

Braud, I., 2014. Multi-scale hydrometeorological observation and modelling strategy for flash-flood understanding 16, 2580.

Brooks, R.H., Corey, T., 1964. Hydraulic properties of porous media. Hydrol Pap. 3 Colo. State Univ. Fort Collins.

Burdine, N.T., 1953. Relative permeability calculation from pore size distribution data. Petr TransAmInst Min Met. Eng 198, 71–77.

Canone, D., Previati, M., Bevilacqua, I., Salvai, L., Ferraris, S., 2015. Field measurements based model for surface irrigation efficiency assessment. Agric. Water Manag. 156, 30–42. https://doi.org/10.1016/j.agwat.2015.03.015

Cannavo, P., Vidal-Beaudet, L., Béchet, B., Lassabatère, L., Charpentier, S., 2010. Spatial distribution of sediments and transfer properties in soils in a stormwater infiltration basin. J. Soils Sediments 10, 1499–1509. https://doi.org/10.1007/s11368-010-0258-7

Castellini, M., Stellacci, A.M., Mastrangelo, M., Caputo, F., Manici, L.M., 2020. Estimating the soil hydraulic functions of some olive orchards: soil management implications for water saving in soils of Salento peninsula (Southern Italy). Agronomy 10, 177. https://doi.org/10.3390/agronomy10020177

Castellini, M., Fornaro, F., Garofalo, P., Giglio, L., Rinaldi, M., Ventrella, D., Vitti, C., Vonella, A.V., 2019a. Effects of no-tillage and conventional tillage on physical and hydraulic properties of fine textured soils under winter wheat. Water Switz. 11. https://doi.org/10.3390/w11030484

Castellini, Mirko, Stellacci, A.M., Tomaiuolo, M., Barca, E., 2019b. Spatial variability of soil physical and hydraulic properties in a durum wheat field: An assessment by the BEST-procedure. Water 11, 1434. https://doi.org/10.3390/w11071434

Castellini, M., Di Prima, S., Iovino, M., 2018. An assessment of the BEST procedure to estimate the soil water retention curve: A comparison with the evaporation method. Geoderma 320, 82–94. https://doi.org/10.1016/j.geoderma.2018.01.014

Castellini, M., Iovino, M., Pirastru, M., Niedda, M., Bagarello, V., 2016. Use of BEST procedure to assess soil physical quality in the Baratz lake catchment (Sardinia, Italy). Soil Sci. Soc. Am. J. 0, 0. https://doi.org/10.2136/sssaj2015.11.0389

Cerdà, A., 1999. Seasonal and spatial variations in infiltration rates in badland surfaces under Mediterranean climatic conditions. Water Resour. Res. 35, 319–328. https://doi.org/10.1029/98WR01659

Cerdà, A.,Ibáñez, S., Calvo, A., 1997. Design and operation of a small and portable rainfall simulator for rugged terrain. Soil Technol. 11, 163–170. https://doi.org/10.1016/S0933-3630(96)00135-3

Cerdà, A., 1996. Seasonal variability of infiltration rates under contrasting slope conditions in southeast Spain. Geoderma 69, 217–232. https://doi.org/10.1016/0016-7061(95)00062-3

Cheik, S., Bottinelli, N., Minh, T.T., Doan, T.T., Jouquet, P., 2019a. Quantification of three dimensional characteristics of macrofauna macropores and their effects on soil hydraulic conductivity in northern Vietnam. Front. Environ. Sci.

Cheik, S., Bottinelli, N., Soudan, B., Harit, A., Chaudhary, E., Sukumar, R., Jouquet, P., 2019b. Effects of termite foraging activity on topsoil physical properties and water infiltration in Vertisol. Appl. Soil Ecol. 133, 132–137.

Cheik, S., Shanbhag, R.R., Harit, A., Bottinelli, N., Sukumar, R., Jouquet, P., 2019c. Linking termite feeding preferences and soil physical functioning in Southern-Indian Woodlands. Insects 10, 4. https://doi.org/10.3390/insects10010004

Chen, L., Sela, S., Svoray, T., Assouline, S., 2013. The role of soil-surface sealing, microtopography, and vegetation patches in rainfall-runoff processes in semiarid areas. Water Resour. Res. 49, 5585–5599. https://doi.org/10.1002/wrcr.20360

Coutinho, A.P., Lassabatere, L., Montenegro, S., Antonino, A.C.D., Angulo-Jaramillo, R., Cabral, J.J.S.P., 2016. Hydraulic characterization and hydrological behaviour of a pilot permeable pavement in an urban centre, Brazil. Hydrol. Process. 30, 4242–4254. https://doi.org/10.1002/hyp.10985

Cullotta, S., Bagarello, V., Baiamonte, G., Gugliuzza, G., Iovino, M., La Mela Veca, D.S., Maetzke, F., Palmeri, V., Sferlazza, S., 2016. Comparing different methods to determine soil physical quality in a Mediterranean forest and pasture land. Soil Sci. Soc. Am. J. 0, 0. https://doi.org/10.2136/sssaj2015.12.0447

Dikinya, O., Hinz, C., Aylmore, G., 2008. Decrease in hydraulic conductivity and particle release associated with self-filtration in saturated soil columns. Geoderma 146, 192–200. https://doi.org/10.1016/j.geoderma.2008.05.014

Di Prima, S., Winiarski, T., Angulo-Jaramillo, R., Stewart, R. D., Castellini, M., Abou Najm, M. R., & Biddoccu, M. 2020. Detecting infiltrated water and preferential flow pathways through time-lapse ground-penetrating radar surveys. Science of The Total Environment, 138511. https://doi.org/10.1016/j.scitotenv.2020.138511

Di Prima, S., Concialdi, P., Lassabatere, L., Angulo-Jaramillo, R., Pirastru, M., Cerda, A., Keesstra, S., 2018a. Laboratory testing of beerkan infiltration experiments for assessing the role of soil sealing on water infiltration. Catena 167, 373–384. https://doi.org/10.1016/j.catena.2018.05.013

Di Prima, S., Marrosu, R., Lassabatere, L., Angulo-Jaramillo, R., Pirastru, M., 2018b. In situ characterization of preferential flow by combining plot- and point-scale infiltration experiments on a hillslope. J. Hydrol. 563, 633–642. https://doi.org/10.1016/j.jhydrol.2018.06.033

Di Prima, S., Rodrigo-Comino, J., Novara, A., Iovino, M., Pirastru, M., Keesstra, S., Cerdà, A., 2018c. Soil physical quality of citrus orchards under tillage, herbicide, and organic managements. Pedosphere 28, 463–477. https://doi.org/10.1016/S1002-0160(18)60025-6

Di Prima, S., Bagarello, V., Lassabatere, L., Angulo-Jaramillo, R., Bautista, I., Burguet, M., Cerdà, A., Iovino, M., Prosdocimi, M., 2017. Comparing beerkan infiltration tests with rainfall simulation experiments for hydraulic characterization of a sandy-loam soil. Hydrol. Process. 31, 3520–3532. https://doi.org/10.1002/hyp.11273

Di Prima, S., Lassabatere, L., Bagarello, V., Iovino, M., Angulo-Jaramillo, R., 2016. Testing a new automated single ring infiltrometer for beerkan infiltration experiments. Geoderma 262, 20–34. https://doi.org/10.1016/j.geoderma.2015.08.006

Di Prima, S., 2015. Automated single ring infiltrometer with a low-cost microcontroller circuit. Comput. Electron. Agric. 118, 390–395. https://doi.org/10.1016/j.compag.2015.09.022

Dohnal, M., Vogel, T., Dusek, J., Votrubova, J., Tesar, M., 2016. Interpretation of ponded infiltration data using numerical experiments. J. Hydrol. Hydromech. 64, 289–299. https://doi.org/10.1515/johh-2016-0020

Durand-Bessart, C., Tixier, P., Quinteros, A., Andreotti, F., Rapidel, B., Tauvel, C., Allinne, C., 2020. Analysis of interactions amongst shade trees, coffee foliar diseases and coffee yield in multistrata agroforestry systems. Crop Prot. 133, 105137. https://doi.org/10.1016/j.cropro.2020.105137

Fohrer, N., Berkenhagen, J., Hecker, J.-M., Rudolph, A., 1999. Changing soil and surface conditions during rainfall: Single rainstorm/subsequent rainstorms. CATENA 37, 355–375. https://doi.org/10.1016/S0341-8162(99)00026-0

Gette-Bouvarot, M., Mermillod-Blondin, F., Angulo-Jaramillo, R., Delolme, C., Lemoine, D., Lassabatere, L., Loizeau, S., Volatier, L., 2014. Coupling hydraulic and biological measurements highlights the key influence of algal biofilm on infiltration basin performance. Ecohydrology 7, 950–964. https://doi.org/10.1002/eco.1421

Gonzalez-Merchan, C., Barraud, S., Bedell, J.-P., 2014. Influence of spontaneous vegetation in stormwater infiltration system clogging. Environ. Sci. Pollut. Res. 21, 5419–5426. https://doi.org/10.1007/s11356-013-2398-y

Gonzalez-Sosa, E., Braud, I., Dehotin, J., Lassabatère, L., Angulo-Jaramillo, R., Lagouy, M., Branger, F., Jacqueminet, C., Kermadi, S., Michel, K., 2010. Impact of land use on the hydraulic properties of the topsoil in a small French catchment. Hydrol. Process. 24, 2382–2399. https://doi.org/10.1002/hyp.7640

Goutaland, D., Winiarski, T., Lassabatere, L., Dubé, J.S., Angulo-Jaramillo, R., 2013. Sedimentary and hydraulic characterization of a heterogeneous glaciofluvial deposit: Application to the modeling of unsaturated flow. Eng. Geol. 166, 127–139. https://doi.org/10.1016/j.enggeo.2013.09.006

Haverkamp, R., Ross, P.J., Smettem, K.R.J., Parlange, J.Y., 1994. Three-dimensional analysis of infiltration from the disc infiltrometer: 2. Physically based infiltration equation. Water Resour. Res. 30, 2931–2935. https://doi.org/10.1029/94WR01788

Kanso, T., Tedoldi, D., Gromaire, M.-C., Ramier, D., Saad, M., Chebbo, G., 2018. Horizontal and vertical variability of soil hydraulic properties in roadside Sustainable Drainage Systems (SuDS)—Nature and implications for hydrological performance evaluation. Water 10, 987. https://doi.org/10.3390/w10080987

Keller, T., Sutter, J.A., Nissen, K., Rydberg, T., 2012. Using field measurement of saturated soil hydraulic conductivity to detect low-yielding zones in three Swedish fields. Soil Tillage Res. 124, 68–77.https://doi.org/10.1016/j.still.2012.05.002

Khaledian, M., Shabanpour, M., Alinia, H., 2016. Saturated hydraulic conductivity variation in a small garden under drip irrigation. Geosystem Eng. 19, 266–274. https://doi.org/10.1080/12269328.2016.1188030

Khodaverdiloo, H., Cheraghabdal, H.K., Bagarello, V., Iovino, M., Asgarzadeh, H., Dashtaki, S.G., 2017. Ring diameter effects on determination of field-saturated hydraulic conductivity of different loam soils. Geoderma 303, 60–69. https://doi.org/10.1016//j.geoderma.2017.04.031.

King, B.A., Bjorneberg, D.L., 2012. Transient soil surface sealing and infiltration model for bare soil under droplet impact. Trans. ASABE 55, 937–945

Lassabatere, L., Di Prima, S., Angulo-Jaramillo, R., Keesstra, S., Salesa, D., 2019a. Beerkan multi-runs for characterizing water infiltration and spatial variability of soil hydraulic properties across scales. Hydrol. Sci. J. 64 (2), 165–178. https://doi.org/10.1080/02626667.2018.1560448

Lassabatere, L., Di Prima, S., Angulo-Jaramillo, R., Keesstra, S., Cerda, A., 2019b. Beerkan multi-runs for characterizing water infiltration and spatial variability of soil hydraulic properties across scales. Hydrol. Sci. J. https://doi.org/10.1080/02626667.2018.1560448

Lassabatere, L., Di Prima, S., Bouarafa, S., Iovino, M., Bagarello, V., Angulo Jaramillo, R., 2019c. BEST-2K for characterizing dual-permeability unsaturated soils with ponded and tension infiltrometers. Vadose Zone J.

Lassabatere, L., Angulo-Jaramillo, R., Goutaland, D., Letellier, L., Gaudet, J.P., Winiarski, T., Delolme, C., 2010. Effect of the settlement of sediments on water infiltration in two urban infiltration basins. Geoderma 156, 316–325. https://doi.org/10.1016/j.geoderma.2010.02.031

Lassabatere, L., Angulo-Jaramillo, R., Soria Ugalde, J.M., Cuenca, R., Braud, I., Haverkamp, R., 2006. Beerkan estimation of soil transfer parameters through infiltration experiments—BEST. Soil Sci. Soc. Am. J. 70, 521. https://doi.org/10.2136/sssaj2005.0026

Lavrnić, S., Alagna, V., Iovino, M., Anconelli, S., Solimando, D., Toscano, A., 2020. Hydrological and hydraulic behaviour of a surface flow constructed wetland treating agricultural drainage water in northern Italy. Sci. Total Environ. 702, 134795. https://doi.org/10.1016/j.scitotenv.2019.134795

Le Bissonnais, Y.L., Singer, M.J., 1992. Crusting, runoff, and erosion response to soil water content and successive rainfalls. Soil Sci. Soc. Am. J. 56, 1898–1903

Leite, P.A.M., de Souza, E.S., dos Santos, E.S., Gomes, R.J., Cantalice, J.R., Wilcox, B.P., 2017. The influence of forest regrowth on soil hydraulic properties and erosion in a semiarid region of Brazil. Ecohydrology n/a-n/a. https://doi.org/10.1002/eco.1910

Levy, G., Shainberg, I., Morin, J., 1986. Factors affecting the stability of soil crusts in subsequent storms. Soil Sci. Soc. Am. J. 50, 196–201. https://doi.org/10.2136/sssaj1986.03615995005000010037x

Lozano-Baez, S.E., Cooper, M., de Barros Ferraz, S.F., Ribeiro Rodrigues, R., Lassabatere, L., Castellini, M., Di Prima, S., 2020. Assessing water infiltration and soil water repellency in brazilian Atlantic forest soils. Appl. Sci. 10, 1950. https://doi.org/10.3390/app10061950

Lozano-Baez, S.E., Cooper, M., Ferraz, S., Ribeiro Rodrigues, R., Pirastru, M., Di Prima, S., 2018. Previous land use affects the recovery of soil hydraulic properties after forest restoration. Water 10, 453. https://doi.org/10.3390/w10040453

Marichal, R., Grimaldi, M., Feijoo M., A., Oszwald, J., Praxedes, C., Ruiz Cobo, D.H., del Pilar Hurtado, M., Desjardins, T., Silva Junior, M.L. da, Silva Costa, L.G. da, Miranda, I.S., Delgado Oliveira, M.N., Brown, G.G., Tsélouiko, S., Martins, M.B., Decaëns, T., Velasquez, E., Lavelle, P., 2014. Soil macroinvertebrate communities and ecosystem services in deforested landscapes of Amazonia. Appl. Soil Ecol., XVI International Colloquium on Soil Zoology & XIII International Colloquium on Apterygota, Coimbra, 2012 – Selected papers 83, 177–185. https://doi.org/10.1016/j.apsoil.2014.05.006

Minasny, B., McBratney, A.B., 2007. Estimating the water retention shape parameter from sand and clay content. Soil Sci. Soc. Am. J. 71, 1105. https://doi.org/10.2136/sssaj2006.0298N

Montenegro, S.M., da Silva, B.B., Antonino, A.C., Lima, J.R., de Souza, E.S., de Oliveira, L.M., de Moura, A.E., Souza, R.M.S., 2014. Hydrological studies in experimental and representative basins in Pernambuco State, Brazil. Proc. Int. Assoc. Hydrol. Sci. 364, 422–428

Morbidelli, R., Saltalippi, C., Flammini, A., Cifrodelli, M., Picciafuoco, T., Corradini, C., Govindaraju, R.S., 2017. In situ measurements of soil saturated hydraulic conductivity: assessment of reliability through rainfall–runoff experiments. Hydrol. Process. https://doi.org/10.1002/hyp.11247

Morin, J., Benyamini, Y., 1977. Rainfall infiltration into bare soils. Water Resour. Res. 13, 813–817. https://doi.org/10.1029/WR013i005p00813

Mubarak, I., Angulo-Jaramillo, R., Mailhol, J.C., Ruelle, P., Khaledian, M., Vauclin, M., 2010. Spatial analysis of soil surface hydraulic properties: Is infiltration method dependent? Agric. Water Manag. 97, 1517–1526. https://doi.org/10.1016/j.agwat.2010.05.005

Mubarak, I., Mailhol, J.C., Angulo-Jaramillo, R., Bouarfa, S., Ruelle, P., 2009a. Effect of temporal variability in soil hydraulic properties on simulated water transfer under high-frequency drip irrigation. Agric. Water Manag. 96, 1547–1559. https://doi.org/10.1016/j.agwat.2009.06.011

Mubarak, I., Mailhol, J.C., Angulo-Jaramillo, R., Ruelle, P., Boivin, P., Khaledian, M., 2009b. Temporal variability in soil hydraulic properties under drip irrigation. Geoderma 150, 158–165. https://doi.org/10.1016/j.geoderma.2009.01.022

Nasta, P., Lassabatere, L., Kandelous, M.M., Šimůnek, J., Angulo-Jaramillo, R., 2012. Analysis of the role of tortuosity and infiltration constants in the beerkan method. Soil Sci. Soc. Am. J. 76, 1999–2005

Ndiaye, B., Esteves, M., Vandervaere, J.-P., Lapetite, J.-M., Vauclin, M., 2005. Effect of rainfall and tillage direction on the evolution of surface crusts, soil hydraulic properties and runoff generation for a sandy loam soil. J. Hydrol. 307, 294–311. https://doi.org/10.1016/j.jhydrol.2004.10.016

Palácio Filho, A.M., Maciel Netto, A., Corrêa, M.M., Rolim Neto, F.C., Silva, L.P.D., Malta, S.H.D.S., Palácio Filho, A.M., Maciel Netto, A., Corrêa, M.M., Rolim Neto, F.C., Silva, L.P.D., Malta, S.H.D.S., 2020. Hydrodinamic and hydrodispersive characterization of a fluvic cambisol in the northeast region of Brazil 1. Rev. Caatinga 33, 160–171. https://doi.org/10.1590/1983-21252020v33n118rc

Parlange, J.-Y., 1975. On solving the flow equation in unsaturated soils by optimization: Horizontal infiltration. Soil Sci. Soc. Am. J. 39, 415–418

Philip, J.-R., 1969. Theory of infiltration, in: Advances in Hydroscience. Elsevier, pp. 215–296.

Picciafuoco, T., Morbidelli, R., Flammini, A., Saltalippi, C., Corradini, C., Strauss, P., Blöschl, G., 2019. On the estimation of spatially representative plot scale saturated hydraulic conductivity in an agricultural setting. J. Hydrol. 570, 106–117. https:// doi.org/10.1016/j.jhydrol.2018.12.044

Ramos, M.C., Nacci, S., Pla, I., 2000. Soil sealing and its influence on erosion rates for some soils inthe Mediterranean area. Soil Sci. 165, 398–403. https:/doi.org/10.1097/00010694-200005000-00003

Reyes Gómez, V.M., Viramontes Olivas, O., Arredondo Moreno, J.T., Huber Sannwald, E., Rodríguez, A.R., 2015. Functional ecohydrological differences among native and exotic grassland covers in sub-urban landscapes of Chihuahua city, Mexico. Landsc. Urban Plan. 139, 54–62. https://doi.org/10.1016/j.landurbplan.2015.03.005

Reynolds, W.D., 2008. Saturated hydraulic properties: ring infiltrometer. Carter MR Gregor. EG Eds Soil Sampl. Methods Anal. 2nd Ed CRC Press Boca Raton Pp 1043–1056.

Reynolds, W.D., Bowman, B.T., Brunke, R.R., Drury, C.F., Tan, C.S., 2000. Comparison of tension infiltrometer, pressure infiltrometer, and soil core estimates of saturated hydraulic conductivity. Soil Sci. Soc. Am. J. 64, 478–484. https://doi.org/10.2136/sssaj2000.642478x

Sales, E.G., Almeida, C.D.N., Farias, A.S., Coelho, V.H.R., 2014. Hydrodynamic characterization of soils within a representative watershed in northeast Brazil. Proc. Int. Assoc. Hydrol. Sci. 364, 94–99. https://doi.org/10.5194/piahs-364-94-2014

Scalenghe, R., Ferraris, S., 2009. The first forty years of a Technosol. Pedosphere 19, 40–52.

Siltecho, S., Hammecker, C., Sriboonlue, V., Clermont-Dauphin, C., Trelo-ges, V., Antonino, A.C.D., Angulo-Jaramillo, R., 2015. Use of field and laboratory methods for estimating unsaturated hydraulic properties under different land uses. Hydrol. Earth Syst. Sci. 19, 1193–1207. https://doi.org/10.5194/hess-19-1193-2015

Silva Ursulino, B., Maria Gico Lima Montenegro, S., Paiva Coutinho, A., Hugo Rabelo Coelho, V., Cezar dos Santos Araújo, D., Cláudia Villar Gusmão, A., Martins dos Santos Neto, S., Lassabatere, L., Angulo-Jaramillo, R., 2019. Modelling soil water dynamics from soil hydraulic parameters estimated by an alternative method in a tropical experimental basin. Water 11, 1007. https://doi.org/10.3390/w11051007

Somaratne, N.M., Smettem, K.R.J., 1993. Effect of cultivation and raindrop impact on the surface hydraulic properties of an Alfisol under wheat. Soil Tillage Res. 26, 115–125. https://doi.org/10.1016/0167-1987(93)90038-Q

Souza, E.S., Antonino, A.C.D., Heck, R.J., Montenegro, S.M.G.L., Lima, J.R.S., Sampaio, E.V.S.B., Angulo-Jaramillo, R., Vauclin, M., 2014. Effect of crusting on the physical and hydraulic properties of a soil cropped with Castor beans (Ricinus communis L.) in the northeastern region of Brazil. Soil Tillage Res. 141, 55–61. https://doi.org/10.1016/j.still.2014.04.004

Souza, R., Souza, E., Netto, A.M., Almeida, A.Q. de, Júnior, G.B., Silva, J.R.I., de Sousa Lima, J.R., Antonino, A.C.D., 2017. Assessment of the physical quality of a Fluvisol in the Brazilian semiarid region. Geoderma Reg. https://doi.org/10.1016/j.geodrs.2017.07.008

Stewart, R.D., Abou Najm, M.R., 2018. A Comprehensive model for single ring infiltration ii: estimating field-saturated hydraulic conductivity. Soil Sci. Soc. Am. J. 0, 0. https://doi.org/10.2136/sssaj2017.09.0314

Torri, D., Regüés, D., Pellegrini, S., Bazzoffi, P., 1999. Within-storm soil surface dynamics and erosive effects of rainstorms. Catena 38, 131–150. https://doi.org/10.1016/S0341-8162(99)00059-4

Touma, J., Voltz, M., Albergel, J., 2007. Determining soil saturated hydraulic conductivity and sorptivity from single ring infiltration tests. Eur. J. Soil Sci. 58, 229–238. https://doi.org/10.1111/j.1365-2389.2006.00830.x

van de Giesen, N.C., Stomph, T.J., de Ridder, N., 2000. Scale effects of Hortonian overland flow and rainfall-runoff dynamics in a West African catena landscape. Hydrol.Process. 14, 165–175.

van Genuchten, M.T., 1980. A closed-form equation for predicting the hydraulic conductivity of unsaturated soils. Soil Sci. Soc. Am. J. 44, 892–898

Vandervaere, J.-P., Vauclin, M., Elrick, D.E., 2000. Transient flow from tension infiltrometers I. The two-parameter equation. Soil Sci. Soc. Am. J. 64, 1263–1272

Van Meir, N., Gaudet, J.P., Phrommavanh, V., Laurent, J.P., Bugai, D., Biron, R., 2012. Flow in the unsaturated zone around a shallow subsurface radioactive waste trench: Interpretation of an infiltration–drainage test at the Chernobyl Pilot Site. Appl. Geochem. 27, 1297–1303. https://doi.org/10.1016/j.apgeochem.2011.08.009

Votrubova, J., Dohnal, M., Vogel, T., Tesar, M., Jelinkova, V., Cislerova, M., 2017. Ponded infiltration in a grid of permanent single-ring infiltrometers: Spatial versus temporal variability. J. Hydrol. Hydromech. 65, 244–253. https://doi.org/10.1515/johh-2017-0015

White, I., Sully, M.J., Melville, M.D., 1989. Use and hydrological robustness of time-to-incipient-ponding. Soil Sci. Soc. Am. J. 53, 1343–1346. https://doi.org/10.2136/sssaj1989.03615995005300050007x

Wu, S., Chen, L., Wang, N., Xu, S., Bagarello, V., Ferro, V., 2019. Variable power-law scaling of hillslope Hortonian rainfall-runoff processes. Hydrol. Process. https://doi.org/10.1002/hyp.13538.

Xiao, B., Sun, F., Hu, K., Kidron, G.J., 2019. Biocrusts reduce surface soil infiltrability and impede soil water infiltration under tension and ponding conditions in dryland ecosystems. J. Hydrol. 568, 792–802. https://doi.org/10.1016/j.hydrol.2018.11. 051

Xu, X., Lewis, C., Liu, W., Albertson, J.D., Kiely, G., 2012. Analysis of single-ring infiltrometer data for soil hydraulic properties estimation: Comparison of BEST and Wu methods. Agric. Water Manag. 107, 34–41. https://doi.org/10.1016/j.agwat.2012.01.004

Xu, X., Kiely, G., Lewis, C., 2009. Estimation and analysis of soil hydraulic properties through infiltration experiments: comparison of BEST and DL fitting methods. Soil Use Manag. 25, 354–361. https://doi.org/10.1111/j.1475-2743.2009.00218.x

Yang, J., Xu, X., Liu, M., Xu, C., Luo, W., Song, T., Du, H., Kiely, G., 2016. Effects of Napier grass management on soil hydrologic functions in a karst landscape, southwestern China. Soil Tillage Res. 157, 83–92. https://doi.org/10.1016/j.still.2015.11.012

Yilmaz, D., Bouarafa, S., Peyneau, P.-E., Angulo-Jaramillo, R., Lassabatere, L., 2019. Assessment of hydraulic properties of technosols using Beerkan and multiple tension disc infiltration methods. Eur. J. Soil Sci. 70, 1049–1062. https://doi.org/10.1111/ejss.12791

Yilmaz, D., Lassabatere, L., Deneele, D., Angulo-Jaramillo, R., Legret, M., 2013. Influence of carbonation on the microstructure and hydraulic properties of a basic oxygen furnace slag. Vadose Zone J. 12, 0. https://doi.org/10.2136/vzj2012.0121

Yilmaz, D., Lassabatere, L., Angulo-Jaramillo, R., Deneele, D., Legret, M., 2010. Hydrodynamic characterization of basic oxygen furnace slag through an adapted best method. Vadose Zone J. 9, 107. https://doi.org/10.2136/vzj2009.0039

CHAPTER 4: Intensive soil characterization with automatic single-ring infiltrometers

4.1. Introduction

Knowledge of the water quantity in the vadose zone is interesting for the optimum management of water resources and the quality of soil.

Estimating soil hydraulic properties, such as hydraulic conductivity, is important for planning efficient irrigation and erosion control practices, and for understanding hydrological processes like rainfall and irrigation partition. Infiltration experiments are widely used for measuring infiltration rates and for an in situ determination of the soil hydraulic conductivity.

They are commonly performed in the field by visually noting the water level drop in a Mariotte column or recording the time needed for the water to infiltrate into the soil. However, this technique requires an operator for the monitoring of the infiltration process that may also last several hours for achieving steady state conditions, depending on the soil textural and structural characteristics. To overcome this limitation, many different infiltrometer devices, including tension, single-ring, mini disk, and double-ring infiltrometers, have been automated using different approaches (**Table 4.1**).

Table 4.1 Examples of different automated devices developed to characterize soil hydraulic properties

References	Type of device	Storage system
Ankeny et al. (1988)	tension infiltrometer	two pressure transducers (one installed at the top, and the other at the bottom of the Mariotte column) and a data logger
Casey and Derby (2002)		differential transducer connected to a data logger
Castiglione et al (2005)		the water level in the reservoir (monitored by the pressure transducer) is managed by the data logger that controls the valves
Moret et al (2004)		the reflection of the TDR(time domain reflectometry) measurement is automatically transferred to a computer
Selker et al. (2009)		transducer and microprocessor
Špongrová et al (2009)		differential pressure transducer connected to data logger through a set of solenoid valves
Constantz and Murphy (1987)	single-ring infiltrometer	pressure transducer linked to programmable data logger
Prieksat et al. (1992)		
Di Prima (2015; 2016)		data acquisition system based on the open source Arduino board
Rodríguez-Juárez et al. (2018)		
Cernicchiaro et al. (2019)		
Milla and Kish (2006)	The system can be adapted to single- and dual-ring infiltrometers	infrared distance-measuring sensor and microcontroller
Madsen and Chandler (2007).	mini disk infiltrometer	pressure transducers connected to compact data loggers
Klipa et al (2015)		the load cell measures depth of water in the reservoirs and it is connected to a datalogger
Arriaga et al (2010)	double-ring infiltrometer	pressure transducer and datalogger
Fatehnia et al (2016)		Arduino microcontroller, a Hall effect sensors, and a constant-level float valve

Automated measurements of Marriotte reservoir water levels were first introduced by Constanz and Murphy (1987), who used single gage transducers. The quality of the acquisition was then improved by using two gage (Ankeny et al., in 1988) or differential transducers (Casey and Derby, 2002).
The interest in automating has considerably increased. Indeed, automated infiltrometers may be used to collect simultaneous measurements at multiple locations for relatively long periods of time, thus providing accurate data at high spatial and temporal resolutions. Also, the automatic systems not require a continuous presence of the operator.
Considering all these aspects, in 2020 Concialdi et al. improved the automated single-ring infiltrometer proposed by Di Prima (2015).
Our objectives were: i) developing an instrumentation package to automatically collect data from multiple infiltrometers working simultaneously, ii) improving the treatment of the raw data recorded by the transducers, iii) assessing the use of the infiltrometers in conjunction with different methods for estimating the soil parameters from infiltrometer data, and iv) evaluating instrument performance under specific and challenging field conditions, such as highly permeable, slightly sorptive and water repellent conditions.
This chapter is divided into two sections and an appendix. In particular, the research activity on this subject, developed during the PhD course is shortly introduced in the 4.2 section and summarized in the article by Concialdi et al. (2020).

4.2. An innovative instrumentation package for soil characterization

A part of PhD research activity was spent abroad, at the Laboratoire d'Ecologie des Hydrosystèmes Naturels et Anthropisés (LEHNA), in Lyon (France). During this period a new acquisition system made of ten automatic infiltrometers linked to two data acquisition systems for automatic recording of ten simultaneous experiments was developed. Each infiltrometer is composed of a Mariotte reservoirs equipped with differential transducers to monitor the drop of the water level. The data acquisition systems consist of low-cost components and an Arduino open-source microcontroller. The devices were tested both in the laboratory and on four different urban and agricultural soils in France and India. The design of the devices was improved over a previously presented prototype in terms of reservoir capacity, diameter of the air entry tube, and number of infiltrometers that can be simultaneously operated. Also, a new algorithm for the automatic processing of the raw transducer data was developed, and it can be downloaded from the website bestsoilhydro.net. The use of the automatic infiltrometers allows the user to obtain more accurate estimates of soil hydraulic parameters, while also reducing the amount of effort needed to run multiple experiments.
This research activity was summarized in the paper Concialdi et al. (2020). This paper is reported below in the **Appendix E**.

Appendix E:

Journal of Hydrology 582 (2020) 124492

Contents lists available at ScienceDirect

Journal of Hydrology

journal homepage: www.elsevier.com/locate/jhydrol

Research papers

An open-source instrumentation package for intensive soil hydraulic characterization

Paola Concialdi[a], Simone Di Prima[b,c,*], Harsh M. Bhanderi[d], Ryan D. Stewart[e], Majdi R. Abou Najm[f], Murari Lal Gaur[d], Rafael Angulo-Jaramillo[b], Laurent Lassabatere[b]

[a] University of Palermo, Department of Agricultural, Food and Forest Sciences, Palermo, Italy
[b] Univ. Lyon, Univ. Claude Bernard Lyon 1, CNRS, ENTPE, UMR5023 LEHNA, F-69518, Vaulx-en-Velin, France
[c] University of Sassari, Department of Agricultural Sciences, Sassari, Italy
[d] College of Agricultural Engineering, Anand Agricultural University, Godhra, Gujarat, India
[e] School of Plant and Environmental Sciences, Virginia Polytechnic Institute and State University, Blacksburg, VA, United States
[f] Department of Land, Air and Water Resources, University of California, Davis, CA 95616, United States

ARTICLE INFO

This manuscript was handled by Corrado Corradini, Editor-in-Chief, with the assistance of Renato Morbidelli, Associate Editor

Keywords:
Automatic infiltrometer
Infiltration rate measurements
Soil hydraulic properties
Arduino

ABSTRACT

We present a new open-source and modular instrumentation package composed of up to ten automatic infiltrometers connected to data acquisition systems for automatic recording of multiple infiltration experiments. The infiltrometers are equipped with differential transducers to monitor water level changes in a Mariotte reservoir, and, in turn, to quantify water infiltration rates. The data acquisition systems consist of low-cost components and operate on the open-source microcontroller platform Arduino. The devices were tested both in the laboratory and on different urban and agricultural soils in France and India. More specifically, we tested three procedures to treat the transducers readings, including a filtering algorithm that substantially improved the ability to determine cumulative infiltration from raw data. We combined these three procedures with four methods for estimating the soil parameters from infiltrometer data, showing pros and cons of each scenario. We also demonstrated advantages in using the automatic infiltrometers when infiltration measurements were hindered by: i) linearity in cumulative infiltration curves owing to gravity-driven flow, ii) an imprecise description of the transient state of infiltration, and iii) the occurrence of soil water repellency. The use of the automatic infiltrometers allows the user to obtain more accurate estimates of soil hydraulic parameters, while also reducing the amount of effort needed to run multiple experiments.

1. Introduction

Different automated devices have been developed to measure water infiltration rates in the field. Automation strategies have involved the use of many different set-ups and sensors, including pressure transducers (e.g., Ankeny et al., 1988; Casey and Derby, 2002; Constantz and Murphy, 1987; Di Prima, 2015; Madsen and Chandler, 2007; Prieksat et al., 1992), infrared sensor systems (Milla and Kish, 2006), micro flow-meters (Moret-Fernández et al., 2012), reflectometry probes (Moret et al., 2004), and load cell sensors (Klípa et al., 2015; Zumr et al., 2019). Among these approaches, pressure transducers are widely used for field applications given their simplicity of use and low price. These sensors allow the user to monitor water level changes in a Mariotte reservoir, and, in turn, to quantify water infiltration rates. Automation of a Mariotte reservoir was firstly proposed by Constantz and Murphy (1987). These authors used a pressure transducer connected at the top of a Mariotte reservoir to monitor the head-space tension during the drop of the water level. This technique was used by Ankeny et al. (1988) to automate a tension infiltrometer for infiltration rates measurements under negative suction. These authors tested two different set-ups: the first configuration had a single pressure transducer located at the top of the Mariotte reservoir, while the second configuration added another pressure transducer at the base of the water column. The use of two transducers overcame some of the difficulties generated from the tension fluctuations caused by bubbling. This strategy was further improved by Casey and Derby (2002), who used a differential transducer with two ports to automate an SW-080B tension infiltrometer, and Madsen and Chandler (2007), who automated a mini-disk infiltrometer (Decagon, 2014) using pressure transducers. Selker et al. (2009) incorporated pressure transducers and pneumatic reed switches

* Corresponding author.
E-mail address: sdiprima@uniss.it (S. Di Prima).

https://doi.org/10.1016/j.jhydrol.2019.124492
Received 23 June 2019; Received in revised form 16 December 2019; Accepted 17 December 2019
Available online 20 December 2019
0022-1694/ © 2019 Elsevier B.V. All rights reserved.

to create a tension infiltrometer with automated, near-instantaneous control over the tension applied to the water source. Pressure transducers have also been used to automate single-ring infiltrometers (Prieksat et al., 1992).

The single-ring infiltrometer technique (Reynolds and Elrick, 1990) is a widespread method (e.g., Braud et al., 2017), which has the advantages of speed and simplicity over more cumbersome procedures for performing field-saturated soil hydraulic conductivity measurements, such as the Guelph permeameter and the double-ring infiltrometer (Di Prima et al., 2019). These infiltrometers maintain a quasi-constant head in a containment ring, allowing to calculate infiltration rates under ponding conditions (Angulo-Jaramillo et al., 2016). Recently, Di Prima (2015) presented a new automated single-ring infiltrometer. This device is equipped with a differential transducer to measure the stepwise drop of water level in a Mariotte reservoir. The data acquisition system consists of low-cost components and uses the open-source Arduino microcontroller platform.

The potential of this automated infiltrometer to reliably derive saturated hydraulic conductivity, K_s, and sorptivity, S, was tested by using three existing BEST algorithms, i.e., BEST-slope (Lassabatere et al., 2006), BEST-intercept (Yilmaz et al., 2010) and BEST-steady (Bagarello et al., 2014). This approach demonstrated that the total volume applied with the prototype version of the infiltrometer (130 mm) may not be sufficient to evaluate steady state conditions, compromising the reliability of the estimates in some cases (e.g., loamy soil). The importance to collect an appropriate number of data points during the transient state was investigated, using analytically generated data, by increasing the precision of the collected information, namely decreasing the cumulative infiltration interval from 5 mm to 2.5 mm. In the case of readings every 2.5 mm, the number of points used to describe the same curve doubled and generated enough points to accurately model the transient state of infiltration. Based on these results, Di Prima et al. (2016) proposed guidelines for the optimization of the design in terms of capacity of the Mariotte reservoir (which affects the cumulative amount of infiltration that can be measured) and the radius of air entry tube (which affects the increment size between two successive measurements). These guidelines thus suggest ways to optimize infiltrometers to accurately measure transient and steady-state infiltration conditions, yet the actual effectiveness of these improvements have not been assessed using experimental data.

Another limitation on the use of the initial prototype is the need to filter raw data recorded by the transducer. The transducer readings produce a step-shaped or stair-like relationship between time and recorded voltage. These artifacts tend to be caused by air bubble formation in the Mariotte system, and the magnitude and rate of change of the resulting steps tend to depend on the infiltrometer set-up. Di Prima (2015) and Di Prima et al. (2016, 2017) manually processed the data, which complicated post-processing step and required a tremendous amount of work and time to determine cumulative infiltration curves. While previous work has attempted to ease the analysis of infiltration data from automated infiltrometers, for instance using the FLOWDATA software developed by Ankeny et al. (1993), such methods are not able to filter out “stair-like” relationships that are often obtained with the proposed infiltrometer.

Lastly, previous studies have shown that the strong spatial variability of hydraulic properties and water infiltration at the field scale may affect measurement of water cumulative infiltration and related estimates for hydraulic parameters (e.g., Zimmermann et al., 2008). For instance, Lassabatere et al. (2019a) developed the concept of the BMR (Beerkan Multi Run) showing the need for a large dataset of experimental data for a proper representation of the average response and its variability. Automated infiltrometers may be used to collect simultaneous measurements at multiple locations for relatively long periods of time, thus providing accurate data at high spatial and temporal resolutions. The use of automated infiltrometers may therefore improve characterization of spatial variability in soil hydraulic characteristics, making it important to develop a system that can collect and integrate measurements from multiple units

In this investigation we present a new modular instrumentation package, based on the original design of Di Prima (2015), that has been updated to include up to ten automatic infiltrometers for automatic recording of simultaneous infiltration experiments. Following the guidelines in Di Prima et al. (2016), we improved the design of the devices in terms of reservoir capacity to ensure steady state at the end of the experiment, accuracy of the description of the transient phase of the infiltration process, and number of infiltrometers that can be simultaneously operated. This set of new devices should produce an optimum description of the cumulative infiltration for an optimum hydraulic characterization. The main objectives of this paper were to: i) testing the potential of the instrumentation package to automatically collect data from multiple infiltrometers working simultaneously, ii) improving the treatment of the raw data recorded by the transducers, iii) assessing the use of the infiltrometers in conjunction with different methods for estimating the soil parameters from infiltrometer data, and iv) evaluating instrument performance under specific and challenging field conditions, such as highly permeable, slightly sorptive and water repellent conditions.

2. Materials and methods

2.1. Improved infiltrometer design

The main components of the complete system are illustrated in Fig. 1. Each infiltrometer consists of a Mariotte bottle with a 94-mm inner diameter and a height of 850 mm, with effective water storage height of 740 mm. It provides the capacity to hold the volume of water corresponding to a total cumulative infiltration of 280 mm based on a 150 mm infiltration ring diameter. This water volume represents 150 mm of additional water available for infiltration compared to the prototype proposed by Di Prima (2015).

An air entry tube is positioned with its lower end at short distance from the reservoir base, which controls the air entry in the Mariotte bottle and thus the water level inside the ring. The air entry tube has a 7 mm inner diameter, compared to the 6.5 mm inner diameter used in the original prototype. Using this larger diameter tube changed the cumulative infiltration interval from ~ 4.5 mm in the original prototype to ~ 2 mm in the updated version (see section 3.3). This change was implemented with the goals of increasing the precision of the collected information and allowing the collection of many data points during the first stage of the process.

The Mariotte bottle is closed by a top and a bottom plug (Fig. 1c–e) and sustained through a tripod (Fig. 1f–g) made of four interlocking parts (3 legs and 1 circular support). The design of the tripod allows the user to easily regulate the distance between the base of the infiltrometer and the infiltration surface, with an adjustable range from 2 to 3 mm at the closest setting up to 90 mm at the most distant setting. The tripod components were manufactured through an online laser cutting service. This type of service is offered by a number of online companies, which typically allow users to choose the thickness and the type of material and then upload a file (e.g., .eps, .svg or .dxf) that specifies the cutting lines. An illustration of the cutting lines is provided in Fig. 1f. The plugs can be realized by different 3D printing technologies, such as stereolithography (SLA), selective laser sintering (SLS), and Multi Jet Fusion (MJF). The project files for the realization of the plugs (Fig. 1c) and the tripod (Fig. 1f) can be downloaded from the website bestsoilhydro.net. We note that online manufacturer services tend to be cost-effective, allowing the user to build the system for relatively low cost.

2.2. Data acquisition system and differential pressure sensor

The core of the data acquisition system consists of an Arduino Mega microcontroller board, an Arduino wireless shield with an onboard

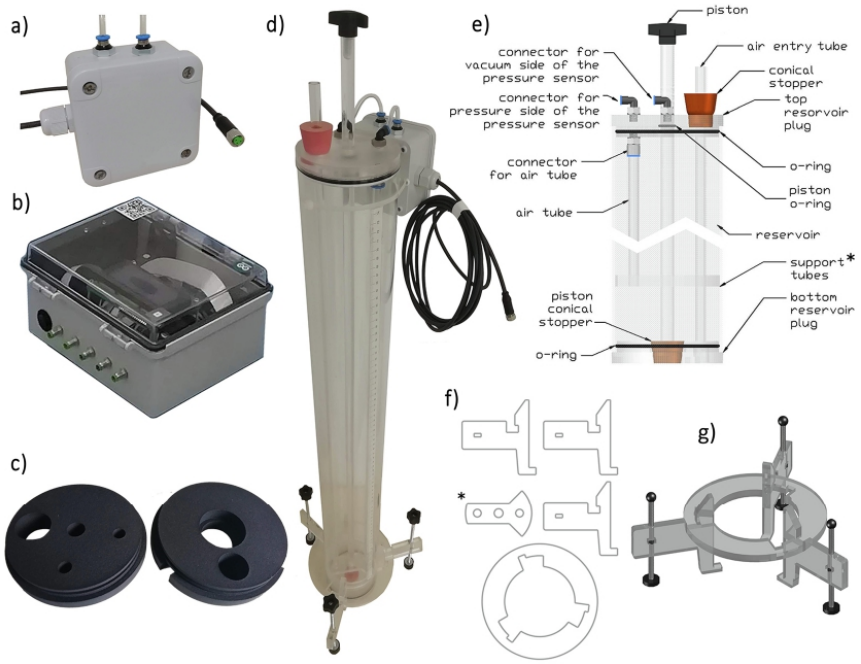

Fig. 1. Main components of the automatic system. (a) Box with differential pressure sensor MPXV5010DP; (b) data acquisition system with Arduino MEGA 2560 Rev3; (c) 3D printed top and bottom plugs realized by Multi Jet Fusion (MJF) printing technology; (d) Infiltrometer; (e) detailed scheme of the infiltrometer; (f) laser cutting project for the realization of the (g) tripod and (*) support tubes. The project files for the manufacture of the plugs and the tripod can be downloaded from the website bestsoilhydro.net.

micro-SD socket and a LCD module shield (20 columns and 4 rows) and a differential pressure transducer. The list of components and the Arduino code can be downloaded from the website bestsoilhydro.net. The LCD module requires that a specific library (LiquidCrystal_I2C) be installed into the Arduino IDE; this library can be downloaded from the website wiki.sunfounder.cc. The data acquisition system (Fig. 1b) is connected to differential pressure sensors (Fig. 1a) using 3-m-long cables. Each system simultaneously connects to as many as five infiltrometers. The differential pressure sensor box is mounted on the top of the infiltrometer (Fig. 1d). The two ends of the transducer are connected using small plastic flexible tubes (outer diameter = 4 mm) to the head-space of the reservoir and to an acrylic tube (outer diameter = 10 mm, inner diameter = 7 mm, height = 790 mm) descending inside the reservoir. This configuration enables measurement of the pressure difference between the head-space and the bottom of the column of water. The differential pressure transducer used for this application is the piezoresistive differential pressure transducer MPXV5010DP, from NXP semiconductors (nxp.com; other companies that provide similar transducers include SMI and Honeywell). This sensor requires a power supply of 5 V and has an integrated temperature compensation and signal amplification circuit. The transducer provides a linear voltage output for a differential pressure range from 0 to 1000 mm H_2O. The data are recorded on a SD card and simultaneously displayed on the LCD display. The software generates a new comma-separated values (CSV) file every time that the microcontroller is activated. The name of the generated file appears on the LCD.

2.3. Infiltrometer system calibration

Laboratory calibration of the devices was carried out by visually monitoring the height of the water column inside the Mariotte bottle during the complete emptying of the reservoirs. Each infiltrometer was placed within a 150-mm inner diameter cylinder; a quasi-constant water head of 5 mm was maintained inside the cylinder. Visual readings of the water levels were done on a 740-mm long ruler with the zero positioned 10 mm above the bottom end of the tube connected to the pressure side of the differential pressure sensor. Then, a calibration function was created via linear regression between the visual readings of the heights of the water column and the corresponding recorded volts. The calibration function for each infiltrometer was used in subsequent experiments to convert recorded transducer outputs into water column heights, which were then used to estimate infiltration amounts.

2.4. Laboratory testing

All of the infiltrometers were also tested in the laboratory (example shown in Fig. 2). Similar to the calibration procedure, the infiltrometer was used to maintain a quasi-constant head of water inside a 150-mm inner diameter cylinder that was connected via an outlet pipe to a collection container set on a balance (Fig. 2a). The experiments were carried out by recording the transducer output during the complete emptying of the reservoir while weighing the mass of discharged water (Fig. 2a and b). In the example of Infiltrometer #3, the transducer voltage was constant during intervals where bubbles form in the air-entry tube, reflecting a constant water level in the reservoir. Once a bubble reached sufficient size to enter the water column, e.g., at time t = 509 s (observations in Fig. 2b and left-most red triangle in Fig. 2c), the transducer readings fluctuated and generated easily detectable outliers (blue solid circles in Fig. 2c), as already discussed by Ankeny et al. (1988). The transducer readings then stabilized at a constant value until the subsequent bubbling event, e.g., the transducer output stayed at 2.85 V between t = 510 and 517 s. As highlighted by Di Prima

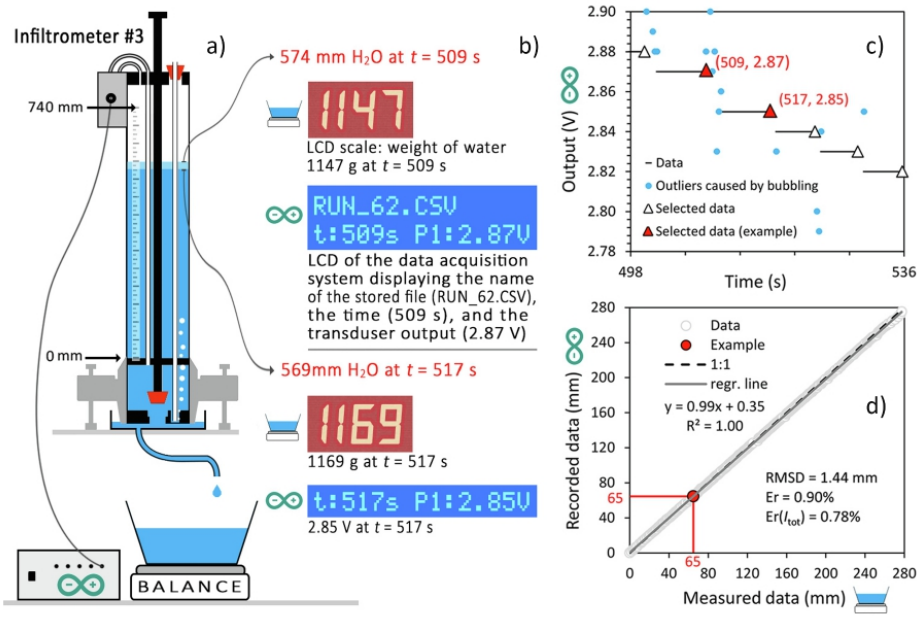

Fig. 2. (a) Sketch of the testing procedure; (b) weight of the discharged water and transducer output at time immediately preceding two consecutive bubbling events; (c) manual selection of data at the end of the constant height stages in Mariotte bottle; and (d) comparison between recorded and measured cumulative flow data. Note that the recorded data in subpanel d were firstly converted into water column heights using the calibration function for Infiltrometer #3, and then used to estimate infiltration amounts.

(2015) and Di Prima et al. (2016), this typically behavior produces a step-shaped relationship between time and recorded voltage (Fig. 2c).

2.5. Field testing

After laboratory calibration and testing, we also tested the devices during four experimental campaigns in the field, with three sites in France and one in India. The first two sites (ENTPE-1 and ENTPE-2 sites) are located in the garden of the École Nationale des Travaux Publics de l'État (ENTPE) in the municipality of Vaulx-en-Velin (France). The third site (DOUA site) is a drainage ditch located at the La DOUA scientific campus in the municipality of Villeurbanne (France), which receives runoff mainly originating from adjacent parking lots and sidewalks. These municipalities belong to the Metropolis of Lyon in Auvergne-Rhône-Alpes region in eastern France. The three sites are part of the Lyon city Field Observatory for Urban Water Management (OTHU). The sampled soils ranged in texture from silt to sand (Bouarafa et al., 2019). The fourth experimental site is a sandy loam soil covered by maize crop that is located at the Anand Agricultural University in the western Indian state of Gujarat.

For each site in France, a total of four undisturbed soil cores (50 mm in height and 50 mm in diameter) were collected at randomly sampled points and used to determine both the soil bulk density, ρ_b (g cm^{-3}), and the initial volumetric soil water content, θ_i (cm^3 cm^{-3}) (Table 1). We used the infiltrometers to carry out a total of fifteen infiltration experiments, with five simultaneous experiments conducted at each French site (Fig. 3a). We used stainless steel rings with an inner diameter of 150 mm, inserted shallowly into the soil (~10 mm) according to the Beerkan procedure for single-ring infiltration experiments (Lassabatere et al., 2006). Following the procedure described in Di Prima et al. (2016), we firstly positioned a plastic film on the soil surface inside each ring and applied a small water head of few millimeters (2–3 mm), depending on the surface roughness. The plastic film was also used to minimize disturbance on the soil surface while establishing ponding conditions and to have an accurate data acquisition from the beginning of the run. The infiltrometers were positioned inside the rings and regulated in height so that the bases were in contact with the ponding water. The Mariotte bottles were filled with tap water and then activated through lifting the pistons. A few seconds before flow began, the data acquisition was started by simply switching on the data acquisition system. Finally, the infiltration experiments started when the plastic films were removed. A video tutorial showing this procedure can be viewed online (Di Prima, 2014). At the ENTPE-1 site, we also used all the automatic infiltrometers connected to two data acquisition systems for automatic recording of ten simultaneous infiltration experiments. These experiments were aimed to test the potential of the proposed instrumentation package to capture soil heterogeneity.

Table 1
Coordinates, dry soil bulk density, ρ_b (g cm^{-3}), and initial volumetric soil water content, θ_i (cm^3 cm^{-3}) for the three sampled soils in France (sample size for each soil, $N = 4$). Standard deviations are indicated in parentheses.

Site	ENTPE-1	ENTPE-2	DOUA
Coordinates	45°46′42.46″N 4°55′33.68″E	45°46′42.40″N 4°55′30.62″E	45°47′5.67″N 4°52′17.31″E
ρ_b (g cm^{-3})	1.276 (0.150)	1.280 (0.154)	1.166 (0.043)
θ_i (cm^3 cm^{-3})	0.378 (0.048)	0.400 (0.057)	0.273 (0.045)

The hypothesis of an improved description of the cumulative infiltration curve was investigated through a comparison with the prototype proposed by Di Prima (2015). At this aim, we made a comparison between 45 curves collected with the prototype during previous field campaigns (Di Prima, 2015; Di Prima et al., 2017, 2016), and the curves collected with new infiltrometers at the ENTPE-1, ENTPE-2 and DOUA sites.

At the experimental site in India, we conducted a total of six

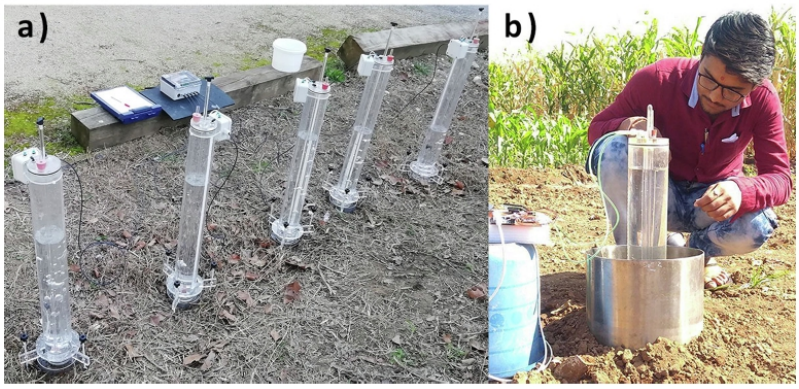

Fig. 3. Automated infiltration experiments of the (a) single- and (b) double-ring type carried out respectively at the DOUA site and at the Anand Agricultural University.

infiltration experiments. Three runs of the double-ring type were carried out using an inner ring of 150 mm diameter and outer ring of 300 mm diameter. The automatic infiltrometer was used to maintain constant water depths in the inner rings of 25 mm (Run 1), 50 mm (Run 2), and 75 mm (Run 3), while the same water depths were maintained in the outer ring manually by pouring the water during the experiments. Assuming that water infiltration below the inner ring was one-dimensional (1D) and that the final steady flow was only gravity driven, we estimated the saturated soil hydraulic conductivity based on the steady infiltration rate (Reynolds et al., 2002). The other three runs used single rings with 150 mm inner diameter. The infiltrometers were used to maintain constant depths of 25 mm (Run 4), 50 mm (Run 5), and 75 mm (Run 6).

2.6. Treatment of the raw data recorded by the transducers

In this investigation, we propose three different procedures to treat the raw data recorded by the transducer. The first procedure, proposed by Di Prima (2015) and applied by Di Prima et al. (2016, 2017), requires the user to manually select values at the end of the constant height stages, i.e., by sampling the transducer readings at time immediately preceding the bubbling. The second procedure automatically selects these values through an algorithm coded with the open-source software Scilab. The code can be downloaded from the website bestsoilhydro.net. Because the code may fail in certain cases owing to unpredictable noise in the transducer readings, in this investigation we decided to apply both procedures. Further, these two procedures cannot be adopted whenever rapid emptying of the Mariotte bottle causes uninterrupted air bubbling, which may occur during high infiltration rates (Di Prima et al., 2016). Following the suggestion by Di Prima et al. (2016), we therefore applied a third procedure that calculated a moving median to identify the underlying trend of transducer output with time. In the laboratory, the accuracy of these procedures was evaluated through the comparison between recorded and measured cumulative flow data (Fig. 2d) in terms of relative error, *Er* (%), and root mean squared differences, *RMSD* (mm), defined as:

$$Er = 100 \times \sqrt{\frac{\sum_{i=1}^{n} (I_i^{exp} - I_i)^2}{\sum_{i=1}^{n} (I_i^{exp})^2}} \quad (1)$$

$$RMSD = \sqrt{\frac{\sum_{i=1}^{n} (I_i^{exp} - I_i)^2}{n}} \quad (2)$$

where n is the total number of data pairs, I_i^{exp} (mm) are the measured data, estimated from the mass of discharged water during laboratory tests, and I_i (mm) are the values estimated from the recorded transducer data using the calibration functions. Also, the recorded total cumulative flow, I_{tot} (mm), were compared with the corresponding measured data, I_{tot}^{exp} (mm), using the relative error, $Er(I_{tot})$ (%), defined as follows:

$$Er(I_{tot}) = 100 \times \frac{I_{tot} - I_{tot}^{exp}}{I_{tot}^{exp}} \quad (3)$$

The three procedures presented above to treat the transducer output (i.e., manual selection, automatic selection and moving median) were subsequently applied to determine the cumulative infiltration curves. In addition, we also considered a fourth procedure described below. According to Angulo-Jaramillo et al. (2016), an expected advantage of the use of the automatic infiltrometers is better accuracy during the transient flow state. In this paper we investigated this hypothesis by processing the raw data in order to obtain “Beerkan-like data”, i.e., cumulative infiltration curves having the same increments (8.5 mm) as manually pouring water volumes into the containment ring. More specifically, the curves obtained by manually sampling the transducer readings were further processed and polynomial regression functions were applied to cumulative data to model the discretized infiltration measurements.

2.7. Estimating hydrodynamic parameters from field experiments

All the cumulative infiltration curves from the four different procedures were subsequently inverted by three different approaches to estimate the soil sorptivity, S (mm $h^{-0.5}$) and the saturated hydraulic conductivity, K_s (mm h^{-1}). The three approaches represented different algorithms within the Beerkan Estimation of the Soil Transfer parameters (BEST) solution introduced by Lassabatere et al. (2006), Yilmaz et al. (2010), and Bagarello et al. (2014), and differed from one another in the manner by which they fit the experimental cumulative infiltration to the approximate expansion for transient and steady states defined by Haverkamp et al. (1994) and to derive S and K_s. More specifically, BEST-slope (Lassabatere et al., 2006) uses the slope of the straight line defined by the last points (representative of the steady state) to constrain S and K_s, before fitting the transient model to the experimental data by the optimization of S. BEST-intercept (Yilmaz et al., 2010) uses the intercept of the steady state model to constrains S and K_s, priori fitting the experimental data. Lastly, BEST-steady (Bagarello et al., 2014) uses both the slope and the intercept to resolve a set of two equations (Di Prima et al., 2016), leading to the estimation of the two unknowns, S and K_s. More information on BEST can be found in

Table 2
Calibration parameters of the ten infiltrometers.

Infiltrometer	1	2	3	4	5	6	7	8	9	10
Slope (V/mm H_2O)	0.00433	0.00435	0.00436	0.00435	0.00436	0.00433	0.00432	0.00433	0.00436	0.00435
Intercept (V)	0.366	0.346	0.371	0.353	0.354	0.390	0.383	0.347	0.328	0.337
R^2	1.0000	0.9999	0.9999	0.9999	0.9998	0.9999	0.9999	0.9998	0.9998	0.9999

Angulo-Jaramillo et al. (2019).

K_s values were also estimated using Approach 4 in Stewart and Abou Najm (2018), in which the macroscopic capillary length, λ, was assumed to have a constant value of λ = 150 mm, following the recommendation of Stewart and Abou Najm (2018). Note that this approach does not require additional information (e.g., particle size distribution, initial and final soil water content and dry soil bulk density) to estimate K_s from infiltration runs. Therefore, it is particularly useful when a large number of locations needs to be sampled, particularly when time and financial resources are limited (Di Prima et al., 2019). At the Indian site, K_s values were estimated using Approach 4, as this method is also usable for both quasi-zero (i.e., the French sites) and positive values (Indian site) of ponded depth on the infiltration surface.

3. Results and discussion

3.1. Calibration and laboratory testing

Each infiltrometer had a unique calibration function between the visual readings of the water column heights and the corresponding voltage recorded during the emptying of the Mariotte bottle (Table 2). All transducers provided a nearly linear relationship between the voltage output and the heights of the water columns; as an example, R^2 = 1.0 for the calibration relationship collected using Infiltrometer #3 (Fig. 4, Table 2). They also had nearly identical values of the calibration multiplier ranging from 4.32×10^{-3} and 4.36×10^{-3} V/mm H_2O, while, as also noted by Ankeny (1992), the intercept yielded more variable values ranging from 0.328 and 0.390 mm. Nonetheless, while the calculation of the water levels is affected by the intercept value, the calculation of the water volume change between readings is independent from this parameter (Casey and Derby, 2002). However, the intercept value is still useful to exclude the water levels measured below the zero of the rule from the calculation of the water volumes, as the internal geometry of the Mariotte bottles changes below this level (Fig. 2a). In the laboratory, the accuracy of the three procedures to treat the transducer output (i.e., manual selection, automatic selection and moving median) was evaluated through a comparison between recorded and measured cumulative flow data. All procedures yielded

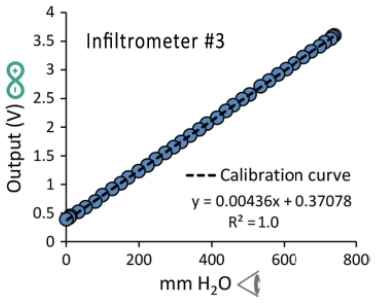

Fig. 4. Experimental calibration curve of the MPXV5010DP sensor mounted on Infiltrometer #3. The calibration multiplier is 4.36×10^{-3} V/mm H_2O (R^2 = 1.0). (∞) Recorded transducer outputs. (◁) Visual readings of the heights of the water column inside the Mariotte bottle during the complete emptying of the reservoir.

Table 3
Minimum (Min), maximum (Max), mean, and coefficient of variation (CV) of the root mean squared differences, *RMSD* (mm), relative error, *Er* (%), and relative error, $|Er(I_{tot})|$ (%), of the total cumulative flow, I_{tot} (mm), for the three procedures to treat the transducer output. Sample size for each procedure, N = 10.

Error	Data treatment	Min	Max	mean	CV (%)
RMSD	Manual selection	0.41	3.06	1.60 A	48.3
	Automatic selection	0.46	2.66	1.52 A	50.9
	Moving median	0.81	2.73	1.71 A	41.2
Er	Manual selection	0.28	2.06	1.06 A	48.2
	Automatic selection	0.31	1.83	1.02 A	50.5
	Moving median	0.52	1.77	1.11 A	40.5
$\|Er(I_{tot})\|$	Manual selection	0.11	1.41	0.79 A	47.8
	Automatic selection	0.29	1.76	0.86 A	53.3
	Moving median	0.06	1.60	0.86 A	63.9

For a given variable, means followed by the same letter are not significantly different according to a paired, two-tailed *t*-test ($P < 0.05$).

small errors (Table 3), suggesting that the ten infiltrometers had good accuracy when measuring water flow. More specifically, the three procedures yielded *RMSD* ranging between 0.41 and 3.06 mm, *Er* between 0.28 and 2.06%, and $Er(I_{tot})$ between 0.06 and 1.76%. The three procedures did not yield significantly different errors (Table 3 and Fig. 5). This result suggests that adopting a simplified procedure to treat the transducer output, such as a moving median, does not negatively affect determination of flow data. In addition, the laboratory experiments, with a quasi-constant head of water maintained inside a cylinder, allowed us to test the infiltrometers with a similar set-up to that one used on the field, thus increasing our confidence in the field measurements.

3.2. Field testing

3.2.1. Optimum case and peculiarities

Cumulative infiltration into an unsaturated porous medium typically exhibits a concave shape as a function of time, due to a decreasing hydraulic gradient as the wetting front moves away from the source and the influence of capillarity decreases (Xu et al., 2012). As flow rates approach steady state, cumulative infiltration becomes approximately linear with time (Angulo-Jaramillo et al., 2016). An example of this behavior is depicted in Fig. 6a–e. In this example, the measured infiltration rates showed the typical stepwise drop in water level within the reservoir, yielding the same kind of stair-like output (Fig. 6a) as the one reported for the laboratory experiments (Fig. 2c). All three procedures used to treat the transducer output (i.e., manual selection, automatic selection and moving median) were successfully applied to these data (Fig. 6c and e) and yielded similar cumulative infiltration curves as one another (Fig. 6b). Besides, all combinations of treatment procedure and BEST algorithms gave similar results for this example. This result suggests that in case of stair-like output, using the automatic procedure to treat the raw data is preferable, given that it avoids the tremendous amount of work and time required when manually processing the data.

The success of this example case above did not translate to all infiltration tests. Certain combinations of data treatment procedures and soil characterization algorithms failed to successfully characterize soil properties, yielding success rates as low as 40% for the manual selection

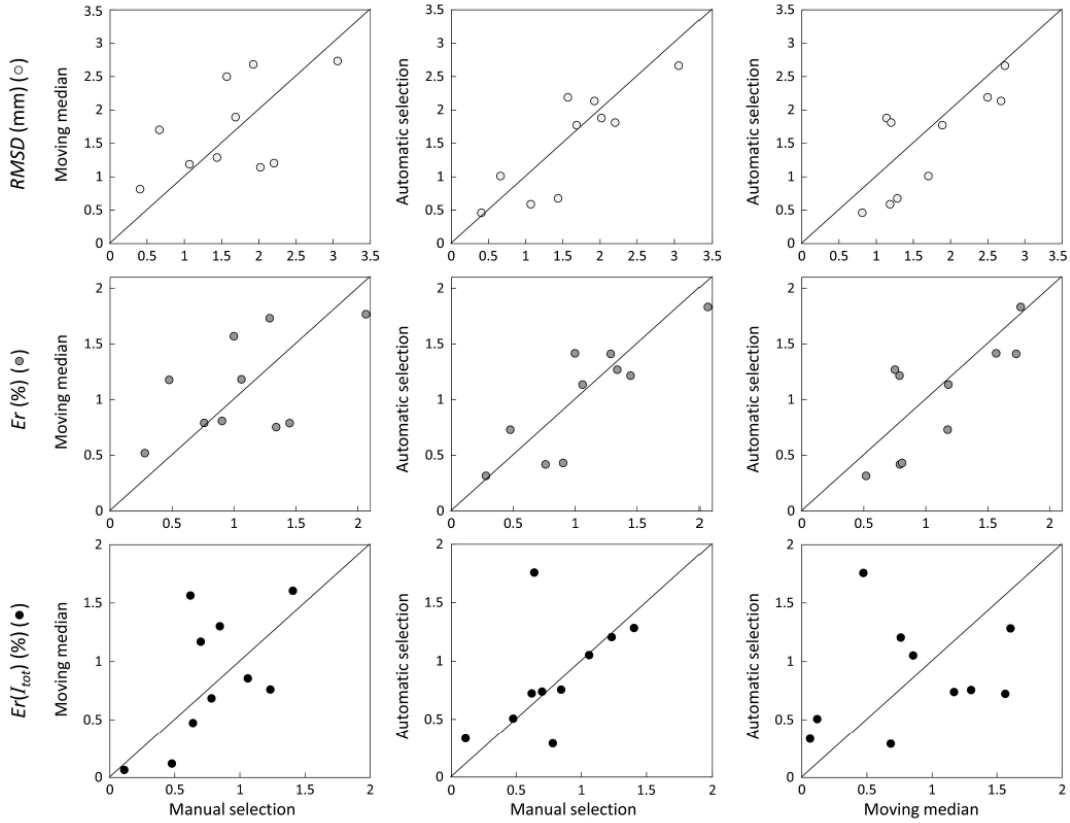

Fig. 5. Comparison between the errors obtained from the three procedures used to treat the transducer output.

method combined with BEST-slope (Table 4, Fig. 7a).

Further, for each site and treatment procedure, the four methods (i.e., BEST-slope, BEST-intercept, BEST-steady and Approach 4) provided different success rates (Table 4). These differences then carried over to the overall distributions for K_s (Fig. 7b) and S (Fig. 7c). Thus, as demonstrated by these results, different assumptions and analysis structures inherent to the four methods and three alternative procedures used to treat the transducer output (i.e., manual selection, automatic selection and moving median) makes each combination sensitive to different kinds of non-ideal conditions. Below we discuss different types of obstacles that may commonly hinder infiltration measurements in the field, including: i) linearity in cumulative infiltration curves owing to gravity-driven flow, ii) imprecise description of the transient state of infiltration, and iii) occurrence of soil water repellency. We also discuss related advantages provided by automatic infiltrometers when dealing with these issues.

3.2.2. High flow rate experiments

For six out of fifteen experiments, the infiltration processes were entirely dominated by the influence of preferential flow paths, with infiltration rates ranging between 1529.8 and 5215.1 mm h^{-1} (as estimated by the moving median approach). In such circumstances, we distinguished two different scenarios depending on the rapidity of the process. In three cases (first scenario), one at the ENTPE-1 site and two at the DOUA site, we measured infiltration rates equal or lower than 3159.3 mm h^{-1} (Table 4). Still, the rapid infiltration process and the high measured infiltration rates did not cause uninterrupted bubbling within the Mariotte bottle. Therefore, the emptying process was characterized by the typical stepwise drop of water level in the reservoirs, yielding the same kind of stair-like output reported previously (Figs. 2c and 6a), and all the three procedures to treat the transducer output were successful applied. However, the influence of preferential flow paths on the infiltration processes made it impossible to evaluate any effect of the capillary flow. Obviously, in such condition the use of transient models to fit infiltration data was inappropriate, and BEST-slope and BEST-intercept failed to provide S and K_s values (Lassabatere et al., 2019b). Three other experiments at the DOUA sites yielded even higher infiltration rates, ranging from 3496.3 and 5215.1 mm h^{-1} (second scenario). Under these conditions, the manual and automatic procedures to treat the raw data could not be applied owing to the rapid emptying of the Mariotte bottle causing an uninterrupted air bubbling that spoiled the transducer readings (Fig. 6h and i; also discussed in Di Prima et al., 2016). On the contrary, the application of a moving median successfully revealed the underlying trend of the transducer output with time (Fig. 6f and j), thus allowing cumulative infiltration to be determined (Fig. 6g). It also should be noted that, when the infiltration process was mainly driven by gravity and cumulative infiltration curves were near-linear (Lassabatere et al., 2019b), BEST-slope and BEST-intercept failed to provide S and K_s estimates, while BEST-steady was successfully applied. Indeed, according to Bagarello et al. (2014), BEST-steady does not require data from the transient stage of the run but rather relies solely on the regression analysis of the final

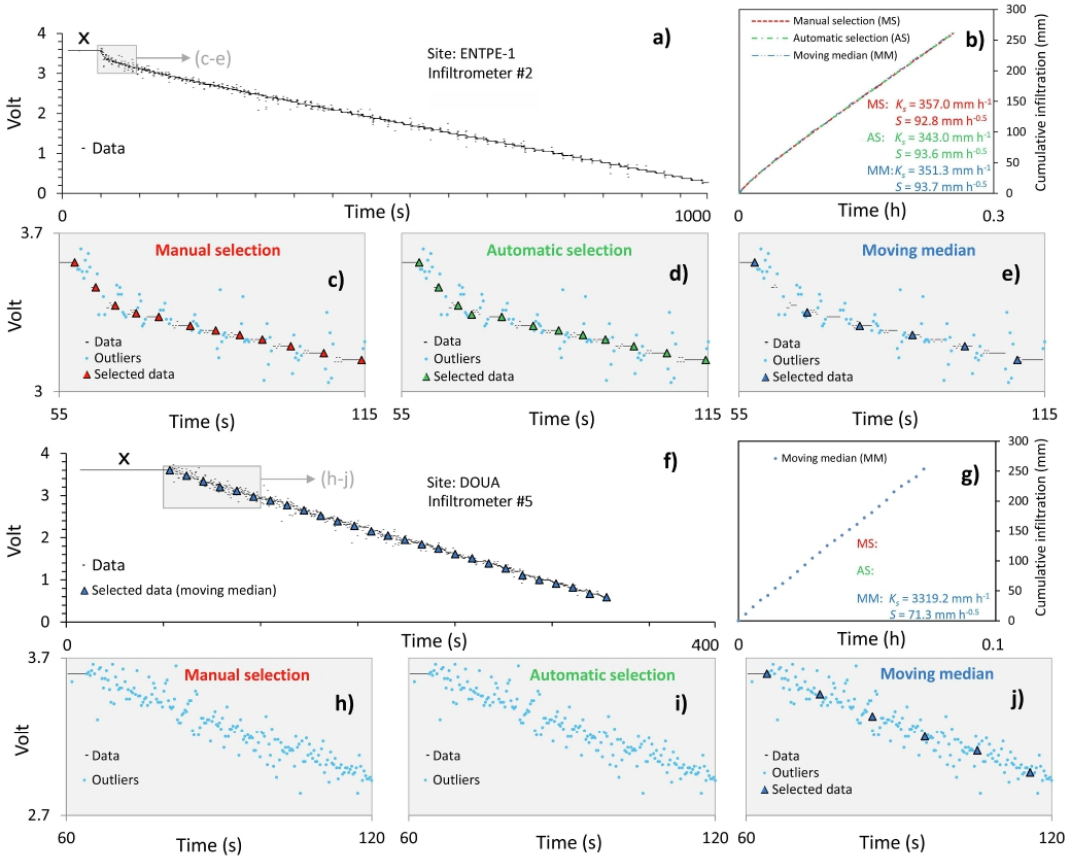

Fig. 6. Examples of transducer output for (a) stair-like data and (f) a rapid infiltration process. Subpanels c-e present close views of the transducer readings reported in the gray rectangle of subpanel a and subpanels h-j show close views of the readings reported in the gray rectangle of subpanel f. Note that the manual and automatic procedures could not be applied to treat the raw data in case of rapid infiltration process (h and i) owing to an uninterrupted air bubbling that spoiled the transducer readings. (b and g) Determined cumulative infiltration amounts. The BEST-slope deduced S and K_s values are also reported. Note that the Mariotte bottles were filled with tap water and then activated through lifting the pistons, at which time data acquisition began. Then, the infiltration experiments started when the plastic films were removed. This procedure facilitated accurate data acquisition from the beginning of the run, with a constant transducer output during the first seconds of the experiments (×).

few cumulative infiltration depths. This particular algorithm avoided the uncertainties due to the linearity of the cumulative infiltration, which can obscure the distinction between the early- and late-time infiltration processes (Di Prima et al., 2018).

3.2.3. Improved description of the transient phase

The hypothesis of a better description of the transient phase when using the automatic infiltrometers was investigated through a comparison between the cumulative infiltration curves obtained from transducer output and discretized curves having the same increments as manually pouring water volumes into the containment ring. In the reported example (Fig. 8), the infiltration reached steady state early (i.e., within the first 0.03 h) and only one discretized data point occurred within the transient flow regime. As a consequence, the transient infiltration models in BEST-slope and BEST-intercept could not be fitted to the discretized data. Conversely, the high-resolution cumulative infiltration curve obtained from the transducer output captured 14 points during the transient state, allowing for the BEST-slope (Fig. 8c) and BEST-intercept algorithms to be fitted. In some cases, too few points could be identified for the description of the transient state. Such a problem occurred at the ENTPE-1 site, likely due to the high local initial soil water content there (Table 1). In addition to this example, BEST-slope also failed in two cases at the ENTPE-2 site whereas BEST-intercept was successfully applied; consequently, the former method had the lowest success rate (Fig. 7). This shortcoming was already investigated in several investigations (e.g., Castellini et al., 2018; Di Prima et al., 2018). More specifically, when the early- and late-time infiltration stages greatly differ in terms of infiltration rates, the strong concavity of cumulative infiltration results in an over-estimation of soil sorptivity. Such overestimations result in negative values for K_s, as already suggested by Yilmaz et al. (2010).

3.2.4. Water repellent soils

The first obvious advantage in using automatic infiltrometer in case of water repellent soils is that data collection is automated and it does not require any further manipulation by the user once the device is installed. Therefore, tests can be successfully (and simultaneously) performed even if water repellency impedes infiltration and causes long

Table 4
Parameter values for the three data treatment approaches (i.e., manual selection, automatic selection and moving median) and the four methods to estimate hydrodynamic parameters (i.e., BEST-slope, BEST-intercept, BEST-steady and Approach 4). k_{tot} is the total number of measured data points, i_s is the steady infiltration rate (mm h^{-1}), S is the soil sorptivity (mm $h^{-0.5}$), K_s is the saturated soil hydraulic conductivity (mm h^{-1}), k_{step} is the number of datapoints used to fit the model, and Er is the fitting error (%). Descriptive statistics are reported in bold.

Site	Statistic	k_{tot}	i_s	BEST-slope				BEST-intercept				BEST-steady		Approach 4
				S	K_s	k_{step}	Er	S	K_s	k_{step}	Er	S	K_s	K_s
Manual selection														
ENTPE-1		71	1512.5									55.9	1290.4	354.8
		93	969.2	96.7	303.8	45	1.9	94.2	368.2	31	2.5	92.8†	357.0†	227.3
		159	74.6											17.5
		79	179.5	45.3	33.3	79	0.8	44.7	49.6	43	1.3	43.3	46.4	42.1
		75	339.9	41.2	219.3	14	4.3	41.0	220.8	13	4.6	41.0	220.3	79.7
	N	**5**	**5**	**3**	**3**	**3**	**3**	**3**	**3**	**3**	**3**	**4**	**4**	**5**
	mean	**95.4**	**615.1**	**61.1**	**185.5**	**46.0**	**2.3**	**60.0**	**212.9**	**29.0**	**2.8**	**58.2**	**478.5**	**144.3**
	CV (%)	**38.3**	**99.2**	**50.7**	**74.6**	**70.7**	**76.8**	**49.5**	**74.9**	**52.1**	**59.3**	**41.1**	**116.2**	**99.2**
ENTPE-2		97	232.8	48.4	32.6	97	1.2	47.4	57.0	68	1.6	45.8	53.2	54.6
		157	419.1					53.0	153.5	31	5.5	54.7	163.3	98.3
		232	136.5					33.9	35.0	119	4.7	34.3	35.7	32.0
		249	316.8	52.1	84.3	108	2.2	51.9	128.2	58	4.6	48.8	113.3	74.3
		155	166.4	40.2	28.1	155	0.8	39.1	42.1	85	1.4	38.3	40.5	39.0
	N	**5**	**5**	**3**	**3**	**3**	**3**	**5**	**5**	**5**	**5**	**5**	**5**	**5**
	mean	**178.0**	**254.3**	**46.9**	**48.4**	**120.0**	**1.4**	**45.1**	**83.1**	**72.2**	**3.5**	**44.4**	**81.2**	**59.7**
	CV (%)	**35.0**	**45.3**	**13.0**	**64.6**	**25.7**	**52.1**	**18.4**	**65.0**	**45.3**	**54.2**	**18.3**	**68.3**	**45.3**
DOUA		47	2684.4									101.3	2326.8	629.7
		50	3129.0									111.4	2697.0	734.0
	N	**2**	**2**									**2**	**2**	**2**
	mean	**48.5**	**2906.7**									**106.3**	**2511.9**	**681.8**
	CV (%)	**4.4**	**10.8**									**6.7**	**10.4**	**10.8**
Automatic selection														
ENTPE-1		77	1511.9									50.2	1332.8	354.6
		104	965.7	97.6	287.7	54	1.6	95.2	355.1	36	2.3	93.6†	343.0†	226.5
		153	74.2											17.4
		77	179.6	45.4	32.7	77	0.9	44.8	49.3	43	1.2	43.3	46.1	42.1
		74	339.2	45.9	189.2	18	1.8	44.7	217.3	15	2.3	43.4	205.0	79.6
	N	5	5	3	3	3	3	3	3	3	3	4	4	5
	mean	97.0	614.1	63.0	169.9	49.7	1.4	61.6	207.2	31.3	1.9	57.6	481.7	144.1
	CV (%)	34.6	99.2	47.6	75.7	59.9	34.9	47.3	73.9	46.5	32.3	41.9	120.4	99.2
ENTPE-2		95	229.7	48.6	27.8	95	1.3	47.6	53.0	75	1.5	45.9	49.4	53.9
		163	418.8					53.1	151.8	32	5.2	54.8	161.8	98.2
		223	135.8					34.2	34.1	121	4.7	34.4	34.5	31.8
		233	315.0	51.5	88.2	91	1.8	50.9	122.7	58	3.1	48.7	112.2	73.9
		154	166.2	40.2	27.9	154	0.8	39.1	41.9	85	1.4	38.4	40.3	39.0
	N	5	5	3	3	3	3	5	5	5	5	5	5	5
	mean	173.6	253.1	46.7	48.0	113.3	1.3	45.0	80.7	74.2	3.2	44.4	79.6	59.4
	CV (%)	32.4	45.5	12.5	72.6	31.1	37.9	17.9	65.8	44.4	56.2	18.3	69.7	45.5
DOUA		65	2680.1									111.4	2247.9	628.7
		38	3113.5									75.9	2912.8	730.3
	N	**2**	**2**									**2**	**2**	**2**
	mean	**51.5**	**2896.8**									**93.6**	**2580.4**	**679.5**
	CV (%)	**37.1**	**10.6**									**26.8**	**18.2**	**10.6**
Moving median														
ENTPE-1		61	1529.8									53.4	1327.3	358.8
		82	975.3	98.44	285.99	36	1.4	95.3	363.8	20	1.8	93.7†	351.3†	228.8
		177	75.5											17.7
		96	178.1	46.08	27.06	96	1.3	45.4	44.7	67	1.7	43.8	41.6	41.8
		73	339.1	44.94	195.42	15	3.7	44.2	205.5	13	4.0	43.8	202.4	79.5
	N	**5**	**5**	**3**	**3**	**3**	**3**	**3**	**3**	**3**	**3**	**4**	**4**	**5**
	mean	**97.8**	**619.6**	**63.2**	**169.5**	**49.0**	**2.2**	**61.6**	**204.6**	**33.3**	**2.5**	**58.7**	**480.7**	**145.3**
	CV (%)	**47.1**	**99.6**	**48.4**	**77.5**	**85.8**	**62.2**	**47.4**	**78.0**	**88.1**	**51.7**	**40.5**	**120.3**	**99.6**
ENTPE-2		106	237.8	48.64	35.27	106	1.3	47.8	61.4	67	1.6	46.0	56.9	55.8
		161	426.3	40.59	285.22	6	9.1	52.3	180.8	22	5.9	53.0	185.8	100.0
		239	136.7	25.94	79.08	13	5.3	34.2	34.8	118	4.2	34.4	35.2	32.1
		238	316.8	51.89	86.34	89	1.7	51.3	127.9	42	3.5	48.6	114.7	74.3
		166	167.3	40.43	27.32	166	0.5	39.5	42.1	91	0.8	38.5	40.2	39.2
	N	**5**	**5**	**5**	**5**	**5**	**5**	**5**	**5**	**5**	**5**	**5**	**5**	**5**
	mean	**182.0**	**257.0**	**41.5**	**102.6**	**76.0**	**3.6**	**45.0**	**89.4**	**68.0**	**3.2**	**44.1**	**86.5**	**60.3**
	CV (%)	**31.2**	**45.7**	**24.2**	**102.6**	**88.4**	**100.6**	**17.5**	**70.4**	**56.1**	**62.8**	**17.1**	**73.8**	**45.7**
DOUA		16	5215.1									231.3	3351.3	1223.3
		22	4221.7									131.9	3615.3	990.3
		35	2707.8									112.2	2268.9	635.2
		30	3159.3									105.1	2774.2	741.1
		27	3496.3									71.3††	3319.2††	820.1
	N	**5**	**5**									**5**	**5**	**5**
	mean	**26.0**	**3760.0**									**130.4**	**3065.8**	**882.0**
	CV (%)	**28.1**	**26.2**									**46.4**	**17.6**	**26.2**

N = sample size, CV = coefficient of variation.
† Values reported in Fig. 6b.
†† Values reported in Fig. 6g.

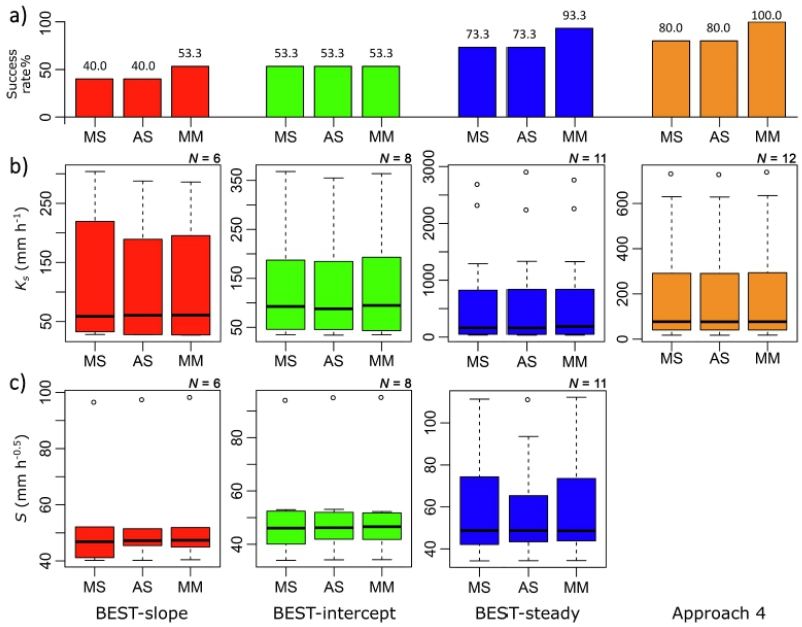

Fig. 7. (a) Comparison between the success rates obtained for the three data treatments (i.e., manual selection, MS, automatic selection AS, and moving median, MM), and the four methods for estimating the hydrodynamic parameters (i.e., BEST-slope, BEST-intercept, BEST-steady and Approach 4). Box plots of the (b) saturated soil hydraulic conductivity, K_s (mm h^{-1}), and (c) soil sorptivity, S (mm h$^{-0.5}$), pairs data for the different scenarios. The sample size (N) for each box plot is also reported.

testing durations (Alagna et al., 2018). In addition, the automatic infiltrometer used in this investigation was capable of maintaining a small water head on the soil surface, which helps to prevent excessive positive pressure from overcoming the soil water repellency (Nyman et al., 2010). For one experiment at the ENTPE-1 site, this experimental approach was useful to signal the occurrence of soil water repellency, as identified by cumulative infiltration having a convex curve shape (Di Prima et al., 2017). The cumulative infiltration data in that instance yielded a negative value for the intercept of the regression line fitted to the data points describing steady-state conditions (e.g., Alagna et al., 2018; Di Prima et al., 2019, 2017; Lozano-Baez et al., 2018). This circumstance led to the failure of all the BEST-algorithms (Lassabatere et al., 2019a); only Approach 4 provided an estimate of K_s. More specifically, BEST-slope and BEST-intercept failed because both algorithms required fitting transient models to early infiltration data that must be concave instead of convex as determined by soil water repellency. The BEST-steady algorithm avoids most problems associated with the use of the transient infiltration data, yet still estimates meaningless K_s data in case of negative intercept values. On the other hand, Approach 4 by Stewart and Abou Najm (2018) differs by the term expressing steady-state condition, considering exclusively the final infiltration rate, i.e., the slope of regression line fitted to the last data points of the cumulative infiltration. The exclusive use of this term allowed to consider only the final stage of the infiltration process, i.e., when the water repellency had diminished or no effect on infiltration. Therefore, we suggest to use steady state methods, such as Approach 4, in case of water repellent soils (Angulo-Jaramillo et al., 2019). This example also illustrates that, when the physics of infiltration change, as in the case of water infiltration into water repellent soils, all the BEST methods are questionable (Bauters et al., 2003).

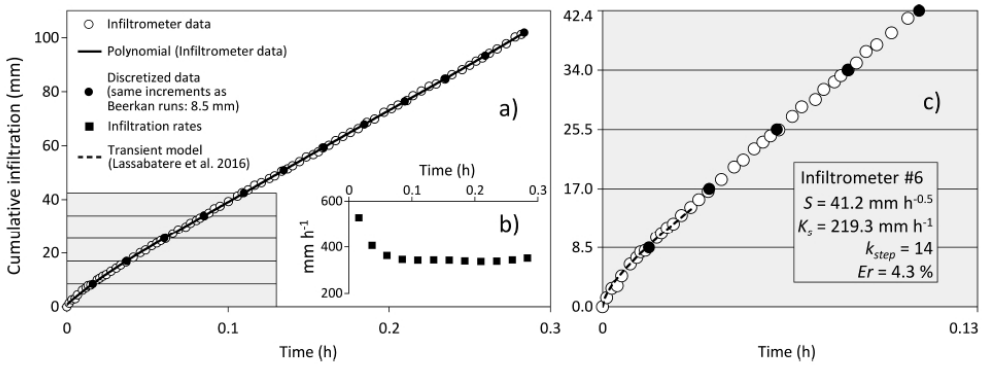

Fig. 8. (a) Comparison between cumulative infiltration curves obtained from transducer output (open circles ○) and discretized data (solid circles ●). The solid line is the polynomial function used to model the discretized data with the same increments as manually collected infiltration curves, i.e., 8.5 mm ("Beerkan-like data"). (b) Infiltration rates of the discretized data. (c) Detailed view of the early-time infiltration stage. The dotted line is the fitted cumulative infiltration model to the transient infiltration data. k_{step} is the number of datapoints used to fit the model.

3.3. Comparison with the prototype

We also compared the cumulative infiltrations curves collected using the new infiltrometers with those measured by the prototype proposed by Di Prima (2015) on different soils analyzed during previous field campaigns (Di Prima, 2015; Di Prima et al., 2017, 2016). Fig. 9 depicts a comparison between 45 curves collected with the prototype (Fig. 9a) versus the curves collected with new infiltrometers at the ENTPE-1, ENTPE-2 and DOUA sites (Fig. 9b). The mean value of the cumulative infiltration intervals, ΔI, decreased from 4.65 mm with the original prototype to 2.15 mm with the new version (Fig. 9c). Therefore, the new infiltrometers had more than twice the resolution (i.e., shorter increments between readings) of the prototype. Returning the example shown in Fig. 8, the updated version of the automated infiltrometer provided 14 measurements during the transient regime (Fig. 8c), whereas the prototype would only have the capability to capture 3–4 points. Accurately modeling the transient state requires a minimum of five measurements (Angulo-Jaramillo et al. 2019), meaning that the prototype system would be inadequate in that scenario. At the same time, the new devices were able to collect measurements for longer durations (and greater cumulative infiltration amounts) due to their larger storage capacity. Thus, compared to the prototype system the new version of the infiltrometer can generate more data points during both transient and steady-state flow regimes.

3.4. Application of the proposed device to double-ring measures

An automatic infiltrometer constructed at the Anand Agricultural University was used to run both of the single- and double-ring infiltration experiments. K_s values ranged between 15.0 and 105.8 mm h^{-1} (Table 5). The different experimental set-ups, including multiple imposed water depths (25, 50 and 75 mm), showed the versatility of the device to execute experiments with multiple positive water heads, such as the one requested for the two- or multiple-ponding-depth approaches (Reynolds and Elrick, 2002a). For the double-ring experiments, the use of the infiltrometer to maintain the water level in the inner ring improved monitoring of the infiltration process while reducing the amount of effort needed to maintain a constant depth of water in both rings (Lai and Ren, 2007). The main advantage of using the automated infiltrometer in this scenario was its simplicity, in that it allowed a single operator to carry out the field experiments. In addition, the limited cost of the device means that it can contribute to more widespread applications of accurate and automated infiltration rates measurements, even when combined with cumbersome experiments such as the double-ring infiltrometer.

Table 5
Results of the single- and double-ring infiltration experiments.

Method	Water depth (mm)	Steady infiltration rate (mm h^{-1})	K_s (mm h^{-1})
Single-ring	25	105.8	43.6
	50	80.5	30.6
	75	73.3	25.8
Double-ring	25	22.7	22.7
	50	22.5	22.5
	75	15.0	15.0

3.5. On the advantage of multiple infiltration experiments

The ability of the proposed instrumentation package to automatically collect data from up to ten infiltrometers working simultaneously, i.e., when using ten infiltrometers connected to two data acquisition systems, was tested at the ENTPE-1 site (Fig. 10). Such a protocol had many advantages. Indeed, ten replicates enabled the identification of specific runs, revealing either the effect of preferential flow (e.g., Fig. 10b, run n. 10) or, on the contrary, the impedance of flux owing to water repellency (e.g., Fig. 10b, runs n. 4 and 8). In addition, ten replicates should be appropriate to obtain representative mean values of soil hydrodynamic parameters at the field scale (Reynolds and Elrick, 2002b; Verbist et al., 2010). This protocol can help to overcome uncertainties in the hydraulic characterization of highly heterogeneous soils. The new instrumentation package may constitute a valuable tool for the application of the Beerkan multi-runs procedure proposed by Lassabatere et al. (2019a), which consists in carrying out ten Beerkan infiltration experiments along a transect. The use of the automatic infiltrometers in this protocol may both provide sufficient water supply to reach steady state and provide measurement resolution needed to improve the description of the transient state. These advances allow the user to obtain more accurate estimates of soil hydraulic parameters, while also reducing the amount of effort needed to run multiple experiments.

4. Summary and conclusions

In this investigation we designed and manufactured a set of ten devices that automatically provide water at a constant head and record the resulting infiltration rates. The design of the devices was improved over a previously presented prototype in terms of reservoir capacity (which controls the duration of the test), diameter of the air entry tube (which controls the measurement resolution and corresponding accuracy of infiltration measurements), and number of infiltrometers that can be simultaneously operated (here up to ten at one time). We also

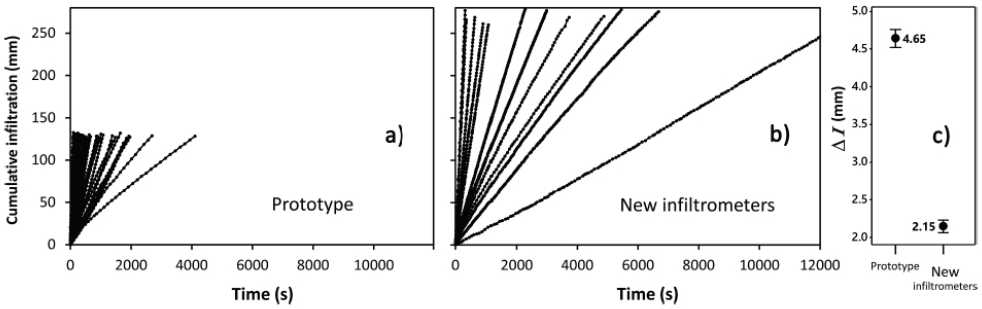

Fig. 9. Comparison between cumulative infiltration curves collected with (a) the prototype proposed by Di Prima (2015) on different soils analyzed during previous field campaigns (Di Prima, 2015; Di Prima et al., 2017, 2016), versus (b) the curves collected with new infiltrometers at the ENTPE-1, ENTPE-2 and DOUA sites. Subpanel c displays the interval plots with the mean values of the cumulative infiltration intervals, ΔI (mm), and the 95% confidence interval bars. Individual standard deviations were used to calculate the intervals.

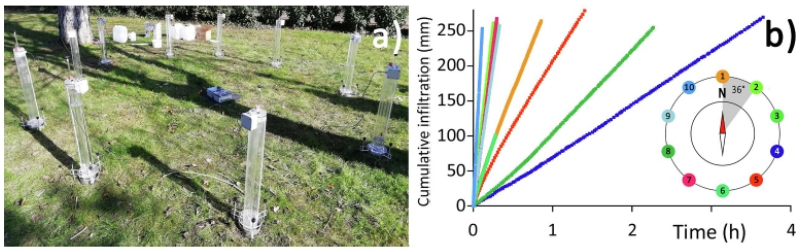

Fig. 10. (a) Experimental setup consisting of ten infiltrometers working simultaneously and connected to two data acquisition systems, and (b) measured cumulative infiltration curves.

proposed a new algorithm for the automatic processing of the transducer readings, which substantially reduced the amount of work necessary to analyze the raw data. We encourage the readers to check the website bestsoilhydro.net for the latest updates, and also to download: Arduino sketches, electronic schemes, codes for data treatment, lists of components, models for 3D printing and laser cutting projects.

The devices were firstly tested in the laboratory and then on four different experimental sites under specific and challenging field conditions, such as highly permeable, slightly sorptive and water repellent conditions. The field campaigns highlighted the ease of use of the devices when performing either single-ring or double-ring infiltration experiments. The new instrumentation package provided in this study allows the user to intensively measure soil infiltration rates, with the capability of automatically recording multiple experiments. Automated measurements also facilitate better detection of preferential flow and soil water repellency conditions in the field.

Funding

This work was supported through the INFILTRON Project (ANR-17-CE04-0010, Package for assessing infiltration & filtration functions of urban soils in stormwater management; https://infiltron.org/) funded by the French National Research Agency (ANR). Funding was also provided in part by: i) the Virginia Agricultural Experiment Station and the Hatch Program of the National Institute of Food and Agriculture, U.S. Department of Agriculture, ii) the European Regional Development Fund (ERDF) and the Italian Ministry of Education, University and Research (MIUR) through the "Programma Operativo Nazionale (PON) Ricerca e Innovazione 2014-2020 (Linea 1 – Mobilità dei ricercatori, AIM1853149, CUP: J54I18000120001), and iii) the University of California – Davis Agricultural Experiment Station.

CRediT authorship contribution statement

Paola Concialdi: Conceptualization, Investigation, Formal analysis, Writing - original draft, Validation, Visualization. **Simone Di Prima:** Conceptualization, Investigation, Formal analysis, Writing - original draft, Validation, Visualization. **Harsh M. Bhanderi:** Investigation, Validation, Visualization, Writing - original draft. **Ryan D. Stewart:** Validation, Visualization, Writing - original draft. **Majdi R. Abou Najm:** Validation, Visualization, Writing - original draft. **Murari Lal Gaur:** Validation, Visualization, Writing - original draft. **Rafael Angulo-Jaramillo:** Validation, Visualization, Writing - original draft. **Laurent Lassabatere:** Supervision, Software, Funding acquisition, Validation, Visualization, Writing - original draft.

Declaration of Competing Interest

The authors declare that they have no known competing financial interests or personal relationships that could have appeared to influence the work reported in this paper.

Acknowledgements

The authors wish to thank the Lyon city Field Observatory for Urban Water Management (OTHU), the Department of Agricultural, Food and Forest Sciences of the University of Palermo (Italy), and Pier Nicola Labate and Andrea Melis from the laboratory FabLab UniSS of the University of Sassari (Italy) for technical and scientific support. P. Concialdi and S. Di Prima realized the devices, outlined the investigation and carried out the experimental activity in France. H. Bhanderi realized the device and carried out the experimental activity at the Anand Agricultural University. L. Lassabatere coded the algorithm in Scilab for the automatic treatment of the transducer output. All authors contributed to discussing the results and writing the manuscript. S.D.P. also thanks labandadipalermo.it for their contribution to keep the spirit up.

References

Alagna, V., Iovino, M., Bagarello, V., Mataix-Solera, J., Lichner, Ľ., 2018. Alternative analysis of transient infiltration experiment to estimate soil water repellency. Hydrol. Process. https://doi.org/10.1002/hyp.13352.

Angulo-Jaramillo, R., Bagarello, V., Iovino, M., Lassabatère, L., 2016. Infiltration Measurements for Soil Hydraulic Characterization. Springer International Publishing.

Angulo-Jaramillo, R., Bagarello, V., Di Prima, S., Gosset, A., Iovino, M., Lassabatere, L., 2019. Beerkan Estimation of Soil Transfer parameters (BEST) across soils and scales. J. Hydrol. 576, 239–261. https://doi.org/10.1016/j.jhydrol.2019.06.007.

Ankeny, M.D., 1992. Methods and theory for unconfined infiltration measurements. SSSA Special Publication Series (USA), pp. 123–141.

Ankeny, M.D., Kaspar, T.C., Horton, R., 1988. Design for an automated tension infiltrometer. Soil Sci. Soc. Am. J. 52, 893. https://doi.org/10.2136/sssaj1988.03615995005200030054x.

Ankeny, M.D., Prieksat, M.A., Kaspar, T.C., Noh, K.M., 1993. FLOWDATA: software for analysis of infiltration data from automated infiltrometers. Agron. J. 85, 955–959. https://doi.org/10.2134/agronj1993.00021962008500040030x.

Bagarello, V., Di Prima, S., Iovino, M., 2014. Comparing alternative algorithms to analyze the Beerkan infiltration experiment. Soil Sci. Soc. Am. J. 78, 724. https://doi.org/10.2136/sssaj2013.06.0231.

Bauters, T.W.J., Steenhuis, T.S., DiCarlo, D.A., Nieber, J.L., Dekker, L.W., Ritsema, C.J., Parlange, J.Y., Haverkamp, R., 2003. Physics of hydrophobic soils. Soil Water Repellency 215–224. https://doi.org/10.1016/B978-0-444-51269-7.50022-9.

Bouarafa, S., Lassabatere, L., Lipeme-Kouyi, G., Angulo-Jaramillo, R., 2019. Hydrodynamic characterization of sustainable urban drainage systems (SuDS) by using Beerkan infiltration experiments. Water 11, 660. https://doi.org/10.3390/w11040660.

Braud, I., Desprats, J.-F., Ayral, P.-A., Bouvier, C., Vandervaere, J.-P., 2017. Mapping topsoil field-saturated hydraulic conductivity from point measurements using different methods. J. Hydrol. Hydromech. 65. https://doi.org/10.1515/johh-2017-0017.

Casey, F.X.M., Derby, N.E., 2002. Improved design for an automated tension infiltrometer. Soil Sci. Soc. Am. J. 66, 64–67.

Castellini, M., Di Prima, S., Iovino, M., 2018. An assessment of the BEST procedure to estimate the soil water retention curve: a comparison with the evaporation method. Geoderma 320, 82–94. https://doi.org/10.1016/j.geoderma.2018.01.014.

Constantz, J., Murphy, F., 1987. An automated technique for flow measurements from Mariotte reservoirs. Soil Sci. Soc. Am. J. 51, 252. https://doi.org/10.2136/sssaj1987.03615995005100010051x.

Decagon, 2014. Minidisk Infiltrometer User's Manual. Decagon Devices, Inc., Pullman, USA, pp. 24.

Di Prima, S., 2015. Automated single ring infiltrometer with a low-cost microcontroller circuit. Comput. Electron. Agric. 118, 390–395. https://doi.org/10.1016/j.compag.2015.09.022.

Di Prima, S., Lassabatere, L., Bagarello, V., Iovino, M., Angulo-Jaramillo, R., 2016. Testing a new automated single ring infiltrometer for Beerkan infiltration experiments. Geoderma 262, 20–34. https://doi.org/10.1016/j.geoderma.2015.08.006.

Di Prima, S., Bagarello, V., Angulo-Jaramillo, R., Bautista, I., Cerdà, A., del Campo, A., González-Sanchis, M., Iovino, M., Lassabatere, L., Maetzke, F., 2017. Impacts of thinning of a Mediterranean oak forest on soil properties influencing water infiltration. J. Hydrol. Hydromech. 65, 276–286. https://doi.org/10.1515/johh-2017-0016.

Di Prima, S., Concialdi, P., Lassabatere, L., Angulo-Jaramillo, R., Pirastru, M., Cerda, A., Keesstra, S., 2018. Laboratory testing of Beerkan infiltration experiments for assessing the role of soil sealing on water infiltration. CATENA 167, 373–384. https://doi.org/10.1016/j.catena.2018.05.013.

Di Prima, S., Castellini, M., Abou Najm, M.R., Stewart, R.D., Angulo-Jaramillo, R., Winiarski, T., Lassabatere, L., 2019. Experimental assessment of a new comprehensive model for single ring infiltration data. J. Hydrol. 573, 937–951. https://doi.org/10.1016/j.jhydrol.2019.03.077.

Di Prima, Simone, Lassabatere, L., Bagarello, V., Iovino, M., Angulo-Jaramillo, R., 2016. Testing a new automated single ring infiltrometer for Beerkan infiltration experiments. Geoderma 262, 20–34. https://doi.org/10.1016/j.geoderma.2015.08.006.

Di Prima, S., 2014. A new automated single ring infiltrometer for Beerkan infiltration experiments [https://www.youtube.com/watch?v=2nok8MJWV9s].

Haverkamp, R., Ross, P.J., Smettem, K.R.J., Parlange, J.Y., 1994. 3-Dimensional analysis of infiltration from the disc infiltrometer. 2. Physically-based infiltration equation. Water Resources Res. 30, 2931–2935.

Klípa, V., Sněhota, M., Dohnal, M., 2015. New automatic minidisk infiltrometer: design and testing. J. Hydrol. Hydromech. 63. https://doi.org/10.1515/johh-2015-0023.

Lai, J., Ren, L., 2007. Assessing the size dependency of measured hydraulic conductivity using double-ring infiltrometers and numerical simulation. Soil Sci. Soc. Am. J. 71, 1667. https://doi.org/10.2136/sssaj2006.0227.

Lassabatere, L., Angulo-Jaramillo, R., Soria Ugalde, J.M., Cuenca, R., Braud, I., Haverkamp, R., 2006. Beerkan estimation of soil transfer parameters through infiltration experiments—BEST. Soil Sci. Soc. Am. J. 70, 521. https://doi.org/10.2136/sssaj2005.0026.

Lassabatere, L., Di Prima, S., Bouarafa, S., Iovino, M., Bagarello, V., Angulo-Jaramillo, R., 2019b. BEST-2K method for characterizing dual-permeability unsaturated soils with ponded and tension infiltrometers. Vadose Zone J. 18. https://doi.org/10.2136/vzj2018.06.0124.

Lassabatere, L., Di Prima, S., Angulo-Jaramillo, R., Keesstra, S., Salesa, D., 2019a. Beerkan multi-runs for characterizing water infiltration and spatial variability of soil hydraulic properties across scales. Hydrol. Sci. J. 64, 165–178. https://doi.org/10.1080/02626667.2018.1560448.

Lozano-Baez, S.E., Cooper, M., Ferraz, S.F.B., Ribeiro Rodrigues, R., Pirastru, M., Di Prima, S., 2018. Previous land use affects the recovery of soil hydraulic properties after forest restoration. Water 10. https://doi.org/10.3390/w10040453.

Madsen, M.D., Chandler, D.G., 2007. Automation and use of mini disk infiltrometers. Soil Sci. Soc. Am. J. 71, 1469. https://doi.org/10.2136/sssaj2007.0009N.

Milla, K., Kish, S., 2006. A low-cost microprocessor and infrared sensor system for automating water infiltration measurements. Comput. Electron. Agric. 53, 122–129. https://doi.org/10.1016/j.compag.2006.05.001.

Moret, D., López, M.V., Arrúe, J.L., 2004. TDR application for automated water level measurement from Mariotte reservoirs in tension disc infiltrometers. J. Hydrol. 297, 229–235. https://doi.org/10.1016/j.jhydrol.2004.04.003.

Moret-Fernández, D., González, C., Lampurlanés, J., Vicente, J., 2012. An automated disc infiltrometer for infiltration rate measurements using a microflowmeter. Hydrol. Process. 26, 240–245. https://doi.org/10.1002/hyp.8184.

Nyman, P., Sheridan, G., Lane, P.N.J., 2010. Synergistic effects of water repellency and macropore flow on the hydraulic conductivity of a burned forest soil, south-east Australia. Hydrol. Process. 24, 2871–2887. https://doi.org/10.1002/hyp.7701.

Prieksat, M.A., Ankeny, M.D., Kaspar, T.C., 1992. Design for an automated, self-regulating, single-ring infiltrometer. Soil Sci. Soc. Am. J. 56, 1409. https://doi.org/10.2136/sssaj1992.03615995005600050013x.

Reynolds, W.D., Elrick, D.E., 1990. Ponded Infiltration From a Single Ring: I. Analysis of Steady Flow. Soil Sci. Soc. Am. J. 54, 1233. https://doi.org/10.2136/sssaj1990.03615995005400050006x.

Reynolds, W.D., Elrick, D.E., 2002a. 3.4.3.3 Constant Head Well Permeameter (Vadose Zone). In: Methods of Soil Analysis: Part 4 Physical Methods, SSSA Book Series. Soil Science Society of America, Madison, WI, pp. 844–858. https://doi.org/10.2136/sssabookser5.4.c33.

Reynolds, W., Elrick, D., 2002b. 3.4.3.2. Pressure infiltrometer. In: Dane, J.H., Topp, G.C. (Eds.), Methods of Soil Analysis, Part 4, Physical Methods, SSSA Book Series, No. 5. Soil Sci. Soc. Am.: Madison, Wisconsin, USA 4, pp. 826–836.

Reynolds, W., Elrick, D., Youngs, E., 2002. 3.4.3.2 Ring or cylinder infiltrometers (vadose zone). In: Dane, J.H., Topp, G.C. (Eds.), Methods of Soil Analysis, Part 4, Physical Methods, SSSA Book Series, No. 5. Soil Sci. Soc. Am.: Madison,Wisconsin, USA, pp. 818–820.

Selker, J.S., Suter, J.D., Cuenca, R.H., Flugstad, B.A., Kelly, S.F., 2009. Tension infiltrometer enhancements with automated pneumatic control and more durable base plate: enhanced tension infiltrometer. Water Resour. Res. 45, n/a-n/a. https://doi.org/10.1029/2008WR007075.

Stewart, R.D., Abou Najm, M.R., 2018. A Comprehensive model for single ring infiltration II: estimating field-saturated hydraulic conductivity. Soil Sci. Soc. Am. J. 82, 558–567. https://doi.org/10.2136/sssaj2017.09.0314.

Verbist, K., Torfs, S., Cornelis, W.M., Oyarzún, R., Soto, G., Gabriels, D., 2010. Comparison of single- and double-ring infiltrometer methods on stony soils. Vadose Zone J. 9, 462–475. https://doi.org/10.2136/vzj2009.0058.

Xu, X., Lewis, C., Liu, W., Albertson, J.D., Kiely, G., 2012. Analysis of single-ring infiltrometer data for soil hydraulic properties estimation: comparison of BEST and Wu methods. Agric. Water Manag. 107, 34–41. https://doi.org/10.1016/j.agwat.2012.01.004.

Yilmaz, D., Lassabatere, L., Angulo-Jaramillo, R., Deneele, D., Legret, M., 2010. Hydrodynamic characterization of basic oxygen furnace slag through an adapted BEST method. Vadose Zone J. 9, 107. https://doi.org/10.2136/vzj2009.0039.

Zimmermann, B., Zehe, E., Hartmann, N.K., Elsenbeer, H., 2008. Analyzing spatial data: an assessment of assumptions, new methods, and uncertainty using soil hydraulic data: analyzing spatial data. Water Resour. Res. 44, n/a-n/a. https://doi.org/10.1029/2007WR006604.

Zumr, D., Jeřábek, J., Klípa, V., Dohnal, M., Sněhota, M., 2019. Estimates of tillage and rainfall effects on unsaturated hydraulic conductivity in a small central European Agricultural Catchment. Water 11, 740. https://doi.org/10.3390/w11040740.

References

Ankeny, M.D., Kaspar, T.C., Horton, R., 1988. Design for an automated tension infiltrometer. Soil Sci. Soc. Am. J. 52, 893. https://doi.org/10.2136/sssaj1988.03615995005200030054x

Arriaga, F.J., Kornecki, T.S., Balkcom, K.S., Raper, R.L., 2010. A method for automating data collection from a double-ring infiltrometer under falling head conditions: Modified double-ring infiltrometer. Soil Use Manag. 26, 61–67. https://doi.org/10.1111/j.1475-2743.2009.00249.x

Bagarello, V., Di Prima, S., Iovino, M., 2014. Comparing alternative algorithms to analyze the beerkan infiltration experiment. Soil Sci. Soc. Am. J. 78, 724. https://doi.org/10.2136/sssaj2013.06.0231

Casey, F.X.M., Derby, N.E., 2002. Improved design for an automated tension infiltrometer. Soil Sci Soc Am J 66, 64–67

Castiglione, P., Shouse, P.J., Mohanty, B., Hudson, D., van Genuchten, M.T., 2005. Improved tension infiltrometer for measuring low fluid flow rates in unsaturated fractured rock. Vadose Zone J. 4, 885. https://doi.org/10.2136/vzj2004.0135

Cernicchiaro, G., Barmak, R., Teixeira, W.G., 2019. Digital interface device for field soil hydraulic conductivity measurement. J. Hydrol. 576, 58–64. https://doi.org/10.1016/j.jhydrol.2019.06.034

Concialdi, P., Di Prima, S., Bhanderi, H.M., Stewart, R.D., Abou Najm, M.R., Lal Gaur, M., Angulo-Jaramillo, R., Lassabatere, L., 2020. An open-source instrumentation package for intensive soil hydraulic characterization. J. Hydrol. 582, 124492. https://doi.org/10.1016/j.jhydrol.2019.124492

Constantz, J., Murphy, F., 1987. An automated technique for flow measurements from mariotte reservoirs1. Soil Sci. Soc. Am. J. 51, 252. https://doi.org/10.2136/sssaj1987.03615995005100010051x

Di Prima, S., Lassabatere, L., Bagarello, V., Iovino, M., Angulo-Jaramillo, R., 2016. Testing a new automated single ring infiltrometer for Beerkan infiltration experiments. Geoderma 262, 20–34. https://doi.org/10.1016/j.geoderma.2015.08.006

Di Prima, S., 2015. Automated single ring infiltrometer with a low-cost microcontroller circuit. Comput. Electron. Agric. 118, 390–395. https://doi.org/10.1016/j.compag.2015.09.022

Fatehnia, M., Paran, S., Kish, S., Tawfiq, K., 2016. Automating double ring infiltrometer with an Arduino microcontroller. Geoderma 262, 133–139. https://doi.org/10.1016/j.geoderma.2015.08.022

Klípa, V., Sněhota, M., Dohnal, M., 2015. New automatic minidisk infiltrometer: design and testing. J. Hydrol. Hydromech. 63. https://doi.org/10.1515/johh-2015-0023

Lassabatere, L., Di Prima, S., Angulo-Jaramillo, R., Keesstra, S., Cerda, A., 2019. Beerkan multi-runs for characterizing water infiltration and spatial variability of soil hydraulic properties across scales. Hydrol. Sci. J. https://doi.org/10.1080/02626667.2018.1560448

Lassabatere, L., Angulo-Jaramillo, R., Soria Ugalde, J.M., Cuenca, R., Braud, I., Haverkamp, R., 2006. Beerkan estimation of soil transfer parameters through infiltration experiments—BEST. Soil Sci. Soc. Am. J. 70, 521. https://doi.org/10.2136/sssaj2005.0026

Logsdon, S.D., Jaynes, D.B., 1996. Spatial variability of hydraulic conductivity in a cultivated field at different times. Soil Sci. Soc. Am. J. 60, 703. https://doi.org/10.2136/sssaj1996.03615995006000030003x

Madsen, M.D., Chandler, D.G., 2007. Automation and use of mini disk infiltrometers. Soil Sci. Soc. Am. J. 71, 1469. https://doi.org/10.2136/sssaj2007.0009N

Milla, K., Kish, S., 2006. A low-cost microprocessor and infrared sensor system for automating water infiltration measurements. Comput. Electron. Agric. 53, 122–129. https://doi.org/10.1016/j.compag.2006.05.001

Moret, D., López, M.V., Arrúe, J.L., 2004. TDR application for automated water level measurement from Mariotte reservoirs in tension disc infiltrometers. J. Hydrol. 297, 229–235. https://doi.org/10.1016/j.jhydrol.2004.04.003

Prieksat, M.A., Ankeny, M.D., Kaspar, T.C., 1992. Design for an automated, self-regulating, single-ring infiltrometer. Soil Sci. Soc. Am. J. 56, 1409. https://doi.org/10.2136/sssaj1992.03615995005600050013x

Reynolds, W.D., Elrick, D.E., 1990. Ponded infiltration from a single ring: i. analysis of steady flow. Soil Sci. Soc. Am. J. 54, 1233. https://doi.org/10.2136/sssaj1990.03615995005400050006x

Rodríguez-Juárez, P., Júnez-Ferreira, H.E., González Trinidad, J., Zavala, M., Burnes-Rudecino, S., Bautista-Capetillo, C., 2018. Automated laboratory infiltrometer to estimate saturated hydraulic conductivity using an arduino microcontroller board. Water 10, 1867. https://doi.org/10.3390/w10121867

Selker, J.S., Suter, J.D., Cuenca, R.H., Flugstad, B.A., Kelly, S.F., 2009. Tension infiltrometer enhancements with automated pneumatic control and more durable base plate: enhanced tension infiltrometer. Water Resour. Res. 45, n/a-n/a. https://doi.org/10.1029/2008WR007075

Špongrová, K., Kechavarzi, C., Dresser, M., Matula, S., Godwin, R.J., 2009. Development of an automated tension infiltrometer for field use. Vadose Zone J. 8, 810. https://doi.org/10.2136/vzj2008.0135

Yilmaz, D., Lassabatere, L., Angulo-Jaramillo, R., Deneele, D., Legret, M., 2010. Hydrodynamic characterization of basic oxygen furnace slag through an adapted BEST Method. Vadose Zone J. 9, 107. https://doi.org/10.2136/vzj2009.0039

CHAPTER 5: Additional investigations on soil hydraulic characterization by single-ring infiltration methods

This chapter describes the research activity on soil hydraulic characterization by single-ring infiltration methods that is still in progress. To be clearer, this activity started during the PhD course but it was not fully concluded with respect to the analysis of the results. However, the work that was carried out and the results obtained till now were considered to have a certain scientific interest and therefore they were also included in this thesis.
This chapter is composed by two sections. The first section deals with parameterization of the comprehensive model for single-ring infiltration recently proposed by Stewart and Abou Najm (2018a,b). The second section attempts to establish if there is a link between the applied methodology to perform a single-ring infiltration experiment and the detected temporal variability of the saturated soil hydraulic conductivity, K_s.
Both investigations were based on field campaigns of soil sampling. The methodological starting point was the protocol already described in detail by Auteri et al. (2020), that is beerkan infiltration runs carried out with 30 water volumes (each-one of 57 ml), each establishing an initial ponded depth of water of nearly 0.01 m on the infiltration surface, and both low (height of water pouring = 0.03 m) and high (1.5 m) heights of water pouring. In short, this experimental protocol was applied at three different field sites (Aranceto, AR; Orleans, OR; Roccamena, RO) and at different times in the former site.
The data collected with the low runs at the three sites were used for the investigation on the infiltration model proposed by Stewart and Abou Najm (2018a,b). The data repeatedly collected at the AR site with both low and high runs were used to perform the investigation on temporal variability of K_s. The data obtained at the OR site with the high runs were not used in this thesis but they were stored to develop a homogeneous dataset for future use. The data collected with the low and high runs at the RO site were used in Auteri et al. (2020) paper.

5.1. Parameterization of an explicit model for single-ring infiltration

5.1.1.Introduction

Stewart and Abou Najm (2018a) combined the single-ring infiltration models by Reynolds and Elrick (1990) and Wu et al. (1999) to develop a new comprehensive model for single-ring infiltration. According to the authors, this new infiltration model is simple, easy to parameterize and interpret, applicable to most initial conditions and soil types with minimal error, and capable of describing both early-time and steady-state infiltration behaviors. In a companion paper, Stewart and Abou Najm (2018b) used the developed infiltration model to derive four methods for estimating the saturated soil hydraulic conductivity (K_s) from single-ring infiltration data. Di Prima et al. (2019) later tested the suggested methods for determining K_s and they concluded that the new infiltration model represents a valuable tool for analyzing both transient and steady-state infiltration as well as experiments carried out with different depths of ponded water, ring sizes and ring insertion depths. Therefore, the model by Stewart and Abou Najm (2018a) deserves additional testing.
A point to be considered is related to the parameterization of the infiltration model. In particular, the a constant that appears in this model should be equal to 0.9084 according to Wu and Pan (1997) and to 0.45 according to Stewart and Abou Najm (2018a). Currently, there is not any independent check of the most appropriate choice that should be made with reference to this constant.
The objective of this investigation was to improve parameterization of the infiltration model by Stewart and Abou Najm (2018a). A theoretical analysis was initially developed to demonstrate that the a constant can directly be estimated by a single-ring experiment that includes both the transient and the steady-state phase of the infiltration process. Single-ring infiltration data collected in the field were then used to determine a and to check consistency with theoretical expectations.

5.1.2. Infiltration model

Stewart and Abou Najm (2018a) developed the following explicit expressions of transient and steady-state three-dimensional (3D) cumulative infiltration, I (L), from a surface circular source under a positive pressure head, by building on the Wu et al. (1999) and Reynolds and Elrick (1990) solutions for 3D flow from within a ring inserted into the initially unsaturated soil to a short depth:

$$I = \sqrt{\frac{(\theta_s - \theta_i)(h_{source} + \lambda)K_s}{b}}\sqrt{t} + a\, f\, K_s\, t \qquad t < t_{crit} \qquad (1a)$$

$$I = \frac{(\theta_s - \theta_i)(h_{source} + \lambda)}{4\, f\, b(1-a)} + f\, K_s\, t \qquad t \geq t_{crit} \qquad (1b)$$

$$t_{crit} = \frac{(\theta_s - \theta_i)(h_{source} + \lambda)}{4 b K_s\, f^2 (1-a)^2} \qquad (1c)$$

where t (T) is the time, t_{crit} (T) is the time of transition between early-time and steady-state infiltration behaviors, θ_s (L^3L^{-3}) and θ_i (L^3L^{-3}) are the saturated and initial volumetric soil water contents, respectively, h_{source} (L) is the established ponded depth of water on the infiltration surface, λ (L) is the capillary length of the soil, K_s (L T^{-1}) is the saturated soil hydraulic conductivity, a and b are dimensionless constants (with $b \approx 0.55$; White and Sully, 1987), and f is a correction factor that depends on soil initial and boundary conditions and ring geometry:

$$f = \frac{h_{source} + \lambda}{d + r_d/2} + 1 \qquad (2)$$

where d (L) is the depth of ring insertion and r_d (L) is the radius of the ring. The t_{crit} time in eq.(1c) is defined as the time when the infiltration rate (dI/dt) is equal between eqs.(1a) and (1b). Eqs.(1) can be simplified as follows:

$$I = c_1\sqrt{t} + c_2 t \qquad t < t_{crit} \qquad (3a)$$

$$I = c_3 + c_4 t \qquad t \geq t_{crit} \qquad (3b)$$

$$t_{crit} = \frac{1}{4}\left(\frac{c_1}{c_4 - c_2}\right)^2 \qquad (3c)$$

where the infiltration coefficients c_1 (L $T^{-0.5}$) and c_2 (L T^{-1}) can be determined by fitting eq.(3a) to the data while the intercept, c_3 (L), and the slope, c_4 (L T^{-1}), of eq.(3b) are estimated by linear regression analysis of the $I(t)$ vs. t data points denoting steady-state conditions. The four infiltration coefficients can be used to estimate λ and K_s from a single-ring infiltration experiment (Stewart and Abou Najm, 2018b; Di Prima et al., 2019). Taking into account that the same I value has to be obtained by eqs.(3a) and (3b) at $t = t_{crit}$ and considering eq.(3c), the constraint among the four infiltration coefficients can be written as:

$$c_3 = \frac{c_1^2}{4(c_4 - c_2)} = t_{crit}(c_4 - c_2) \qquad (4)$$

Some perplexity can emerge with reference to the *a* constant of eqs.(1). Wu and Pan (1997) fitted a dimensionless infiltration equation to the numerically simulated single-ring infiltration data for three representative soils (sand, clay, sandy-clay-loam) and they obtained $a = 0.9084$. This value was subsequently used in the infiltration model by Wu et al. (1999). By analogy with Philip (1990), Stewart and Abou Najm (2018a) suggested that *a* should instead be equal to 0.45, that is approximately one half of the value recommended by Wu and Pan (1997). Stewart and Abou Najm (2018a) supported their suggestion by a sensitivity analysis of the model results. Both recommendations (Wu and Pan, 1997; Stewart and Abou Najm, 2018a) originated from theoretical reasoning and simulations for idealized porous media. A common suggestion between the two research groups was that *a*, being a constant, should not depend on the soil and its initial water content. The novel and simple reasoning that is made here is that the mentioned perplexity has no reason to exist since *a* can directly be estimated by a single-ring experiment that includes both the transient and the steady-state phase of the infiltration process. In particular, determination of c_2 and c_4 yields an experimental value of this constant by the following relationship:

$$\frac{c_2}{c_4} = \frac{a\, f\, K_s}{f\, K_s} = a \tag{5}$$

Therefore, it is not necessary to fix the *a* constant in advance for estimating soil hydraulic properties. Taking into account the constraint between c_2 and c_4 defined by eq.(5), eqs.(3c) and (4) can be written as:

$$t_{crit} = \frac{1}{4}\left[\frac{c_1}{c_4(1-a)}\right]^2 \tag{6}$$

$$c_3 = \frac{c_1^2}{4c_4(1-a)} \tag{7}$$

Eqs.(6) and (7) indicate that values of $a \geq 1$ should not be expected. Both equations are undefined for $a = 1$ and eq.(7) yields a negative c_3 coefficient, which is physically implausible, for $a > 1$.
According to Di Prima et al. (2019), an estimate of t_{crit} can be obtained with the empirical criterion by Bagarello et al. (1999). If it is possible to presume that steadiness was reached before the end of the run, a linear regression analysis is carried out on the last three data pairs (I, t). In this case, t_{crit} is the first experimental t value, starting from the beginning of the experiment, for which the following criterion (Bagarello et al., 1999) applies:

$$\hat{E} = \left|\frac{I(t) - I_{reg}(t)}{I(t)}\right| \times 100 \leq E \tag{8}$$

where $I_{reg}(t)$ is estimated from the linear regression analysis for the last three data points at steady-state and E (%) defines a threshold for error ($E = 2\%$ according to Bagarello et al., 1999). Steady-state conditions exist for $t > t_{crit}$ (i.e., when $\hat{E} \leq 2$). Transient infiltration conditions occur from $t = 0$ until $t = t_{crit}$ (i.e., when $\hat{E} > 2$).

5.1.3. Materials and methods

Three Sicilian soils were chosen for this investigation. Two loam soils (AR and OR sites) were located at the Department of Agricultural, Food and Forest Sciences of the Palermo University (Italy). A silty-clay soil (RO site) was located near Roccamena, approximately 70 km south of Palermo. The AR soil supported a citrus orchard under no tillage. The OR soil was tilled approximately six months

before performing the infiltration runs and a spontaneous herbaceous vegetation cover was present at the time of the experiment. The RO soil supported a fruit orchard under no tillage. Soil at the AR site was sampled on five different dates (November 2017, April, May and September 2018, April 2019) to encompass a range of environmental conditions. Soil was sampled only once at the other two sites (OR: January 2018; RO: June 2019). The same experimental protocol was applied for each of the overall seven sampling campaigns.

A total of 10 infiltration runs were carried out at randomly selected locations during each sampling campaign. To conduct an infiltration run, a bare area of approximately 150 m^2 was selected and the sampled soil surface was gently leveled and smoothed by manual implements. Small diameter (0.08 m) rings were inserted on the soil surface to a depth of 0.01 m following the beerkan infiltration procedure (Lassabatere et al., 2006; Di Prima et al., 2019). Ring insertion was conducted manually, if necessary by gently using a rubber hammer, while ensuring that the upper rim of the ring remained horizontal during insertion. Then, 30 water volumes, each of 57 mL, were successively poured onto the confined infiltration surface over a period of ~3 s. A relatively large number of water volumes was used to attain quasi-steady state conditions. For each water volume, the infiltration time was measured from water application to disappearance of all water, when the subsequent water volume was poured on the infiltration surface. Water was applied at a small distance from the infiltration surface, i.e. approximately at a height, h_w, of 0.03 m, with the practitioner's fingers used to dissipate the kinetic energy of the falling water and thereby minimize soil disturbance due to water application. After the infiltration test, two undisturbed soil cores (0.05 m in height by 0.05 m in diameter) were collected nearby at 0 to 0.05 m and 0.05 to 0.10 m depths. These cores were used to determine the dry soil bulk density, ρ_b, and the antecedent soil water content, θ_i. The data were averaged over the two depths and paired with the corresponding infiltration run (**Table 5.1.1**).

Table 5.1.1 Mean and coefficient of variation, *CV*, of the soil water content, θ_i, and the dry soil bulk density, ρ_b, at the beginning of the infiltration run (sample size, $N = 10$ for each summarized dataset)

Site	Date	θ_i (m^3/m^3)		ρ_b (g/cm^3)	
		mean	CV (%)	mean	CV (%)
AR	November 2017	0.215	6.5	0.966	6.0
	April 2018	0.199	15.3	0.957	11.1
	May 2018	0.137	12.0	0.979	7.9
	September 2018	0.103	11.8	1.037	6.9
	April 2019	0.158	21.8	1.064	5.5
OR	January 2018	0.251	11.4	1.138	12.0
RO	June 2019	0.184	16.1	0.998	7.1

For each infiltration run, I was plotted against t and t_{crit} was estimated using eq.(8). Eq.(3a) was then fitted to the transient portion of the run to estimate c_1 and c_2 by using the cumulative infiltration fitting method (Vandervaere et al., 2000). Following Lassabatere et al. (2006), the quality of the fit was evaluated by calculating the relative error, Er (%):

$$Er = 100\sqrt{\frac{\sum_{i=1}^{k}\left(I_i^{\exp} - I_i\right)^2}{\sum_{i=1}^{k}\left(I_i^{\exp}\right)^2}} \quad (9)$$

where $I_i^{\exp}$ and I_i are the experimental and modeled cumulative infiltrations, respectively, and k is the number of experimental data pairs. Linear regression analysis of the $I(t)$ data was used to estimate the c_3 and c_4 coefficients of eq.(3b) by only considering the steady-state portion of the run. Finally, a was calculated by eq.(5). A run was considered successful when all coefficients (c_1, c_2, c_3 and c_4) were positive since, according to eq.(1), they cannot be negative or null.
An attempt was made to verify the possible existence of a link between the shape of the experimentally determined infiltration curve and the results of the a calculations. At this aim, the empirical Horton (1940) infiltration model was fitted to the data:

$$I = i_f t + \frac{i_0 - i_f}{k}\left(1 - e^{-kt}\right) \quad (10)$$

where i_0 (L T^{-1}) is the initial infiltration rate (t = 0), i_f (L T^{-1}) is the final infiltration rate and the constant k (T^{-1}) determines the rate at which i_0 approaches i_f.
This model was chosen since it describes in some detail the infiltration curve, making use of three parameters, and also because it was found to give a good representation of the experimentally determined $I(t)$ relationships in other investigations (Shukla et al., 2003).

5.1.4. Results

The average duration of the 70 infiltration tests was of 1.06 h (CV = 109.0%). The mean t_{crit} value was equal to 0.61 h (CV = 105.4%) and the critical time increased with the duration of the run (**Figure. 1a**). Taking into account that a common water volume was used for each infiltration run, this result supported the reliability of the developed analysis since equilibration times are expected to be longer when infiltration proceeds more slowly (Reynolds et al., 2002).
The runs were successful (positive infiltration parameters) in 44 out of 70 cases (63% of the total, with a mean duration of 0.96 h and a mean t_{crit} of 0.58 h) and unsuccessful in 26 cases (37%, mean duration = 1.23 h, mean t_{crit} = 0.67 h). In particular, all experiments carried out at the OR site failed. Reasons of failure included obtaining c_1 = 0 (9 cases), c_1 = 0 and c_3 < 0 (4 cases), and c_2 = 0 (13 cases). The c_2 = 0 result was associated with basically high c_1 values (> 170 mm/$h^{0.5}$), that are indicative of a high sorptivity (**Figure. 5.1.1b**). On the other hand, c_1 = 0 was associated with basically high c_2 values (> 700 mm/h), that indicate high saturated conductivity.
Figure. 5.1.2 shows an example of the cumulative infiltration curve for each reason of failure. In short, runs failed when i) I was soon nearly linear with t (lack or very short duration of an initial transient phase, **Figure. 5.1.2a**) (Angulo-Jaramillo et al., 2019), ii) the infiltration rates increased with time, as expected in water repellent soil conditions (**Figure. 5.1.2b**) (Lassabatere et al., 2010; Alagna et al., 2019), and iii) concavity was or appeared to be particularly pronounced (Di Prima et al., 2018) (**Figure. 5.1.2c**).

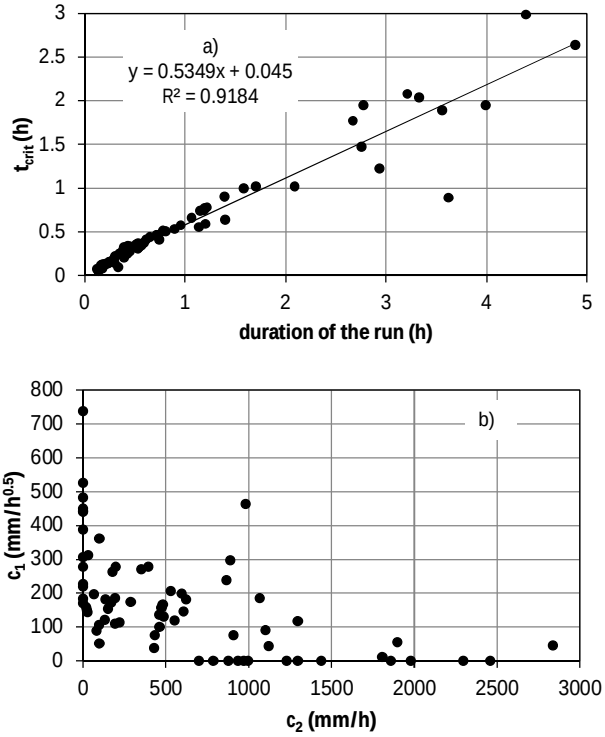

Figure 5.1.1 Relationship between the estimated t_{crit} time and total duration of the field run (a) and scatter plot of the c_1 vs. c_2 coefficients (b) (sample size, N = 70)

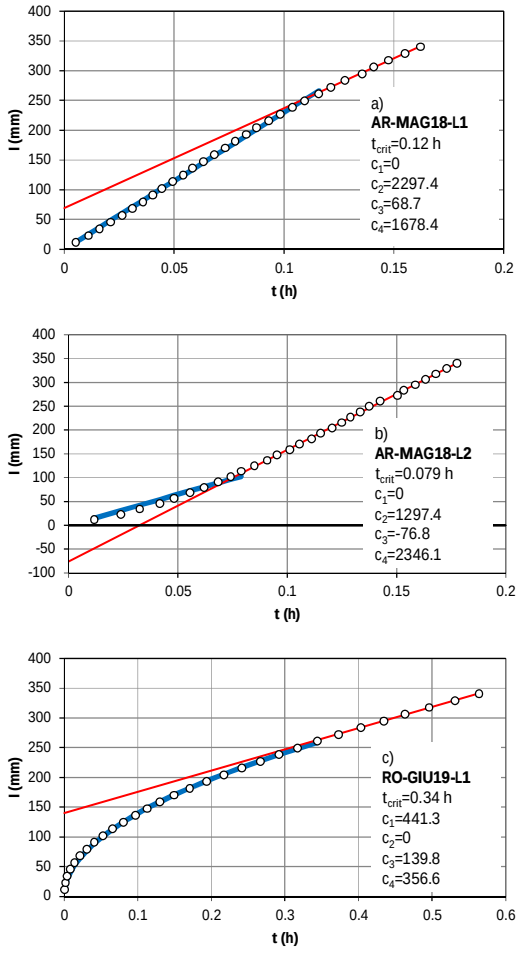

Figure 5.1.2 Examples of unsuccessful runs: a) $c_1 = 0$; b) $c_1 = 0$ and $c_3 < 0$; and c) $c_2 = 0$. Blue lines indicate the fitting of the transient model to the data and red lines indicate the adaption of the steady-state model to the data

For the 44 runs yielding positive *a* results, the relative error of the transient infiltration model, *Er*, was ≤ 6.1% and, on average, it was equal to 2.2%. In addition, *Er* did not exceed 3.5%, denoting a good fit of the model to the data (Lassabatere et al., 2006), in the 86.4% of the cases. For these 44 runs, the estimates of *I* calculated for $t = t_{crit}$ with the transient (eq.3a) and the steady-state (eq.3b) models compared favorably one with the other, since the percentage differences between two corresponding values of *I* varied from -4.4% to 2.9%, depending on the run (**Figure. 5.1.3**).

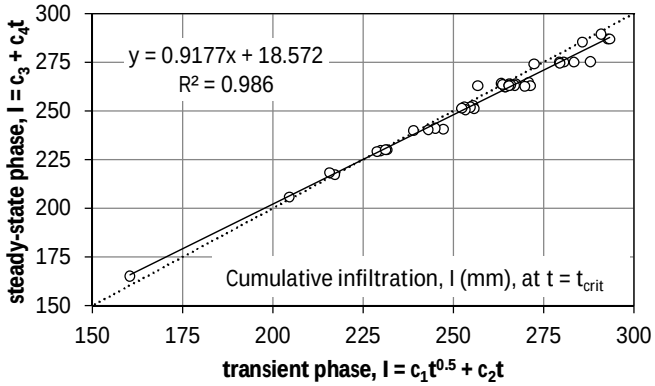

Figure 5.1.3 Comparison between cumulative infiltration calculated at the transition time $I(t_{crit})$ by eq.(3a) (transient phase) and eq. (3b) (steady-state phase) for the 44 field experiment yielding positive *a* estimates

The valid infiltration runs yielded *a* values varying from 0.239 (**Figure. 5.1.4a**) to 1.364 (**Figure. 5.1.4b**). **Figures. 5.1.4c** and **5.1.4d** show runs yielding an *a* value close to those suggested by Stewart and Abou Najm (2018a) and Wu and Pan (1997), respectively.

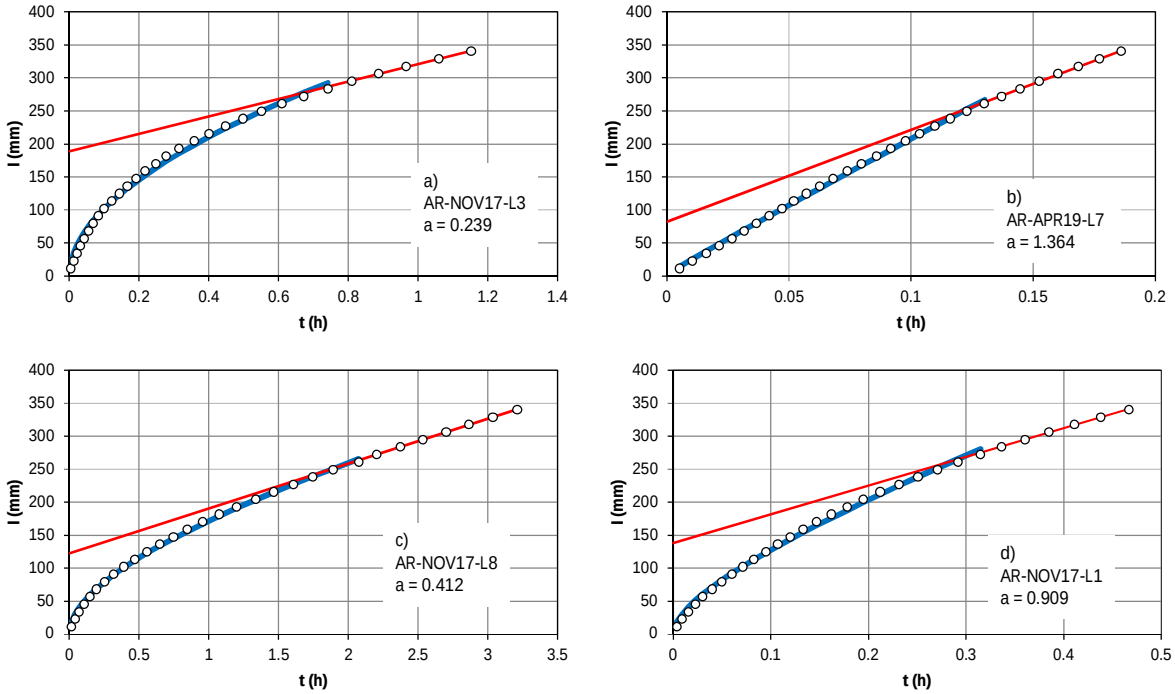

Figure 5.1.4 Successful runs yielding a) the lowest *a* value; b) the highest *a* value; c) an *a* value close to that suggested by Stewart and Abou Najm (2018a); and d) an *a* value close to that suggested by Wu and Pan (1997). Blue lines indicate the fitting of the transient model to the data and red lines indicate the adaption of the steady-state model to the data

According to the Lilliefors (1967) test at $P = 0.05$, the hypothesis that the positive *a* values were normally distributed was not rejected and, consequently, the results were summarized by the mean

and the associated *CV*. The average value of the *a* constant (*a* = 0.933) was closer to the suggested value by Wu and Pan (1997) than that by Stewart and Abou Najm (2018a). The *CV* of the individual estimates of *a* (30.7%) was much lower than the *CV*s of c_2 and c_4 (105.2% and 91.8%, respectively). A rather high percentage of calculated *a* values were implausible according to eq.(7) since the 45.5% of the individual values were greater than one. Excluding these values from the analysis yielded a mean value of *a* of 0.735 and an associated *CV* of 32.3% (*N* = 24).

Therefore, according to this field investigation, *a* was intermediate between the suggested values in the literature (*a* = 0.91 and 0.45). However, the field experiment was successful with respect to the estimation of *a* in a limited number of cases, that is for only the 34.3% of the infiltration runs that were overall carried out.

The Horton model was successfully fitted to the data for 62 out of the 70 infiltration experiments, and all failures occurred at the AR site. The *Er* values varied from 0.41 to 5.60% (**Figure. 5.1.5**) and they were lowest at the AR site and highest at the OR site (**Table 5.1.2**). The *k* constant, expressing the rate at which i_0 approaches i_f (Tindall et al., 1999), varied between 0.09 and 70 h^{-1}. Regardless of the considered central tendency index (mean, median), this rate was greater at the OR and RO sites than at the AR site.

For the 44 infiltration runs yielding an estimate of the *a* constant, a scattered but rather clear relationship was detected between *a* and k/i_f (R^2 = 0.659), representing a normalized *k* constant (**Figure. 5.1.6**), while appreciably lower R^2 values ($\leq$ 0.298) were obtained with other parameters of the Horton model or with combinations among them (i_0, i_f, k, i_0-i_f, (i_0-i_f)/k). For these runs, the k/i_f ratio varied between 0.011 and 0.067 mm^{-1}. For the 26 cases in which estimation of *a* failed, the Horton model was not applicable (eight runs) or k/i_f was either greater than 0.67 mm^{-1} (14 runs) or smaller than 0.011 mm^{-1} (three runs). In a single case, an estimate of *a* was not obtained even if k/i_f was in the range 0.011-0.067 mm^{-1} (in particular, equal to 0.025 mm^{-1}).

Table 5.1.2 Summary statistics of the initial infiltration rate, i_0, final infiltration rate, i_f, and the constant *k* of the Horton infiltration model for each sampled site

Site	Statistic	i_0 (mm h^{-1})	i_f (mm h^{-1})	*k* (h^{-1})	Er (%)
AR (N=42)	Min	200.1	9.53	0.093	0.41
	Max	4675.1	1370.2	67.1	4.10
	Mean	1470.0	320.7	8.05	1.29
	Median	1300.0	150.8	3.90	0.99
	CV (%)	62.4	89.6	152.0	61.1
OR (N=10)	Min	1176.7	42.4	6.55	2.88
	Max	7985.0	219.6	44.6	5.60
	Mean	3595.2	93.5	20.6	4.60
	Median	2984.2	64.8	17.6	4.83
	CV (%)	64.8	62.1	59.9	22.8
RO (N=10)	Min	416.1	131.0	3.69	1.55
	Max	11243.0	716.1	70.1	4.46
	Mean	2734.2	328.6	19.9	2.89
	Median	890.3	247.5	6.73	2.45
	CV (%)	125.7	55.9	110.7	34.8

N = sample size, *Min* = minimum value, *Max* = maximum value, *CV* = coefficient of variation

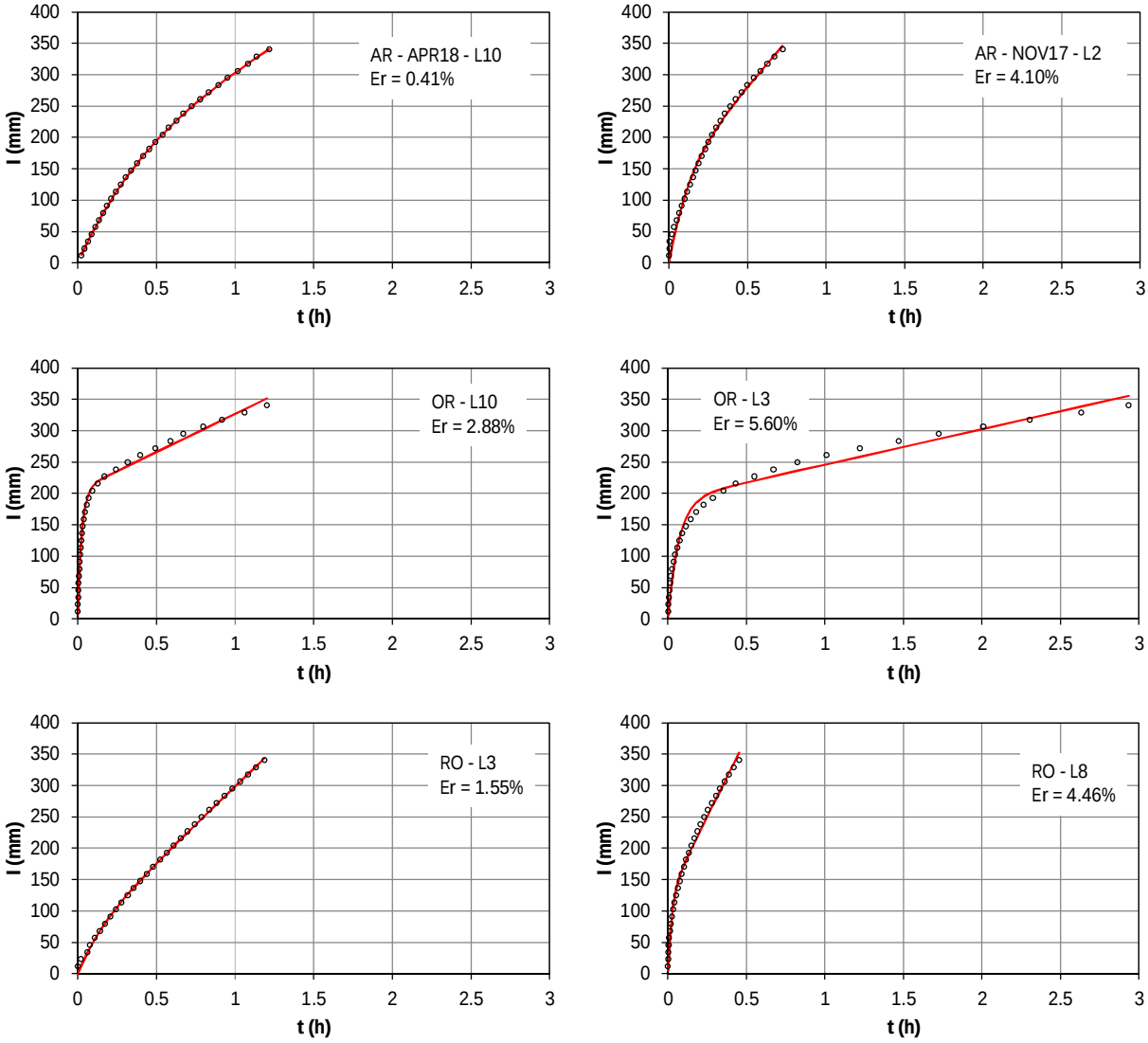

Figure 5.1.5 Best and poorest fitting of the Horton model (continuous line) to the cumulative infiltration, *I*, vs. time, *t*, data (white dots) for each sampled site

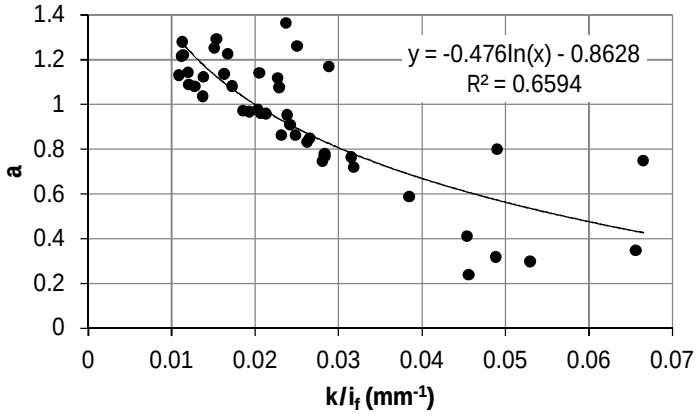

Figure 5.1.6 Relationship between the estimated *a* parameter and the normalized *k* constant of the Horton infiltration model

Therefore, the normalized *k* constant explained both variability of *a* and the success or the failure of the experiment. According to the fitted relationship of **Figure. 5.1.6**, obtaining $a < 1$ requires a normalized *k* constant of more than 0.02 mm^{-1}.

5.1.5. Conclusions

In conclusion, a does not need to be fixed a priori but it can be estimated by the infiltration run. The number of successful runs, that is yielding a physically valid estimate of this constant, seems to be a reduced percentage of the total runs performed in the field for two reasons: i) an estimate of a cannot be obtained; or ii) an estimate of a is obtained but it has to be rejected as it is not in accordance with theory ($a \geq 1$).

With reference to the physically plausible estimations of a, this constant settles around 0.735, that is an approximately intermediate value between the two currently available suggestions (0.91 and 0.45). The experimental value of a could be used to identify the cases in which the new infiltration model is applicable (positive values smaller than one). The shape of the infiltration curve controls the success of the experiment with reference to estimation of a.

5.2: Monitoring saturated hydraulic conductivity of a loam soil by different application methodologies of a beerkan infiltration run

5.2.1. Introduction

The investigation described in this section represents an extension of the work carried out by Auteri et al. (2020), already introduced in this PhD thesis. In particular, Auteri et al. (2020) only considered the April 2019 sampling campaign, but a soil monitoring program with the same experimental protocol as that applied by Auteri et al. (2020) started on November 2017 on the basis of two different premises.

The first premise was that the soil hydrodynamic properties, depending on soil structure, can vary also appreciably with time (e.g, Prieksat et al., 1994) and a temporal variability of the saturated soil hydraulic conductivity, K_s, determined in the field with single-ring infiltration methods was previously detected at the same field site sampled in this investigation (Bagarello and Sgroi, 2007; Alagna et al., 2016).

The other premise was that the low-high methodology developed by Bagarello et al. (2014) was found to be able to signal the impact of the initial soil water content on the K_s values determined with runs with different soil perturbing effects (Alagna et al., 2016). In particular, soil alteration due to a high run was found to be greater when the initial soil water content was low. However, this information was obtained with reference to only three sampling dates and also with a simpler methodology than the one subsequently applied in other investigations. In particular, Alagna et al. (2016) only used 15 water volumes for each type of run.

It was therefore thought that it would have made sense exploring the temporal variability of the K_s values determined with different application methodologies of a beerkan run, also in the perspective to possibly support the conclusions by Alagna et al. (2016). Consequently, starting on November 2017, campaigns of measurements were realized at different dates. All experiments were carried out by performing longer runs than those performed by Alagna et al. (2016), that is using more water to better follow possible soil deterioration processes associated with a perturbing run.

A total of five sampling campaigns were performed in the period November 2017 – April 2019. The monitoring program is still active but the data collected until now were subjected to a first analysis, that is the one reported here, also with the objective to verify if methodological changes or adaptions are advisable in the perspective to develop a dataset that contains the largest possible amount of information and hence to make interpretation of the results easier and more robust.

The general objective of this investigation was the same as that by Auteri et al. (2020), that is to verify if performing a beerkan infiltration run with more water than that corresponding to the standard experimental protocol could be justified in the perspective to obtain realistic soil data for simulation of hydrological processes. A loam soil was sampled by L and H runs using a relatively large number of water volumes on different occasions to i) verify water volume and water pouring height effects on the established infiltration process; ii) explore if soil deterioration changes with the sampling date,

that is under different antecedent soil water content and perhaps also soil bulk density conditions; iii) compare the saturated soil hydraulic conductivity values obtained with infiltration runs differing by both the number of poured water volumes and the height of water application; iv) verify the effect of the applied experimental methodology on the detected temporal variability of K_s; and v) establish if the K_s data can be explained by the gravitational potential energy of the water used for the infiltration experiment.

5.2.2. Materials and methods

Field site

The study was performed at the Agricultural, Food and Forest Sciences Department of the University of Palermo (Italy), in a citrus orchard under conventional tillage with trees spaced 4 m × 4 m apart (coordinates 33S 355511E 4218990N). The soil at the field site (Typic Rhodoxeralf) has a relatively high gravel content and it is mostly sandy-loam or loam down to a depth of at least 0.30 m (Bagarello and Provenzano, 1996; Bagarello, 1997; Bagarello et al., 2014; Concialdi et al., 2020). This investigation was performed on an area of approximately 200 m^2, in which the soil had mainly a loam texture, according to the USDA classification system (clay = 15.4%, silt = 36.2%, sand = 48.4%), and a soil organic carbon content equal to 3.1% (Auteri et al., 2020). The soil structural stability index calculated according to Pieri (1992) was equal to 10.5%, suggesting a stable structure (Reynolds et al., 2009). The soil surface was gently leveled and smoothed by manual implements before sampling. To sample a bare area, the superficial herbaceous vegetation was cut with a knife when it was present, while the roots remained in situ.

Experimental field methods

Small diameter (D = 0.08 m) rings were inserted on the soil surface to a depth of 0.01 m for the beerkan infiltration runs (Lassabatere et al., 2006). Ring insertion was conducted manually or by gently using a rubber hammer and ensuring that the upper rim of the ring remained horizontal during insertion. The rings were particularly small to more clearly detect possible effects of soil disturbance due to water application.

On a given sampling date, a total of 20 infiltration runs were carried out at randomly selected locations. For each run, 30 water volumes, each of 57 mL, were successively poured in approximately 3 s on the confined infiltration surface. For each water volume (1^{st}, 2^{nd}, …, 30^{th}), the infiltration time was measured from water application to disappearance of all water, when the subsequent water volume was poured on the infiltration surface. Despite other choices could have been made to establish when adding a new volume of water (Smith, 1999), waiting for complete disappearance of water from the infiltration surface was preferred to reduce operator's subjectivity when the infiltration surface was disturbed as a consequence of repeated, soil perturbing water applications. Ten runs were carried out by applying water at a small distance from the infiltration surface, i.e. approximately at a height, h_w, of 0.03 m. Water energy was dissipated on the fingers of the hand in an attempt to minimize soil disturbance due to water application (low, L, runs). Water was applied from h_w = 1.5 m at the other 10 sampling points (high, H, runs). The soil surface was not shielded in this case to maximize possible disruptive effects of water impact. To ensure flow verticality and prevent wind effects, the device developed by Bagarello et al. (2014) and Alagna et al. (2016) was used. Only nine H runs were performed on September 2018 due to the adverse meteorological conditions during this field campaign.

At least one L and one H run were carried out on a given day at a distance of no more than 1.5-2.0 m from each other. In an intermediate position between the two sampling points for infiltration, two undisturbed soil cores (0.05 m in height by 0.05 m in diameter) were collected at the 0 to 0.05 m and 0.05 to 0.10 m depths, in accordance with other investigations (e.g., Lassabatere et al., 2019). These cores were used to determine the dry soil bulk density, ρ_b, and the antecedent volumetric soil water

content, θ_i. The soil porosity, *f*, was calculated from ρ_b assuming a soil particle density of 2.65 g/cm^3. According to other investigations, the field saturated soil water content, θ_s, was assumed to coincide with *f* (Mubarak et al., 2009; Bagarello et al., 2011; Angulo-Jaramillo et al., 2016, 2019). The data were averaged over the two depths and they were associated with the couple of L and H runs performed in the vicinity of the soil sampling location. A nearly uniform vertical profile of θ_i was assumed because the soil was not irrigated and no rainfall occurred for several weeks before sampling. The experiment was repeated on five different dates during a 18 months period (November 2017, April, May and September 2018, April 2019) to encompass how environmental conditions and hence of antecedent soil water content.

Calculations and data analysis

Infiltration data were plotted on cumulative infiltration, *I* (L), vs. time, *t* (T), and infiltration rate, i_r (L/T), vs. *I* plots to take an initial look at the general response of the two types of experiments (L and H) for each sampling date. The i_r vs. *I* plot was used since durations changed from run to run, making presentation of all data on a single i_r vs. *t* plot confuse. For each campaign, the mean infiltration time of each applied water volume (1st, 2nd, …, 30th) was calculated for both the low, Δt_L (T), and the high, Δt_H (T), runs. The $\Delta t_H/\Delta t_L$ ratio was then plotted against the number of the applied water volumes, n_v, to detect the effect of the height of water pouring on infiltration.

For each run, the BEST-steady algorithm (Bagarello et al., 2014) was applied to calculate saturated soil hydraulic conductivity, K_s (L/T), from the experimentally determined intercept, b_s (L), and slope, i_s (L/T), of the straight line fitted to the data describing steady-state conditions on the *I* vs. *t* plot. BEST-steady was preferred over BEST-slope (Lassabatere et al., 2006) and BEST-intercept (Yilmaz et al., 2010) because it was the only algorithm that, in another investigation, allowed a successful treatment of runs involving soil alteration and led to K_s values close to those obtained by rainfall simulation (Di Prima et al., 2018).

Two K_s values were determined for each infiltration run (L and H). In particular, an estimate of this parameter was obtained by considering a run with 15 water volumes, that represents the standard number of water volumes for a beerkan experiment and was used in previous investigations on height effects (Lassabatere et al., 2006; Bagarello et al., 2014; Alagna et al., 2016). Another estimate of K_s was obtained for a run with 30 water volumes, that is using the complete experimental information. Consequently, four different experimental methodologies were considered to calculate K_s: 15L (15 water volumes and low, L, height of water pouring), 30L (30 water volumes, L runs), 15H (15 water volumes and high, H, height of water pouring) and 30H (30 water volumes, H runs). The 15L methodology represents the standard beerkan infiltration experiment according to Lassabatere et al. (2006). The 30L methodology was expected to be perhaps more reliable with respect to attainment of steady-state infiltration rates. The 15H methodology was the most soil perturbing methodology in previous investigations on height effects (Bagarello et al., 2014; Alagna et al., 2016). The 30H methodology had the most perturbing character in this investigation.

For each experimental methodology, the gravitational potential energy, E_p (J/m^2), of the water used for the infiltration run was calculated taking into account that both the mass of water and the height of fall were known (Auteri et al., 2020).

Each dataset was summarized by calculating the mean, *M*, and the associated coefficient of variation, *CV*. The arithmetic mean and the associated *CV* were calculated for ρ_b and θ_i. For K_s, the statistical frequency distribution of the data was preliminarily checked with the Lilliefors (1967) test by considering both a normal and a ln-normal distribution. Ln-normally distributed data were summarized by the geometric mean and the associated *CV* (Lee et al., 1985).

For each sampling date, comparisons were established between different experimental methodologies. In particular, differences in K_s between the least (15L) and the most (30H) soil altering experiments were checked. The dependence of these differences on the two experimental factors that were allowed to vary was then determined by comparing the 15L and 30L (water volume) and the 30L and 30H (height of pouring) methodologies.

A comparison was also established for each experimental methodology (15L, 30L, 15H, 30H) among the different sampling dates.
The infiltration data corresponding to the 15L scenario were also analysed by the so-called method 1 by Wu et al. (1999) and a comparison with the BEST-steady calculations of K_s was carried out. This comparison was made because method 1 does not require attainment of steady-state conditions (Stewart and Najm, 2018). Therefore, stabilization of the late phase of the 15L run was considered plausible if the K_s dataset developed with BEST-steady on the basis of this assumption compared favorably with the K_s dataset obtained without making any hypothesis on flow steadiness. Only the 15L scenario was considered for this check since the uncertainties about attainment of steady-state infiltration rates were highest in this case.
The relationship between the mean values of K_s obtained with the four experimental methodologies and E_p was then tested to verify if the gravitational potential energy of the water used for the infiltration experiment explained changes in the saturated soil hydraulic conductivity. Exponential, linear, logarithmic and power relationships were considered and the relationship having the highest coefficient of determination, R^2, was retained for further analysis.
Two-tailed t tests were carried out to compare two datasets while the Tukey Honestly Significant Difference (THSD) test was used to compare more than two datasets (Daniel, 1996). Ln-transformed values were considered when the data were found to be ln-normally distributed. A two-tailed t test was also used to establish the statistical significance of the fitted regression line to the data (Glantz, 2012). All test were carried out at $P = 0.05$.

5.2.3. Results and discussion

Soil water content and dry soil bulk density
During the study period, the mean soil water content at the beginning of a beerkan infiltration campaign, θ_i, varied by approximately two times, that is between 0.103 and 0.215 m^3/m^3 (**Table 5.2.1**).
The mean θ_i values at each date differed according to the sequence NOV17 = APR18 > APR19 = MAY18 > SEP18.
In general, the soil was wettest in the autumn season and driest at the end of summer.
Both wet and intermediate soil water conditions were detected in the spring months.
The dry bulk density varied between 0.97 and 1.06 g/cm^3 and the mean ρ_b value at each date differed according to the sequence APR19 $\geq$ SEP18 = MAY18 $\geq$ NOV17 = APR18 (**Table 5.2.1**).
Therefore, the bulk density was lower in the early stages (first sampling dates) than in the later stages of the experiment.
A temporally increasing dry soil bulk density was detected in another zone of the same orchard, with mainly a sandy-loam soil, by Bagarello and Sgroi (2007).
The low values of ρ_b were probably indicative, at least in part, of a large presence of macropores formed by earthworms that were frequently observed, but they could also be expressive of the fact that collecting undisturbed soil cores was not always easy due to the widespread presence of gravel and stones at the field site (Bagarello and David, 2020).

Infiltration experiments
With reference to the classical protocol for a beerkan run, that is a low height of water application, using 30 volumes of water (cumulative infiltration, $I = 340.2$ mm) instead of 15 volumes ($I = 170.1$ mm) determined longer infiltration times by 2.2 to 3.8 times, depending on the sampling date (**Table 5.2.2**).

Table 5.2.1 Statistics of the initial volumetric soil water content, θ_i, dry soil bulk density, ρ_b, and saturated soil hydraulic conductivity, K_s, obtained with different experimental methods in the five sampling dates

Variable	Statistic	November 2017	April 2018	May 2018	September 2018	April 2019
θ_i (m^3/m^3)	N	10	10	10	10	10
	Min	0.191	0.161	0.099	0.082	0.119
	Max	0.236	0.258	0.161	0.118	0.238
	Mean	0.215 a	0.199 a	0.137 b	0.103 c	0.158 b
	CV (%)	6.5	15.3	12.0	11.8	21.8
ρ_b (g/cm^3)	N	10	10	10	10	10
	Min	0.881	0.804	0.849	0.943	0.970
	Max	1.056	1.172	1.116	1.157	1.193
	Mean	0.966 a	0.957 a	0.979 ab	1.037 ab	1.064 b
	CV (%)	6.0	11.1	7.9	6.9	5.5
$K_{s,15L}$ (mm/h)	N	10	10	7	7	7
	Min	19.0	11.7	169.5	195.0	87.0
	Max	545.3	531.4	2182.1	2087.5	1003.2
	Mean	94.6 a	105.1 a	601.6 b	553.2 b	293.8 ab
	CV (%)	129.3	209.8	133.8	95.6	107.6
$K_{s,30L}$ (mm/h)	N	10	10	7	7	7
	Min	6.4	4.0	65.7	52.6	21.2
	Max	60.0	115.4	1637.0	671.1	181.4
	Mean	16.4 a	29.9 ac	173.4 b	181.8 b	83.8 bc
	CV (%)	95.9	171.0	167.3	117.2	88.9
$K_{s,15H}$ (mm/h)	N	9	10	8	8	9
	Min	10.6	4.4	9.1	26.0	12.1
	Max	72.1	270.9	466.7	587.1	112.1
	Mean	22.1 a	29.9 a	49.2 a	69.6 a	31.0 a
	CV (%)	88.1	181.2	240.2	169.2	95.4
$K_{s,30H}$ (mm/h)	N	9	10	8	8	9
	Min	3.7	3.3	4.7	5.3	2.5
	Max	55.8	23.4	65.0	22.3	17.9
	Mean	7.7 a	10.9 a	12.4 a	8.8 a	6.3 a
	CV (%)	114.9	60.8	105.6	53.2	67.6

$K_{s,15L}$: 15 water volumes and low runs; $K_{s,30L}$: 30 water volumes and low runs; $K_{s,15H}$: 15 water volumes and high runs; $K_{s,30H}$: 30 water volumes and high runs. *N* = sample size; *Min* = minimum value; *Max* = maximum value; Mean = arithmetic mean for θ_i and ρ_b and geometric mean for K_s; *CV* = coefficient of variation. Values in a row followed by the same lowercase letter are not significantly different according to the Tukey Honestly Significant Difference test at $P = 0.05$

Table 5.2.2 Statistics of the duration (h) of the infiltration process for each experimental methodology in the five sampling dates

Methodology	Statistic	November 2017	April 2018	May 2018	September 2018	April 2019
L15	N	10	10	10	10	10
	Mean	0.345	0.452	0.143	0.166	0.155
	CV (%)	84.0	89.9	36.5	48.8	51.8
L30	N	10	10	10	10	10
	Mean	1.27	1.37	0.325	0.383	0.368
	CV (%)	79.2	97.7	44.7	54.3	59.9
H15	N	10	10	10	9	10
	Mean	0.717	0.996	0.484	0.278	0.587
	CV (%)	60.5	77.5	66.0	41.7	49.8
H30	N	10	10	10	9	10
	Mean	2.54	3.16	1.75	1.62	2.34
	CV (%)	55.2	62.6	60.0	49.2	41.7

L15: 15 water volumes and low runs; L30: 30 water volumes and low runs; H15: 15 water volumes and high runs; H30: 30 water volumes and high runs. *N* = sample size; Mean = arithmetic mean; *CV* = coefficient of variation

The smallest d30/d15 (d30 and d15 = duration of the run with 30 and 15 volumes of water, respectively) values were detected in MAY18, SEP18 and APR19 (2.2 < d30/d15 < 2.4) while the highest ratios were observed for the NOV17 and APR18 campaigns (2.8 < d30/d15 < 3.8). Obtaining d30/d15 ratios greater than two was plausible since the initial stage of an infiltration process into an initially unsaturated soil is typically faster than the later stage (e.g., Elrick and Reynolds, 1992). To be clearer, a value of d30 exactly twice that of d15 can only occur if the mean infiltration rate does not change between the early (first 170.1 mm of infiltration) and the later stage (subsequent 170.1 mm) of the run. This equality presupposes that the infiltration process has a steady-state character from the beginning of the experiment (lack of the initial transient phase with decreasing infiltration rates) and also that the soil does not experience any deterioration as water application continues.
On NOV17, the mean d30/d15 values were similar between the L and H runs (3.8 and 3.9, respectively). In all the other cases, d30/d15 was higher for the H runs (> 3.5, depending on the campaign) than the L runs (< 2.8). The H experiment with 15 water volumes was 1.7-3.8 times (mean = 2.6) longer than the corresponding L experiment, depending on the sampling date. With 30 volumes, a H run determined a 2.0-6.3 times (mean = 4.1) longer process than an L run. Therefore, this initial check suggested that a high height of water pouring slowed down infiltration. This slowdown was perceivable with a relatively small amount of applied water (15 water volumes) but it was more noticeable with more water (30 volumes). Taking into account that the H experiments were expected to have a more soil perturbing character than the L ones, total duration of the run was a synthetic index of water pouring height effects on the infiltration process.
Total infiltration time was also used by Lassabatere et al. (2019) to summarize the general behavior of a set of field infiltration data.
Both the cumulative infiltration (I vs. t) and the infiltration rate (i_r vs. I) curves signaled that the infiltration processes were generally consistent with theory (**Figure 5.2.1**). In particular, the concavity of the I vs. t curves was generally facing downwards and the infiltration
rates decreased during the run. In some cases, however, the I vs. t relationship was nearly linear, indicating a nearly steady-state infiltration process from the beginning of the run, or it yielded some weak sign of a concavity facing upwards, as expected in consequence of some soil hydrophobicity (Lassabatere et al., 2010, Alagna et al., 2019). Infiltration rates were generally greater for the L runs than the H runs.
In general, the mean infiltration time of a fixed water volume increased during the run (Figure 5.2.2). However, with reference to the L runs, two types of response were detected. In particular, Δt appeared to steadily and appreciably increase with the number of the applied water volumes, nv, for the former two campaigns while it increased at an appreciably smaller rate on the last three occasions. The H runs yielded in general greater Δt values than the L runs. On a Δt vs. nv graph, stabilization of the infiltration process is signaled by nearly horizontal data points. A near stabilization of the infiltration rates close to the end of the experiment was perceivable for three of the five sampling campaigns with the L runs (MAY18, SEP18, APR19) and four of the five campaigns with the H runs (APR18, MAY18, SEP18, ,and, with some uncertainty APR19), although with some uncertainty and/or approximation due to the data scattering. Signs of stabilization after applying 15 water volumes were weak or, more frequently, not perceivable. In particular, there was not any sign of a stabilization of the process for the L runs performed on the first two sampling dates and for all the H runs.
The $\Delta t_H/\Delta t_L$ ratio was generally greater than one and it increased, for at least a part of the run, with the number of applied water volumes (**Figure 5.2.3**). In particular, $\Delta t_H/\Delta t_L$ increased only a little with n_w in the first two sampling campaigns and it stabilized around a value of almost 2.0-2.5 after applying approximately ten water volumes.

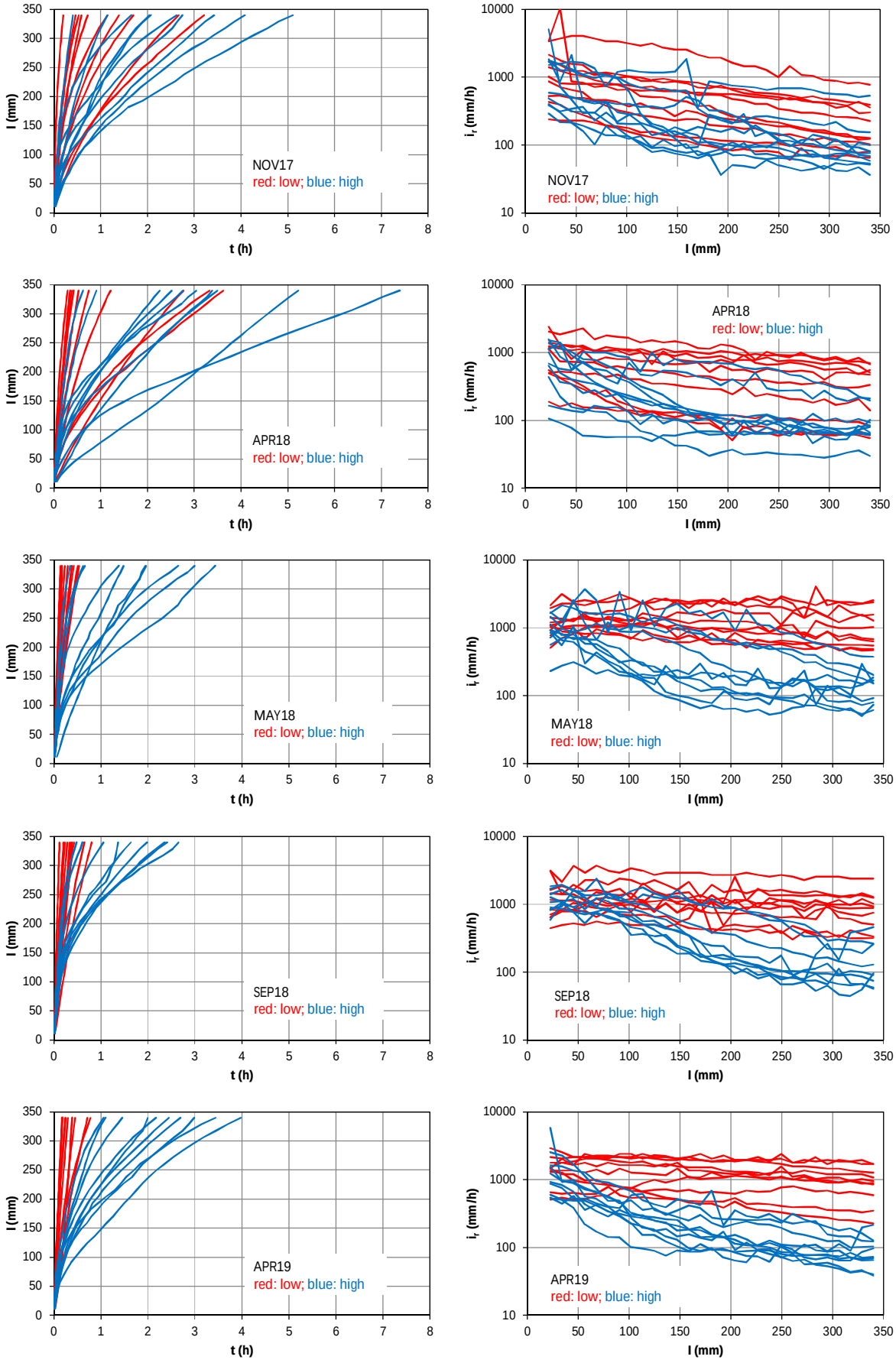

Figure 5.2.1 Cumulative infiltration, I, vs. time, t, and infiltration rates, ir, vs. I for the five sampling campaigns and the two heights of water pouring (sample size, N = 10 for each site and type of run; N = 9 for the H runs on SEP18)

For the MAY18 and APR19 sampling campaigns, $\Delta t_H/\Delta t_L$ increased steadily and it only stabilized in the final part of the run (approximately, last 4 or 5 water volumes) around an appreciably greater value, that is between 7 and 9. For the SEP18 campaign, $\Delta t_H/\Delta t_L$ initially increased slowly with n_v. About halfway through the test, $\Delta t_H/\Delta t_L$ started to increase more appreciably and then it stabilized around a value of approximately 7. A value of $\Delta t_H/\Delta t_L$ greater than one indicates deterioration of the surface soil layer (Bagarello et al., 2014; Alagna et al., 2016; Auteri et al., 2020). According to this investigation, the same soil reacted differently to the disturbance effects associated with a high height of pouring. In particular, the experimental methodology and also the operator did not change among the sampling campaigns but soil disturbance effects were relatively limited on two occasions and more noticeable in the other three cases.
Attempting to interpret this result, it was preliminarily noted that the lowest $\Delta t_H/\Delta t_L$ ratios (**Figure 5.2.3**) were associated with the slowest L runs (largest Δt values in **Figure 5.2.2**).

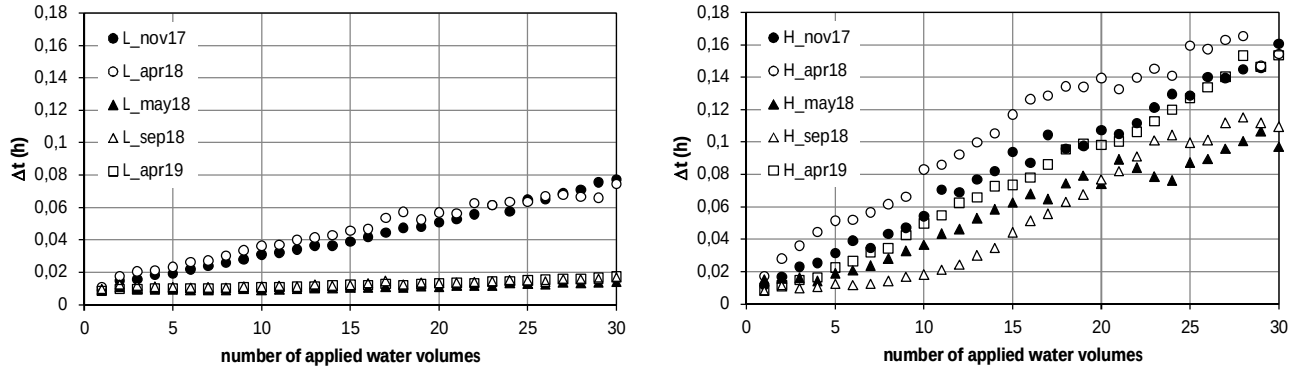

Figure 5.2.2 Mean infiltration time, Δt, of each applied water volume for the two types of runs (low, L, and high, H) at each sampling date (each data point in the graphs is the mean of 9 or 10 individual Δt values)

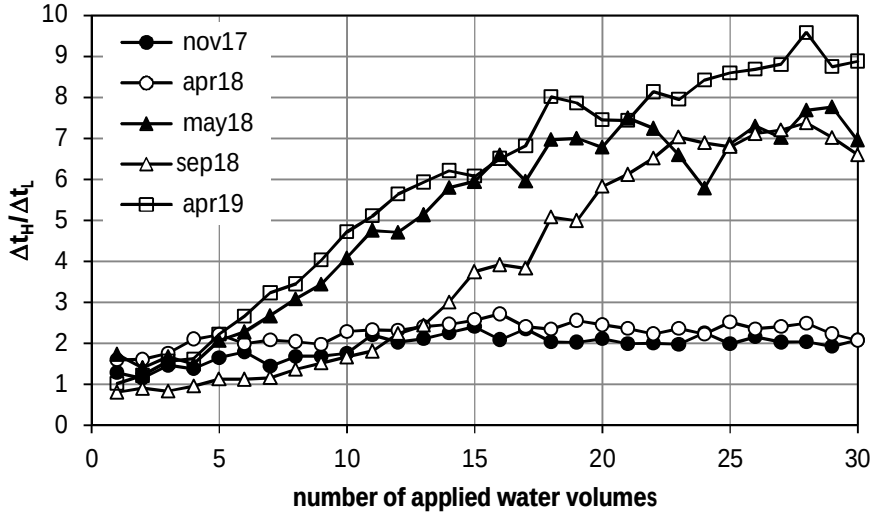

Figure 5.2.3 Ratio between the mean infiltration time for a water application height of 1.5 m (Δt_H) and 0.03 m (Δt_L) during the beerkan runs plotted against the number of the applied volumes of water for the five sampling campaigns

A possible physical interpretation of this circumstance could be that low infiltration rates are typical of soils having an overall limited permeability to water. In this case, there are few opportunities for the H run to determine further slowdowns of the infiltration process. Instead, L runs yielding high infiltration rates denote a permeable porous medium, with a presumably high presence of large pores, that are known to be particularly unstable (Jarvis et al., 2013). In this case, the H run has a more noticeable impact on the established infiltration process since the mechanical solicitation caused by

the impact of water is more effective in altering the macropores. In other terms, it seems that the ΔtH/ΔtL ratios of this investigation were mainly controlled by the denominator. These ratios were relatively small on NOV17 and APR18 because the denominator was high. Instead, they were relatively high on MAY18, SEP19 and APR19 because the denominator was small.

A single sampling campaign does not yield a long-term valid information for a soil of interest since the soil response is temporally variable. However, the experimental methodology used in this investigation appeared appropriate to obtain a complete information on the dynamics of the disturbance processes in different circumstances since ΔtH/ΔtL nearly stabilized by the end of the run in all cases.

Plotting the coefficient of variation, *CV*, of the Δt values measured, for a given water volume (1^{st}, 2^{nd}, … 30^{th}), on the five sampling dates against n_v revealed a different response of the L and the H runs (**Figure 5.2.4**). In particular, the *CV* values stabilized during the later phase of the infiltration process, that is after applying approximately 20 water volumes. However, they initially increased with reference to the L runs. For the H runs, *CV* first increased (four water volumes) and then decreased. The stabilized *CV* values were approximately four times larger for the L runs (nearly 80%) than the H runs (nearly 20%). A lower *CV* value was obtained with the H runs than the L runs starting from the seventh water volume. The increasing relationship between *CV* and n_v for the L runs could be a consequence of the fact that some Δt values did not vary much during the experiment (MAY18, SEP18, APR19) while others increased appreciably with n_v (NOV17, APR18). The generally smaller *CV* values for the H runs was viewed as denoting a homogenization of the soil response, regardless of the sampling date. In other terms, the soil subjected to a mechanical solicitation loses part of its variability and behaves like a basically homogeneous medium.

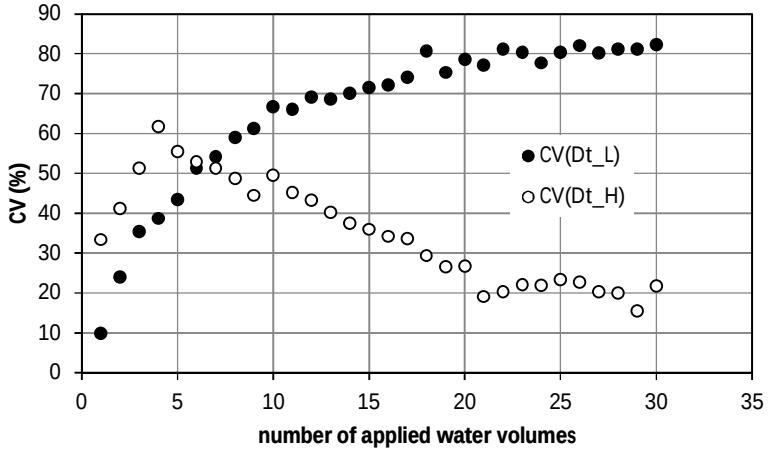

Figure 5.2.4 Coefficient of variation, *CV*, of the infiltration times of a given water volume measured on the five sampling dates with the L and H runs plotted against the number of the applied water volumes

Saturated soil hydraulic conductivity

According to the Lilliefors (1967) test, the hypothesis of a normal distribution of the untransformed K_s data was rejected for three of the 20 tested datasets (**Table 5.2.3**) while it was never rejected with reference to the ln-transformed data. Moreover, the largest difference between the empirical cumulative distribution function and the corresponding theoretical function was generally smaller with reference to these last data. Therefore, Ks was assumed to be ln-normally distributed, and the data were summarized by calculating the geometric mean and the associated coefficient of variation. Valid calculations of Ks were obtained for 7 to ten runs for a given sampling date and an experimental methodology. Invalid calculations occurred as a consequence of a negative estimate of the intercept of the straight line passing through the last three data points for the nearly linear or slightly concave upwards cumulative infiltration curves.

Table 5.2.3 Results of the normality test by Lilliefors (1967) for the saturated soil hydraulic conductivity, K_s, values obtained with the 15L, 30L, 15H and 30H experimental methodologies

Sampling date	L runs		H runs		D_{max}							
	N_s	D_{crit}	N_s	D_{crit}	15L		30L		15H		30H	
					N	LN	N	LN	N	LN	N	LN
November 2017	10	0.258	9	0.271	0.220 NR	0.104 NR	0.191 NR	0.166 NR	0.254 NR	0.166 NR	0.338 R	0.265 NR
April 2018	10	0.258	10	0.258	0.131 NR	0.111 NR	0.151 NR	0.174 NR	0.279 R	0.144 NR	0.157 NR	0.098 NR
May 2018	7	0.300	8	0.285	0.152 NR	0.138 NR	0.290 NR	0.187 NR	0.218 NR	0.106 NR	0.199 NR	0.083 NR
September 2018	7	0.300	8	0.285	0.190 NR	0.141 NR	0.101 NR	0.130 NR	0.289 R	0.160 NR	0.239 NR	0.160 NR
April 2019	7	0.300	9	0.271	0.135 NR	0.116 NR	0.089 NR	0.145 NR	0.192 NR	0.111 NR	0.129 NR	0.071 NR

N_s = sample size. D_{crit} = critical D value at a significance level of 0.05. N = normality test of the non-transformed variable (K_s). LN = normality test of ln(K_s). D_{max} = maximum absolute difference between the sample cumulative distribution function and the cumulative normal distribution function with mean and variance equal to the sample mean and variance, respectively. NR = the normal distribution hypothesis was not rejected. R = the normal distribution hypothesis was rejected. For given sampling date and experimental methodology, the closer distribution to the normal one between the non-transformed and the ln-transformed data is underlined

The individual values of K_s determined in this investigation varied by nearly three orders of magnitude, that is from 2182 to 2.5 mm/h (**Table 5.2.1**). The means of K_s varied with the sampling date and the applied experimental methodology by two orders of magnitude (**Table 5.2.1**). The highest mean value, equal to 602 mm/h, was obtained on MAY18 with the 15L experiment. The lowest value, equal to 6.3 mm/h, was obtained on APR19 with the 30H experiment.
On all sampling dates, the highest and the lowest K_s values were obtained with the experiments that induced the lowest (15L) and the highest (30H) soil disturbance, respectively (**Table 5.2.1**), and all differences between two extreme mean values were statistically significant (**Table 5.2.4**). Therefore, the applied experimental methodology always had a statistically detectable impact on determination of both soil hydrodynamic parameters. The changes of K_s were more noticeable on the last three sampling dates (MAY18, SEP18 and APR19: decrease by 46.5-62.9 times from the 15L to the 30H experiment, **Table 4**) than on the first two sampling dates (NOV17 and APR18: decrease by 9.6-12.3 times). This result confirmed that K_s is a sentinel property since it is highly sensitive to the applied experimental methodology (Reynolds et al., 2000; Auteri et al., 2020).

Table 5.2.4 Statistical difference between the saturated soil hydraulic conductivity values obtained in the five sampling dates with different experimental methodologies and ratio between the two mean values (highest K_s value/lowest K_s value) for given comparison and sampling date

Comparison	November 2017	April 2018	May 2018	September 2018	April 2019
$K_{s,30H}$ vs. $K_{s,15L}$	Smaller 12.3	Smaller 9.64	Smaller 48.4	Smaller 62.9	Smaller 46.5
$K_{s,30L}$ vs. $K_{s,15L}$	Smaller 5.77	Smaller 3.51	Smaller 3.47	Smaller 3.04	Smaller 3.51
$K_{s,30H}$ vs. $K_{s,30L}$	Not different (2.13)	Smaller 2.74	Smaller 13.9	Smaller 20.7	Smaller 13.3

$K_{s,15L}$: 15 water volumes and low runs; $K_{s,30L}$: 30 water volumes and low runs; $K_{s,15H}$: 15 water volumes and high runs; $K_{s,30H}$: 30 water volumes and high runs. Non-paired, two-tailed t test for the $K_{s,30H}$ vs. $K_{s,15L}$ and $K_{s,30H}$ vs. $K_{s,30L}$ comparisons. Paired, two-tailed t test for the $K_{s,30L}$ vs. $K_{s,15L}$ (P = 0.05 in both cases). All comparisons were carried out on the ln-transformed K_s data. The ratio between the highest and the lowest mean K_s values is reported in parenthesis in the case of not statistically significant differences

However, sensitivity of the K_s determination to the applied methodology differed between the sampling dates. In particular, it appeared to be smaller when the soil was initially wet and the saturated conductivity determined with the standard protocol (Lassabatere et al., 2006) was relatively low (**Table 5.2.1**). Given that the soil texture did not vary since the same zone was sampled on each sampling date, smaller K_s values should denote less macropores in the soil. This circumstance could then suggest that, on the first two sampling dates, there were less opportunities to modify the soil pore arrangement as compared with the latter three sampling dates, in which the K_s values determined with the standard protocol were higher by 2.8 or more times. In other terms, on the two first two sampling dates was less permeable and hence inherently less modifiable as compared with the last three sampling dates.

The results of this investigation were consistent with those obtained by Alagna et al. (2016), working on a sandy-loam zone of the same field and only using 15 water volumes to perform L and H runs. In particular, these authors noticed that the dry soil was more sensitive to the height from which water was poured than a wet soil and they also suggested that, in more macroporous conditions (lower θ_i, higher K_s), there were more opportunities for aggregate breakdown, compaction of the exposed soil surface and macropore obstruction, that are expected phenomena when the applied water has a mechanical impact on the soil surface. In addition, a greater stability of an initially wetter soil is documented in the literature. For example, Truman et al. (1990) concluded that an increase in initial water conditions increased the resistance of the aggregates to the forces of raindrops, thereby lessening particle detachment. Fohrer et al. (1999) reported that, under continuous rainfall conditions, an initially dry soil showed a higher compaction than an initially moist soil.

The saturated conductivity decreased by 3.0 to 5.8 times, depending on the sampling date, for increasing water volumes (comparison between 15L and 30L methodologies, **Table 5.2.4**) and by 2.1 to 20.7 times for increasing height of water pouring (30L vs. 30H methodologies). More in particular, the height of water pouring had a larger influence than the used water volume when the soil was initially dry and highly permeable.

A run making use of more water (30L instead of 15L) can be expected to yield smaller K_s values for different reasons. The most obvious is a closer attainment of nearly steady-state conditions with the longer run (Reynolds and Elrick, 2002). In this investigation, stabilization after applying 15 water volumes was questionable on the whole in several circumstances (**Figure 5.2.2**) although each individual run did not appear visually evidently unsteady (**Figure 5.2.1**). The 15L methodology was suggested as a sort of standard method to perform a beerkan infiltration run in the field (Lassabatere et al., 2006) although other procedures could be applied. For example, water can be added until two (Mubarak et al., 2009) or three (Mubarak et al., 2010) consecutive infiltration times are identical or until the differences in infiltration times between consecutive water applications become negligible (Lassabatere et al., 2019). The practical advantage of the protocol by Lassabatere et al. (2006) is that the amount of water to be used for an experiment is rather small and it can be fixed in advance, which greatly simplifies planning of sampling campaigns in general and especially in remote areas. Instead, perfect identity of two or three consecutive infiltration times does not always assure that steady-state was reached (Bagarello et al., 1999) and establishing when differences between two infiltration times are negligible is unavoidably rather subjective.

With reference to the 15L scenario, calculations of K_s were successful with both BEST-steady and method 1 by Wu et al. (1999) for 34 of the 50 runs. Attempting to perform a reliable comparison between the two K_s calculation methods, a single dataset including these 34 runs was considered. A possible alternative choice, that is considering separately each sampling date, was excluded since in some instances K_s calculations were valid with both methods in only a few cases (in particular, three runs for the MAY18 sampling campaign), likely making a comparison based on such small datasets not very informative. Although there were generally similarities between the two developed K_s datasets ($K_{s,BS}$ and $K_{s,WU1}$), particularly low K_s values were provided by the transient method but not the steady one in a few instances (**Figure 5.2.5**). For both datasets, the hypothesis of a normal distribution was rejected for the untransformed K_s data but not with reference to the ln-transformed

data (Lilliefors, 1967). Consequently, K_s was assumed to be ln-normally distributed, and the data were summarized by calculating the geometric mean and the associated *CV* (**Figure 5.2.5**).

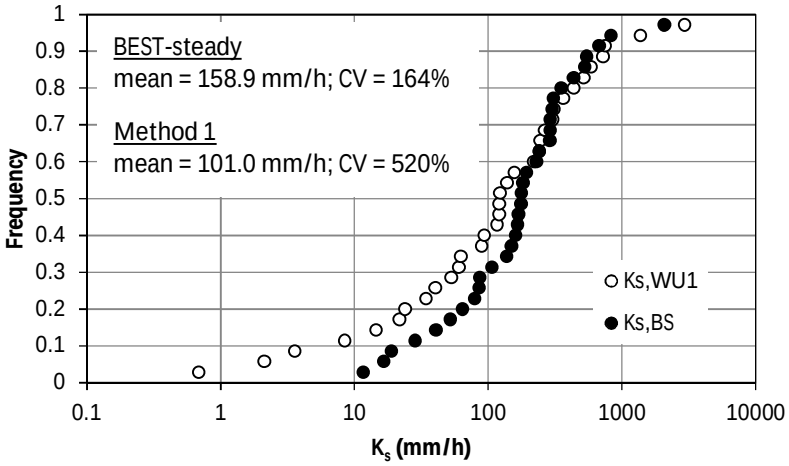

Figure 5.2.5 Cumulative empirical frequency distribution of the saturated soil hydraulic conductivity values obtained with BEST-steady ($K_{s,BS}$) and method 1 by Wu et al. (1999) ($K_{s,WU1}$) with reference to the 15L infiltration runs (sample size, N = 34)

The two datasets differed widely with reference to relative variability. Moreover, the two means were significantly different according to a two-tailed paired t test performed on the ln-transformed K_s values. In particular, the two means differed by 1.6 times which indicated, within the validity limits of the established comparison, that on average the steady method overestimated K_s for no more than a small quantity according to the suggested criterion by Elrick and Reynolds (1992). Therefore, this comparison gave a partial support to the assumption that near steady-state conditions were approximately reached, or at least approached, by using 15 water volumes, as expected according to the rule of thumb by Lassabatere et al. (2006). More precisely, the BEST-steady calculations overestimated K_s but not appreciably. With BEST-steady, the mean K_s values obtained with the 15L and 30L methodologies differed by 3.0 to 5.8 times, depending on the sampling date (**Table 5.2.1**). Also assuming that the steady state was not obtained and thus decreasing the means of Ks obtained with the shortest experiment by a factor of 1.6, the means of short run remained higher than those obtained with the longer run by 1.9 to 3.6 times. This result did not demonstrate unequivocally that this last decrease was a consequence of soil deterioration due to a prolonged wetting but induced to believe that this could be a plausible interpretation since the concerns about achievement of steadiness with the shortest run, possibly influencing the differences between the two compared datasets (15L and 30L), were removed or, at least, mitigated in the established comparison.

More water implies larger sampled volumes (Elrick and Reynolds, 1992) which could suggest that the different response of the 15L and 30L runs was a consequence of small scale spatial variability of soil hydraulic properties (Price and Bauer, 1984; Mallants et al., 1996). However, each individual 30L run yielded a smaller K_s value than the corresponding 15L run and it was unlikely that each smaller soil bulb was systematically embedded in a less permeable bulb. It is therefore more likely that increased water volume promoted some soil structural changes (Or, 1996; Bagarello and Sgroi, 2004; Lado et al., 2004; Dikinya et al., 2008). The infiltration run was longer and therefore there was more time for a weakening of the bonds between soil particles and more chances that detached soil particles were transported, with a subsequent modification of the soil pore system.

Applying water from a higher height (30H instead of 30L) can be expected to yield smaller infiltration rates as a consequence of mechanical effects on the soil surface, such as compaction and vertical displacement of detached soil particles and small aggregates. Vertical heterogeneity of soil hydraulic properties was not considered to explain the detected differences between the 30L and 30H runs since the same water volume was used for these runs. Areal heterogeneity was also viewed as an unlikely

explanation because the sampled area was rather small and the number of replications was relatively large.
The applied experimental methodology had a clearly perceivable impact on temporal variability of K_s. In particular, the 15L methodology indicated that the soil had a greater conductivity on MAY18 and SEP18 than on NOV17 and APR18 and also that the saturated conductivity of APR19 was similar to the other four dates (**Table 5.2.1, Figure 5.2.6**).

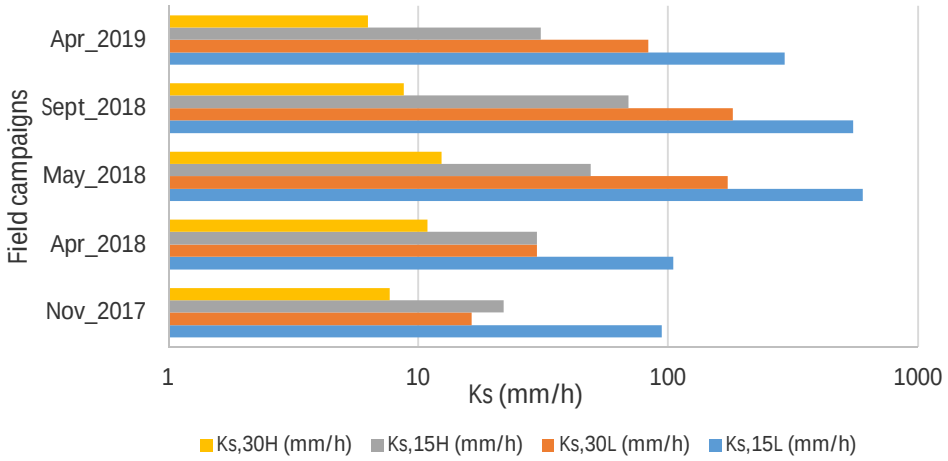

Figure 5.2.6 Comparison between field campaigns

The result was similar, although not identical, with the 30L methodology. Instead, neither the 15H nor the 30H methodologies signaled any difference among the five sampling dates. Therefore, the soil was found to be temporally stable in this case. The summary of the mean K_s values obtained on the five sampling dates showed a clear general decrease of this hydrodynamic soil property in the passage from the 15L to the 30H experimental methodology and it also revealed a clear homogenizing effect of the more soil perturbing experiments (lower *CV* and lower ratio between the two extreme mean values of K_s for a given methodology, **Table 5.2.5**).
Therefore, it appeared that the saturated conductivity of the sampled soil tended to collapse towards a rather narrow range of small values, likely compatible with surface runoff formation in many instances, when a soil perturbing run was carried out.
High or very high K_s values are typical of macroporous soils and the macropores that dominate flow at saturation are known to be fragile (Jarvis et al., 2013) and less stable than matrix pores (Kutílek et al., 2006). Likely, changing the experimental method to perform an infiltration run in the field implied passing from a process mainly governed by the unstable structural macroporosity (Watson and Luxmoore, 1986; Jarvis and Messing, 1995; Jarvis et al., 2013) to a process that was more controlled by the soil matrix, which did not vary. According to this investigation, a decline of the soil hydrodynamic properties can have a nearly abrupt character, that is a single infiltration run is enough to deeply modify the detectable hydrodynamic response of the soil.
The results of this investigation appear attractive in a hydrological perspective. For example, Hortonian surface runoff is expected to occur as a consequence of prolonged and intense rainfall events, often inducing development of an altered layer at the soil surface (Assouline and Mualem, 2002, 2006). As shown in this investigation, the soil sampled with classical methodologies only differing by the run duration (15L and 30L) had a conductivity standing on values of $\geq$ 100 mm/h, that denote the impossibility to have runoff in most natural situations. However, a more soil perturbing infiltration experiment, that likely reproduces better what happens at the soil surface when heavy rainfall occurs, yielded an information on the same soil hydrodynamic property that, at least potentially, appeared compatible with rainfall excess formation (K_s equal on average to 9.2 mm/h, **Table 5.2.5**).

Table 5.2.5 Mean and coefficient of variation, *CV*, of the mean values of the saturated soil hydraulic conductivity, K_s (mm/h), obtained on the five sampling dates with different experimental methodologies and ratio between the two extreme mean values of K_s

Statistic	15L	30L	15H	30H
Mean	329.7	97.1	40.4	9.2
CV (%)	72.9	80.1	47.4	26.5
Ratio	6.4	11.1	3.1	2.0

15L: 15 water volumes and low runs; 30L: 30 water volumes and low runs; 15H: 15 water volumes and high runs; 30H: 30 water volumes and high runs

Therefore, it seems that the methodology can be adapted to obtain hydrologically relevant soil data (Auteri et al., 2020). More clearly, a soil can be characterized under different conditions, ranging from a nearly undisturbed situation (non-perturbing and, perhaps, short run) to heavily disturbed (long and perturbing run). In the former case, the temporal variability of K_s cannot be neglected and soil sampling campaigns have to be replicated over time to fully characterize the porous medium. Instead, temporal variation of K_s does not represent a matter of great concern when it is determined by a soil perturbing experiment. In this case, sampling the soil only once could be enough to obtain an information usable at different times for the field site.
The gravitational potential energy, E_p, of the water used for the infiltration run generally explained a large proportion of the variance in K_s and the relationship between K_s and E_p was statistically significant in three of the five sampling dates (**Table 5.2.6**).

Table 5.2.6 Shape and statistical significance of the relationship between the mean saturated soil hydraulic conductivity and the gravitational potential energy of the applied water by considering three different scenarios: i) all experimental methodologies (N = 4; 15L, 30L, 15H, 30H), ii) excluding the 30L methodology (N = 3), and iii) excluding the 15L methodology (N = 3)

Sampling date	All methodologies		Excluding 30L		Excluding 15L	
	Relationship	R^2	Relationship	R^2	Relationship	R^2
November 2017	Power	0.5356 ns	Logarithmic	0.9998 s	Exponential	0.4937 ns
April 2018	Exponential	0.6931 ns	Logarithmic	0.9973 s	Exponential	0.7595 ns
May 2018	Power	0.9143 s	Logarithmic	0.9929 ns	Exponential	0.9998 s
September 2018	Exponential	0.9326 s	Exponential	1.0000 s	Linear	0.9673 ns
April 2019	Exponential	0.9053 s	Logarithmic	0.9961 s	Exponential	0.9854 ns

R^2 = coefficient of determination; s = R significantly greater than zero at P = 0.05; ns = R not significantly greater than zero

However, as shown in the example of **Figure 5.2.7** for the APR18 sampling campaign and also in Figure 4 by Auteri et al. (2020), reporting the same result for the APR19 campaign, the points corresponding to the 15L and 30L methods had similar E_p values (50 and 100 J/m^2, respectively) but also appreciably different means of K_s (**Table 5.2.1**).

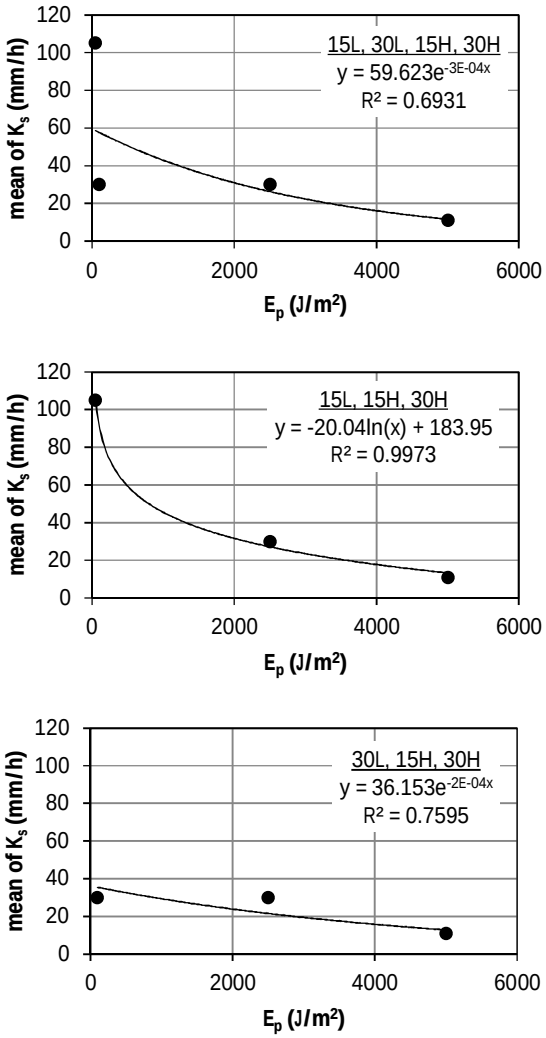

Figure 5.2.7 Example of the relationships between the mean saturated soil hydraulic conductivity, K_s, and the gravitational potential energy of the applied water, E_p, for the April 2018 sampling campaign

Excluding the data obtained with the 30L method from the regression analysis determined an increase of the R^2 value for the regression line between the two variables and a very limited scattering of the data around the fitted line in all cases and also a larger number of times in which the regression was statistically significant (four cases, **Table 5.2.6**). Excluding the data obtained with 15L method was generally advantageous in terms of R^2 but not with reference to alignment of the data around the fitted line and to statistical significance of the regression, that was recognized only once.

Therefore, it was confirmed that the energy of the applied water for a beerkan run can be useful to predict the K_s changes that could be expected when different methodologies are applied but this conclusion cannot be considered valid in general. In particular, it seems that there is an incompatibility between the 15L and 30L methodologies in the perspective to develop a K_s vs. E_p relationship. On the basis of the results of this investigation, it seems that the best choice could be to use the K_s value obtained with the 15L methodology as representative of a more or less totally undisturbed soil condition. The 15H and 30H methodologies are usable to explain how this undisturbed K_s value varies as a consequence of the mechanical perturbation at the soil surface and probably accounts of different factors (i.e., soil layering, vertical heterogeneity in initial soil water content. Perhaps, the 30L methodology does not work well in this context because the K_s decrease as compared with the 15L methodology does not actually signal effects of water impact on the soil surface and probably accounts of different factors (i.e., soil layering, vertical heterogeneity in initial soil water content).

Supporting this approximate reasoning needs additional investigations. In particular, each data point considered to develop the K_s vs. E_p relationships was deemed to be rather reliable since it was obtained

as the mean of a relatively large number of replications. However, the check performed in this study was based on a limited number of data points (three or four), which represents an obvious limit. Therefore, more experimental scenarios should be considered but, according to this investigation, it is something worth doing to improve our ability to predict the soil's response in hydrologically relevant situations.

5.2.4. Conclusions

This investigation confirmed that the single-ring beerkan infiltration run can be adapted in an attempt to induce a soil disturbance that is likely similar to the one expected when a rainfall event produces runoff. In particular, using much water for the experiment and applying water from a relatively high height on the infiltration surface determined an appreciable decrease of saturated soil hydraulic conductivity, K_s, as compared with the standard beerkan run. These data seem more hydrologically relevant than those obtained with standard experimental methodologies since they were obtained in a soil condition that is closer to that expected when runoff is formed.

Height of water pouring effects were more noticeable when the soil was initially dry and highly permeable. Probably, this result was a consequence of the fact that, in these conditions, the soil had a more unstable macroporosity.

The gravitational potential energy, E_p, of the water used for the infiltrometer experiment explained much of the variance of the K_s values obtained by different experimental methodologies. However, there was some sign that the four considered experimental methodologies are not simultaneously usable to develop a single relationship between K_s and E_p. The suggestion was that this kind of relationship could be expected to work well in the prediction of the mechanical impact effects on the conductivity of an initially unaltered soil but not when other factors also contribute to induce a decrease of K_s as compared with the target value.

Assessing of K_s temporal variability should be expected to depend on the applied experimental methodology. If the objective is to characterize the soil with a non-perturbing experiment, that is obtaining data for a nearly undisturbed situation, sampling has to be repeated over time to also describe temporal variability of the investigated soil hydrodynamic property. However, if the same soil has to be characterized in the perspective to predict runoff formation, a perturbative experiment performed only once could be enough to obtain an information usable at different times for the field site.

In conclusion, an infiltrometer experiment can be carried out in such a way to mimic what happens in real situations when rainfall produces Hortonian runoff. Soil disturbance can be controlled by changing the water volume used for the run and, especially, the height of water pouring. The field experiment remains rather simple and, therefore, the attractiveness of infiltrometer methods is not reduced.

Some advancements in the experimental methodology to be applied in this ongoing monitoring program could be indicated. In particular, it could be advisable to perform longer runs (e.g., 45 water volumes or something of similar) to reduce possible uncertainties on attainment of really near steady infiltration rates. However, this is not the only advancement to be made in this perspective because more water and longer runs also imply more opportunities for deterioration of soil structure. In other terms, some doubts on the interpretation of the data could remain. Perhaps, pairing tension infiltrometer experiments, that are among the less soil perturbing devices currently available, could be an option to be considered. Still another option could be to analyze the data collected with the standard protocol (15 water volumes) with analytical methods and procedures that do not require attainment of steady-state. However, the relative performances of these methods as compared with the BEST-steady calculations of K_s should initially be established for ideal soil conditions, that is using analytically or numerically simulated infiltration data, to avoid the risk to misinterpret the results of a comparison established on field data. More data should also be collected to better establish what are the factors that control the relationship between K_s and the gravitational potential energy. This investigation could have modelling interest since such a kind of relationship could easily be implemented into hydrological models.

References

Alagna, V., Bagarello, V., Di Prima, S., Guaitoli, F., Iovino, M., Keesstra, S., Cerdà, A., 2019. Using beerkan experiments to estimate hydraulic conductivity of a crusted loamy soil in a Mediterranean vineyard. J. Hydrol. Hydromech. 67. https://doi.org/10.2478/johh-2018-0023

Alagna, V., Bagarello, V., Di Prima, S., Giordano, G., Iovino, M., 2016. Testing infiltration run effects on the estimated water transmission properties of a sandy-loam soil. Geoderma 267, 24–33. https://doi.org/10.1016/j.geoderma.2015.12.029

Angulo-Jaramillo, R., Bagarello, V., Di Prima, S., Gosset, A., Iovino, M., Lassabatere, L., 2019. Beerkan Estimation of Soil Transfer parameters (BEST) across soils and scales. J. Hydrol. 576, 239–261. https://doi.org/10.1016/j.jhydrol.2019.06.007

Angulo-Jaramillo, R., Bagarello, V., Iovino, M., Lassabatère, L., 2016. Infiltration measurements for soil hydraulic characterization. Springer International Publishing.

Assouline, S., Mualem, Y., 2006. Runoff from heterogeneous small bare catchments during soil surface sealing. Water Resour. Res. 42, W12405. https://doi.org/10.1029/2005WR004592

Assouline, S., Mualem, Y., 2002. Infiltration during soil sealing: The effect of areal heterogeneity of soil hydraulic properties. Water Resour. Res. 38, 1286. https://doi.org/10.1029/2001WR001168

Auteri, N., Bagarello, V., Concialdi, P., Iovino, M., 2020. Testing an adapted beerkan infiltration run for a hydrologically relevant soil hydraulic characterization. J. Hydrol. 584, 124697. https://doi.org/10.1016/j.jhydrol.2020.124697

Bagarello, V., Cecere, N., David, S.M., Prima, S.D., 2020. Determining short-term changes in the hydraulic properties of a sandy-loam soil by a three-run infiltration experiment. Hydrol. Sci. J.

Bagarello, V., Castellini, M., Di Prima, S., Iovino, M., 2014a. Soil hydraulic properties determined by infiltration experiments and different heights of water pouring. Geoderma 213, 492–501. https://doi.org/10.1016/j.geoderma.2013.08.032

Bagarello, V., Baiamonte, G., Castellini, M., Di Prima, S., Iovino, M., 2014b. A comparison between the single ring pressure infiltrometer and simplified falling head techniques. Hydrol. Process. 28, 4843–4853. https://doi.org/10.1002/hyp.9980

Bagarello, V., Di Prima, S., Iovino, M., Provenzano, G., Sgroi, A., 2011. Testing different approaches to characterize Burundian soils by the BEST procedure. Geoderma 162, 141–150. https://doi.org/10.1016/j.geoderma.2011.01.014

Bagarello, V., Sgroi, A., 2007. Using the simplified falling head technique to detect temporal changes in field-saturated hydraulic conductivity at the surface of a sandy loam soil. Soil Tillage Res. 94, 283–294. https://doi.org/10.1016/j.still.2006.08.001

Bagarello, V., Sgroi, A., 2004. Using the single-ring infiltrometer method to detect temporal changes in surface soil field-saturated hydraulic conductivity. Soil Tillage Res. 76, 13–24. https://doi.org/10.1016/j.still.2003.08.008

Bagarello, V., Iovino, M., Reynolds, W.D., 1999. Measuring hydraulic conductivity in a cracking clay soil using the Guelph permeameter. Trans. ASAE 42.

Bagarello, V., 1997. Influence of well preparation on field-saturated hydraulic conductivity measured with the Guelph permeameter. Geoderma 80, 169–180.

Bagarello, V., Provenzano, G., 1996. Factors affecting field and laboratory measurement of saturated hydraulic conductivity. Trans. ASAE USA.

Dikinya, O., Hinz, C., Aylmore, G., 2008. Decrease in hydraulic conductivity and particle release associated with self-filtration in saturated soil columns. Geoderma 146, 192–200. https://doi.org/10.1016/j.geoderma.2008.05.014

Di Prima, S., Concialdi, P., Lassabatere, L., Angulo-Jaramillo, R., Pirastru, M., Cerda, A., Keesstra, S., 2018. Laboratory testing of beerkan infiltration experiments for assessing the role of soil sealing on water infiltration. Catena 167, 373–384. https://doi.org/10.1016/j.catena.2018.05.013

Di Prima, S., Castellini, M., Abou Najm, M.R., Stewart, R.D., Angulo Jaramillo, R., Winarski, T., Lassabatere, L., 2019. Experimental assessment of a new comprehensive model for single ring infiltration. 2019. J. Hydrol. 573. Pp. 937-951. https://doi.org/10.1016/j.jhydrol.2019.03.077

Elrick, D.E., Reynolds, W.D., 1992. Methods for analyzing constant-head well permeameter data. Soil Sci. Soc. Am. J. 56, 320. https://doi.org/10.2136/sssaj1992.03615995005600010052x

Daniel W. W., 1996. Biostatistica. Concetti di base per l'analisi statistica delle scienze dell'area medico-sanitaria. Edises.

Fohrer, N., Berkenhagen, J., Hecker, J.-M., Rudolph, A., 1999. Changing soil and surface conditions during rainfall: Single rainstorm/subsequent rainstorms. Catena 37, 355–375. https://doi.org/10.1016/S0341-8162(99)00026-0

Glantz S., Primer of Biostatistics. 2012. Mc Graw Hill.

Horton, R.E., 1940. The infiltration-theory of surface-runoff. Eos Trans. Am. Geophys. Union 21, 541–541. https://doi.org/10.1029/TR021i002p00541-1

Jarvis, N., Koestel, J., Messing, I., Moeys, J., Lindahl, A., 2013. Influence of soil, land use and climatic factors on the hydraulic conductivity of soil. Hydrol Earth Syst Sci 17, 5185–5195. https://doi.org/10.5194/hess-17-5185-2013

Jarvis, N.J., Messing, I., 1995. Near-saturated hydraulic conductivity in soils of contrasting texture measured by tension infiltrometers. Soil Sci. Soc. Am. J. 59, 27–34.

Kutilek, M., Jendele, L., Panayiotopoulos, K., 2006. The influence of uniaxial compression upon pore size distribution in bi-modal soils. Soil Tillage Res. 86, 27–37. https://doi.org/10.1016/j.still.2005.02.001

Lado, M., Ben-Hur, M., Shainberg, I., 2004. Soil wetting and texture effects on aggregate stability, seal formation, and erosion. Soil Sci. Soc. Am. J. 68, 1992–1999. https://doi.org/10.2136/sssaj2004.1992

Lassabatere, L., Di Prima, S., Bouarafa, S., Iovino, M., Bagarello, V., Angulo Jaramillo, R., 2019. BEST-2K for characterizing dual-permeability unsaturated soils with ponded and tension infiltrometers. Vadose Zone J.

Lassabatere, L., Angulo-Jaramillo, R., Goutaland, D., Letellier, L., Gaudet, J.P., Winiarski, T., Delolme, C., 2010. Effect of the settlement of sediments on water infiltration in two urban infiltration basins. Geoderma 156, 316–325. https://doi.org/10.1016/j.geoderma.2010.02.031

Lassabatere, L., Angulo-Jaramillo, R., Soria Ugalde, J.M., Cuenca, R., Braud, I., Haverkamp, R., 2006. Beerkan estimation of soil transfer parameters through infiltration experiments—BEST. Soil Sci. Soc. Am. J. 70, 521. https://doi.org/10.2136/sssaj2005.0026

Lilliefors, H.W., 1967. On the Kolmogorov-Smirnov test for normality with mean and variance unknown. J. Am. Stat. Assoc. 62, 399–402. https://doi.org/10.1080/01621459.1967.10482916

Mallants, D., Mohanty, B.P., Jacques, D., Feyen, J., 1996. Spatial variability of hydraulic properties in a multi-layered soil profile. Soil Sci. 161, 167–181.

Mubarak, I., Angulo-Jaramillo, R., Mailhol, J.C., Ruelle, P., Khaledian, M., Vauclin, M., 2010. Spatial analysis of soil surface hydraulic properties: Is infiltration method dependent? Agric. Water Manag. 97, 1517–1526. https://doi.org/10.1016/j.agwat.2010.05.005

Mubarak, I., Mailhol, J.C., Angulo-Jaramillo, R., Ruelle, P., Boivin, P., Khaledian, M., 2009. Temporal variability in soil hydraulic properties under drip irrigation. Geoderma 150, 158–165. https://doi.org/10.1016/j.geoderma.2009.01.022

Or D., 1996. Wetting-induced soil structural changes: The theory of liquid phase sintering. Water. 3041-3049. https://doi.org/10.1029/96WR02279

Philip, J.R., 1990. Inverse solution for one-dimensional infiltration, and the ratio A/K1. Water Resour. Res. 26, 2023–2027. https://doi.org/10.1029/WR026i009p02023

Pieri, C.J.M.G. 1992. Fertility of soils a future for farming in the West African savannah. Springer-Verlag, Berlin.

Price, A.G., Bauer, B.O., 1984. Small-scale heterogeneity and soil-moisture variability in the unsaturated zone. J. Hydrol. 70, 277–293. https://doi.org/10.1016/0022-1694(84)90127-6

Prieksat, M.A., Kaspar, T.C., Ankeny, M.D., 1994. Positional and temporal changes in ponded infiltration in a corn field. Soil Sci. Soc. Am. J. 58, 181. https://doi.org/10.2136/sssaj1994.03615995005800010026x

Reynolds, W.D., and D.E. Elrick. 2002. Pressure infiltrometer In: J.H. Dane and G.C. Topp, editors, Methods of soil analysis. Part 4. Physical methods. SSSA Book Ser. 5. SSSA, Madison, WI. p. 826–836. doi:10.2136/sssabookser5.4.c32

Reynolds, W.D., Bowman, B.T., Drury, C.F., Tan, C.S., Lu, X., 2002. Indicators of good soil physical quality: density and storage parameters. Geoderma 110, 131–146.

Reynolds, W.D., Drury, C.F., Tan, C.S., Fox, C.A., Yang, X.M., 2009. Use of indicators and pore volume-function characteristics to quantify soil physical quality. Geoderma 152, 252–263. https://doi.org/10.1016/j.geoderma.2009.06.009

Reynolds, W.D., Bowman, B.T., Brunke, R.R., Drury, C.F., Tan, C.S., 2000. Comparison of tension infiltrometer, pressure infiltrometer, and soil core estimates of saturated hydraulic conductivity. Soil Sci. Soc. Am. J. 64, 478–484. https://doi.org/10.2136/sssaj2000.642478x

Reynolds, W.D., Elrick, D.E., 1990. Ponded Infiltration From a Single Ring: I. Analysis of Steady Flow. Soil Sci. Soc. Am. J. 54, 1233. https://doi.org/10.2136/sssaj1990.03615995005400050006x

Shukla, M.K., Lal, R., Unkefer, P., 2003. Experimental evaluation of infiltration models for different land use and soil management systems. Soil Sci. 168, 178–191. doi: 10.1097/01.ss.0000058890.60072.7c

Stewart, R.D., Abou Najm, M.R., 2018a. A comprehensive model for single ring infiltration i: initial water content and soil hydraulic properties. Soil Sci. Soc. Am. J. 0, 0. https://doi.org/10.2136/sssaj2017.09.0313

Stewart, R.D., Abou Najm, M.R., 2018b. A comprehensive model for single ring infiltration ii: estimating field-saturated hydraulic conductivity. Soil Sci. Soc. Am. J. 0, 0. https://doi.org/10.2136/sssaj2017.09.0314

Truman, C.C., Bradford, J.M., Ferris, J.E., 1990. Antecedent water content and rainfall energy influence on soil aggregate breakdown. Soil Sci. Soc. Am. J. 54, 1385–1392.

Vandervaere, J.-P., Vauclin, M., Elrick, D.E., 2000. Transient flow from tension infiltrometers I. The two-parameter equation. Soil Sci. Soc. Am. J. 64, 1263–1272.

Watson, K.W., Luxmoore, R.J., 1986. Estimating macroporosity in a forest watershed by use of a tension infiltrometer. Soil Sci. Soc. Am. J. 50, 578–582.

White, I., Sully, M.J., 1987. Macroscopic and microscopic capillary length and time scales from field infiltration. Water Resour. Res. 23, 1514–1522. https://doi.org/10.1029/WR023i008p01514

Wu, L., Pan, L., 1997. A generalized solution to infiltration from single-ring infiltrometers by scaling. Soil Sci. Soc. Am. J. 61, 1318–1322.

Wu, L., Pan, L., Mitchell, J., Sanden, B., 1999. Measuring saturated hydraulic conductivity using a generalized solution for single-ring infiltrometers. Soil Sci. Soc. Am. J. 63, 788. https://doi.org/10.2136/sssaj1999.634788x

Yilmaz, D., Lassabatere, L., Angulo-Jaramillo, R., Deneele, D., Legret, M., 2010. Hydrodynamic characterization of basic oxygen furnace slag through an adapted best method. Vadose Zone J. 9, 107. https://doi.org/10.2136/vzj2009.0039

CHAPTER 6: Summary and conclusions

The focus of PhD activity was attempting to give a contribution in the general perspective to improve our ability to obtain a soil hydraulic characterization by infiltration methods. Several experimental investigations were carried out both in the laboratory and in the field.

With regard to the SFH technique, the method used to calculate the established depth of water ponding at the beginning of the infiltration run, D, should not influence very much K_s determination. However, larger D values can yield smaller K_s values in fine-textured soils. Air can escape from the initially unsaturated sampled soil volume when almost all water had infiltrated but this circumstance does not seem to have a great impact on calculation of K_s. A falling-head one-dimensional ponded infiltration process is not recommended to estimate the so-called α^* parameter needed for K_s calculation. The depth of the wetting front at the end of the infiltration process can approximately be predicted before the run. The general conclusion of this investigation was that the SFH technique appears a rather robust method to simply and rapidly determine K_s.

The intensive laboratory and field activity developed during the PhD course with specific reference to the beerkan infiltration runs and the BEST methodologies to analyse the single-ring infiltration data yielded useful information in the perspective to improve our ability to use single-ring infiltration methods to determine the soil hydraulic properties for hydrologically relevant purposes.
In particular, on the basis of the experimental evidence obtained in the laboratory, it was initially concluded that infiltration of simulated rainfall can mainly be driven by the seal and that the so-called BEST-H (H = high) runs should be more appropriate than the classical run when the objective of the experiment is to induce some seal formation. In addition, the joint use of single-ring infiltration and simulated rainfall revealed that the BEST-steady algorithm with BEST-H runs was the best choice to reproduce the saturated conductivity obtained by rainfall simulation. The reason was that this algorithm limits the hydraulic characterization to the stabilized phase of infiltration, that is when the seal is fully developed, avoiding uncertainties due to the seal formation during the early phase of the infiltration process. The other two algorithms (BEST-slope and BEST-intercept), that account for transient data, can be perturbed by the effect of the progressive formation of the seal and related impacts on the infiltration.
The subsequent investigation, developed in the field, demonstrated that the infiltration rate can be expected to decrease due to both water redistribution during a pause and to soil surface perturbation. Moreover, maintaining a small depth of water on the infiltration surface is not an alternative to the classical beerkan experiment. A practically useful conclusion was that a simple experiment can be carried out directly in the field, i.e. in a real world situation, to establish a link between the energy of the applied water and the measured infiltration process in an initially near-saturated soil, that is in a condition particularly favorable to rainfall excess, and hence runoff, generation. Consequently, the collected experimental information could allow us to derive soil hydraulic properties that reflect the appropriate conditions for simulating a specific hydrological process.
Another conclusion of this research activity was that the H (high) runs can be expected to generally alter the soil surface but the response can vary with the soil both in terms of disturbance level and the time required to obtain a complete soil deterioration for the applied experimental method. The infiltration run can be adapted with the aim to induce a soil disturbance likely similar to that expected for a rainfall producing runoff. In a relatively dry initial status, complete deterioration can require less water for a silty-clay soil than a loam soil. The saturated soil hydraulic conductivity is more sensitive than soil sorptivity to the applied experimental methodology. The experimental methods tested in this investigation and in other parts of this thesis could be used to easily measure the seal's saturated hydraulic conductivity for an initially undisturbed bare soil directly impacted by water with minimal experimental efforts, using small volumes of water and easily transportable equipment.

The automatic infiltrometers developed in France allows the user to obtain more accurate estimates of soil hydraulic parameters, while also reducing the effort needed to run multiple experiments.

The thesis also describes a still in progress research activity on parameterization of a recently proposed single-ring infiltration model. In particular, the novel finding was that parameterizing this infiltration model is simpler than expected since the so-calle “a” parameter can be obtained directly from the infiltration data.

Another investigation that has been developed during the PhD course shows that temporal variability of K_s should be expected to depend on the applied experimental methodology to perform the field infiltration experiments. If the objective is to obtain data for a nearly undisturbed situation, sampling has to be repeated over time to also describe temporal variability of the investigated soil hydrodynamic property, that could also be noticeable. However, if the same soil has to be characterized in the perspective to predict runoff formation, a perturbative experiment performed only once could be enough to obtain an information usable at different times for the field site since temporal variability of K_s is greatly reduced and probably negligible under this condition.

The gained experience during this intensive PhD activity allows to hazard some suggestions about other topics that should be investigated in the future.
With reference to the SFH technique, the points deserving further study probably include: i) estimation of the capillarity parameter by a ponded, falling head infiltration experiment; ii) effect of the packing procedure on saturated hydraulic conductivity of repacked soil samples; iii) effect of the reuse of the same soil material on saturated hydraulic conductivity of repacked soil samples; and iv) testing of the multistep falling head infiltration method. Some of these investigations, and particularly the second and the third of the above reported list, could have a larger interest, that is not exclusively limited to the SFH technique.
In the field, the beerkan infiltration method and the BEST methodologies of soil hydraulic characterization should be applied in different soils and initial soil water content conditions against simulated rainfall events differing by both rainfall intensity and duration since rainfall characteristics are among the major factors affecting the dynamics of seal formation. Soil spatial variability issues should also be developed in the future to establish if soil perturbation due to water impact reduces the required sample size to obtain a representative hydrodynamic parameter for an area of interest. In a hydrological perspective, it also seems advisable to improve our knowledge on the short term modifications of K_s and S in an attempt to verify if, under what experimental conditions and to what level they stabilize when a disturbing run is carried out. The lowest possible S and K_s values could be viewed as a sort of hydrologically relevant index since they describe the most favorable condition to runoff occurrence. The experiments should be made more complex to obtain more detailed data in the field. In particular, among the questions to be answered, it should be established if analyzing a short duration run with a steady-state method is a defensible choice not only on the basis of the literature suggestions but also because other experimental methodologies and other methods of data analysis yield an experimental support to this choice. On the other hand, performing long duration runs with large water volume raises other problems because, with more water, the sampled soil volume is expected to increase with obvious consequences, such as a more difficult interpretation of the data, due for example to soil layering or non-homogeneous initial distribution of soil water content. Perhaps, detailed descriptions of the soil profile and soil water content and matric potential sensors located in the presumably wetted soil volume could help to better establish how a long duration infiltration process evolves. Perhaps, pairing tension infiltrometer experiments, that are among the less soil perturbing devices currently available, could be an option to be considered. Still another option could be to analyze the data collected by a short run, representing a sort of standard protocol, with analytical methods and procedures that do not require attainment of steady-state. However, the relative performances of these methods as compared with steady-state calculations of K_s should initially be established for ideal soil conditions, that is using analytically or numerically

simulated infiltration data, to avoid the risk to misinterpret the results. More data should also be collected to better establish what are the factors that control the relationship between K_s and the gravitational potential energy. These investigations could have modelling interest since such a kind of relationship could easily be implemented into hydrological models.

In conclusion, it seems that an infiltrometer experiment can be carried out in such a way to mimic what happens in real situations when rainfall produces Hortonian runoff. Soil disturbance can be controlled by changing the water volume used for the run and, especially, the height of water pouring. The field experiment remains rather simple and consequently the attractiveness of infiltrometer methods is not reduced by adapting the run to a hydrologically representative situation. However, some advancements in the experimental methodology to be applied are necessary and they should be considered in the future.